PART I

IMPACT ASSESSMENT

CHAPTER 1

PURSUING REGIONAL CLIMATE MODELLING AND HYDROLOGICAL MODELLING IN THE ARAB REGION

This chapter provides background information on climate modelling processes and presents the region-specific methodology that was developed and applied under the climate change impact assessment component in RICCAR. The methodology is grounded on the use of regional climate modelling and regional hydrological modelling to generate climate projections over a defined Arab Domain and selected subdomains. It involved selecting a set of climate and hydrological variables that were analysed considering different emission scenarios, resolutions and time periods to facilitate comparability with other climate modelling experiments being conducted at the global, regional and national levels.

1.1 GLOBAL CLIMATE MODELLING

Climate change projections are generated using global climate models (also referred to as general circulation models (GCMs)). These are numerical models that combine physical processes on the land surface and in the ocean, atmosphere and cryosphere to simulate the response of the global climate system to increasing greenhouse-gas concentrations. GCMs are used to study a variety of climate attributes, such as surface temperature, atmospheric temperature profiles, rainfall, atmospheric circulation, ocean circulation, wind patterns, snow and ice distributions and many other variables that are part of the global climate system. More than 100 parameters are available at the global scale to describe the climate observed in the atmosphere, ocean, land or sea ice, or their interaction (e.g. radiative forcing fields).

In these models, the Earth is divided into a three-dimensional grid-like pattern, whereby the values of selected parameters are calculated for each grid point over time to give predictions of their future values and thus provide information on the expected climate for specified conditions and time frame. Each model is characterized by a specific spatial resolution which represents the vertical and the horizontal size of the grid cells (usually expressed in degrees of latitude and longitude or in kilometres) and a temporal resolution or computational "time steps"[1] that establish the temporal sampling rate at which the model-output fields are calculated for each grid box. The interval between each computation depends on the model resolution and the computing capacity.[2]

Global climate models, in conjunction with nested regional climate models, represent the most advanced tools available to provide geographically and physically consistent estimates of regional climate change. GCMs are continuously being improved as scientific understanding of the climate develops and computational power increases. Over the years, several coupled model intercomparison projects (CMIPs) have produced vast ensembles of GCM results that can be used to assess possible future climate changes: the fifth phase of collaboration (CMIP5) supported the preparation of the Fifth Assessment Report (AR5) of the Intergovernmental Panel on Climate Change (IPCC).[3] The typical resolution of CMIP5 models ranges from 100 km to 200 km. Some global models run in horizontal resolutions of about 70 km, however. This represents a significant advancement, since the GCMs developed in the 1990s, which were used in the IPCC First Assessment Report (FAR), had an average model grid-cell resolution of around 500 km.[4] GCM components have also evolved over the years with the state-of-the-art Earth System Models (ESMs) incorporating additional aspects of the climate system, such as sophisticated land-surface models, models of ocean and sea ice, biogeochemical processes and the carbon cycle and, more recently, computationally expensive submodels of atmospheric chemistry and land ice.[5]

Al Hajir, Oman, 2016. Source: Khajag Nazarian.

1.1.1 Reference and projection periods

When creating future climate projections, climate models begin with a period of observed historical climate that is used as a reference period ("control period") that helps to validate the ability of the model to represent the past, as well as to provide a reference point against which climate change projections into the future can be compared. Biases in climate models refer to the differences between the observed long-term mean for a region and the modelled long-term mean results from the control period over the same region. Regional climate modelling outputs are also compared with global outputs and such comparison thus requires uniformity across the compared time periods.

The IPCC and other regional climate modelling experiments generally run climate simulations based on two to three future time periods that are compared with a historical reference period.[6] The following 20-year time periods are generally used: 1986–2005 (reference period), 2016–2035 (near future), 2046–2065 (intermediate future) and 2081–2100 (far future). This report presents climate change analysis with respect to reference period, intermediate future (mid-century time period) and far future (end-century time period), as illustrated in Figure 11. The near-future period is excluded as this 20-year period may be the subject of climate variability rather than climate change, which generally requires a longer time horizon to identify trends emerging from climate projections.

FIGURE 11: Time periods considered for analysis

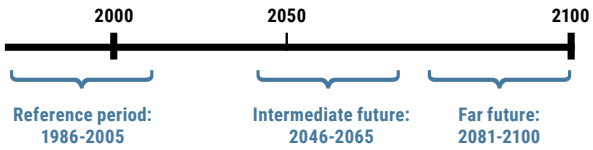

1.1.2 Representative concentration pathways

Different approaches to future scenarios in climate research have been used over time, varying from representations of annual increases in global average concentrations of GHGs to advanced representations of emissions of many gases and particles affecting climate and derived from detailed socio-economic and technology assumptions.

Climate change projections conducted within the framework of RICCAR are based on two of the four representative concentration pathways (RCPs) developed by IPCC for informing global and regional climate modelling work presented in its AR5, which shifted from the former approach based on Special Report on Emissions Scenarios (SRES) used in previous IPCC Assessment Reports.

As shown in Figure 12, there are four RCP scenarios named in accordance with their expected radiative forcing expressed in watts per square metre (W/m^2), namely RCP 2.6, RCP 4.5, RCP 6.0 and RCP 8.5. Each represents a trajectory of GHG concentrations over time to reach a particular radiative forcing in the year 2100. As such, RCPs make no assumptions as to policy changes that may affect the climate; instead they only delimit the range of possible forcings that might occur. Policy analysts and researchers can work back from these trajectories to investigate what may cause them. In this approach, each RCP could result from different combinations of economic, technological, demographic, policy and institutional futures.

FIGURE 12: Representative concentration pathways

	Radiative forcing	CO_2 equivalent concentration in 2010	Rate of change in radiative forcing
RCP 8.5 High Emissions	8.5 W/m^2	1370 ppm	Rising
RCP 6.0 Intermediate Emissions	6.0 W/m^2	850 ppm	Stabilizing
RCP 4.5 Intermediate Emissions	4.5 W/m^2	650 ppm	Stabilizing
RCP 2.6 Low Emissions	2.6 W/m^2	490 ppm	Declining

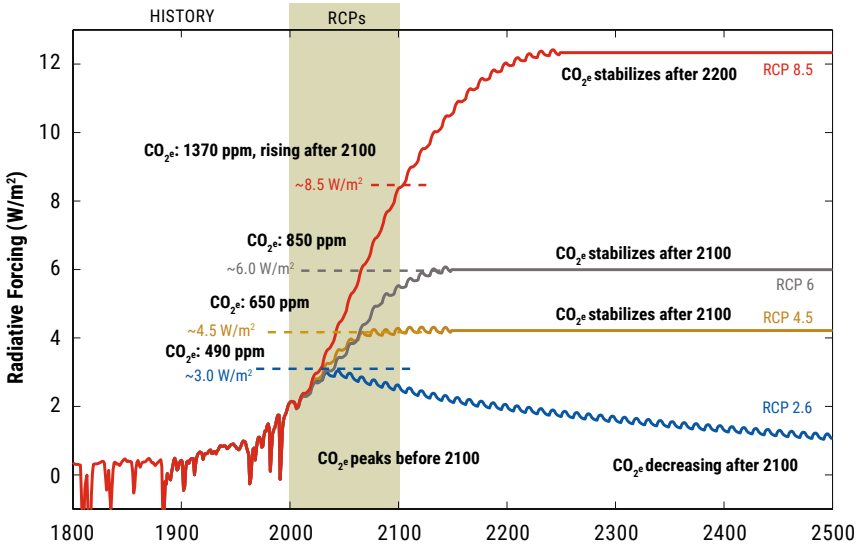

Source: Adapted from Meinshausen et al., 2011

The climate projections studied in RICCAR are based on RCP 4.5 (moderate-case scenario) and RCP 8.5 ("business as usual" – worst-case scenario). RCP 2.6 was examined to a lesser extent, where global GHG emissions peaks by 2020 and then decline thereafter, but are not presented in this report.

To put these scenarios into context, Figure 13 illustrates the corresponding global surface temperature changes projected with respect to these four RCPs that were used to generate climate modelling outputs for IPCC AR5. The figure shows that the mean global surface temperature, with respect to the 1986–2005 reference period, is projected to increase by the end of this century by 1 °C under the optimistic RCP 2.6 scenario, nearly 2 °C under the moderate RCP 4.5, to potentially over 4 °C under the pessimistic RCP 8.5 scenario.

IPCC AR5 reports that global climate risks increase as temperatures rise beyond the 2 °C temperature change, with a high likelihood that extreme weather events become more frequent and intense beyond this threshold.[7]

IPCC has been mandated by the Conference of Parties (COP) to the United Nations Framework Convention on Climate Change (UNFCCC) under the Paris Agreement to provide it with a special report in 2018 on the impacts of global warming of 1.5 °C above pre-industrial levels and related global GHG emission pathways in the context of strengthening the global response to the threat of climate change, sustainable development and efforts to eradicate poverty.

1.2 REGIONAL CLIMATE MODELLING

Despite the rapid progress and development of GCMs, important gaps remain in generating outputs on a smaller scale grid. In order to better understand these smaller-scale processes, climate scientists downscale their models to describe limited areas of the world, which are referred to as domains, through the use of regional climate models (RCMs). A core activity of RICCAR was to produce regionally downscaled future climate projections for the Arab region, which involved setting up a domain. The domain sets the limiting boundaries within which a regional climate model is nested in a GCM. An RCM can then provide a higher-resolution view and an understanding of regional climate conditions by focusing on a specific area (domain) and using the driving forces provided by a GCM as input, as shown in Figure 14. This avoids developing and running a climate model at the global scale when analysis is sought for a specific region.

In this context, there is considerable worldwide cooperation and exchange to promote the advancement of climate science

FIGURE 13: Global temperature change projections for RCP scenarios under CMIP5

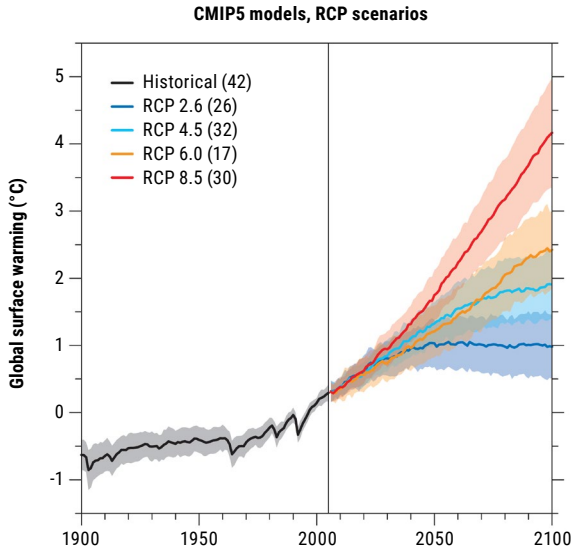

Note: Mean global temperature change relative to 1986–2005 is shown as a colored line and one standard deviation is shown with colored shading. The number of model runs is given in parentheses.

Source: Knutti and Sedláček, 2013

FIGURE 14: Schematic depiction of the one-way RCM nesting technique

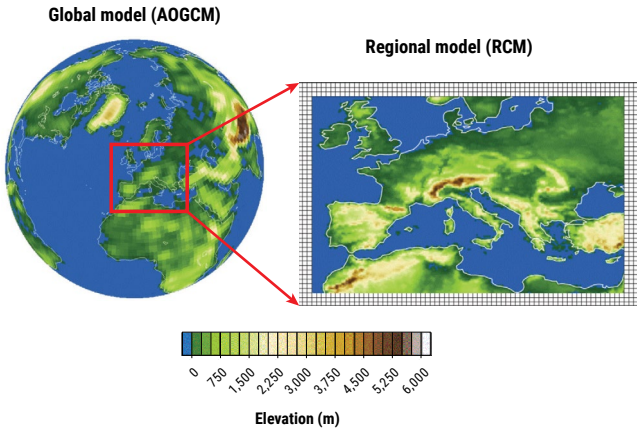

Source: Giorgi and Gutowski, 2015.

at the global and regional levels. An initiative designed to enhance this cooperation is the Coordinated Regional Climate Downscaling Experiment (CORDEX) organized under the World Climate Research Programme (WCRP).[8] Through establishing a standardized approach, CORDEX aims to evaluate and improve regional climate downscaling models and techniques and produce coordinated sets of regional downscaled projections worldwide.

An integral part of this approach is establishing common regional modelling domains to be used by all participating modelling groups.

FIGURE 15: CORDEX domains

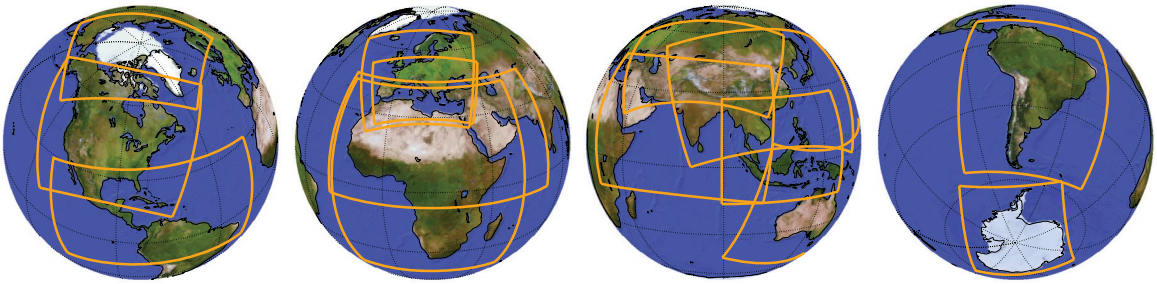

Source: WCRP, 2015a.

A common domain, together with a common list of standard model outputs, provides a framework for comparing model performance and future climate projections over these regions and thus fosters better communication and exchange of regional climate information. Regional climate models are especially suitable to assess changes expected in terms of extreme weather events, which are of great importance to develop adaptation strategies as they better represent the local processes related to weather/climate extremes with respect to GCMs.[9] It was decided at the onset of RICCAR that following the CORDEX approach would enhance the outcomes of the study and provide a productive means for continued development beyond the project's lifetime. At the time of writing, there were 14 established CORDEX regions around the globe (Figure 15). There was no unifying domain covering the Arab region prior to its set-up under RICCAR.

1.2.1 The Arab Domain

The RCM approach was applied to dynamically downscale GCM results to regional scales. This is usually done by first identifying the specific region of the globe in focus for the downscaling. In the case of RICCAR, the region of interest covers all Arab States and their water resources. As the majority of water resources in Arab States originates from outside the region, it was necessary to set up the boundaries of a domain that includes all the headwaters of shared surface-water resources flowing into the region. This encompasses a wider geographic area than those covered by the land areas of Arab States, as it requires extending the area of study to cover the headwaters of the Tigris and Euphrates Rivers in the north, as well as the headwaters of the Nile River in the south.

Defining an appropriate regional domain is not a trivial task and a number of tests were required to determine the ability of different domain configurations to appropriately represent the regional climate. Regional consultation in this regard was organized within the framework of the RICCAR RCM Ensemble Task Force, which was led by SMHI. Testing various domain sizes revealed that it was important to extend the domain sufficiently to the east to be able to appropriately represent the prevailing circulation patterns originating from the Indian Ocean. This concern had to be balanced, however, as a larger domain also requires larger computing needs and disk storage for the output. It was thus desirable to agree on setting up a domain that provides satisfactory results without placing undue demands on computing resources. Five configurations were tested and evaluated, together with regional climate experts, as shown in Figure 16. Focus was on comparing circulation, precipitation and temperature results from the different configurations.

The final CORDEX-MENA Domain (Figure 17) is a hybrid of the tested domain configurations presented in Figure 16. It is based on the minimum domain shown in orange, extended further eastwards and northwards. Nevertheless, it should be noted that CORDEX-MENA is an extended domain that requires substantial computing resources for completing century-long simulations. It is also noted that the Comoros, while an Arab State, is not included in the Arab Domain given its geographic location. The Comoros can be studied, drawing on high-resolution GCMs or RCM outputs covering the CORDEX-AFRICA Domain.

With these considerations, the CORDEX "Region 13: Middle East North Africa (MENA)" regional domain or CORDEX-MENA regional domain (27W–76E, 7S–45N) was established under CORDEX within the WCRP[10] as shown in Figure 17. This is synonymous with the Arab Domain as referred to in this report.

This is a result of the tests conducted together with recommendations from climate scientists in the region that had conducted independent tests with other RCMs. According to the tests made, this choice provides a robust representation of circulation, precipitation and temperature. It thus fulfils both the spatial and performance criteria set forth, while limiting the extent.

FIGURE 16: Different domain configurations tested for the CORDEX-MENA Domain (Arab Domain)

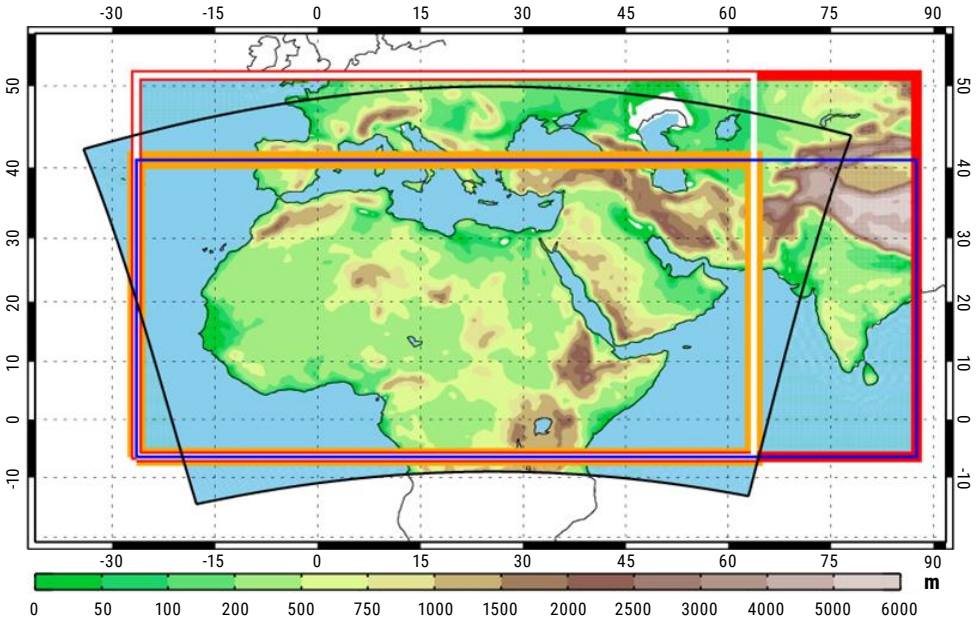

Note: The boundary in orange represents the minimum domain configuration that would satisfy spatial criteria and served as the starting reference for comparison. The boundary in blue represents the eastward extension and the one in white the northward extension. The one in red represents extensions both east and north. The black boundary represents the domain used for previous studies supported by UNESCO.

FIGURE 17: CORDEX-MENA Domain

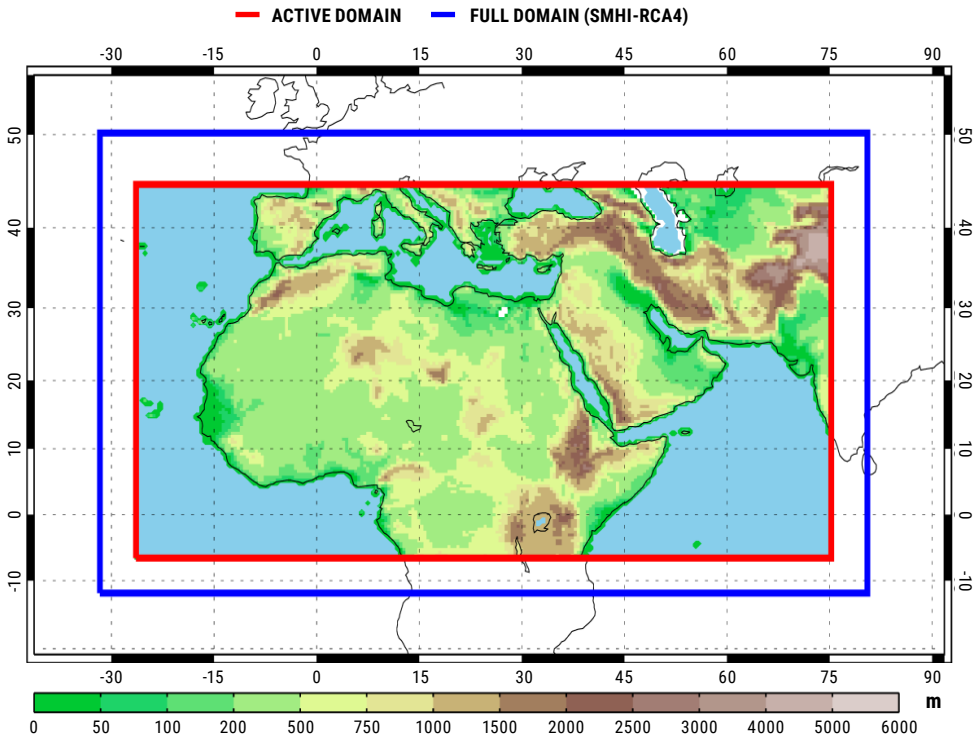

Note: The Active domain (red) contains the area where RCM results are considered usable. The Full domain (blue) indicates the actual area needed for the RCM (RCA4 in this case) to perform properly within the active domain. The area between Active and Full domain is a transition zone between the GCM driving boundaries and the RCM: using results from this zone should be avoided.

1.2.2 Regional climate modelling projections

The list of the available RCM simulations over the CORDEX-MENA domain that were used for the purposes of generating the findings presented in this report are shown in Table 4. The fourth version of the Rossby Centre Regional Atmospheric Model (RCA4) developed at SMHI was the only RCM available for analysis for future simulations in RICCAR. It is built upon its predecessor RCA3 with substantial physical and technical improvements[11] and is developed from the NWP High Resolution Limited Area Model (HIRLAM). There are three types of simulations identified from the table – evaluation, historical and scenario:

- The *evaluation (or hindcast) simulation* is used to assess how well an RCM can represent recent climate over the domain. It was created using ERA-Interim[12] as the driving GCM data at the boundaries and is considered equivalent to driving the RCM with observations.

- The *historical simulation* uses observed emissions data for the period that should statistically represent the historical period from 1950 to 2005.

- For the *scenario simulation* runs performed under RICCAR, downscaled simulations by RCA4 were driven by lateral boundary conditions from three different CMIP5 GCMs, namely EC-EARTH[13], CNRM-CM5[14] and GFDL-ESM2M[15]. As previously outlined, this report focuses on results for RCP 4.5 and RCP 8.5 scenario projections, which began in 2006. The projection under the RCP 2.6 pathway has not been analysed in detail, but is available for use in future research as needed.

A total of nine RCA4 projections are listed in Table 4. Seven of these are at 50-km resolution and two are at 25-km resolution. Six of the 50-km projections based on RCP 4.5 and RCP 8.5 scenarios have been used to create three-member ensemble analyses in RICCAR. The two projections at 25-km resolution were conducted for RCP 8.5 to gain insights as to whether smaller-scale regional climate modelling experiments could generate clearer climate signals under this more pronounced climate scenario. The conclusions relating to the 50-km ensemble outputs are presented in this report, along with a comparison with projections generated at 25-km resolution, as appropriate.

A number of other climate model efforts have also been pursued since the set-up of the CORDEX-MENA Domain for similar or the same domain by other climate modelling centres, such as the Cyprus Institute (Cyprus), Climate Services Center (Germany), Direction de la Météorologie Nationale (Morocco) and the Center of Excellence for Climate Change Research (CECCR) at King Abdulaziz University (Saudi Arabia). These were initiated during or after the impact assessment phase of the RICCAR integrated assessment was completed, however, and thus could not be incorporated into the ensemble analysis used to prepare the integrated vulnerability assessment. Nevertheless, most of them have gone through an early testing stage (setting and optimizing regional models for the Arab Domain, performing hindcast evaluation runs driven by reanalysis data, etc.). Continued work on the domain is expected under the coordination of the CORDEX-MENA Working Group hosted by the Cyprus Institute.

TABLE 4: RCM simulations conducted over the CORDEX-MENA Domain by the Rossby Centre at SMHI under RICCAR

RCM	Driving GCM/ Reanalysis	Evaluation 1979-2010	Historical 1950-2005	RCP 2.6 2006-2100	RCP 4.5 2006-2100	RCP 8.5 2006-2100	RESOLUTION (km)
RCA4	ERA-INTERIM	X					50
RCA4	EC-Earth		X	X	X	X	50
RCA4	EC-Earth		X			X	25
RCA4	CNRM-CM5		X		X	X	50
RCA4	GFDL-ESM2M		X		X	X	50
RCA4	GFDL-ESM2M		X			X	25
HIRAM	GFDL-ESM2M		X				25
REMO	MPI-ESM-LR		X				50

The ability for RCA4 to represent the climate was evaluated by comparing the outputs of the model for the reference period with observed datasets. The higher the coherence between the modelling outputs and the observed datasets, the higher the confidence that the regional model can be used to project climate into the future.

The results of these simulations showed a common tendency for a cold bias in temperature that is more pronounced in winter than in summer for both the RCMs and the GCMs that were used. An exception is the warm bias during summer in the south-eastern part of the Arabian Peninsula, which includes parts of Oman. The GCMs exhibit the same pattern of bias, which indicates that the bias is carried over from the GCMs to the RCMs. This is supported by the fact that RCA4 driven by reanalysis shows more accurate temperature results (ERA-Interim) but the warm bias for the Arabian Peninsula is also apparent with this simulation. It is worth noting that the largest differences between the two observational datasets (CRU and UDEL) also occur for the Arabian Peninsula, so uncertainties in the observational datasets may be in play.

In terms of precipitation, the results show that most of the RCM simulations exhibit a dry bias over Central Africa during summer, but that this appears more pronounced for RCA4. During winter, the dry bias also appears further north in the Atlas Mountains and in the headwaters of the Tigris and Euphrates rivers. This is apparent for the GCM ensemble as well.

It is noted that as model grid-box outputs in general represent area averages, differences compared to station observations result not only from model errors, but also from the scale gap between grid box and point scale.[16] The latter discrepancy, which is not a model error, is known as the representativeness problem.[17] Gridded observations may therefore be considered more appropriate for validating the skill of the RCM to represent the climate.

Further information on these observation dataset comparisons is provided in the RICCAR technical note *Regional Climate Modelling and Regional Hydrological Modelling Applications in the Arab Region (2017)* prepared by SMHI.[18]

1.3 REGIONAL HYDROLOGICAL MODELLING

Although climate models include some representation of hydrological processes, they generally do not resolve the hydrological cycle at a level of detail suitable for hydrological applications. Hydrological models are thus used to further assess the impact of climate change on hydrological processes. The aim within RICCAR was to provide a large-scale overview of hydrological effects over the entire Arab region. Hydrological modelling was carried out at this regional scale, which is referred to as Regional Hydrological Modelling (RHM) in this report. Producing perfect representation of river flows at local scales cannot be expected from such model applications. Efforts were made to produce a reasonable representation of hydrological processes over regional scales, given the sparse data available. The value of these modelling outputs is that they provide a consistent approach for generating information on runoff, evapotranspiration, discharge and other variables with a similar level of detail over the entire region. By providing a regional overview in this way, the regional patterns of projected hydrological change can be seen and trends and areas that would be affected can be identified. The RHM approach does not replace the need to carry out local studies that address water resources management in more detail but it does help to identify key areas that would potentially benefit from more detailed studies.

Flood waters, Lebanon, 2014. Source: Carol Chouchani Cherfane.

1.3.1 Bias correction for hydrological modelling

Even though they are based on physical principles, information generated by GCMs consist of numerical approximations which may lead in some cases to biases resulting in deviation of the simulated climate from that observed.[19] It is thus nowadays widely recognized that climate model results cannot be used directly as inputs to

other more specialized impact models and an adjustment (bias correction) towards the observed climatology is necessary. In particular, there are typically biases in the RCM statistics of key hydrometeorological variables, such as precipitation and temperature.[20] Many of these biases originate from either the driving GCM model or the RCM used for downscaling. Since hydrological models are very sensitive to anomalies in rainfall amounts, direct use of RCM outputs in impact studies is therefore usually not appropriate and the hydrologically important variables precipitation and temperature need first to be adjusted before use in impact studies.[21] While several bias-correction methods exist, all the RCM projections in RICCAR were adjusted using the distribution-based scaling (DBS) method developed by Yang et al. (2010).[22] More detailed information on different bias-correction methods is provided in Nikulin et al. (2015).[23] The following steps were performed within the DBS approach:

- Correction factors were derived by comparing the RCM output with observed climate variables for a similar control period;
- Correction factors were then applied to RCM outputs for the future climate period. This was done for precipitation and temperature for the entire regional domain;
- The WFDEI dataset was used as observed climate to define the DBS parameters for each RCM projection for the control reference period 1980–2009;
- The DBS-corrected precipitation and temperature values were then used as inputs to drive the hydrological models and also in the analysis of extreme events.

The original DBS approach was developed for applications over a wide range of climates in both Europe and Africa. It has been well-tested for areas that usually exhibit a positive bias in precipitation. For the RICCAR region, the climate projections showed tendencies for negative precipitation biases for many areas.[24] Additional focus was thus needed to further develop the DBS techniques to better account for negative precipitation biases. No additional development was needed for the temperature bias-correction technique.
It is important to note that this approach assumes that the biases being corrected are systematic in nature and of similar magnitude for both present and future climate. Although bias correction is essential, it can to some extent also modify the climate change signal. It is also worth noting that applying bias adjustment to climate-model simulations introduces a level of uncertainty in impact modelling. Care should thus be taken with respect to bias-correction assumptions and unavoidable limitations in its application, as also outlined in IPCC (2015). In this context, a Bias Correction Intercomparison Project (BCIP) has recently been established to: address the level of uncertainties that bias adjustment introduces to the flow of climate information; advance the bias-adjustment technique; and provide best practice on use of bias-adjusted climate simulations.[25]

1.3.2 Hydrological models applied

Three different hydrological models (Table 5) were applied within RICCAR. The Hydrological Predictions for the Environment (HYPE) and Variable Infiltration Capacity (VIC) models were used to produce RHM results over the entire Arab region and the HEC-HMS model was used to investigate hydrological impacts from changes in extremes at selected local scales. They all model rainfall runoff processes with primary focus on surface waters.

Both HYPE and VIC are freely available, open-source models. They were chosen as both have been designed for use in large-scale applications and have been successfully used in various regions around the world. Both have been applied to assess hydrological change using future climate projections and can easily accommodate large datasets spanning timescales exceeding 100 years. HEC-HMS is also freely available and is a rainfall-runoff model that has been widely used for a variety of applications. It is not, however, specifically known for large-scale applications. The three models are briefly described hereafter.

TABLE 5: Hydrological models applied under RICCAR

Hydrological model	Application	Set-up
HYPE	Regional approach	Runoff basins
VIC	Regional approach	Grid boxes, 50 km resolution
HEC-HMS	Local extremes	Runoff basins

1.3.2.1 Hydrological Predictions for the Environment (HYPE) model

The HYPE model was developed at SMHI to better address environmental problems affecting hydrological systems, including nutrient transport and the effects of a changing climate.[26] HYPE is based on the widely applied Hydrologiska Byråns Vattenbalansavdelning (HBV) model concept and works on the basis of establishing sub-basins according to topographical data and then assigning different classes within each sub-basin to further represent heterogeneity. These classes – or hydrological response units – are based on land use, soil type and elevation.

Taking river measurements in Penjwen, Iraq, 2014. Source: Sadeq Oleiwi Sulaiman.

The water balance for each class is calculated individually before being combined to generate the overall water balance in each sub-basin. The HYPE model structure was designed to accommodate the large quantities of data needed for modelling large areas and for long time periods, such as with climate change projections. It has been successfully applied in large- and small-scale applications and serves both as a research tool and as an operational forecast model.[27] Input data for this model include forcing data (precipitation, temperature) as well as static data (land cover, soil type, lakes and reservoirs).

1.3.2.2 Variable Infiltration Capacity (VIC) model

The VIC Model is a large-scale, semi-distributed hydrological model that was originally developed as a macroscale hydrological model.[28] As such, it is typically applied on continental or subcontinental scales using a rectangular grid structure ranging from 0.125° to 2.0°, although finer-scale applications have been made in recent years. Within each grid box, multiple land covers can be represented and variable topography is included through the use of elevation bands. VIC allows for two modes of calculation, either water-balance mode with a 24-hour time step or energy balance mode that allows for sub-daily time steps. The water-balance mode was used for this application. Each VIC grid cell is modelled independently to resolve different components of the water balance.[29] Represented processes include infiltration, percolation, evapotranspiration, snow accumulation and snowmelt (not represented are lakes, irrigation, subsurface/groundwater flow and channel losses, including seepage and evaporation). Representation of lateral flows between grid boxes can be done in a separate step for routeing flows, but this was not included in this study. Input data for VIC include daily precipitation, temperature and wind speed in 0.5° resolution from the WFDI dataset, as well as global VIC parameters comprising pre-processed soil and land-cover data.[30]

1.3.2.3 Hydrologic Engineering Center Hydrological Modelling System (HEC-HMS) model

The HEC-HMS model is a modelling package that is designed to accommodate varying hydrological applications over a range of geographical areas.[31] Depending on how it is set up, it can be used for both large river basin applications, as well as urban conditions. It is often used in combination with other modelling tools for a number of water resources management applications. It supersedes the HEC-1 hydrological model from which it is based by offering a number of advancements and modelling options, including different ways to simulate the key variables of precipitation, evapotranspiration and infiltration.

This model was used by ACSAD in RICCAR in order to study hydrological impacts from changes in extremes at the local scale for three different basins, namely Wadi Diqah (Oman), Medjerda River (Tunisia/Algeria), and Nahr el Kabir (Lebanon/Syrian Arab Republic). For this purpose, the GIS extension HEC-GeoHMS was additionally used. This extension provides the user with a set of procedures, tools and utilities to prepare GIS data for import into HEC-HMS and generation of GIS data from HMS output. It allows visualization of spatial information and watershed characteristics, performs spatial analysis, delineates sub-basins and streams, constructs inputs to hydrological models and assists with report preparation.

Additional information on bias correction, as well as model calibration, validation and performance of the applied HYPE and VIC models, is available in the RICCAR technical note *Regional Climate Modelling and Regional Hydrological Modelling Applications in the Arab Region (2017)*.[32] Additional information on HEC-HMS application is available in the RICCAR technical report *Impact of Climate Change on Extreme Events in Selected Basins in the Arab Region (2017)*.[33]

1.4 EXPLANATION OF ANALYSIS AND PRESENTATION OF RESULTS

1.4.1 Ensemble analysis

To derive the best possible estimate of the results from the different climate models, the ensemble method was used, whereby all model simulations based on the same emissions scenario and resolution are grouped and presented as mean values: an ensemble mean. As an ensemble should consist of at least three members – preferably more – the two 25-km resolution projections were not combined as an ensemble. Analysis for them consisted primarily of comparisons against the respective 50-km projections driven by the same GCM (EC-Earth, GFDL-ESM2M) as shown in Table 6. Such analyses show if and where the use of higher resolution would add value.

1.4.2 Regional climate modelling outputs

The different climate models applied under RICCAR provide results of projections for specific variables and are expressed in terms of changes from the reference period. The main variables analysed stem from the application of RCMs, which are most commonly drawn upon to generate projections related to temperature and precipitation (Table 7).

An important consideration concerning the precipitation variable is that, in many studies worldwide, changes in precipitation are often expressed as a percentage change from a base reference period, which provides an easy basis for comparison. Using percentage change can be problematic in regions that have extremely low precipitation, however. Given the small amounts of precipitation for the reference period in such areas, large percentage changes can result even if changes in magnitude are relatively small. The Arab region contains large climatic variations, particularly with regard to precipitation, which is extremely low over large areas. Projected changes in precipitation are thus primarily presented in terms of magnitude (mm) but also expressed as relative terms (%) in the narrative. Concerning results, it is worth noting that larger uncertainties are involved for precipitation than for temperature outputs, whereby the precipitation change signal is more sensitive to the driving GCM rather than the emission scenario.

TABLE 6: Description of the RCA4 ensembles

Scenario/resolution	Global model forcing
RCP 4.5, 50 km	EC-Earth, CNRM-CM5, GFDL-ESM2M
RCP 8.5, 50 km	EC-Earth, CNRM-CM5, GFDL-ESM2M

1.4.3 Regional hydrological modelling outputs

The bias-corrected RCM outputs provide needed inputs to run RHMs. The key parameter studied in RHMs is runoff. Complementary variables include evapotranspiration, soil moisture and river discharge, as well as two discharge-derived parameters, namely high-flow and low-flow discharge values (Table 7).[34] These were simulated based on bias-corrected results for temperature and precipitation generated by the RCMs. To ensure consistency across the integrated assessment components represented in this report, all results are based on the bias-corrected RCM outputs, unless otherwise noted.

When examining the projected changes of runoff, consideration should be given to the fact that these are based on precipitation outputs, which exhibit high uncertainties as mentioned in previous chapters. Runoff output projections also thus demonstrate high uncertainties for both the HYPE and VIC models.

For some rivers and streams pertaining to specific subdomains, no observation datasets on discharge were available against which the model could be verified. It is worth pointing out that the higher the human influence on the river system (water-regulation infrastructure, irrigation, etc.) compared to the size of the river, the higher the uncertainties will be in the results. These factors should be taken into consideration when interpreting and analysing discharge-related results. Moreover, concerning results for discharge and related outputs, it will be recalled that as the VIC model used in this assessment does not take into consideration the lag effects of storage and evaporation from natural lakes or dam features, discharge-related outputs were only completed through the HYPE Model.

Findings related to groundwater recharge and soil moisture are not included in this report as they require further examination based on small-scale analysis. Groundwater recharge is of interest for the region given the significant amount of fossil groundwater resources

TABLE 7: RCM and RHM output variables

Modelling source	Output variables	Absolute/difference unit
Regional climate modelling	Temperature (Tmean, Tmax, Tmin)	°Celsius
	Precipitation	mm
Regional hydrological modelling	Runoff	mm
Related to the Arab region, the Mediterranean Coast and the Moroccan Highlands findings	Evapotranspiration	mm
Regional hydrological modelling	Runoff	mm
Related to presentation of shared surface basins findings	River discharge (only HYPE) - Mean discharge - High flow - Low flow	 m^3/s m^3/s m^3/s or number of days

available and is better assessed in tandem with hydrological modelling. The hydrological models selected for regional application do not directly represent groundwater, however. Change in runoff could be used as a proxy for indicating change in groundwater recharge by interested researchers, while specialized groundwater models at a smaller scale of analysis could be applied, drawing upon the bias-corrected datasets made available for the Arab region.

The interpretation of soil moisture from RHMs should also be made with caution. Preliminary analysis shows that the soil moisture in the VIC model simulations was not at equilibrium for all areas at model initialization and for dry areas in particular. Soil-moisture content in such areas increased over the simulation time until it reached equilibrium state in the model. This means that comparing future soil-moisture states to reference period states does not give an accurate picture of how soil moisture will change in the future for these areas. Addressing this issue would require running the VIC model for an extended time using present climate data to first reach a better soil-moisture equilibrium, often referred to as "model spin-up" and then re-run all the VIC simulations. Model spin-up was considered for VIC, but was apparently not sufficient to respond to conditions in the dry areas of the Arab Domain. Given these issues, HYPE results give a more accurate assessment of change in soil moisture and can be made available upon request.

Examination of future change in soil moisture was conducted to derive a "low soil moisture" indicator based on the HYPE model results for the Arab Domain, which is defined as the mean of the lowest soil moisture occurring every year during the reference period (1986–2005). When comparing future climate to the reference period, the change is identified as the mean number of additional days per year for each future period. The results show an increasing number of days over time. For these two indicators, due to the high uncertainties in value changes in soil moisture, results can be presented as a scale of "high" or "low" change to provide a general idea of these changes without giving exact values and thus avoid misinterpretation. These results are not included in the report.

Nile River, Egypt, 2015. Source: Carol Chouchani Cherfane.

1.4.4 Extreme event indices

Although mean changes in the future climate are of interest for many applications, changes in extreme weather events are sometimes even more important, as they can have severe impacts on human health, built infrastructure, the natural environment, the transportation sector and the economy at large. It is therefore necessary to study these events in order to provide the information needed to inform policy- and decision-making on climate change adaptation and measures to enhance resilience across the Arab region. The list of 27 indices developed by ETCCDI provides metrics for extreme events and is presented in the overview chapter.[35] The present chapter presents analyses of seven indicators from the ETCCDI list and two additional regional-specific indicators that were deemed to be more relevant for examining temperature thresholds in the already hot Arab region, namely summer days over 35 °C (SU35) and summer days over 40 °C (SU40). The nine indices are listed in Table 8. An analysis of additional extreme events indices can be generated from the projections.

Floods in Gaza after thunderstorm Alexa, State of Palestine, 2011.
Source: Alhasan Sweirju/Oxfam-flickr.com

TABLE 8: Extreme events indices studied

Index	Long name	Definition
EXTREME TEMPERATURE INDICES		
SU	Number of summer days	Annual number of days when daily maximum temperature > 25ºC
SU35	Number of hot days	Annual number of days when daily maximum temperature > 35ºC
SU40	Number of very hot days	Annual number of days when daily maximum temperature > 40ºC
TR	Number of tropical nights	Annual number of days when daily minimum temperature > 20ºC
EXTREME PRECIPITATION INDICES		
CDD	Maximum length of dry spell	Maximum number of consecutive days when daily precipitation < 1mm
CWD	Maximum length of wet spell	Maximum number of consecutive days when daily precipitation ≥ 1mm
R10	Annual count of 10mm precipitation days	Annual number of days when daily precipitation ≥ 10mm
R20	Annual count of 20mm precipitation days	Annual number of days when daily precipitation ≥ 20mm
SDII	Simple precipitation intensity index	The ratio of annual total precipitation to the number of wet days (≥ 1mm)

BOX 3: Comparing RICCAR reference period data with observed data in the Arabian Peninsula

Climate scientists can draw upon the regional modelling outputs generated using RCA4 under RICCAR and compare them with simulations generated by applying other RCMs as a means to help review their work and gain insights into climate phenomenon being witnessed across the Arab region or in parts of the region.

As an example, the findings below provide a comparison between the RCA4 simulations for the reference period (1986–2005) and a set of observed records of temperature and precipitation in the Arabian Peninsula for the period 1980–2008. The station data provided by National Meteorological Services comprised the following countries: Bahrain (1 station), Kuwait (1 station), Oman (24 stations), Qatar (1 station), Saudi Arabia (11 stations), UAE (4 stations) and Yemen (2 stations).

Comparisons reveal that RICCAR simulations of the recent past are overall in good agreement with the Arabian Peninsula station data, especially regarding temperature variables, as shown in Table 9. As for extreme temperature indices, comparisons between datasets for SU40 (number of summer days above 40 °C) and TR (number of tropical nights) show better concordance for the latter index. Discrepancies between RICCAR simulations and observed data for SU40 are evident in the tables below. Possible reasons for these discrepancies could be the difference in data periods considered in RCM outputs and station data or different averaging methods of datasets. The coarse RCM resolution (50 km) could also explain these discrepancies.

As for precipitation variables, a noticeable underestimation of the annual values was observed over the high-altitude stations such as the Saiq in Oman, Khamis Mushait in Saudi Arabia and Sana'a station in Yemen, which needs to be taken into consideration when examining results for those countries. Close means are however reported for other countries as shown in Table 10, and were also evident for extreme indices such as CDD, CWD, R10 and R20.

TABLE 9: Comparison of temperature and SU40 indicator results for the RICCAR reference period (1986–2005) and observed station data (1980–2008)

	Temperature (°C)				SU40 (days)			
	Kuwait	**Oman**	**Qatar**	**UAE**	**Kuwait**	**Oman**	**Qatar**	**Bahrain**
RICCAR RCMs	27.5	25.6	27.7	27.3	130.1	2.8	113.0	136.9
Station Data	26.3	22.5	27.3	27.6	139.4	29.6	90.7	30.0

TABLE 10: Comparison of precipitation results between RICCAR RCMs (1986–2005) and station data (1980-2008)

	Precipitation (mm/month)		
	Kuwait	**Oman**	**Qatar**
RICCAR RCMs	8.6	7.5	8.0
Station Data	10.0	9.9	6.4

Source: Said AlSarmi, based on comparative assessment of RICCAR reference period and observed data, as presented in AlSarmi and Washington, 2014.

1.4.5 Seasonal outputs

Although change in annual mean values can be sufficient for some impact applications, it is often important to also see how future changes will likely occur over different seasons. As water is a key focus for this study, evaluating differences between "wet" and "dry" seasons is of considerable interest, and results were thus presented for two seasonal periods; namely April–September and October–March to assess how climate in the Arab region varies between them.

This broadly represents dry and wet periods over the entire domain, although which period is wet and which is dry varies in different subregions.

Two seasons were chosen as robust time periods that could be applied over the entire domain to avoid more complicated analysis of how the length of seasons may change in different subregions in the future.

In addition, some results were generated in terms of three boreal summer months (June, July, August) and three boreal winter months (December, January, February).

This study of projected changes over time at the seasonal level was applied for most of the variables, except for the extreme events indices. Analysis of seasonal and interseasonal variability can also be examined.

1.4.6 Subdomains

The RICCAR Assessment Report provides results presented as both maps and plotted time-series. The maps generally show the entire Arab Domain. On the other hand, the time-series presented are area means summarized over specified subdomains. Selected subdomains have been chosen to give an overview of different areas of special interest over the region (Figure 18 and Table 11).

It should be noted that the Mediterranean Coast (MD) subdomain comprises five small rivers and the Moroccan Highlands (MH) sub-domain includes three rivers (Moulouya, Oum-er-Rbia and Sebou).

Two additional subdomains were identified as areas of interest by Arab States and studied by SMHI, namely the Sana'a River and the Wadi Diqah. The small size of the surface water systems in the Sana'a Basin increased the uncertainty of the results, while the changing situation on the ground complicated efforts to undertake groundwater recharge analysis as initially envisioned. As for Oman, climate projections relating to Wadi Diqah were instead studied by ACSAD within the context of conducting an analysis of extreme climate events using HEC-HMS, and is presented in Chapter 5. Results for the subdomains based on the regional hydrological modelling projections are, however, available for informing further analysis upon request.

FIGURE 18: Location of subdomains identified for analysis

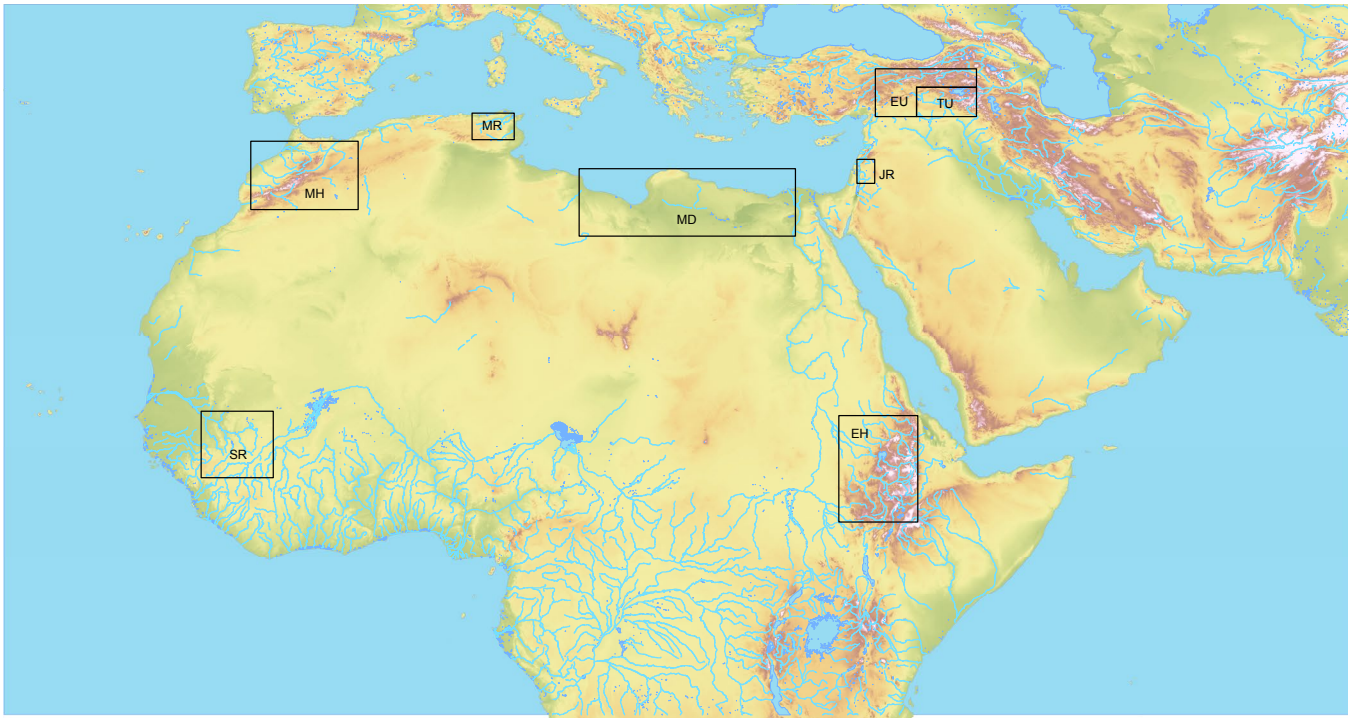

TABLE 11: List of sub-domains considered for analysis

Subdomains	Identifier	Subdomain Name	Coordinates
Selected Subdomains	MH	Moroccan Highlands	9W 1W 30N 35N
	MD	Mediterranean Coast	15E 31E 28N 33N
Shared River Basins	EH	Ethiopian Highlands (Blue Nile Headwaters)	34E 40E 7N 15N
	TU	Upper Tigris (Tigris River Headwaters)	40E 44E 37N 39N
	EU	Upper Euphrates (Euphrates River Headwaters)	37E 44E 39N 40N
	MR	Medjerda River	15E 31E 28N 33N
	JR	Jordan River	35E 37E 32N 34N
	SR	Senegal River Headwaters	12W 7W 10N 15N

ENDNOTES

1 Representing time increments at which equations in the model are resolved.

2 ESCWA, 2011; Flato et al., 2013

3 Taylor et al., 2012

4 Miao et al., 2014

5 Heavens et al., 2013; Flato et al., 2013

6 IPCC, 2013; IPCC, 2014

7 IPCC, 2014

8 Giorgi et al., 2009; WCRP, 2015a

9 Rummukainen, 2010

10 WCRP, 2015b

11 Kjellström et al., 2016; Samuelsson et al., 2011; Strandberg et al., 2014

12 Dee et al., 2011

13 Hazeleger et al., 2010

14 Voldoire et al., 2012

15 Dunne et al., 2012

16 Maraun et al., 2015

17 Klein Tank et al., 2009

18 SMHI, 2017

19 IPCC, 2015

20 For example, Kotlarski et al., 2005; Kay et al., 2006

21 For example, Graham et al., 2007; Lenderink et al., 2007

22 See Yang et al., 2010

23 See Nikulin et al., 2015

24 Bosshard et al., 2014

25 Nikulin et al., 2015. More detailed information on bias-correction methodology can be found in the sources mentioned in this section. Access to bias-corrected datasets as they become available is provided by CORDEX at: http://www.cordex.org

26 Lindström et al., 2010

27 SMHI, 2015

28 Liang et al., 1994

29 Gao, 2010 ; Devia et al., 2015

30 SMHI, 2016

31 US Army Corps of Engineers, 2000

32 SMHI, 2017

33 ESCWA et al., 2017

34 The river discharge is the arithmetic mean discharge value. The high-flow value represents the value with the 100-year return time (probability of 1% to occur or to be exceeded in any given year). The low-flow value represents the arithmetic mean value for all days with values less than the 20th percentile (if expressed in m^3/s) or the number of days with a value less than the 20th percentile in the reference period (if expressed in number of days), noting that it is equal to 73 days in the reference period.

35 Peterson, 2005; Peterson and Manton, 2008

REFERENCES

AlSarmi, S. H. and Washington, R. 2014. Changes in Climate Extremes in the Arabian Peninsula: Analysis of Daily Data. *International Journal of Climatology*, 34: p. 1329-1345.

Bosshard, T., Yang, W., Sjökvist, E., Arheimer, B., et al. 2014. Bias-correction of CORDEX- MENA Projections using the Distribution Based Scaling Method. In *European Geosciences Union General Assembly, Vienna, 27 April –2 May 2014*. Available at: http://meetingorganizer.copernicus.org/EGU2014/EGU2014-12989.pdf

Dee, D. P., Uppala, S. M., Simmons, A. J., Berrisford, P., et al. 2011. The ERA-Interim Reanalysis: Configuration and Performance of the Data Assimilation System. *Quarterly Journal of the Royal Meteorological Society*, 135: p. 553-597.

Devia, G. K., Ganasri, B. P. and Dwarakish, G. S. 2015. A Review on Hydrological Models. *Aquatic Procedia*, 4: p. 1001-1007.

Dunne, J. P., John, J. G., Adcroft, A. J., Griffies, S. M., et al. 2012. GFDL's ESM2 Global Coupled Climate–Carbon Earth System Models. Part I: Physical Formulation and Baseline Simulation Characteristics. *Journal of Climate*, 25(19): p. 6646-6665.

ESCWA (United Nations Economic and Social Commission for Western Asia). 2011. Assessing the Impact of Climate Change on Water Resources and Socio-Economic Vulnerability in the ESCWA Region: A Methodological Framework for Pursuing an Integrated Assessment. New York. Available at: https://www.unescwa.org/publications/assessing-impact-climate-change-water-resources-and-socio-economic-vulnerability-arab.

ESCWA, ACSAD and GIZ (United Nations Economic and Social Commission for Western Asia; Arab Center for the Studies of Arid Zones and Dry Lands; Deutsche Gesellschaft für Internationale Zusammenarbeit). 2017. Integrated Vulnerability Assessment: Arab Regional Applications. *RICCAR Technical Note*. Published by United Nations Economic and Social Commission for Western Asia (ESCWA). Beirut. E/ESCWA/SDPD/2017/RICCAR/TechnicalNote.2.

Flato, G., J., Marotzke, B., Abiodun, P., Braconnot, S. C., et al. 2013. Evaluation of Climate Models (Chapter 9). In *Climate Change 2013: The Physical Science Basis. Contribution of Working Group I to the Fifth Assessment Report of the Intergovernmental Panel on Climate Change*. T. F. Stocker, D. Qin, G.-K. Plattner, M. Tignor, S.K. Allen, J. Boschung, A. Nauels, Y. Xia, V. Bex and P.M. Midgley (eds). Published by Cambridge University Press, Cambridge, United Kingdom and New York, USA. Available at: https://www.ipcc.ch/pdf/assessment-report/ar5/wg1/WG1AR5_Chapter09_FINAL.pdf

Gao, H., Tang, Q., Shi,X., Zhu, C., et al. 2010. Water Budget Record from Variable Infiltration Capacity (VIC) Model. In *Algorithm Theoretical Basis Document for Terrestrial Water Cycle Data Records (in review)*.

Giorgi, F. and Gutowski, W. J. 2015. Regional Dynamical Downscaling and the CORDEX Initiative. *Annual Review of Environment and Resources*, 40(1): p. 467-490.

Giorgi, F., Jones, C. and Asrar, G. R. 2009. Addressing Climate Information Needs at The Regional Level: The CORDEX Framework. *World Meteorological Organization Bulletin*, 58: p. 175-183.

Graham, L. P., Hagemann, S., Jaun, S. and Beniston, M. 2007. On Interpreting Hydrological Change from Regional Climate Models. *Climatic Change*, 81(S1): p. 97-122.

Hazeleger, W., Severijns, C., Semmler, T., Ştefănescu, S., et al. 2010. EC-Earth: A Seamless Earth-System Prediction Approach in Action. *Bulletin of the American Meteorological Society*, 91(1357-1363).

Heavens, N. G., Ward, D. S. and Natalie, M. M. 2013. Studying and Projecting Climate Change with Earth System Models. *Nature Education Knowledge*, 4(5).

IPCC (Intergovernmental Panel on Climate Change). 2013. Climate Change 2013: The Physical Science Basis. Contribution of Working Group I to the Fifth Assessment Report of the Intergovernmental Panel on Climate Change. T. F. Stocker, D. Qin, G.-K. Plattneret al (eds). Published by Cambridge University Press. Cambridge, United Kingdom and New York, NY, USA. Available at: www.climatechange2013.org

IPCC (Intergovernmental Panel on Climate Change). 2014. Climate Change 2014: Synthesis Report. Contribution of Working Groups I, II and III to the Fifth Assessment Report of the Intergovernmental Panel on Climate Change. R. K. Pachauri and L. A. Meyer (eds). Published by Cambridge University Press. Geneva, Switzerland. Available at: https://www.ipcc.ch/pdf/assessment-report/ar5/syr/SYR_AR5_FINAL_full.pdf

IPCC (Intergovernmental Panel on Climate Change). 2015. Workshop Report of the Intergovernmental Panel on Climate Change Workshop on Regional Climate Projections and their Use in Impacts and Risk Analysis Studies In *IPCC Working Group I Technical Support Unit.* T. F. Stocker, D. Qin, G.-K. Plattner and M. Tignor (eds). Published by University of Bern. Bern, Switzerland. Available at: https://www.ipcc.ch/pdf/supporting-material/RPW_WorkshopReport.pdf

Kay, A. L., Reynard, N. S. and Jones, R. G. 2006. RCM Rainfall for UK Flood Frequency Estimation. I. Method and Validation. *Journal of Hydrology*, 318(1-4): p. 151-162.

Kjellström, E., Bärring, L., Nikulin, G., Nilsson, C., et al. 2016. Production and Use of Regional Climate Model Projections – A Swedish Perspective on Building Climate Services. *Climate Services*, 2(3): p. 15-29.

Klein Tank, A. M. G., Zwiers, F. W. and Zhang, X. 2009. Guidelines on Analysis of Extremes in a Changing Climate in Support of Informed Decisions for Adaptation. In *Climate Data and Monitoring, WCDMP-No. 72*. Published by World Meteorological Organization (WMO). Available at: http://www.ecad.eu/documents/WCDMP_72_TD_1500_en_1.pdf.

Knutti, R. and Sedláček, J. 2013. Robustness and Uncertainties In The New CMIP5 Climate Model Projections. *Nature Climate Change*, 3(4): p. 369-373.

Kotlarski, S., Block, A., Bohm, U., Jacob, D., et al. 2005. Regional Climate Model Simulations as Input for Hydrological Applications: Evaluation of Uncertainties. *Advances in Geosciences*, 5: p. 119-125.

Lenderink, G., Buishand, A. and Deursen, W. V. 2007. Estimates of Future Discharges of the River Rhine using Two Scenario Methodologies: Direct Versus Delta Approach. *Hydrology and Earth System Sciences Discussions*, 11(3): p. 1145-1159.

Liang, X., Lettenmaier, D. P., Wood, E. F. and Burges, S. J. 1994. A Simple Hydrologically Based Model of Land Surface Water and Energy Fluxes for General Circulation Models. *Journal of Geophysical Research*, 99(D7): p. 14415-14428.

Lindström, G., Pers, C., Rosberg, J., Strömqvist, J., et al. 2010. Development and Testing of the HYPE (Hydrological Predictions for the Environment) Water Quality Model for Different Spatial Scales. *Hydrology Research*, 41(3-4): p. 295-319.

Maraun, D., Widmann, M., Gutiérrez, J. M., Kotlarski, S., et al. 2015. VALUE - A Framework to Validate Downscaling Approaches for Climate Change Studies. *Earth's Future*, 3(1): p. 1–14.

Meinshausen, M., Smith, S. J., Calvin, K., Daniel, J. S., et al. 2011. The RCP Greenhouse Gas Concentrations and their Extensions from 1765 to 2300. *Climatic Change*, 109: p. 213-241.

Miao, C., Duan, Q., Sun, Q., Huang, Y., et al. 2014. Assessment of CMIP5 Climate Models and Projected Temperature Changes over Northern Eurasia. *Environmental Research Letters*, 9(5).

Nikulin, G., Bosshard, T., Yang, W., Bärring, L., et al. 2015. Bias Correction Intercomparison Project (BCIP): An Introduction and the First Results. Geophysical Research Abstracts Vol. 17. In *European Geosciences Union General Assembly, Vienna, 12 – 17 April 2015*. Available at: http://www.meteo.unican.es/en/node/73279 (Abstract).

Peterson, T. C. 2005. Climate Change Indices. *World Meteorological Organization Bulletin*, 54(2).

Peterson, T. C. and Manton, M. J. 2008. Monitoring Changes in Climate Extremes: A Tale of International Collaboration. *Bulletin of the American Meteorological Society*, 89(9): p. 1266-1271.

Rummukainen, M. 2010. State-of-the-art with Regional Climate Models. *Climate Change*, 1(1): p. 82-96.

Samuelsson, P., Jones, C. G., Willen, U., Llerstig, A. U., et al. 2011. The Rossby Centre Regional Climate Model RCA3: Model Description and Performance. *Tellus*, 63(A): p. 4-23.

SMHI (Swedish Meteorological and Hydrological Institute). 2015. HYPE. Available at: http://www.smhi.se/en/research/research-departments/hydrology/hype-1.7994

SMHI (Swedish Meteorological and Hydrological Institute). 2016. Regional Hydrological Modelling using the HYPE and VIC Models. Presented at the Expert Peer Review of the RICCAR Integrated Assessment Findings, ESCWA, Beirut, 6-9 December 2016. Available at: http://www.smhi.se/en/research/research-departments/hydrology/hype-1.7994

SMHI (Swedish Meteorological and Hydrological Institute). 2017. Regional Climate Modelling and Regional Hydrological Modelling Applications in the Arab Region. *RICCAR Technical Note*. Published by United Nations Economic and Social Commission for Western Asia (ESCWA). Beirut. E/ESCWA/SDPD/2017/RICCAR/TechnicalNote.1.

Strandberg, G., Bärring, L., Hansson, U., Jansson, C., et al. 2014. CORDEX Scenarios for Europe from The Rossby Centre Regional Climate Model RCA4. In *Reports Meteorology and Climatology Vol 116*. Available at: http://www.smhi.se/polopoly_fs/1.90273!/Menu/general/extGroup/attachmentColHold/mainCol1/file/RMK_116.pdf.

Taylor, K. E., Stouffer, R. J. and Meehl, G. A. 2012. An Overview of CMIP5 and the Experiment Design *Bulletin of the American Meteorological Society*, 93: p. 485–498.

US Army Corps of Engineers. 2000. Hydrologic Modeling System (HEC-HMS). Available at: http://www.hec.usace.army.mil/software/hec-hms/.

Voldoire, A., Sanchez-Gomez, E., Salas y Mélia, B., Decharme, B., et al. 2012. The CNRM-CM5.1 Global Climate Model: Description and Basic Evaluation. *Climate Dynamics*, 40: p. 2091–2121.

WCRP (World Climate Research Programme). 2015a. The Coordinated Regional Downscaling Experiment (CORDEX). Available at: http://www.cordex.org/index.php/community/domains.

WCRP (World Climate Research Programme). 2015b. Region 13: Middle East North Africa (MENA). Available at: http://www.cordex.org/index.php/domain-mena-cordex.

Yang, W., Andréasson, J., Graham, P., Olsson, J., et al. 2010. Improved Use of RCM Simulations in Hydrological Climate Change Impact Studies. *Hydrology Research*, 41: p. 211–229.

REGIONAL CLIMATE MODELLING:
ARAB DOMAIN

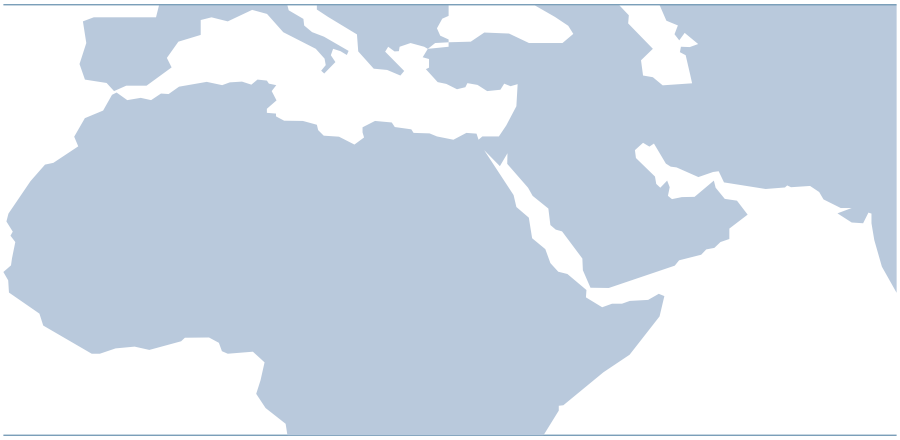

CHAPTER 2

REGIONAL CLIMATE MODELLING RESULTS FOR THE ARAB DOMAIN AND SELECTED SUBDOMAINS

The bias-corrected RCM output presented in this chapter includes temperature, precipitation and selected extreme events indices expressed in terms of change from the reference period. Most results are for the entire Arab Domain or as plotted time-series showing area means summarized over two representative subdomains of special interest, namely the Moroccan Highlands and the Mediterranean Coast. The selection of specific subdomains (presented in Chapter 1) aimed to provide more distinct indicative information over certain areas of interest, including shared river basins. RCM results pertaining to shared river basins are presented alongside their regional hydrological modelling outputs in Chapter 4.

Regional climate modelling outputs were generated by SMHI using the RCA4 model, forced at its boundaries by three state-of-the-art GCMs, namely EC-Earth, CNRM and GFDL-ESM. An average of the three-model output ("ensemble") was derived for RCP 4.5 and RCP 8.5 for the various climate variables up to the end of the 21st century at a horizontal resolution of 50 x 50 km. Due to limited space, selected outputs are presented in this report. Additional results are available in the Technical Annex and online through the regional knowledge hub. As discussed in Chapter 1, the results for temperature are more certain than those for precipitation because the precipitation change signals are correlated more with the driving GCM rather than the emission scenario.

2.1 PROJECTED CHANGE IN CLIMATE ACROSS THE ARAB DOMAIN

2.1.1 Change in temperature

Maps of projected temperature changes (compared to the reference period 1985–2005) over the Arab Domain for the different time periods and the two RCP scenarios are presented in Figure 19. As can be seen, all projections show that temperatures will rise over the Arab region during this century. The general change in temperature for RCP 4.5 shows an increase of 1.2 °C–1.9 °C at mid-century and 1.5 °C– 2.3 °C by end-century. For RCP 8.5, temperatures increase to 1.7 °C–2.6 °C for mid-century and 3.2 °C–4.8 °C towards end-century.

The range of these values represents the variation in results according to different areas in the region. The higher increase at mid-century is shown in the non-coastal areas, with the greatest changes projected in the Sahara Desert. By the end of the century, the increasing change in temperature becomes much more evident throughout the Arab domain. The areas showing higher increases are the broader Sahara region and East Africa, including Morocco and Mauritania. For this period, the increasing temperature signals along the western shores of Yemen and Saudi Arabia under RCP 8.5 are also stronger than under RCP 4.5 in comparison with the rest of the Arabian Peninsula.

Al Ramaa Mountain, Yemen, 2005. Source: Ihab Jnad.

When focusing on seasonal changes, results show no evident tendency for temperature to increase more during one particular season of the year (not shown). The warming is more or less evenly distributed over all seasons. For some areas, there is a larger projected increase in the winter season (e.g. Senegal river headwaters) and for others the summer season sees larger increases (e.g. Tigris river headwaters) which are presented in detail in Chapter 4. However, it seems apparent that for most countries along the Mediterranean, the increase during summer will be larger than during winter.

FIGURE 19: Mean change in annual temperature (°C) for mid- and end-century for ensemble of three RCP 4.5 and RCP 8.5 projections compared to the reference period

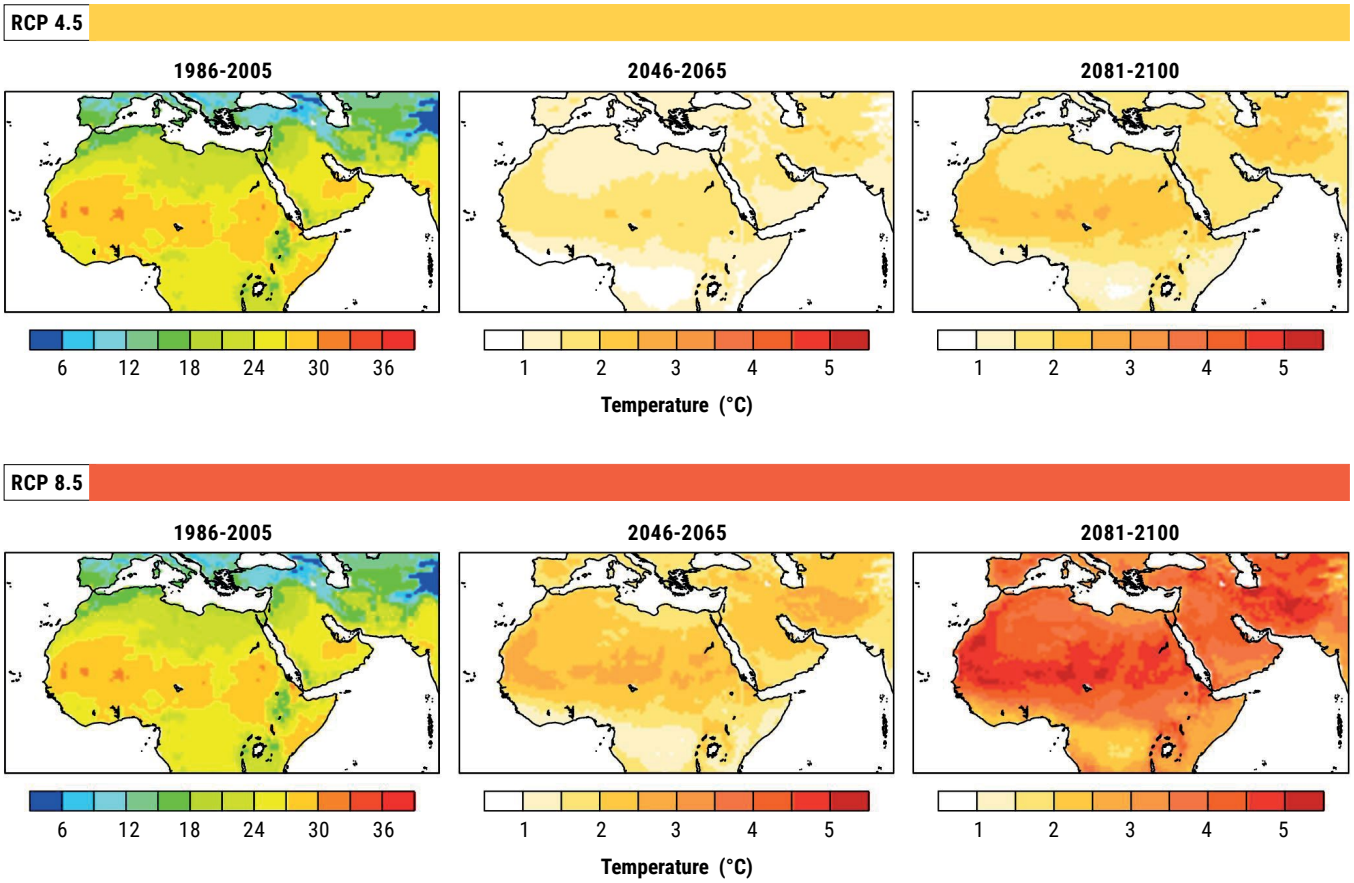

Figure 20 depicts the projected temperature change over the 21st century, averaged over the Arab Domain based on the reference period 1986–2005 and as a 30-year moving average. In agreement with the global and other regional simulations, the different paths of the two RCP emission scenarios start diverging around mid-century. The projected change in temperatures starts becoming discernible for the two scenarios after 2030–2040. As can be seen, all projections are in agreement that temperatures will rise over the Arab region during the next century.

FIGURE 20: Change in mean temperature (°C) over time for the Arab Domain as a 30-year moving average for six individual climate projections

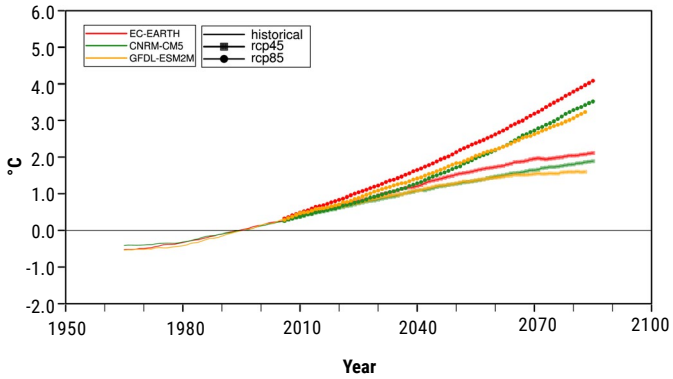

2.1.2 Change in precipitation

As precipitation is much more variable over the domain, there is little benefit to present the area mean time series over the entire Arab Domain in the same way that was done for temperature. This type of figure is more useful when rainfall is averaged over smaller subregions. Such time-series plots are presented in more detail in the following sections of the report.

The maps in Figure 21 show the spatial extent of projected precipitation change over the Arab region averaged for the three-member ensemble, for the mid- and end-21st century sub-periods, considering the two RCP emissions scenarios. Precipitation changes vary considerably across the Arab Domain with no universal trend for annual results as well as

at the seasonal level. Decreasing trends can be seen in most of the Arab region at mid-century. By the end of the century, both scenarios suggest a reduction of the average monthly precipitation reaching 8–10 mm in the coastal areas of the Arab Domain, mainly around the Atlas Mountains in the west and upper Euphrates and Tigris rivers in the east. Some areas, however, show increasing precipitation trends, such as the south-eastern Arabian Peninsula and some parts of the Sahel. This pattern is potentially due to the displacement of the ITCZ bringing precipitation and which, according to several studies tends to move further northwards in response to warming.[1] As increasing temperatures are projected in these areas, this projected precipitation trend concords with this hypothesis.

At the seasonal level (Figure 22 and Figure 23), the stronger precipitation changes for countries along the Mediterranean coast are projected for the winter months and will be negative, as much as –40% in the worst case for the Moroccan Highlands. For this area, a number studies have confirmed the strong influence of the North Atlantic Oscillation (NAO) on precipitation variability in Morocco, and these results are in line with the fact that a positive NAO is associated with reduced rainfall in Morocco in the boreal winter season (December–February).[2] Further south, rainfall changes are more pronounced during the summer months, while the sign of change varies from west to east.

Erosion of river banks in Morocco,2015. Source: Heribert Rustige.

FIGURE 21: Mean change in annual precipitation (mm/month) for mid- and end-century for ensemble of three RCP 4.5 and RCP 8.5 projections compared to the reference period

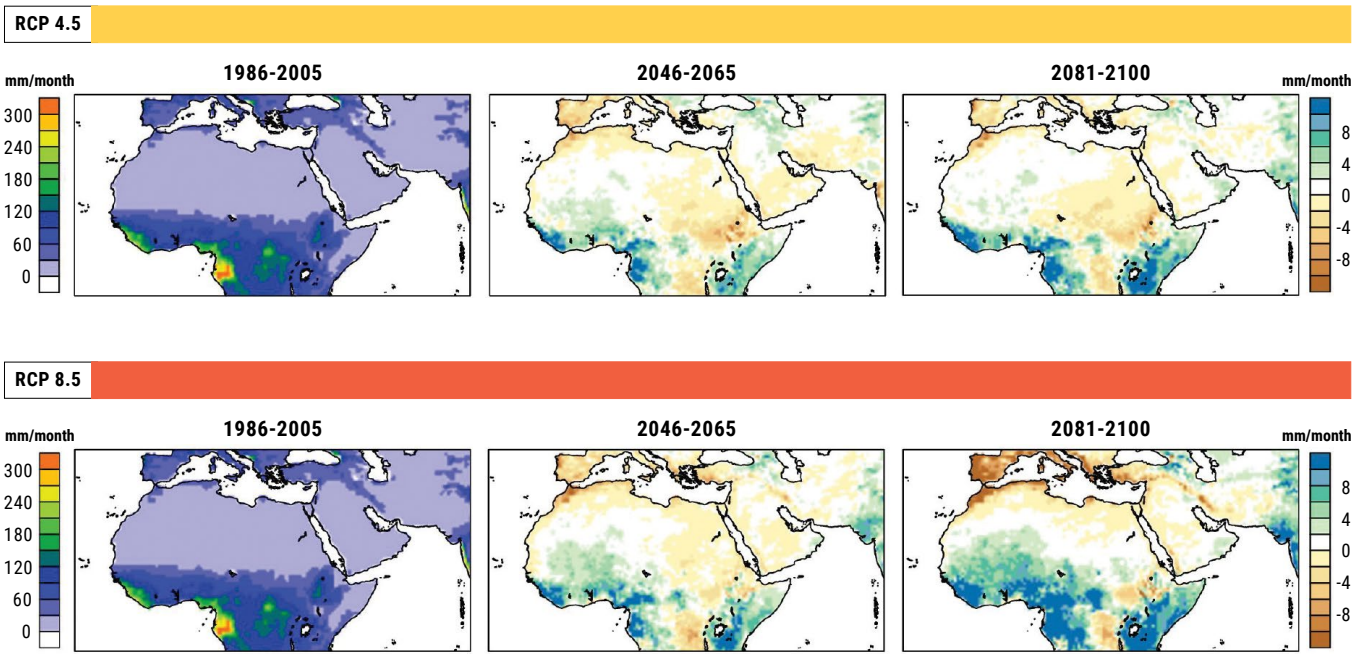

FIGURE 22: Mean change in seasonal precipitation for mid- and end-century for ensemble of three RCP 4.5 projections compared to the reference period

RCP 4.5

APR-SEP

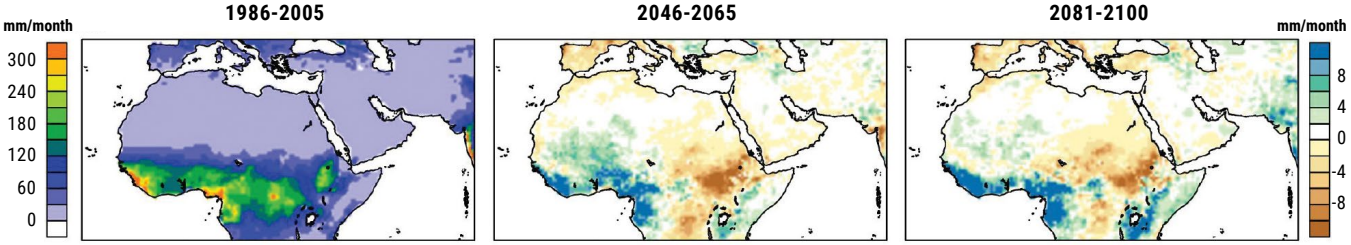

OCT-MAR

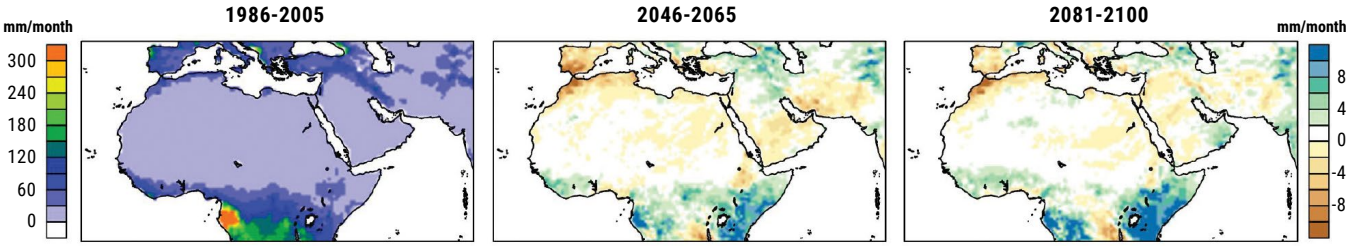

FIGURE 23: Mean change in seasonal precipitation for mid- and end-century for ensemble of three RCP 8.5 projections compared to the reference period

RCP 8.5

APR-SEP

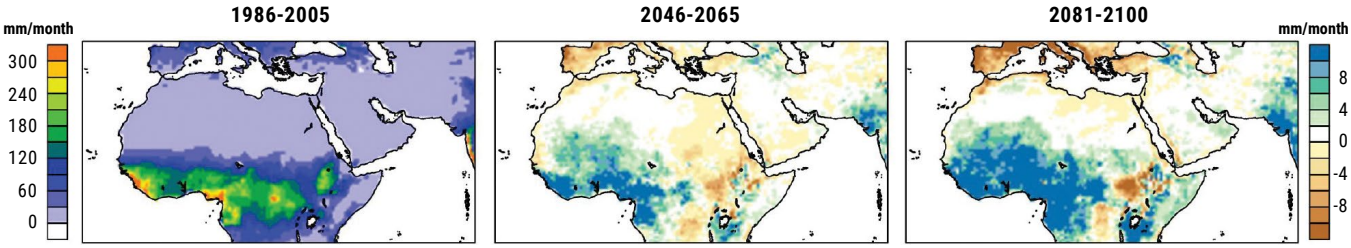

OCT-MAR

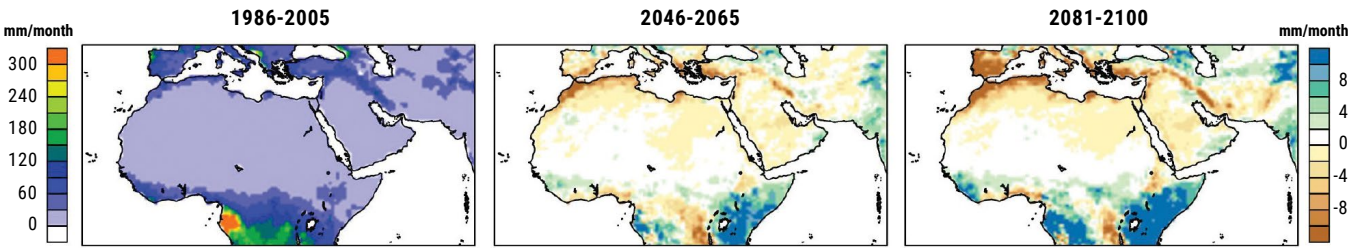

FIGURE 24: Agreement on mean change in annual precipitation from the reference period between the ensemble of three RCP 4.5 and three RCP 8.5 projections for mid- and end-century

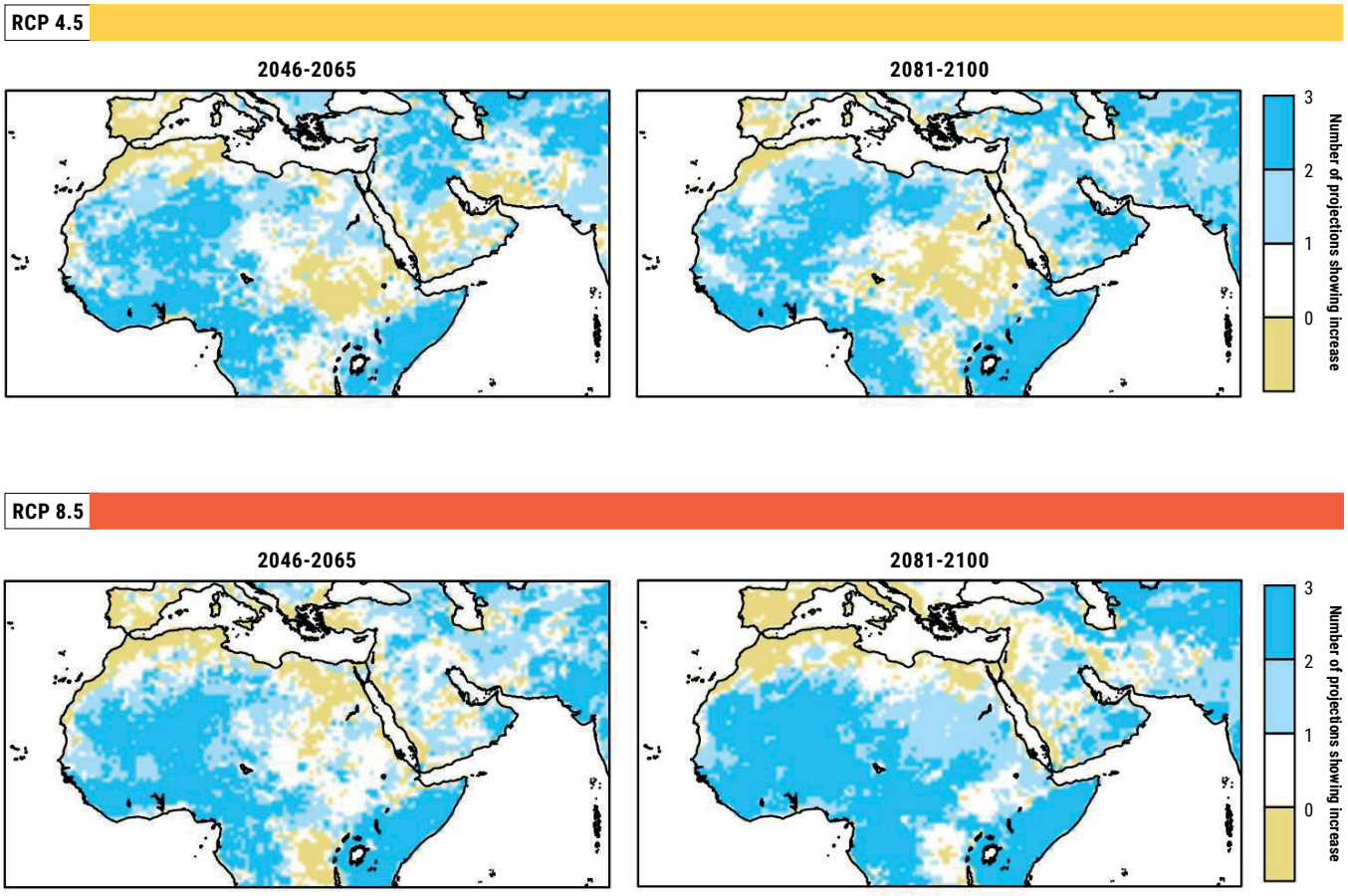

Note: Brown indicates where all ensemble projections agree on a decrease in precipitation, dark blue indicates where all agree on an increase in precipitation, white indicates where two of three projections show a decrease and light blue indicates where two out of three projections show an increase.

Figure 24 indicates where the three ensemble members are in agreement regarding positive or negative change in annual precipitation. This inter-model agreement (disagreement) can be used as a measure of high (low) robustness for the climate change signal.

As can be seen, projections agree on a decrease of rainfall in the Atlas Mountains region, mostly accentuated at mid-century (for both scenarios) and for RCP 8.5 at end-century. For the latter period and scenario, an agreement on a decrease in precipitation is evident for the coastal Mashreq area and for the coastal areas of the Arabian Peninsula along the Red Sea.

Agreement on the projected increases of precipitation appears in various patterns in the Arabian Peninsula across time periods and scenarios such as in the south-eastern Arabian Peninsula and the Sahel.

Sharjah, United Arab Emirates, 2013. Source: Khajag Nazarian.

2.1.3 Changes in extreme temperature indices

Overall, looking at the extremes for temperature, all of the indices relating to hot days show increasing trends as expected. Changes in both the number of hot days (SU35) and the number of very hot days (SU40) show generally larger increases than the number of summer days (SU). The latter finding is not surprising as the number of summer days for present climate is already high over most of the region.

For these indices, the RCP 8.5 scenario at the end of the century stands out as a particularly harsh change for living conditions. This holds for the number of tropical nights (TR) as well, which indicates dwindling chances that there will be a cooler evening after a hot day. The hot days (SU35) indicator shows a particularly strong warming along the Mediterranean coast for eastern Libya and Egypt.

The results towards the end of the century for SU35 (Figure 26) show significant warming trends for both scenarios reaching an increase of up to 80 days in the southern Arabian Peninsula and on the western coast of Africa for the RCP 8.5 emission scenario. Changes for the SU40 indicator (Figure 27) show strong projected warming in the Sahara and central Arabian Peninsula areas for RCP 8.5, indicating that the increase in the extreme temperature on coastal areas would be lower than the inland areas of the region for both scenarios.

As compared to the baseline period, the TR indicator exhibits significant warming trends over time with a projected increase mainly in central Africa and southern Arabian Peninsula regions, particularly for RCP 8.5. According to the literature, there are indications that night-time temperature extremes in the Arabian Peninsula are potentially affected by the Indian Ocean sea-surface temperatures.[3]

This index has considerable implications with regards to cropping systems, as some crops require a substantial difference in temperature between day and night. Furthermore, increased night-time temperatures can also affect human and animal health conditions since it is more difficult for their organisms to recover after a very hot day or a spell of warm days (e.g. heatwave events).

FIGURE 25: Mean change in the number of summer days (SU) (days/yr) for mid- and end-century for ensemble of three RCP 4.5 and RCP 8.5 projections compared to the reference period

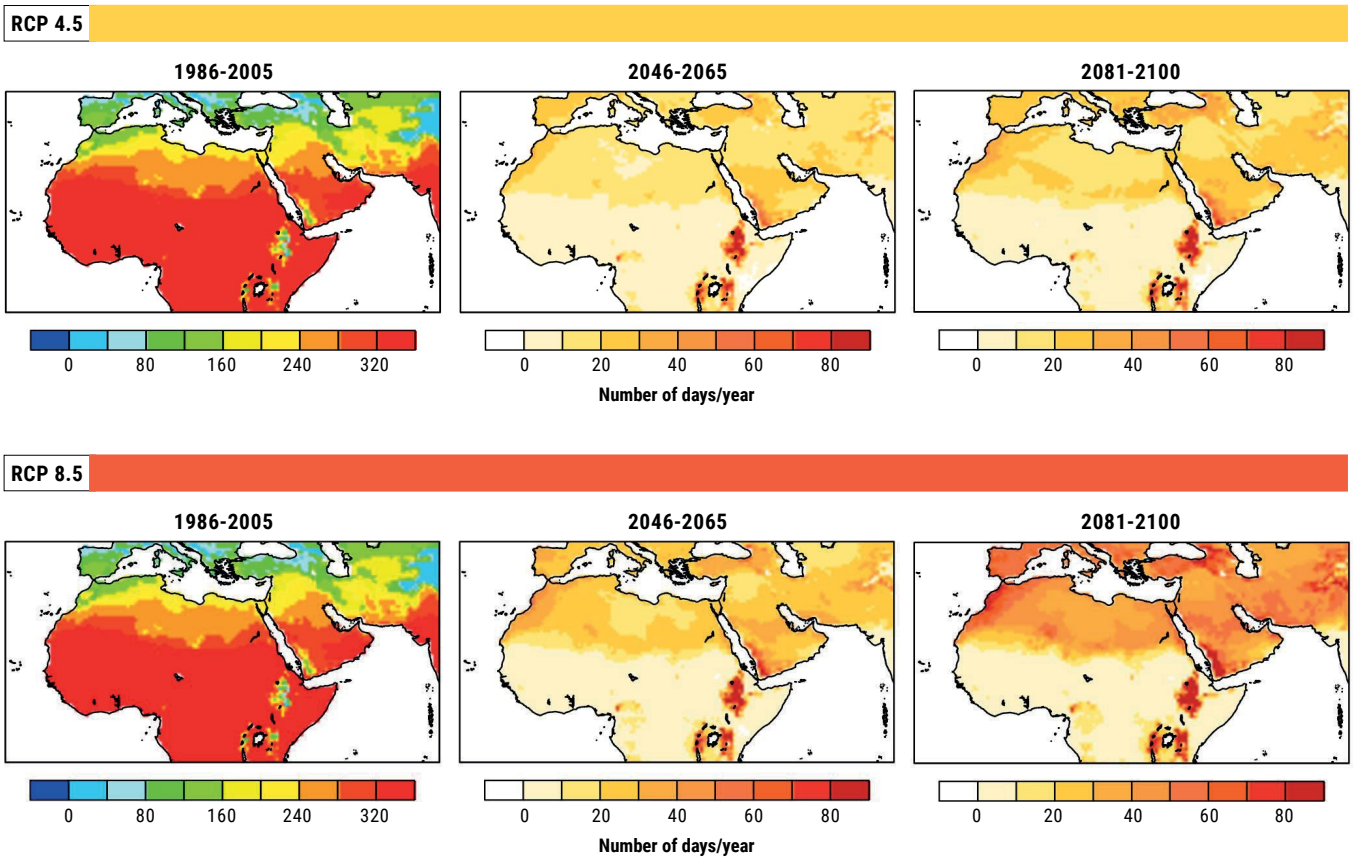

FIGURE 26: Mean change in the number of hot days (SU35) (days/yr) for mid- and end-century for ensemble of three RCP 4.5 and RCP 8.5 projections compared to the reference period

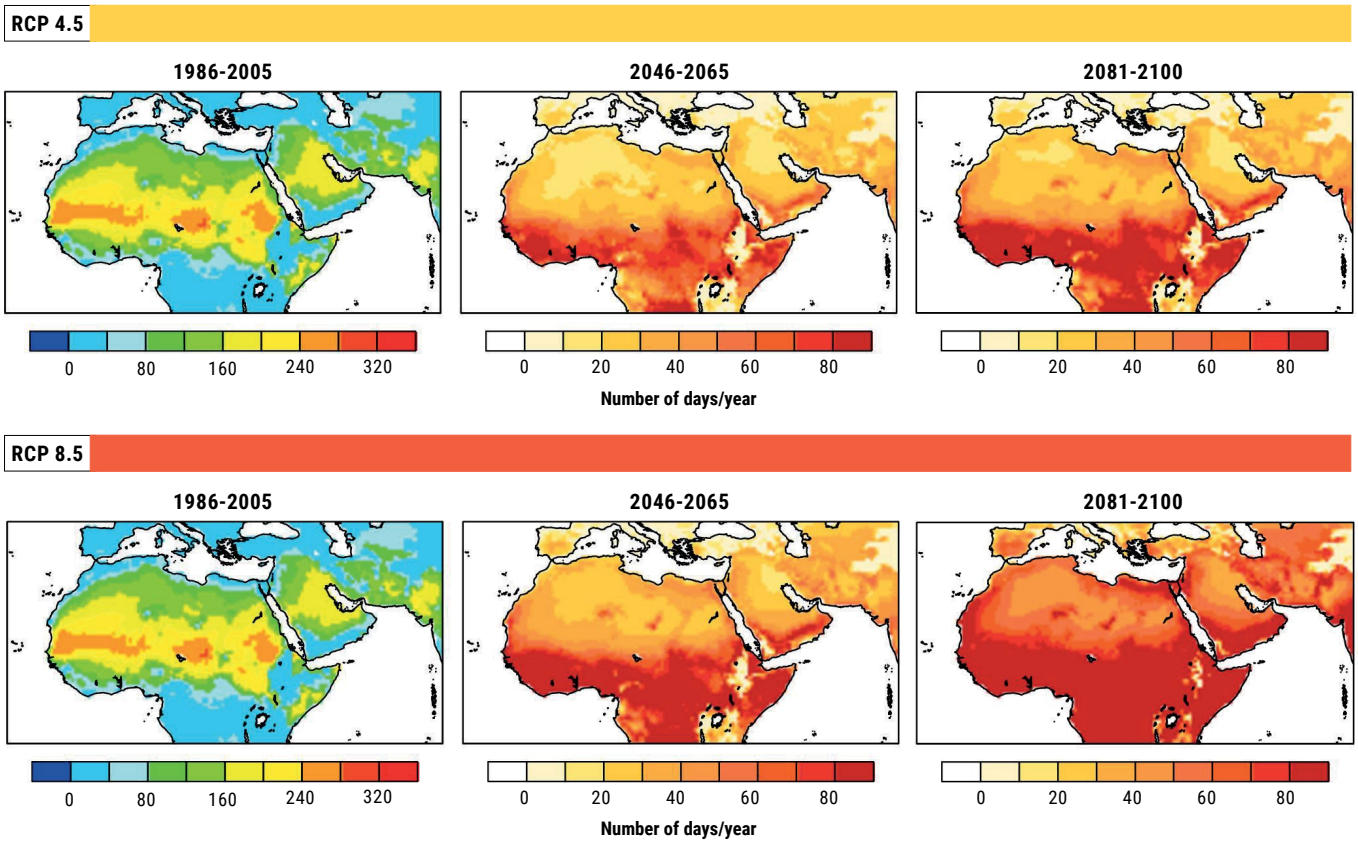

FIGURE 27: Mean change in the number of very hot days (SU40) (days/yr) for mid- and end-century for ensemble of three RCP 4.5 and RCP 8.5 projections compared to the reference period

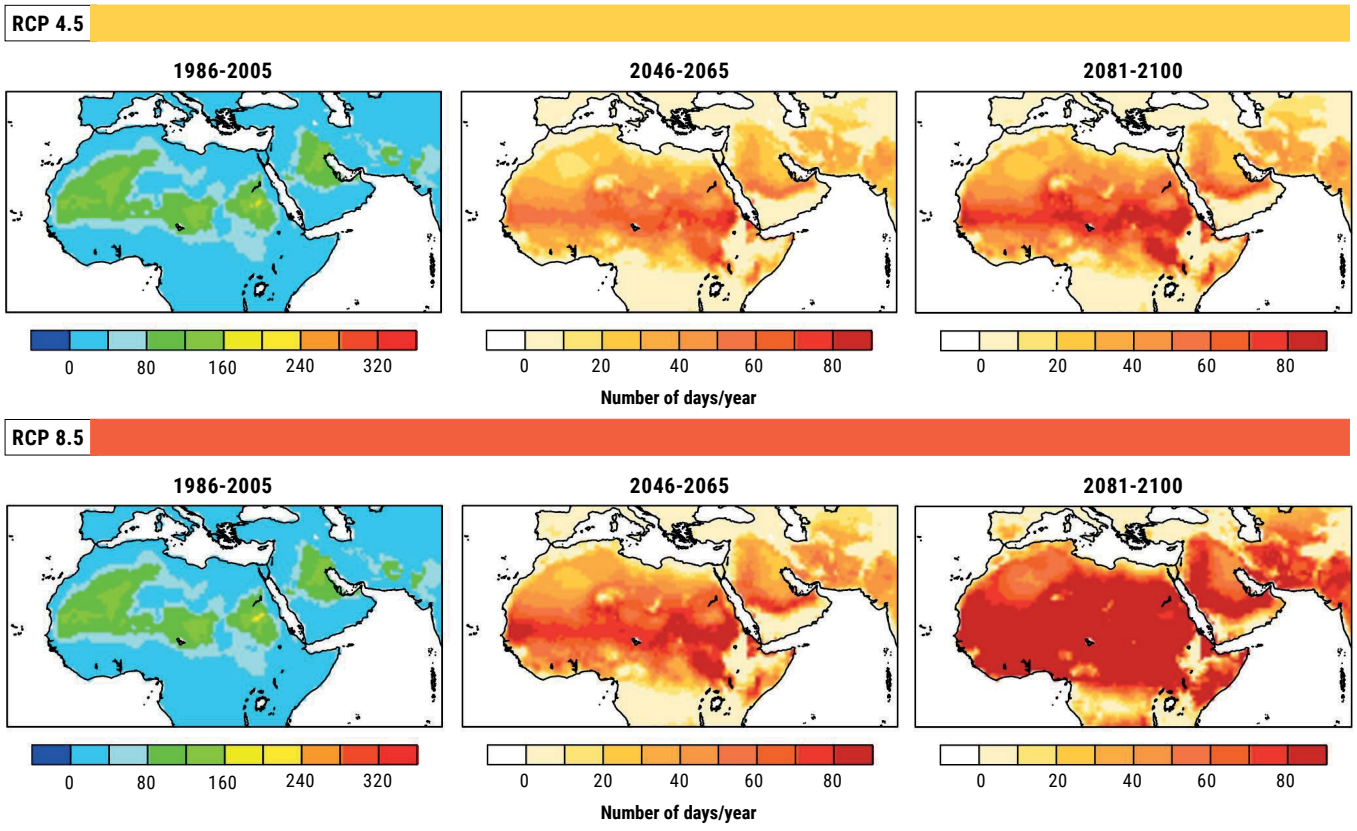

FIGURE 28: Mean change in the number of tropical nights (TR) (days/yr) for mid- and end-century for ensemble of three RCP 4.5 and RCP 8.5 projections compared to the reference period

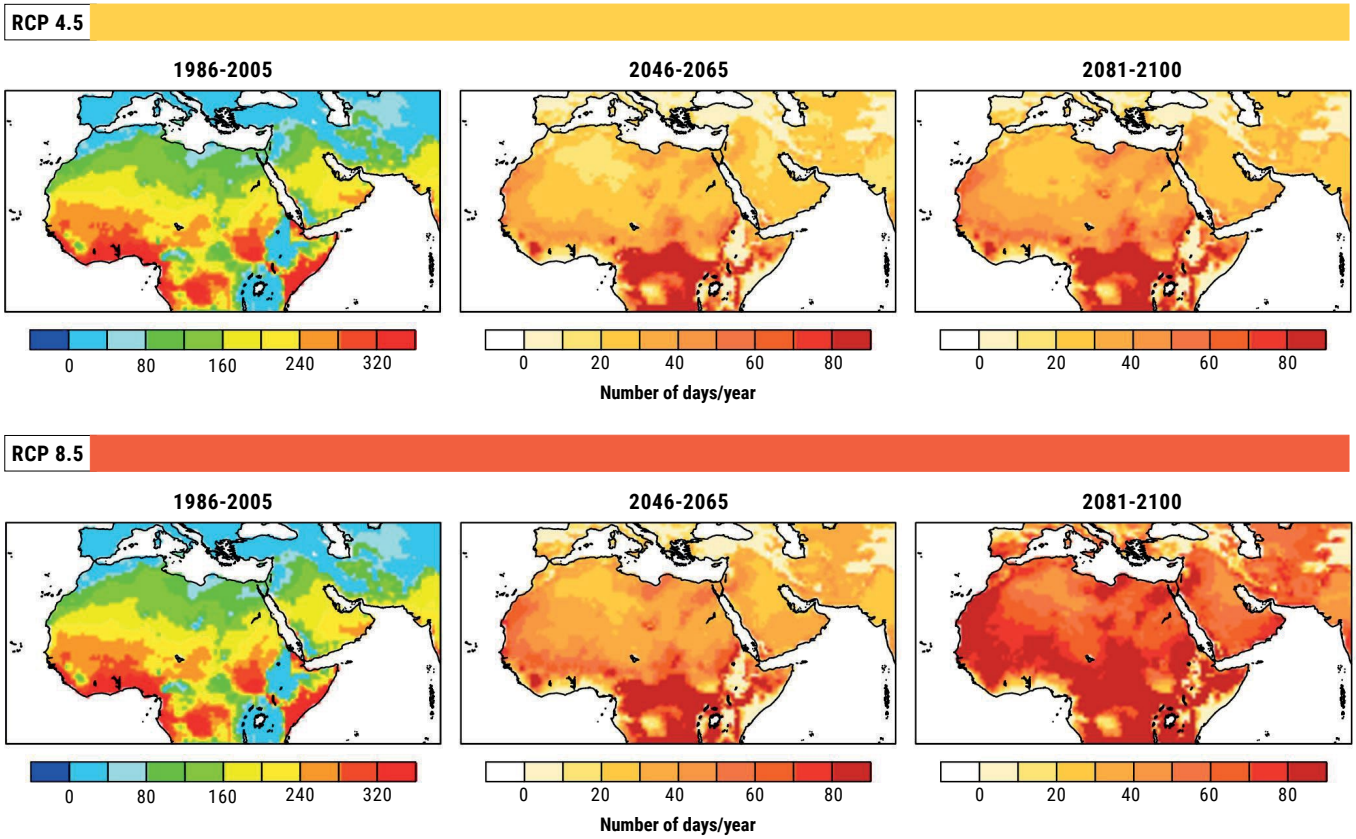

2.1.4 Changes in extreme precipitation indices

Regarding precipitation extremes, there is considerable variation over the region. The projections for the maximum length of dry spell (CDD) suggest trends towards drier conditions with an increase in the number of consecutive dry days specifically for the Mediterranean, as well as the western and northern parts of the Arabian Peninsula by the end of the century (Figure 29). Changes in the length of dry spells are expected to be more significant under the RCP 8.5 scenario and towards the end of the century. The increases in CDD can be an indication that the dry summer season is likely to be extended in length, especially in the aforementioned regions. Some areas in the central and eastern part of North Africa show a decline in CDD. In all cases, results for this indicator ought to be complemented with additional information, since an indication of a shorter dry period does not rule out an increase in drought frequency occurring at the same time.

Changes in the annual number of 10 mm precipitation days (R10) indicate decreasing trends over time compared to the baseline period (Figure 31). Similarly, results for the annual number of 20 mm precipitation days (R20) (Figure 32) for the end of the century are similar to the R10 index, suggesting a projected overall reduction in rainy days with these intensities over the region.

The simple precipitation intensity index (SDII) in Figure 33 shows increasing trends across the majority of the region for all the climate projections, except for the Moroccan Highlands, which stands out as the only one where all projections showed a decreasing trend.

Storm in Beirut, Lebanon, 2014. Source: Carol Chouchani Cherfane.

FIGURE 29: Mean change in the maximum length of dry spell (CDD) (days/yr) for mid- and end-century for ensemble of three RCP 4.5 and RCP 8.5 projections compared to the reference period

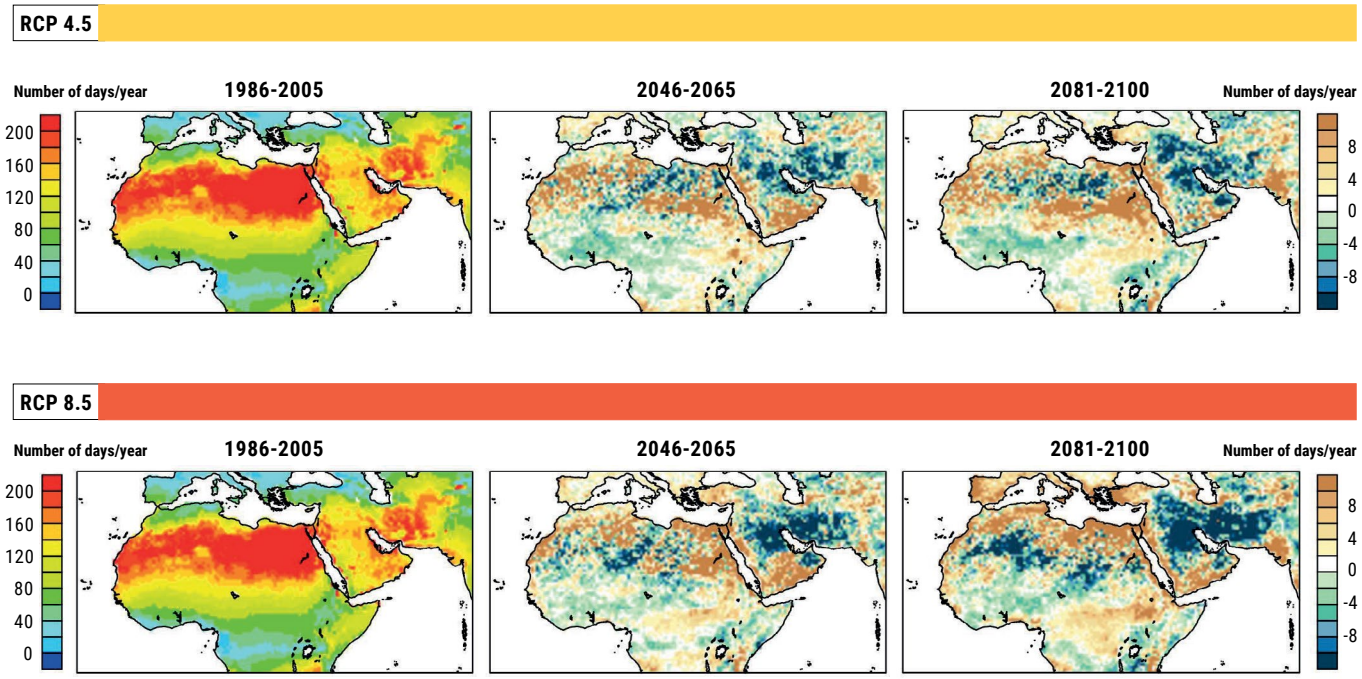

FIGURE 30: Mean change in the maximum length of wet spell (CWD) (days/yr) for mid- and end-century for ensemble of three RCP 4.5 and RCP 8.5 projections compared to the reference period

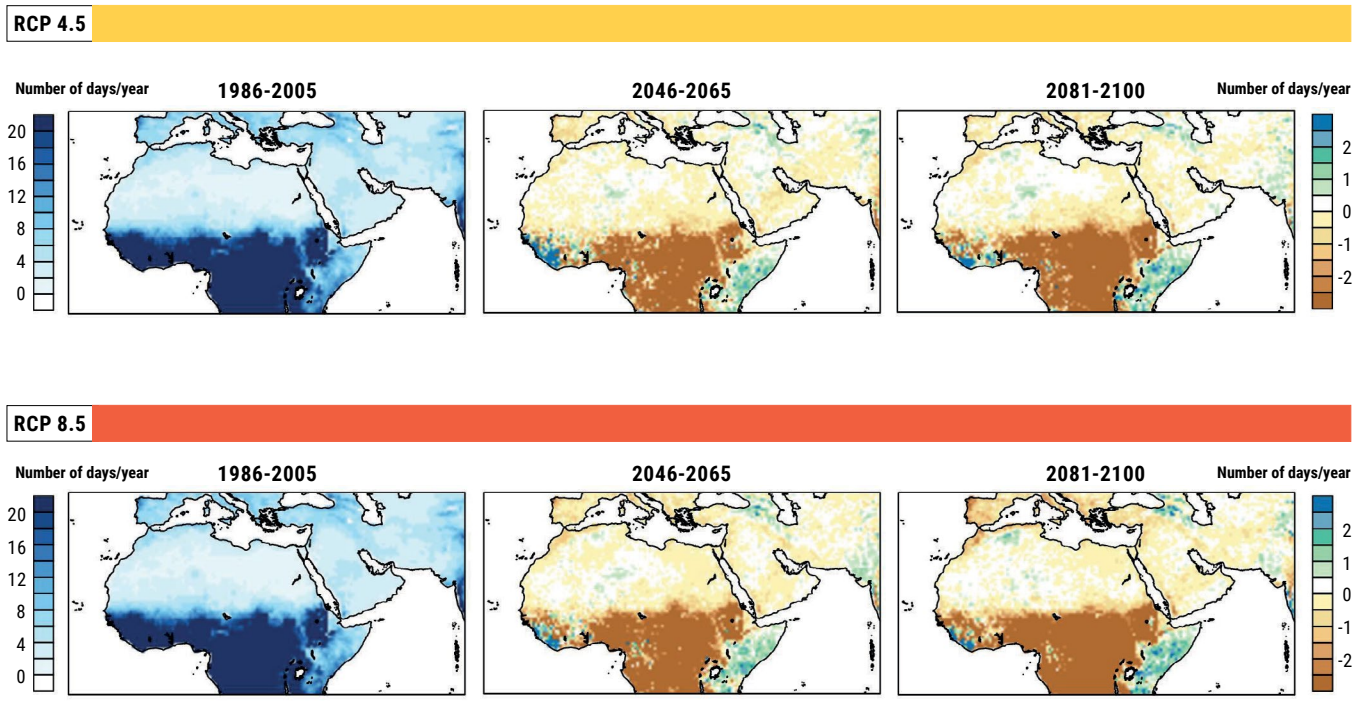

FIGURE 31: Mean change in the number of 10 mm precipitation days (R10) (days/yr) for mid- and end-century for ensemble of three RCP 4.5 and RCP 8.5 projections compared to the reference period

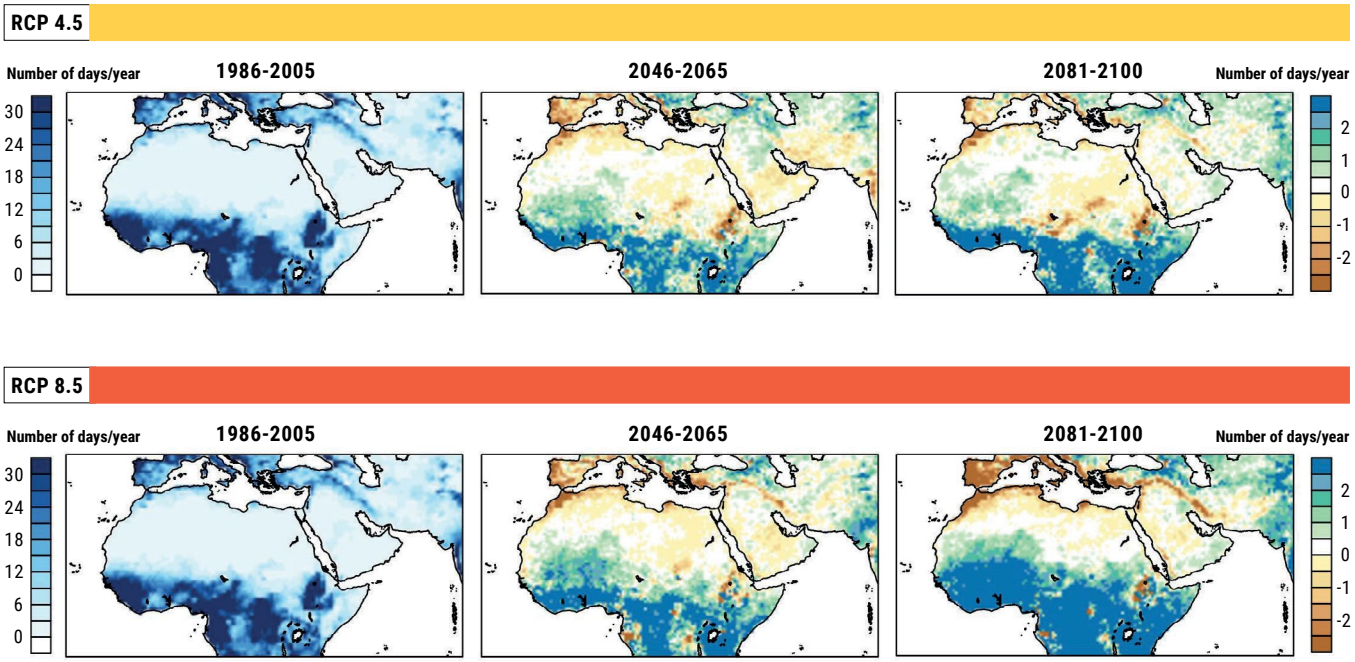

FIGURE 32: Mean change in the number of 20 mm precipitation days (R20) (days/yr) for mid- and end-century for ensemble of three RCP 4.5 and RCP 8.5 projections compared to the reference period

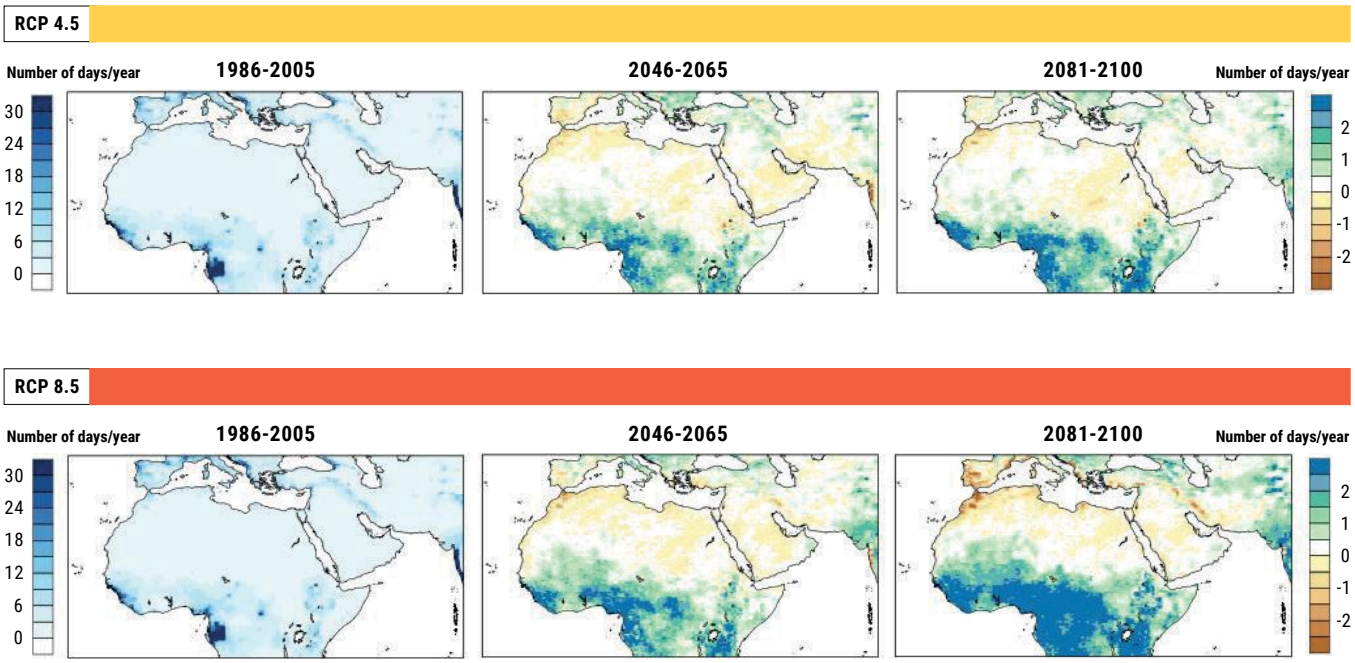

FIGURE 33: Change in the Simple Precipitation Intensity Index (SDII) (mm) for mid- and end-century for ensemble of three RCP 4.5 and RCP 8.5 projections compared to the baseline period

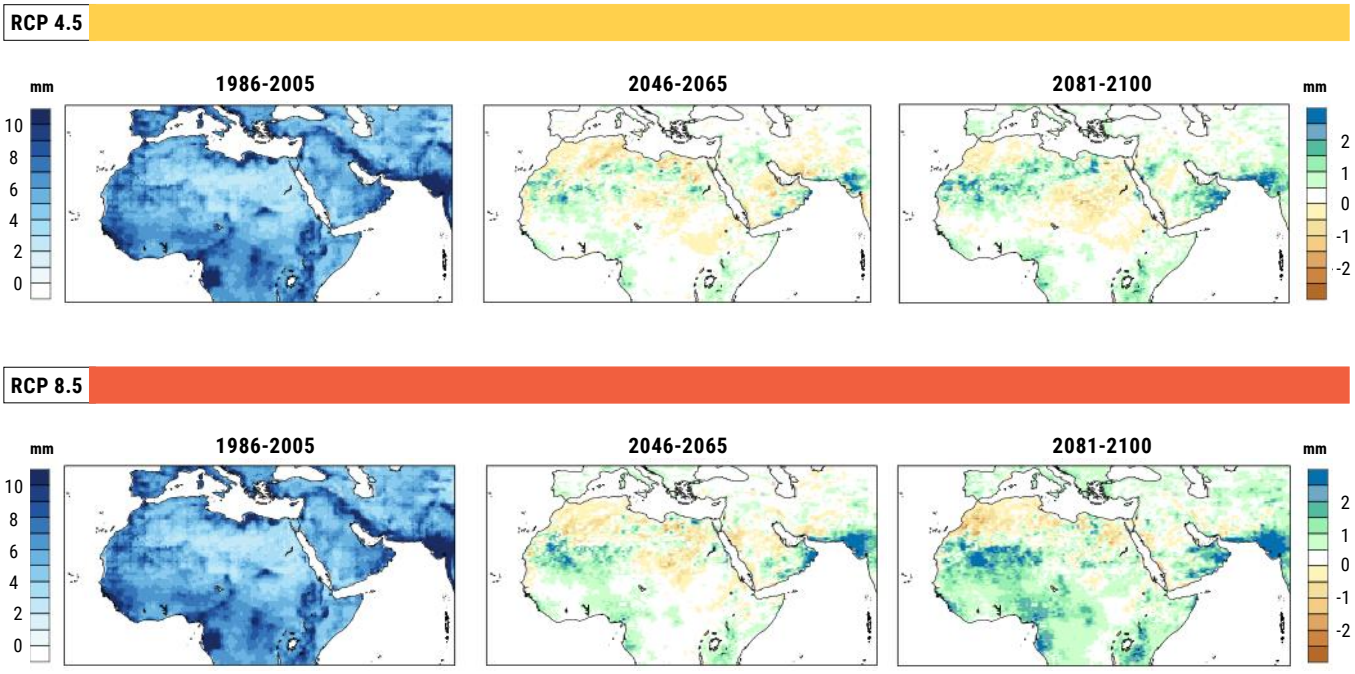

2.2 COMPARATIVE ANALYSIS WITH OTHER REGIONAL CLIMATE MODELLING ASSESSMENTS

2.2.1 IPCC AR5 findings relating to Arab States

Temperature and precipitation projections from the IPCC AR5 are based on a global synthesis output from around 40 GCMs CMIP5 simulations, most of them performed by independent modelling groups. In addition to the focus and discussion mainly of global results (which was the case for the previous reports), IPCC adopted a more systematic regional assessment that was presented in the Atlas of Global and Regional Climate Projections (annex in AR5).[4] This regionalized climate change assessment effort was based purely on the output of global models and no statistical or dynamical downscaling methods were considered.
The corresponding Arab region as defined in RICCAR is encompassed in five of these subregions as shown in Figure 34, namely: South Europe/Mediterranean (MED), Sahara (SAH), West Africa (WAF), East Africa (EAF) and West Asia (WAS). Model projections reveal warming in all seasons in the different subregions under consideration, while precipitation projections are more variable and show some distinct subregional and seasonally dependent changes. The summary of outputs for the different scenarios and time periods presented hereafter are based on the 50th per centile (median) of the CMIP5 ensemble distribution.

In terms of temperature, projections for RCP 4.5 at mid-century suggest an increase of about 2 °C for most of the Arab region, except for the areas of southern Algeria and the central part of the Arabian Peninsula which, according to this scenario, will experience an increase of 3 °C. The projected warming is stronger at end-century compared to the baseline period (overall increase of 3 °C), with the exception of the southern coastal fringe of the Arabian Peninsula (2 °C warming). Projections for RCP 8.5 at mid-century are spatially similar to the RCP 4.5 scenario at the same time period, but with an additional 1 °C temperature increase overall. By end-century, the warming clearly intensifies with a 5 °C increase in temperature in North Africa compared to the reference period, 7 °C in Algeria and Morocco, 5 °C in the Mashreq area and Arabian Peninsula and reaching 7 °C in Iraq and Saudi Arabia.[5]

According to the IPCC, confidence levels for temperature projections for these subregions indicate that it is very likely that all of Africa will continue to warm during the 21st century. The overall quality of the CMIP5 models implies that the Sahara region, which is already hyper-arid, is likely to remain under this regime. There is, however, lower confidence in projection statements about the drying of West Africa.

FIGURE 34: Spatial boundaries of the geographical regions used in the IPCC 5th Assessment Report

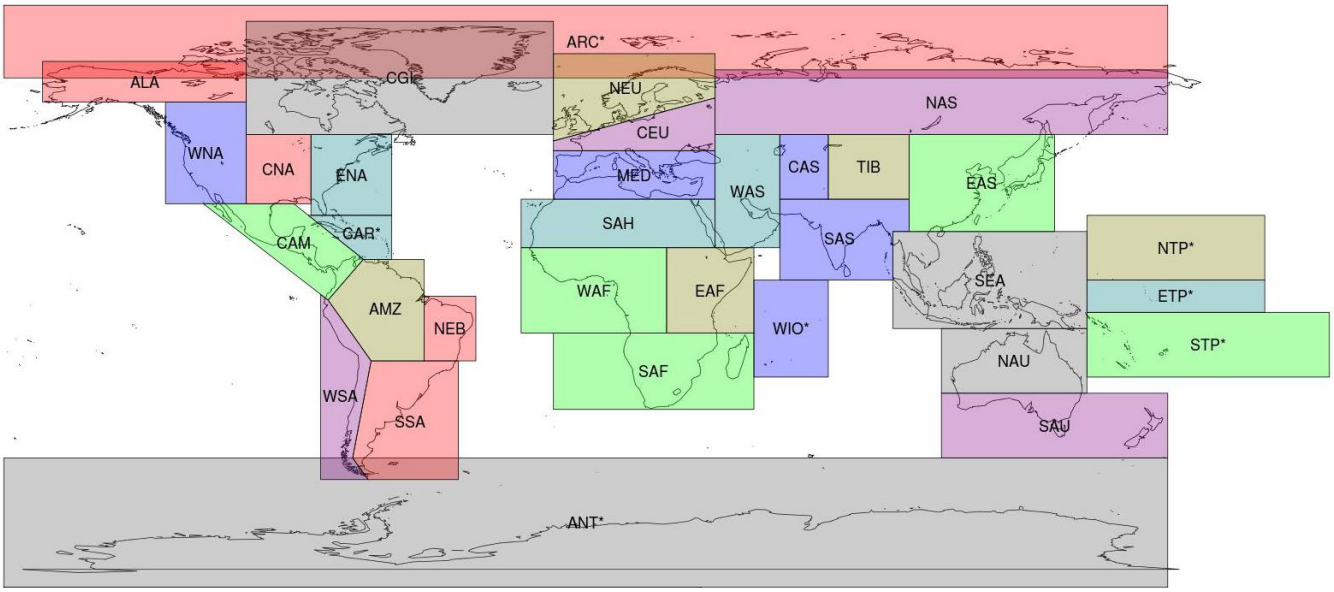

Source: IPCC, 2015

Model agreement for West Asia and for the Mediterranean subregions indicate the likelihood that temperatures will continue to increase throughout the 21st century. Moreover, the length, frequency and/or intensity of warm spells or heatwaves were assessed as being likely to increase throughout the whole Mediterranean region.[6]

Results are much more spatially and temporally variable in terms of precipitation. Projections for the RCP 4.5 scenario at mid-century exhibit decreases in precipitation of about 10% over the Mediterranean, Sahara, Mashreq region and most of the Arabian Peninsula, with a more pronounced reduction (up to 20%) in areas of Morocco, Algeria and Mauritania. This projected decline of up to 20% also spreads over all North Africa at the end of the 21st century. On the other hand, increases in precipitation of up to 10% are projected for mid-century in Sudan, Somalia, north-eastern Saudi Arabia and the southern part of the Arabian Peninsula. According to the CMIP5 models, this increase will likely become widespread over most of the Arabian Peninsula by end-century. Under the business-as-usual RCP 8.5 scenario, the northern African coast, Mauritania and Mashreq will likely experience more dramatic decreases in precipitation compared to the baseline period (up to 20% for mid-century and 30%–40% for end-century), while increases are projected in central Africa for mid-century and intensify when moving south (up to 20% increase) and towards end-century (up to 40%). The major part of the Arabian Peninsula also exhibits increases in precipitation at mid-century (10%) which intensifies at end-century in central and southern parts, but shows decreases of up to 10% in the northern part over this sub-period.[7]

Interestingly, in the AR5 Regional Atlas and over subregions of Africa, the overall confidence in the projected precipitation changes is characterized, in the best case, as only medium, due to the overall limited ability of models to adequately represent the important local phenomena that have a strong influence on African climates. At the seasonal level, African subregions are projected to receive unaltered precipitation by 2081–2100 in the boreal winter half of the year (October to March), although somewhat elevated in RCP 8.5, and little change is projected in the six-month summer season. As for the West Asia subregion, there is medium confidence in projected changes showing an overall reduction in precipitation. At the seasonal level, precipitation in general is projected to decrease in both winter and summer. However, the various interacting dynamical influences on precipitation of the region (that models have varying success in capturing in the current climate) results in uncertainty in both the patterns and magnitude of future precipitation change. Most of the Mediterranean subregion exhibits a likely and notable decrease in summer mean precipitation, while no change or moderate reduction is projected in the winter half of the year.[8]

2.2.2 Findings from other corresponding climate projections

Other climate modelling projections have been undertaken for the CORDEX MENA region as part of a study by Lelieveld et al., 2016, using an ensemble of 26 CMIP5 model output for RCP 4.5 and RCP 8.5 comparing similar mid- and end-century time slices based on the baseline period 1986–2005.

A robustness check to evaluate the level of model agreement indicated that the models consistently project strong temperature changes, whereas precipitation results are much less consistent. In accordance with RICCAR results, model projections suggest that there is a clear projected warming with more marked increases for RCP 8.5 and that climate warming in the region is much stronger in summer than winter. Regarding temperature extremes, the indices studied were different than those selected in RICCAR but exhibit the same warming trends with increasing trends in heat extremes, in particular for the number of warm days and nights. It was shown that, on average, the maximum temperature during the hottest days in the recent past was about 43 °C, which could increase to about 46 °–47 °C by mid-century and would reach nearly 50 °C by the end of century for scenario RCP 8.5. The warm spell duration index (WSDI), which is an indication of present-day heatwaves, is projected to increase steeply from about 16 days in the reference period to 83–118 days by mid-century to more than 200 days by the end of the century for RCP 8.5. Additionally, while the coldest nights (TNn) in the reference period can be below frost point, temperatures turn positive in the first half of the century, increasing further to more than 4 °C by the end of the century for RCP 8.5. Based on these projections, there is an increasing risk that part of the region may become inhabitable for some species, including humans, at least for the warmer months of the year.[9]

The Atmospheric and Climate Modelling group of the Cyprus Institute has recently produced regional climate simulations for the Arab region using a climate version of the Weather Research and Forecasting (WRF) model forced by a bias-corrected version of NCAR's global Community Earth System Model (CESM1).[10] Projected changes of temperature suggest a general warming throughout the Domain. As expected from the climate scenarios used, this temperature increase is higher towards the end of the 21st century and under the business-as-usual RCP 8.5. For the reference period (1986–2005), all local temperature patterns were found to be consistent in both CYI-WRF and RICCAR-RCA4 simulation experiments, which was also evident for the projected changes with comparable results for the warming magnitude range and general spatial patterns. Locally, some discrepancies were apparent, particularly in the location of the hotspots of temperature climate change which are found to have slightly shifted northwards for the WRF simulations over North Africa. Such discrepancies are expected, however, due to the fact that the two regional models have substantial differences, while they are also forced by different global models. Projected rainfall changes have shown that reference period precipitation was in general agreement with the RCA4 simulations of RICCAR. Although not relevant for this study, WRF over parts of the Tropics is wetter than RCA4. Nevertheless, rainfall regimes over the arid and semi-arid parts of the Arab Domain were consistent between the two modelling experiments. Since precipitation is a more challenging variable to be modelled, local discrepancies between the RICCAR and CYI simulations were found. For example, the wetter conditions projected by RCA4 for the northern part of the Domain (more evident for mid-century and RCP 4.5 scenario) were not in agreement with WRF. RCA4 also indicates a slight precipitation increase over the southern Arabian Peninsula of the winter half of the year which was not evident in the WRF simulations. Nevertheless, the global models are also found to disagree on the sign of change over the particular region.[11]

As for other corresponding domains which overlap with the CORDEX-MENA Domain, a number of climate projection studies have been performed on related CORDEX domains such as CORDEX-AFRICA[12] (see following section), EURO-CORDEX[13] and Central Asia[14]. Most of the published East Asia and MEDCORDEX domain studies are, at the time of writing, dedicated to model optimization, evaluation and sensitivity experiments.

Apart from studies focusing on different CORDEX domains that encompass parts of the Arab region, model simulations have also been carried out on areas coinciding with the Arab Domain and are overall consistent with RICCAR projections (see Box 4).

2.2.3 Findings from CORDEX MENA compared to CORDEX AFRICA

Results obtained from CORDEX-MENA were compared to CORDEX-AFRICA simulations, that have a partially overlapping domain (25W–60E, 7S–42N). Because CORDEX-AFRICA data are not bias-corrected, only the RCM outputs from both datasets were analysed. An ensemble for end-century was obtained for CORDEX-AFRICA based on nine differing GCMs at 50-km resolution.

CORDEX-AFRICA outputs were subtracted from CORDEX-MENA outputs and show that, throughout the region, the change in temperature is generally higher for the CORDEX-AFRICA ensemble with an increase up to 1.1 °C noted in North Africa and the Arabian Peninsula. Differences generally decrease from the coastline towards the inland parts of North Africa (Figure 35). This is somehow expected, as parts of the common domain that exhibit the larger discrepancies between the two sets of simulations are located near the edges of one of the two CORDEX domains (e.g. the Tropics or Mediterranean Coast of Africa) and are thus strongly affected by the regional models' buffer zone. The range of the RICCAR CORDEX-MENA simulations is determined by obtaining the minimum and maximum values

between the three ensemble members. For most of the extent of the common domain, one to six of the nine CORDEX-Africa models are within range of the CORDEX-MENA ensemble (Figure 36). Areas with low differences in temperature have better agreement, such as the Atlantic coast and Sahara Desert, where nearly all CORDEX-AFRICA models are within range. Conversely, areas with large differences in temperature have no agreement for range, for example the Tigris-Euphrates basin for RCP 8.5. Worthy of note is that areas where the CORDEX-AFRICA projections are out of the range of the CORDEX-MENA ones are of very limited extent, highlighting the confidence in the RCA4 projections used in this report.

FIGURE 35: Comparison between CORDEX MENA and CORDEX AFRICA outputs for temperature change at end-century

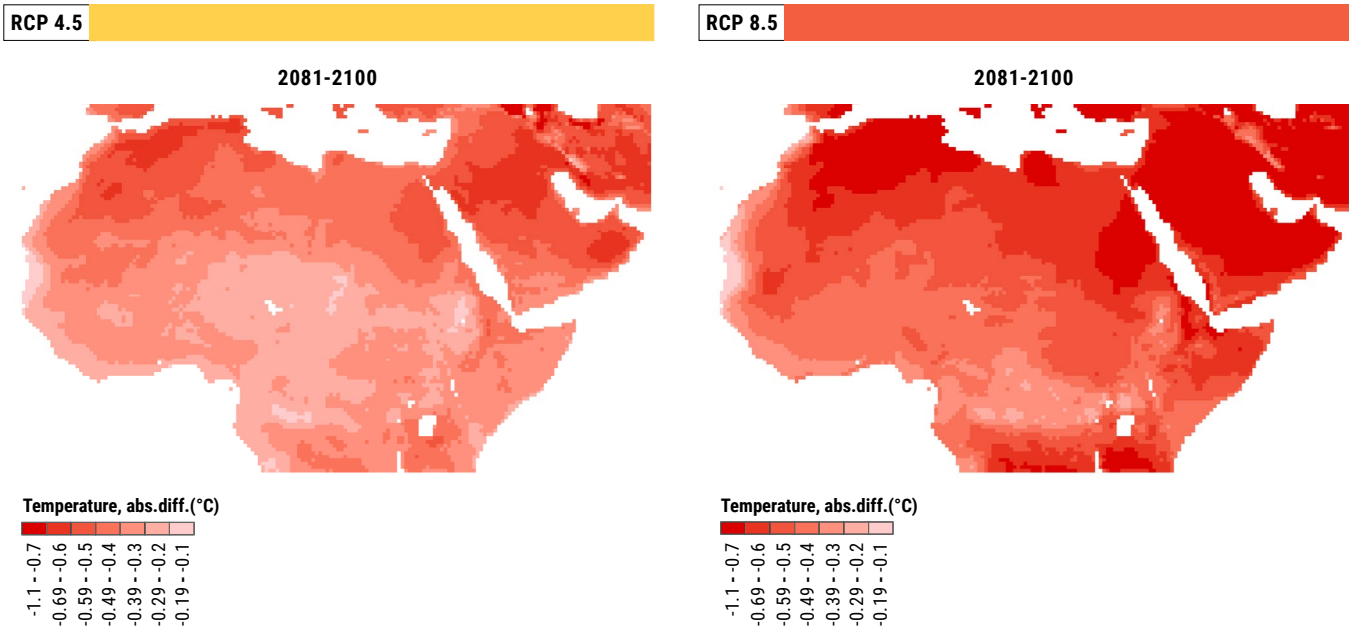

FIGURE 36: Number of CORDEX AFRICA models within the range of CORDEX MENA models for temperature at end-century

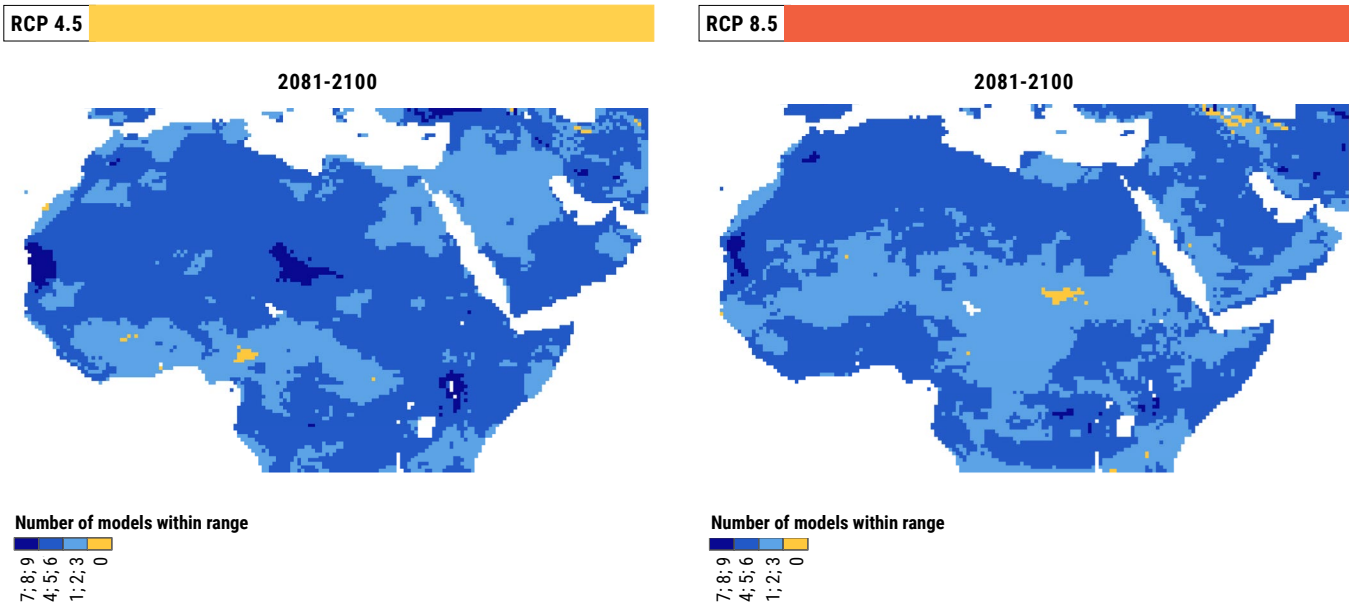

Similar to temperature, differences in precipitation values are determined by subtracting CORDEX- AFRICA from CORDEX-MENA. However, for both ensembles, the data are first normalized by the reference period. Precipitation values tend to be greater for the south-western Arabian Peninsula and sub-Saharan Africa. On the other hand, CORDEX-MENA values tend to be greater in the south-eastern Arabian Peninsula and the Sahara Desert (Figure 37). Nevertheless, these regions are characterized by very low precipitation amounts.

The range of results obtained from the CORDEX-MENA ensemble was also compared to CORDEX AFRICA and the range was determined by the minimum and maximum value obtained from the CORDEX MENA ensemble. Values were normalized by the reference period. Results show that, overall, one to six of the nine models were in agreement. As with temperature, limited areas, spread throughout the common domain are found with low or no agreement (Figure 38).

FIGURE 37: Comparison between CORDEX MENA and CORDEX AFRICA outputs for precipitation change at end-century

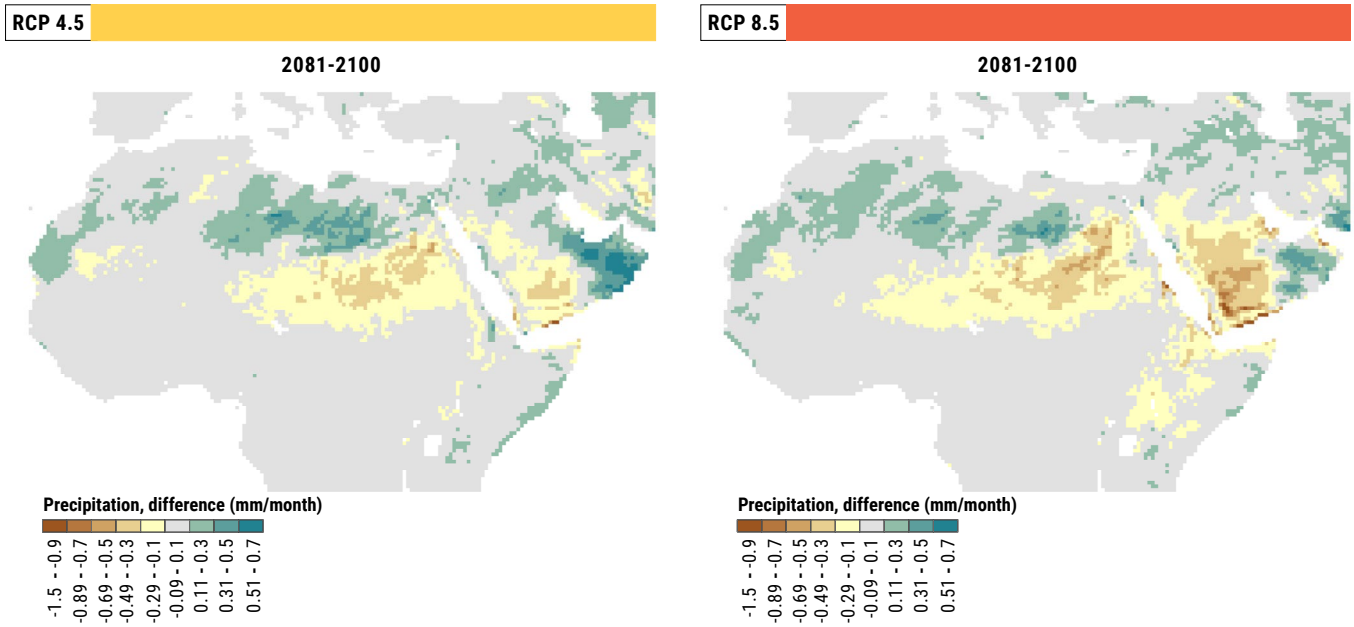

FIGURE 38: Number of CORDEX Africa models within the range of CORDEX MENA models for precipitation at end-century

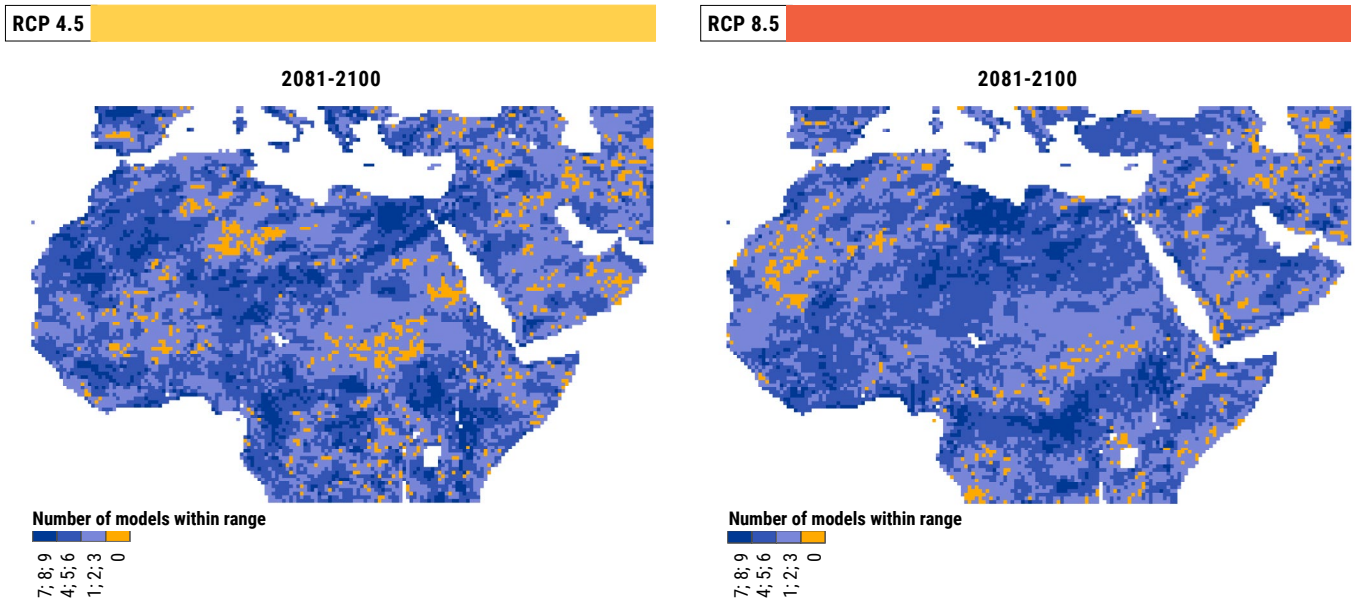

Although this evaluation considered end-century only, it is assumed that similar trends will emerge for mid-century. Because a comparison was conducted using RCM output, it is also assumed that differences in values will be greatly reduced if DBS ensemble output is compared.

BOX 4: ALADIN-Climate projections for the Arab region

A set of climate simulations conducted by Direction de la Météorologie Nationale of Morocco (DMNMOR) assess future climate change over the Arab region using the climate version of the Aire Limitée Adaptation dynamique Développement InterNational (ALADIN) or ALADIN-Climate Model, at a horizontal resolution of 50 km.[15] This dynamic regional climate model follows the same physical characteristics as the general circulation model ARPEGE–Climate[16] used in the CMIP5 exercise (an atmospheric model of CNRM-CM5). It is a bi-spectral RCM with a semi-implicit, semi-lagrangian advection scheme and its configuration includes an 11-point wide bi-periodization zone in addition to the more classical 8-point relaxation zone. ALADIN comprises the Fouquart and Morcrette radiation scheme (FMR15)[17] based on the European Centre for Medium Range Forecasts (ECMWF) model, incorporating effects of greenhouse gases (CO_2, CH_4, N_2O and CFC) and direct effects of aerosols, as well as the first indirect effect of sulphate aerosols. The vertical discretization of this RCM is 31 levels mostly located in the troposphere with a time step of 15 minutes.

Version 5 of ALADIN-Climate was used in this work, as was the case within the framework of MedCORDEX. Version 4 of the RCM was used for the European ENSEMBLES project where it was inter-compared with several European RCMs at 50-km and 25-km resolution,[18] and was also used for the assessment of future climate changes over Morocco.[19]

TABLE 12: Description of simulations

Institute	Model	Resolution	Driving model	Driving experiment	Period
DMN-MOR	ALADIN	0.44°	CNRM-CM5	CNRM-CM5	1971–2005
DMN-MOR	ALADIN	0.44°	CNRM-CM5	RCP 4.5	2006–2100
DMN-MOR	ALADIN	0.44°	CNRM-CM5	RCP 8.5	2006–2100

Three simulations have been carried out by ALADIN-Climate with a horizontal resolution of 50 km driven by CNRM-CM5 (see Table 12).[20] The historical simulation covers the period 1971–2005. The other two were run under the two emission scenarios RCP 4.5 and RCP 8.5 over the period 2006–2100. The full spatial domain (including the Davies relaxation zone) for the RCM is illustrated in Figure 39, noting that the area considered for analysis (red rectangle) coincides with the CORDEX-MENA Domain.

Future changes in the Arab region climate have been assessed by calculating a set of climate change indices covering both mean and extreme aspects, namely the annual mean temperature, the heatwave duration index[21], the annual total rainfall amount and the annual maximum number of consecutive dry days.[22] Figure 40 and Figure 41 show the future changes stemming from ALADIN-Climate for the different variables under RCP 4.5 and RCP 8.5, respectively. The changes are calculated for the future period 2036–2065 compared to the reference period 1971–2000.

FIGURE 39: Spatial extent of the Domain considered using ALADIN-Climate

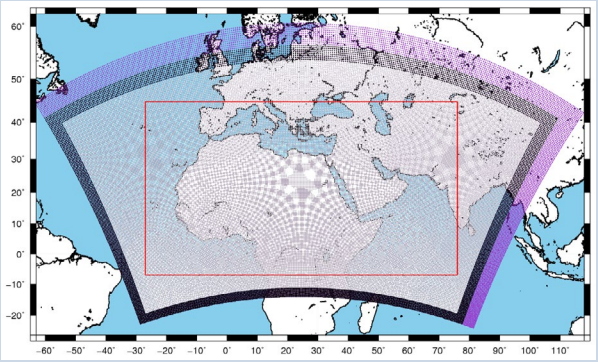

Note: the area within the red rectangle includes the entire Arab region and was considered for analysis.

FIGURE 40: Future changes in different variables from ALADIN-Climate projections for RCP 4.5 for the future period 2036–2065 compared to the reference period 1971–2000

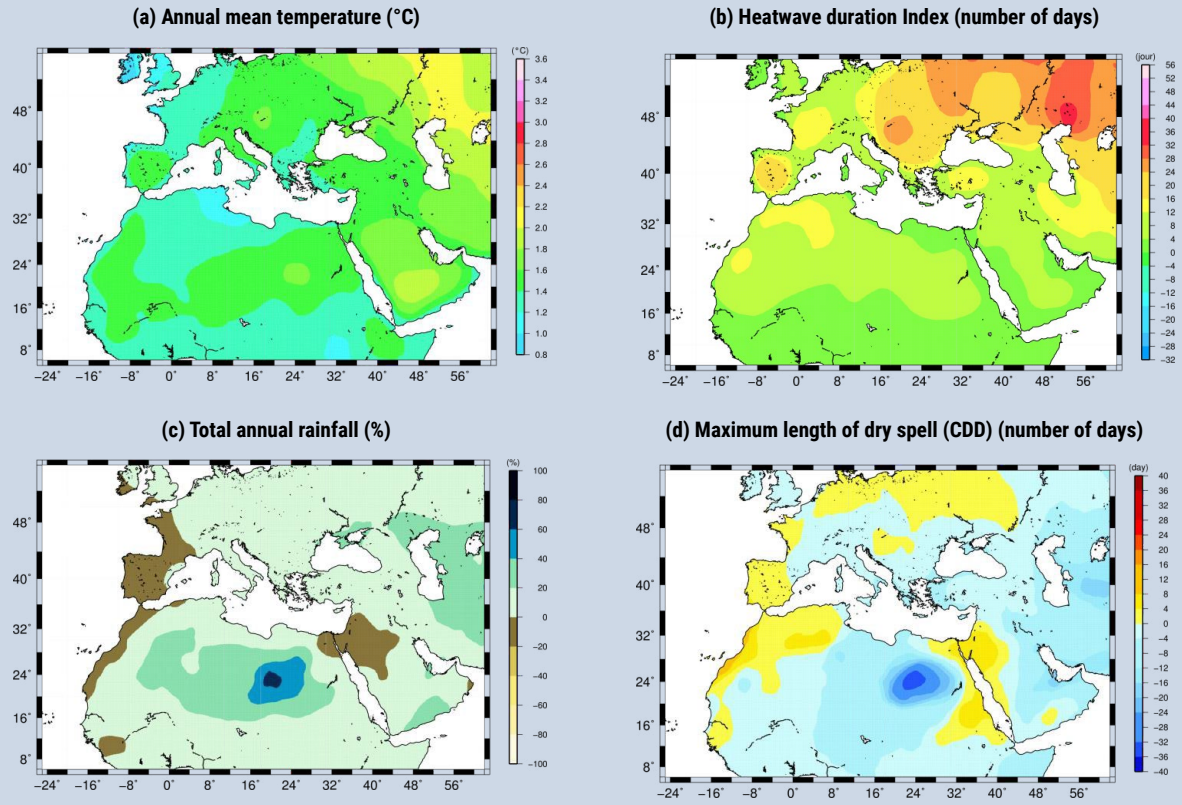

FIGURE 41: Future changes in different variables from ALADIN-Climate projections for RCP 8.5 for the future period 2036–2065 compared to the reference period 1971–2000

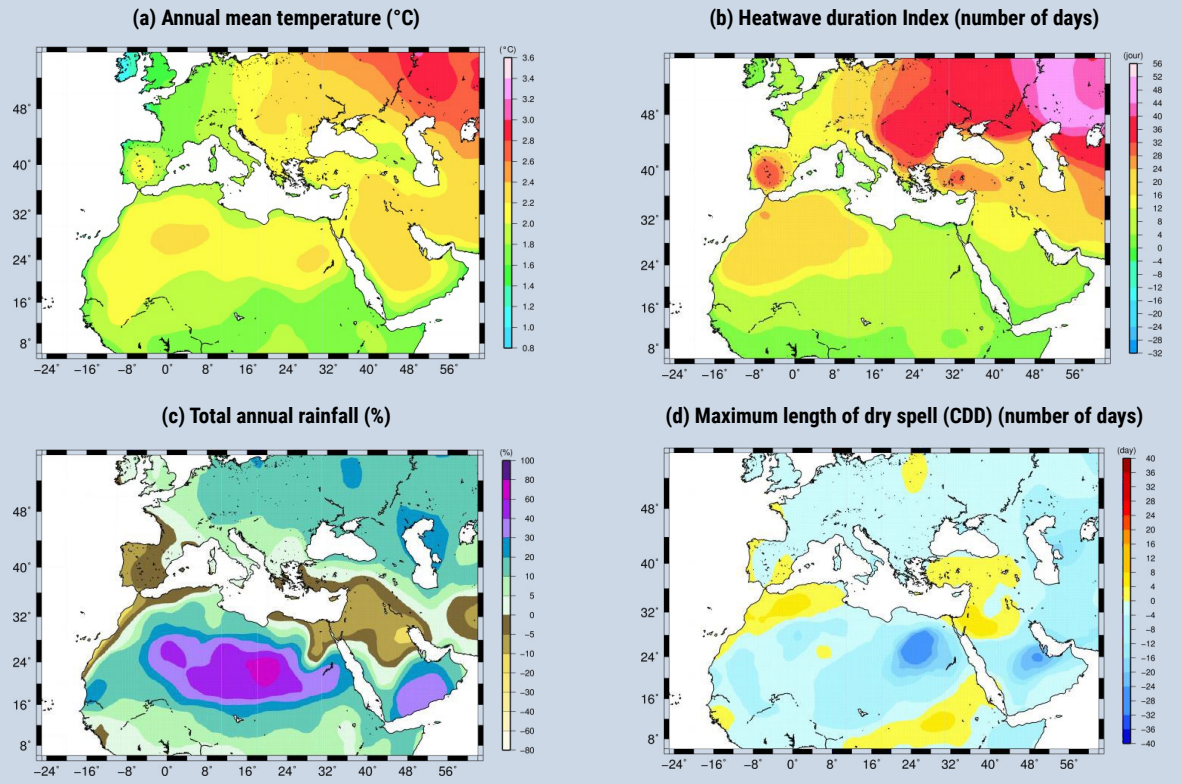

As potentially expected, results show a projected generalized warming for the whole region in the future. This temperature rise generally ranges between 1 °C and 1.2 °C for the emissions scenario RCP 4.5, reaching 2.2 °C to 2.4 °C under RCP 8.5 in the Arabian Peninsula.

Extreme heat events are also projected to increase, with heatwaves longer by about 4–16 days under RCP 4.5 with the highest values located in the western part (Morocco and Algeria) as shown in Figure 40b. The increase in temporal persistence of heatwaves is even higher with RCP 8.5 and reaches 16–20 days over Morocco, Algeria and western Libya (Figure 41b).

In contrast to temperature, precipitation changes show less consistency through the region. For RCP 4.5, a decrease in precipitation of up to 20% is projected in the western part (Morocco) and in the northern part of the Arabian Peninsula. The remaining zones show an increase that can reach 20–40% or even more such as in the southern regions of Algeria, Libya, Egypt and the Arabian Peninsula which are desert regions that register very little precipitation in the current climate (Figure 40c). These projected increases represent not more than 30 mm of total rainfall per year in most cases. Trends under RCP 8.5 are similar in terms of spatial distribution, with more intense changes and an extension of the drying area from Morocco to northern Algeria and over the Arabian Peninsula (Figure 41c).

A seasonal analysis of changes under the RCP 8.5 scenario showed a trend towards less total rainfall amounts in winter generalized to nearly the entire region. The contrasted changes of precipitation across the region have already been reported in previous studies, even when using GCMs with lower resolutions than the one used in this study.[23] In this context, it is important to point out that, although the Arab region displays important climate similarities, there are a number of differences between subregions associated with differing atmospheric circulation and rainfall patterns characterizing the area.[24]

Changes in the maximum length of dry spell (CDD) which represents extreme droughts are generally consistent with the projected future evolution of rainfall amounts (Figures 40d and 41d); with more persistent severe drought over the western part (Morocco), the northern half of Algeria and around the Red Sea. This type of projected evolution is consistent with previous results like those found by Sillmann et al., 2013.

Overall, projected changes in climate for the period 2036–2065 from ALADIN-Climate thus exhibit the following:

- A generalized warming over the entire region, varying from 1 °C to 2.4 °C, depending on the scenario and subregions, which is projected to appear also in terms of increase in heatwave duration;
- A projected decrease in annual total rainfall amounts in the western part of the Domain (mainly in Morocco) and in the northern Arabian Peninsula;
- More persistent extreme droughts in the north-western part of the region (Morocco and Algeria).

Source: Fatima Driouech and Khalid El Rhaz, National Climate Centre, Direction de la Météorologie Nationale, Morocco

Acknowledgements: The authors are grateful to the National Meteorological Service of Morocco (Direction de la Météorologie Nationale) for having provided the necessary computing resources and staff needed for conducting this work.

2.3 PROJECTED CHANGE IN CLIMATE IN THE MOROCCAN HIGHLANDS

Projected changes in temperature, precipitation and extreme events indices for the Moroccan Highlands subdomain are presented in Figure 42.

For scenario RCP 4.5, the change in mean temperature shows an increase of 1.4 °C by mid-century and of 1.8 °C towards the end of the 21st century. Under RCP 8.5, temperature increases are accentuated with a mean of 2.2 °C change for mid-century and 4.1 °C by end-century.

With regard to precipitation, model simulations indicate a reduction over time compared to the baseline period, which is more severe for RCP 8.5. This change is of about –9% for RCP 4.5 at mid-century and –11% at end-century. For RCP 8.5, mean precipitation change is –13% for mid-century and –23% by end-century. This subdomain also stands out in terms of precipitation extremes such as the SDII indicator, whose projections all showed a decreasing trend, unlike the other subdomains which exhibited either an increase or no change in the SDII indicator over time. Looking at seasonal changes, the greatest precipitation changes are projected for the winter months with a reduction of as much as 40% at the end- century sub-period for RCP 8.5. As mentioned in a previous section, this can potentially be explained by the strong influence of the NAO, particularly in winter precipitation. In general, during positive NAO phases, winter rainfall in Morocco tends to be lower than normal.[25] Besides the uncertainties in accurately simulating NAO, future climate models suggest an increasing trend of positive winter NAO for the 21st century.[26]

2.4 PROJECTED CHANGE IN CLIMATE ALONG THE MEDITERRANEAN COAST

Results showing projected changes in temperature, precipitation and extreme events indices for the Mediterranean Coast until the end of the century are presented in Figure 43.

Positive changes in temperature are projected over time. Mean change in temperature for RCP 4.5 is 1.2 °C at mid-century and 1.6 °C at end-century. Changes are stronger for RCP 8.5, with an increase of 1.8° C for mid-century and 3.4 °C for end-century. Regarding precipitation, trends are variable with no change for RCP 4.5 at mid-century and an increase of 4% at end-century. Projected results for RCP 8.5 show decreases (–8% and 16% for mid- and end-century, respectively). Changes in extreme temperature and precipitation generally follow these trends.

Atlas Mountains, Morocco, 2015. Source: Heribert Rustige.

FIGURE 42: Mean change in temperature, precipitation and selected extreme events indices over time for ensemble of three RCP 4.5 and RCP 8.5 projections for the Moroccan Highlands

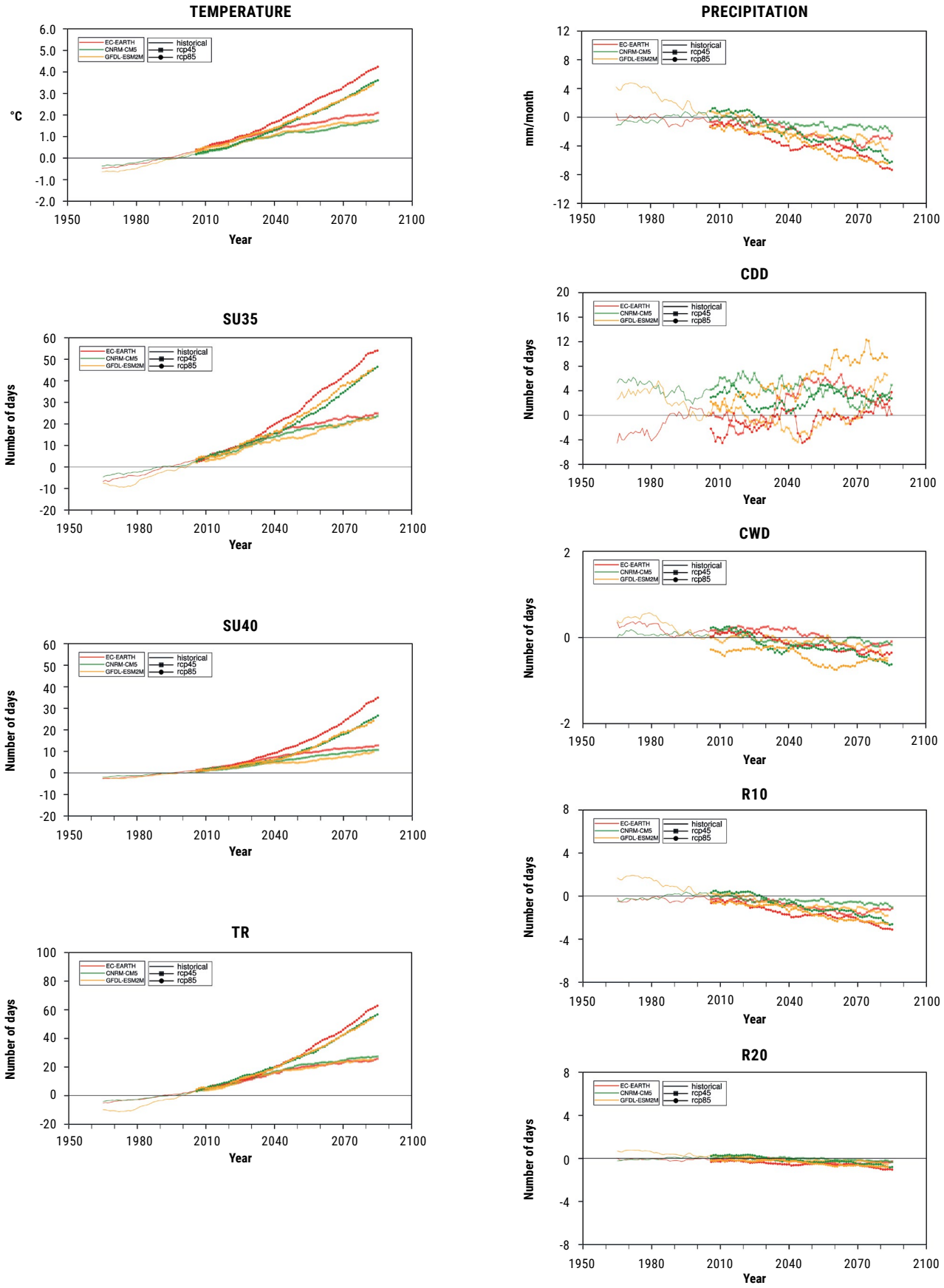

FIGURE 43: Mean change in temperature, precipitation and selected extreme event indices over time for ensemble of three RCP 4.5 and RCP 8.5 projections for the Mediterranean Coast

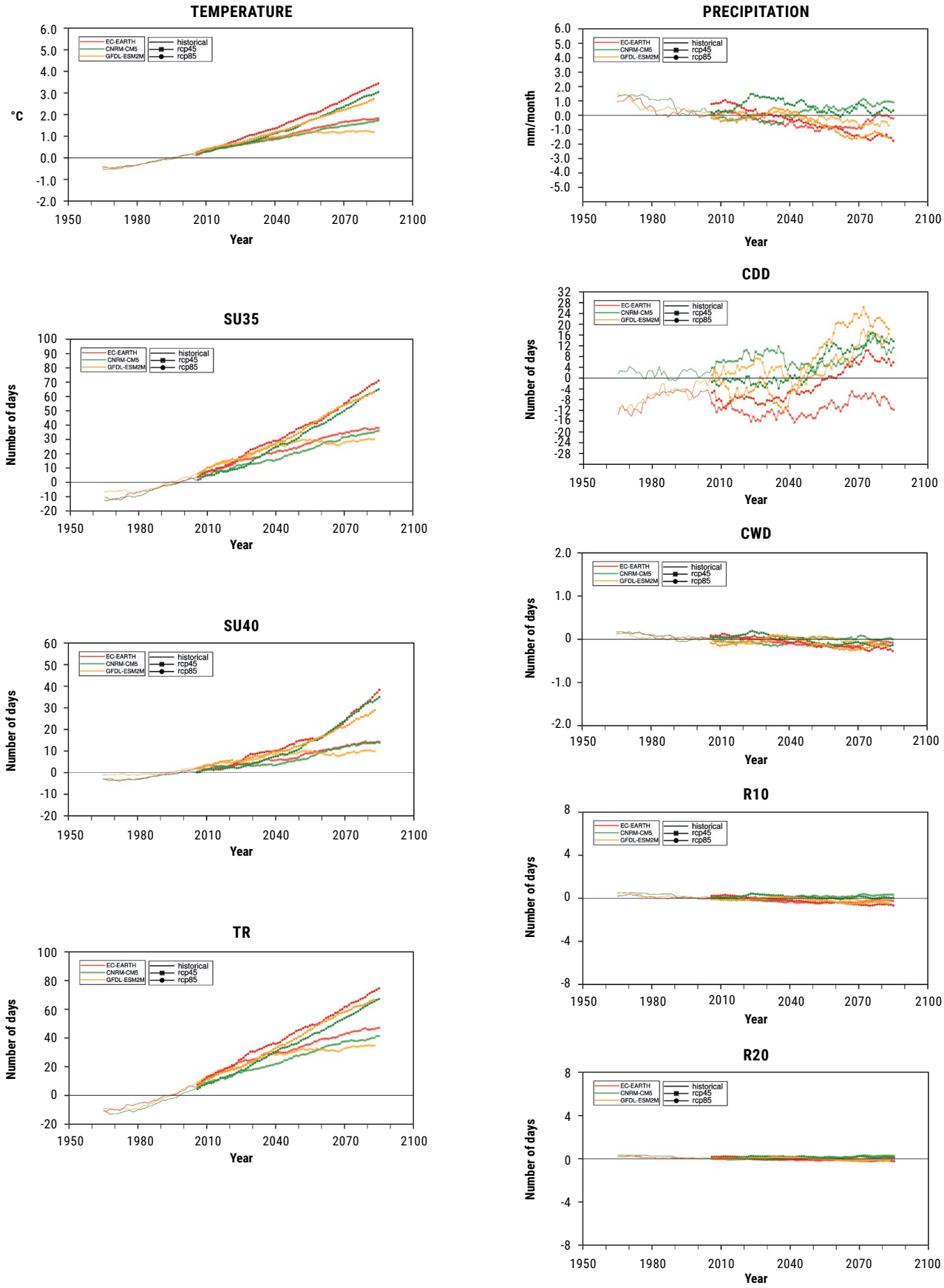

ENDNOTES

1. McGee et al., 2014; Schneider et al., 2014
2. Marchane et al., 2016
3. AlSarmi and Washington, 2014
4. IPCC, 2013a
5. IPCC, 2013a; IPCC, 2013b; IPCC, 2013c
6. Christensen et al., 2013
7. IPCC, 2013a; IPCC, 2013b; IPCC, 2013c
8. Christensen et al., 2013
9. Pal and Eltahir, 2016
10. Monaghan et al., 2014
11. IPCC, 2013a
12. For example, Laprise et al., 2013; Dosio and Panitz, 2016
13. For example,. Jacob et al., 2014
14. For example, Ozturk et al., 2017
15. Radu et al., 2008; Déqué and Somot, 2008; Farda et al., 2010; Colin et al., 2010; Nabat et al., 2015
16. Voldoire et al., 2012
17. Morcrette, 1990
18. Christensen et al., 2008; Sanchez-Gomez et al., 2009; Christensen et al., 2010
19. Driouech et al., 2009; Driouech et al., 2010
20. Salas y Mélia D. et al., 2005; Voldoire et al., 2012
21. The heatwave duration index is percentile-based and corresponds to the maximum number of consecutive days per period where maximum temperature is above its corresponding 90th percentile (Goodess, 2005).
22. Commonly known as maximum length of dry spell (CDD) based on ETCCDI, 2009.
23. i.e Sillmann et al., 2013
24. Donat et al., 2014
25. Marchane et al., 2016
26. For example, Gillett et al., 2003

REFERENCES

AlSarmi, S. H. and Washington, R. 2014. Changes in Climate Extremes in the Arabian Peninsula: Analysis of Daily Data. *International Journal of Climatology*, 34: p. 1329-1345.

Christensen, J. H., Boberg, F., Christensen, O. B. and Lucas-Picher, P. 2008. On the Need for Bias Correction of Regional Climate Change Projections of Temperature and Precipitation. *Geophysical Research Letters*, 35(20).

Christensen, J. H., Kjellström, E., Giorgi, F., Lenderink, G., et al. 2010. Weight Assignment in Regional Climate Models. *Climate Research*, 44: p. 179–194.

Christensen, J. H., Kumar, K. K., Aldrian, E., An, S.-I., et al. 2013. Climate Phenomena and their Relevance for Future Regional Climate Change (Chapter 14). G. J. van Oldenborgh, M. Collins, J. Arblaster, J.H. Christensen, J. Marotzke, S.B. Power, M. Rummukainen and T. Zhou (eds). In *Climate Change 2013: The Physical Science Basis. Contribution of Working Group I to the Fifth Assessment Report of the Intergovernmental Panel on Climate Change.* T. F. Stocker, D. Qin, G.-K. Plattner, M. Tignor, S.K. Allen, J. Boschung, A. Nauels, Y. Xia, V. Bex and P.M. Midgley (eds). Published by Cambridge University Press. Cambridge, United Kingdom and New York, NY, USA. Available at: https://www.ipcc.ch/pdf/assessment-report/ar5/wg1/WG1AR5_Chapter14_FINAL.pdf

Colin, J., Déqué, M., Radu, R. and Somot, S. 2010. Sensitivity Study of Heavy Precipitation in Limited Area Model Climate Simulations: Influence of the Size of the Domain and the Use of the Spectral Nudging Technique. *Tellus*, 62(5): p. 591–604.

Déqué, M. and Somot, S. 2008. Analysis of Heavy Precipitation for France Using High Resolution ALADIN RCM Simulations. *Quaterly Journal of the Hungarian Meteorological Service*, 112(3-4): p. 179-190.

Donat, M. G., Peterson, T. C., Brunet, M., King, A. D., et al. 2014. Changes in Extreme Temperature and Precipitation in the Arab Region: Long-term Trends and Variability Related to ENSO and NAO. *International Journal of Climatology*, 34(3): p. 581-592.

Dosio, A. and Panitz, H.-J. 2016. Climate Change Projections for CORDEX-Africa with COSMO-CLM Regional Climate Model and Differences with the Driving Global Climate Models. *Climate Dynamics*, 46(5-6): p. 1599-1625.

Driouech, F., Déqué, M. and Mokssit, A. 2009. Numerical Simulation of the Probability Distribution Function of Precipitation Over Morocco. *Climate Dynamics*, 32(7): p. 1055–1063.

Driouech, F., Déqué, M. and Sánchez-Gómez, E. 2010. Weather Regimes—Moroccan Precipitation Link in a Regional Climate Change Simulation. *Global and Planetary Change*, 72(1-2): p. 1–10.

ETCCDI (Expert Team on Climate Change Detection and Indices). 2009. ETCCDI/CRD Climate Change Indices: Definition of the 27 Core Indices. Available at: http://etccdi.pacificclimate.org/list_27_indices.shtml.

Farda, A., Déué, M., Somot, S., Horányi, A., et al. 2010. Model ALADIN as Regional Climate Model for Central and Eastern Europe. *Studia Geophysica et Geodaetica*, 54(2): p. 313–332.

Gillett, N. P., Graf, H. F. and Osborn, T. J. 2003. The North Atlantic Oscillation: Climatic Significance and Environmental Impact. In *American Geophysical Union, Geophysical Monograph Series, Volume 134.* Published by American Geophysical Union. Washington, D. C.

Goodess, C. 2005. STARDEX: Downscaling Climate Extremes - Final Report. Published by Climatic Research Unit, University of East Anglia, Norwich, United Kingdom. Available at: https://crudata.uea.ac.uk/projects/stardex/reports/STARDEX_FINAL_REPORT.pdf.

IPCC (Intergovernmental Panel on Climate Change). 2013a. Annex I: Atlas of Global and Regional Climate Projections. G. J. van Oldenborgh, M. Collins, J. Arblaster, J.H. Christensen, J. Marotzke, S.B. Power, M. Rummukainen and T. Zhou (eds). In *Climate Change 2013: The Physical Science Basis. Contribution of Working Group I to the Fifth Assessment Report of the Intergovernmental Panel on Climate Change.* T. F. Stocker, D. Qin, G.-K. Plattner, M. Tignor, S.K. Allen, J. Boschung, A. Nauels, Y. Xia, V. Bex and P.M. Midgley (eds). Published by Cambridge University Press. Cambridge, United Kingdom and New York, NY, USA. Available at: https://www.ipcc.ch/pdf/assessment-report/ar5/wg1/WG1AR5_AnnexI_FINAL.pdf

IPCC (Intergovernmental Panel on Climate Change). 2013b. Annex I: Atlas of Global and Regional Climate Projections Supplementary Material RCP4.5. G. J. van Oldenborgh, M. Collins, J. Arblaster, J.H. Christensen, J. Marotzke, S.B. Power, M. Rummukainen and T. Zhou (eds). In *Climate Change 2013: The Physical Science Basis. Contribution of Working Group I to the Fifth Assessment Report of the Intergovernmental Panel on Climate Change.* T. F. Stocker, D. Qin, G.-K. Plattner, M. Tignor, S.K. Allen, J. Boschung, A. Nauels, Y. Xia, V. Bex and P.M. Midgley (eds). Published by Cambridge University Press. Cambridge, United Kingdom and New York, NY, USA. Available at: https://www.ipcc.ch/pdf/assessment-report/ar5/wg1/supplementary/WG1AR5_AISM4.5_FINAL.pdf

IPCC (Intergovernmental Panel on Climate Change). 2013c. Annex I: Atlas of Global and Regional Climate Projections Supplementary Material RCP8.5. G. J. van Oldenborgh, M. Collins, J. Arblaster, J.H. Christensen, J. Marotzke, S.B. Power, M. Rummukainen and T. Zhou (eds). In *Climate Change 2013: The Physical Science Basis. Contribution of Working Group I to the Fifth Assessment Report of the Intergovernmental Panel on Climate Change.* T. F. Stocker, D. Qin, G.-K. Plattner, M. Tignor, S.K. Allen, J. Boschung, A. Nauels, Y. Xia, V. Bex and P.M. Midgley (eds). Published by Cambridge University Press. Cambridge, United Kingdom and New York, NY, USA. Available at: https://www.ipcc.ch/pdf/assessment-report/ar5/wg1/supplementary/WG1AR5_AISM8.5_FINAL.pdf

IPCC (Intergovernmental Panel on Climate Change). 2015. AR5 Reference Regions. Available at: http://www.ipcc-data.org/guidelines/pages/ar5_regions.html.

Jacob, D., Petersen, J., Eggert, B., Alias, A., et al. 2014. EURO-CORDEX: New High-resolution Climate Change Projections for European Impact Research. *Regional Environmental Change*, 14(2): p. 563-578.

Laprise, R., Hernandez-Dıaz, L., Tete, K., Sushama, L., et al. 2013. Climate Projections over CORDEX Africa Domain using the Fifth-generation Canadian Regional Climate Model (CRCM5). *Climate Dynamics*, 41(11-12): p. 3219-3246.

Lelieveld, J., Proestos, Y., Hadjinicolaou, P., Tanarhte, M., et al. 2016. Strongly Increasing Heat Extremes in the Middle East and North Africa (MENA) in the 21st Century. *Climatic Change*, 137: p. 245–260.

Marchane, A., Jarlan, L., Boudhar, A., Tramblay, Y., et al. 2016. Linkages Between Snow Cover, Temperature and Rainfall and the North Atlantic Oscillation over Morocco. *Climate Research*, 69: p. 229–238.

McGee, D., Donohoe, A., Marshall, J. and Ferreira, D. 2014. Changes in ITCZ Location and Cross-equatorial Heat Transport at the Last Glacial Maximum, Heinrich Stadial 1, and the mid-Holocene. *Earth and Planetary Science Letters*, 390: p. 69-70.

Monaghan, A. J., Steinhoff, D. F., Bruyere, C. L. and Yates, D. 2014. NCAR CESM Global Bias-Corrected CMIP5 Output to Support WRF/ MPAS Research. Published by Research Data Archive at the National Center for Atmospheric Research, Computational and Information Systems Laboratory, USA. Available at: https://rda.ucar.edu/datasets/ds316.1/.

Morcrette, J. J. 1990. Impact of Changes to the Radiation Transfer Parameterizations Plus Cloud Optical. Properties in the ECMWF Model. *Monthly Weather Review*, 118: p. 847-873.

Nabat, P., Somot, S., Mallet, M., Sevault, F., et al. 2015. Direct and Semi-Direct Aerosol Radiative Effect on the Mediterranean Climate Variability Using a Coupled Regional Climate System Model. *Climate Dynamics*, 44(3): p. 1127-1155.

Ozturk, T., Turp, M. T., Türkeş, M. and Kurnaz, M. L. 2017. Projected Changes in Temperature and Precipitation Climatology of Central Asia CORDEX Region 8 by using RegCM4.3.5. *Atmospheric Research*, 183: p. 296-307.

Pal, J. S. and Eltahir, E. A. B. 2016. Future Temperature in Southwest Asia Projected to Exceed a Threshold for Human Adaptability. *Nature Climate Change*, 6: p. 197–200.

Radu, R., Déqué, M. and Somot, S. 2008. Spectral Nudging in a Spectral Regional Climate Model. *Tellus*, 60(5): p. 898–910.

Salas y Mélia D., Chauvin F., Déqué M., Douville H., et al. 2005. Description and Validation of CNRMCM3 Global Coupled Climate Model. In *Note de centre GMGEC (internal publication), CNRM 103*.

Sanchez-Gomez, E., Somot, S. and Déqué, M. 2009. Ability of an Ensemble of Regional Climate Models to Reproduce Weather Regimes Over Europe-Atlantic During the Period 1961–2000. *Climate Dynamics*, 33(5): p. 723–736.

Schneider, T., Bischoff, T. and Haug, G. H. 2014. Migrations and Dynamics of the Intertropical Convergence Zone. *Nature*, 513: p. 45-53.

Sillmann, J., Kharin, V. V., Zwiers, F. W., Zhang, X., et al. 2013. Climate Extremes Indices in the CMIP5 Multi-Model Ensemble. Part 2: Future Projections. *Journal of Geophysical Research*, 118(6): p. 2473–2493.

Voldoire, A., Sanchez-Gomez, E., Salas y Mélia, B., Decharme, B., et al. 2012. The CNRM-CM5.1 Global Climate Model: Description and Basic Evaluation. *Climate Dynamics*, 40: p. 2091–2121.

REGIONAL HYDROLOGICAL MODELLING: ARAB REGION

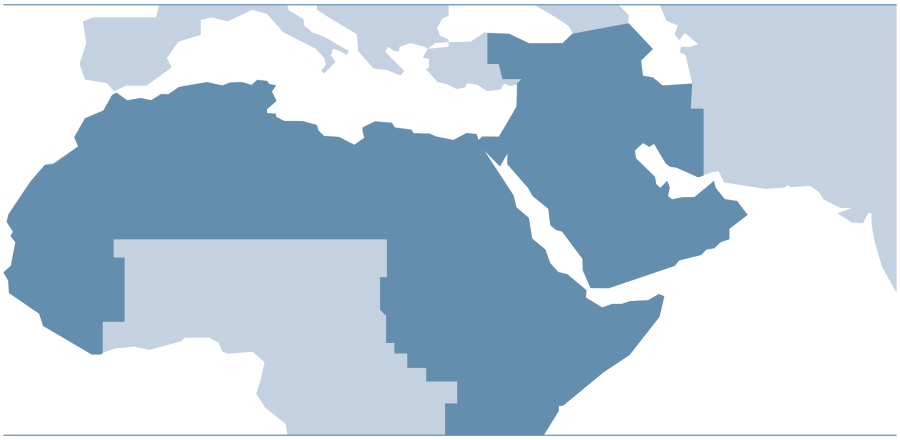

CHAPTER 3

REGIONAL HYDROLOGICAL MODELLING RESULTS FOR THE ARAB REGION AND SELECTED SUBDOMAINS

The regional hydrological modelling (RHMs) variables generated using the VIC and HYPE hydrological models include runoff, evapotranspiration, mean discharge (with related high-flow value and low-flow value), groundwater discharge, soil moisture and low soil moisture,[1] with selected findings reported in this chapter. These were generated for mid- and end-century considering RCP 4.5 and RCP 8.5 emission scenarios at a 50-km resolution. Comparisons with results of 25-km resolution are available for changes in runoff and discharge for the RCP 8.5 projections, noting that only two projections were available at this resolution and were thus not combined as an ensemble. Additional outputs are available in the Technical Annex.

As explained in the overview chapter, the limited quantity of hydrological observation data generates uncertainties regarding the accuracy of the hydrological modelling outputs. For instance, as runoff projections are based on precipitation outputs, they demonstrate high uncertainties for both the HYPE and VIC models. Moreover, for some river and streams pertaining to specific subdomains, no observation datasets on discharge were available to verify the model. This was the case for the Moroccan Highlands (MH) and Mediterranean Coast (MD) subdomains, for which discharge-related outputs (mean discharge, high-flow value, low-flow value) will not be presented in the report due to this uncertainty. It is also worth pointing out at the increasing uncertainties in the results the higher the human influence on the river system compared to the size of the river. This is particularly true for small rivers such as the Jordan River and this issue should be taken into consideration when interpreting and analysing discharge-related outputs. Discharge-related outputs were only completed through the HYPE model but the runoff calculated from the VIC model that contributes to river discharge is included and compared to the HYPE model results.

3.1 PROJECTED CHANGES IN WATER AVAILABILITY DUE TO CLIMATE CHANGE IN THE ARAB REGION

3.1.1 Changes in runoff

Changes in area runoff over the Arab region are shown in Figure 44. Each plot summarizes the three member ensemble results from both the HYPE and VIC models. Although there are differences in some subregions, outcomes from the two hydrological models generally show similar trends of runoff change. The largest discrepancies appear to be at the upper reaches of the White Nile. Changes in runoff largely follow the same pattern of change as for precipitation change. Regional results from the three-member hydrological ensemble are generally in agreement between the two hydrological models used, although there are some differences in the magnitude of change seen in Figure 45.

3.1.2 Changes in evapotranspiration

Changes in evapotranspiration over the Arab region are presented in Figure 46. Each plot summarizes the three member ensemble results from both the HYPE and VIC models. Intuitively, one would expect evapotranspiration to increase with rising temperature and this is most likely the case in places where water is not scarce. For the arid Arab region, however, water quantity is often a limiting factor and evapotranspiration thus decreases over time as there is less water available to evaporate or transpire. The pattern of change for evapotranspiration thus largely follows the pattern of change for runoff. For basins where there is sufficient water, evapotranspiration increases over time, which is a contributing factor to the decrease in runoff in those areas. An example is the headwaters of both the Tigris and Euphrates rivers during the winter season. Overall, projected changes in evapotranspiration are in line with the ensemble projection agreement presented in Figure 47.

FIGURE 44: Mean change in annual runoff (mm/month) for mid- and end-century for the ensemble of three RCP 4.5 and RCP 8.5 projections compared to the reference period using two hydrological models

RCP 4.5

HYPE MODEL

1986-2005 2046-2065 2081-2100

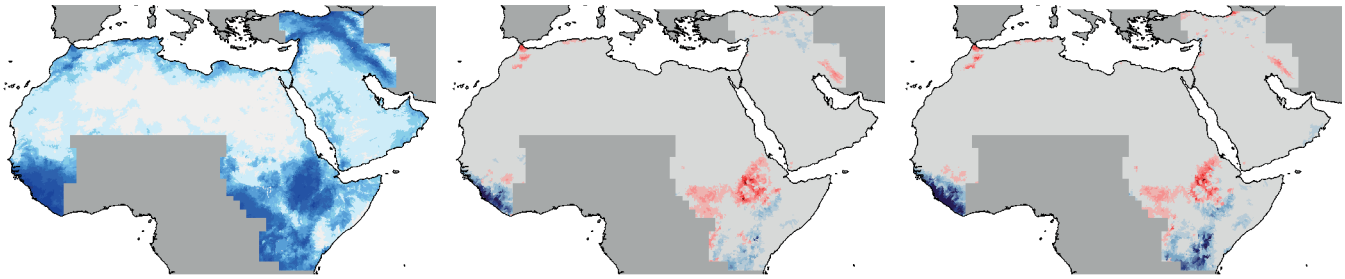

VIC MODEL

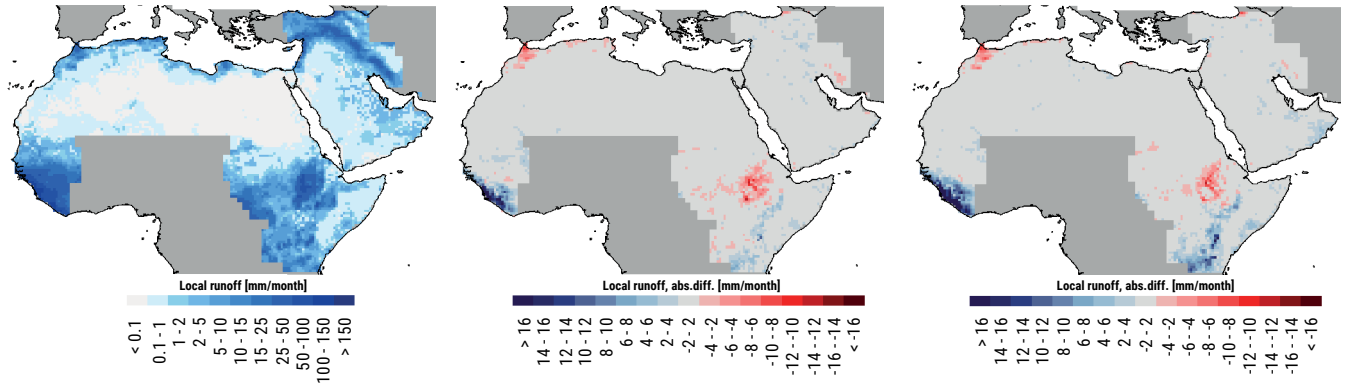

RCP 8.5

HYPE MODEL

1986-2005 2046-2065 2081-2100

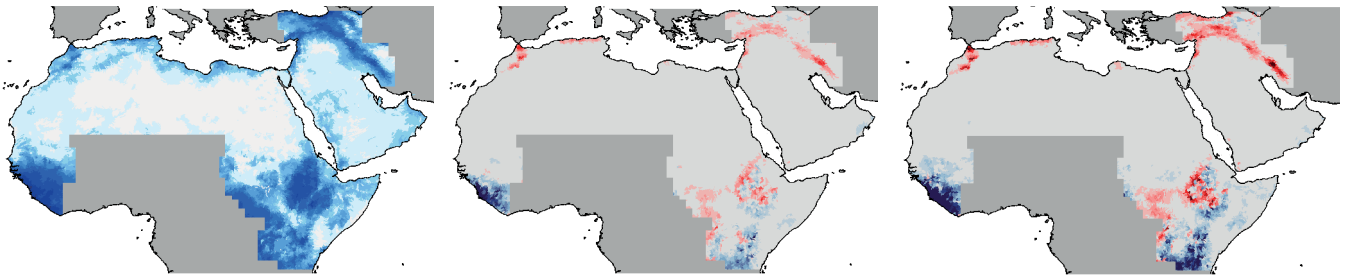

VIC MODEL

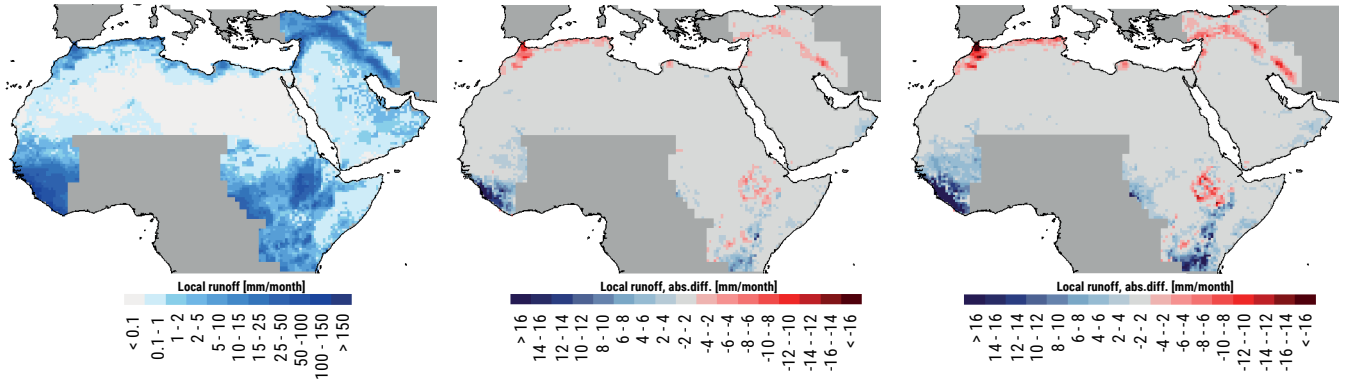

FIGURE 45: Agreement on mean change in annual runoff for mid- and end-century between the ensemble of three RCP 4.5 and RCP 8.5 projections from the reference period

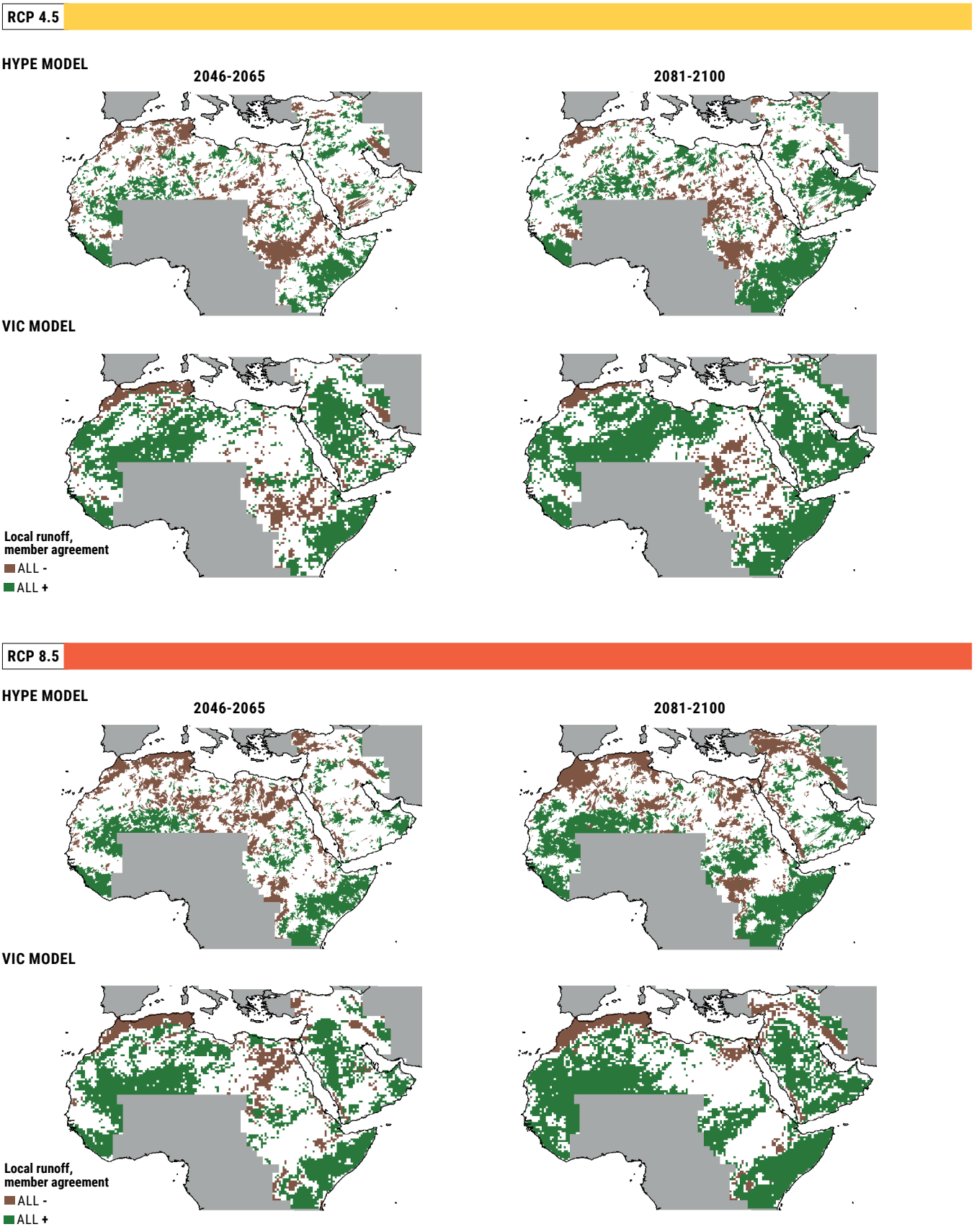

Note: Brown indicates where all ensemble projections agree on a decrease (-) in runoff, and green indicates where all agree on an increase (+) in runoff

FIGURE 46: Mean change in annual evapotranspiration (mm/month) for mid- and end-century for the ensemble of three RCP 4.5 and RCP 8.5 projections compared to the reference period using two hydrological models

RCP 4.5

HYPE MODEL

1986-2005 2046-2065 2081-2100

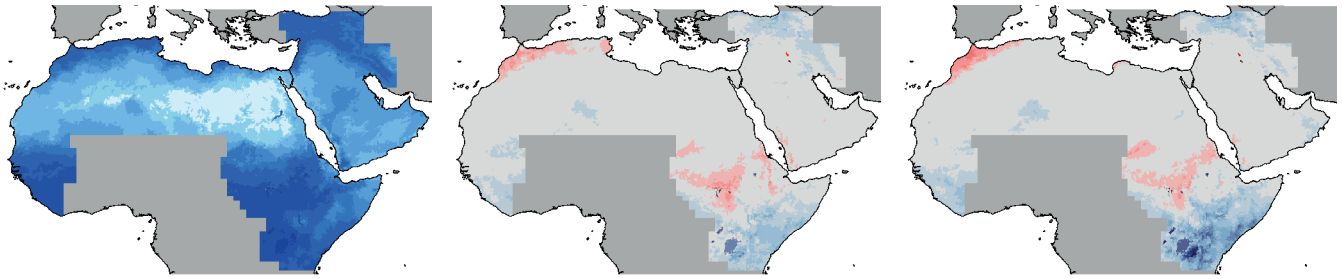

VIC MODEL

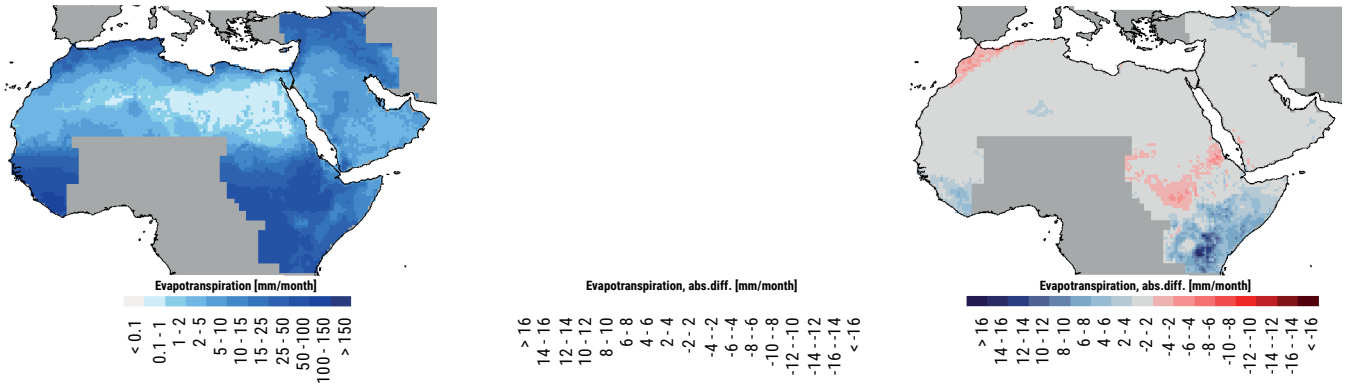

RCP 8.5

HYPE MODEL

1986-2005 2046-2065 2081-2100

VIC MODEL

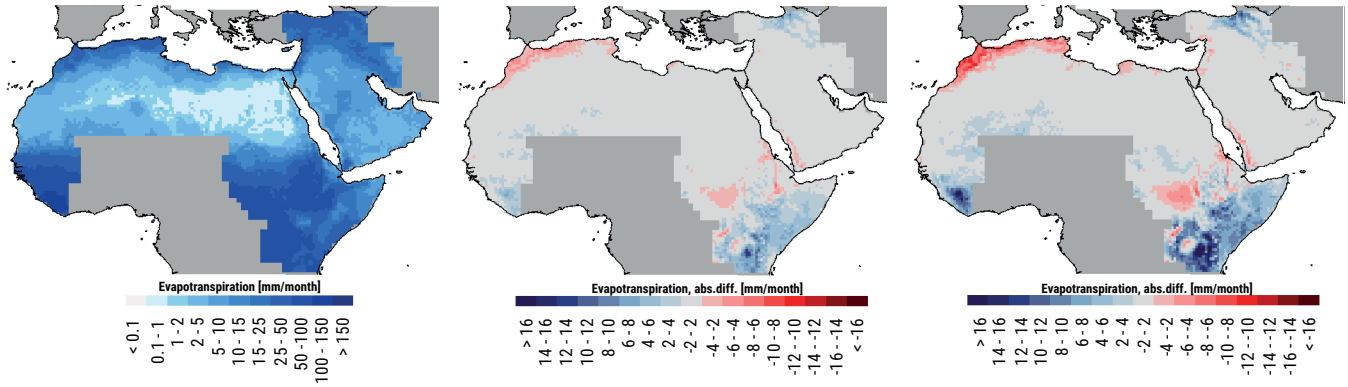

FIGURE 47: Agreement on mean change in annual evapotranspiration for mid- and end-century between the ensemble of three RCP 4.5 and RCP 8.5 projections from the reference period

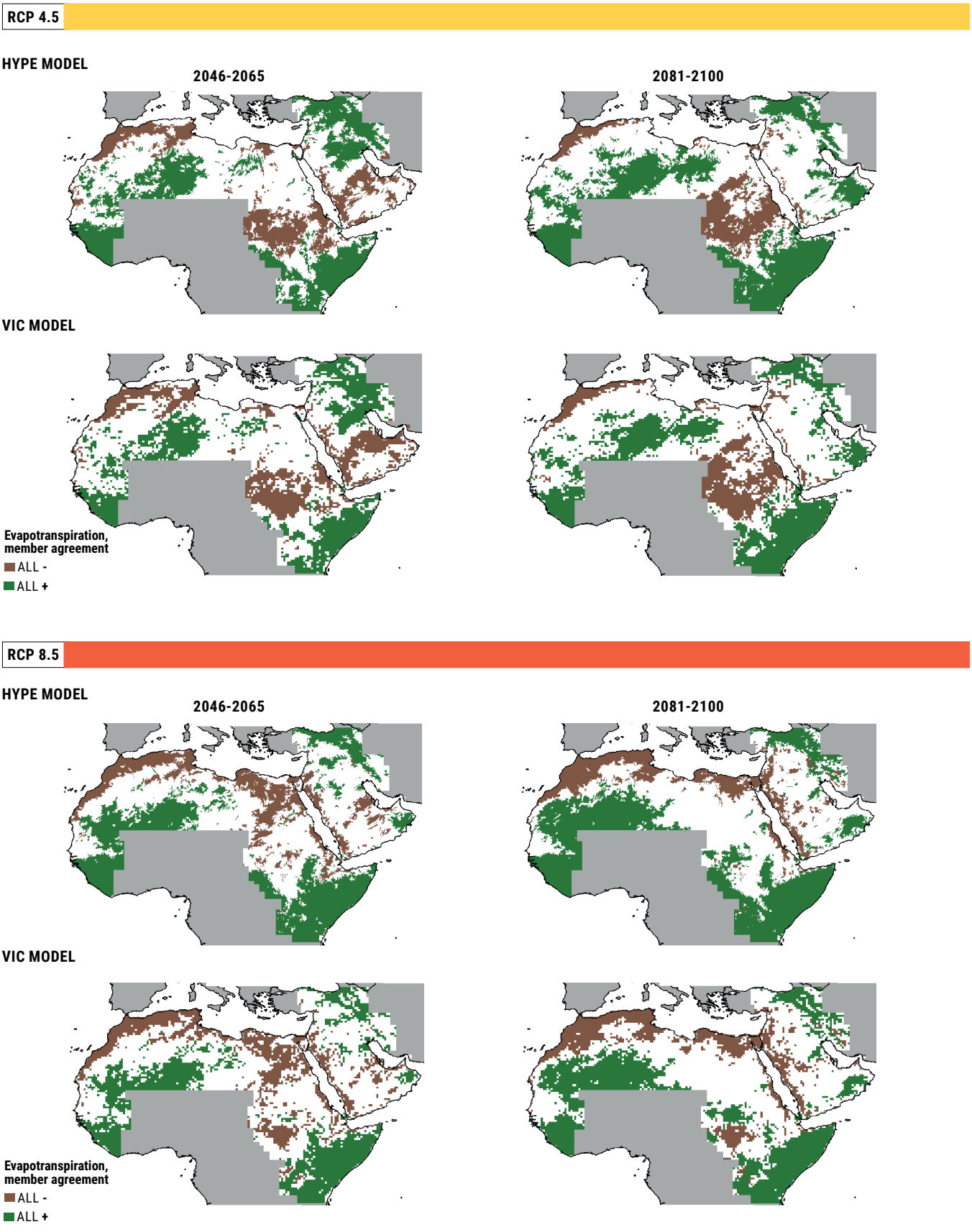

Note: Brown indicates where all ensemble projections agree on a decrease (-) in evapotranspiration, and green indicates where all agree on an increase (+) in evapotranspiration

3.2 MOROCCAN HIGHLANDS

Regional hydrological modelling results for the Moroccan Highlands are presented in Figure 48. This subdomain displays a considerable projected decrease in precipitation. Runoff changes for the Moroccan Highlands appear to follow a marked decrease, in particular for RCP 8.5, representing up to a 32%–40% decrease at mid-century and 48%–59% decrease by end-century, depending on the model. The same pattern is exhibited for changes in evapotranspiration for both models with decreases projected throughout the years reaching a reduction of 10%–11% at end-century for RCP 4.5 and 22%–26% for RCP 8.5.

Similar decreasing trends in runoff are evident whether the HYPE model is applied to generate projections as the 50-km resolution or smaller scale resolution of 25 km, for the RCP 8.5 scenario.

FIGURE 48: Mean change in runoff and evapotranspiration (using HYPE and VIC) over time for ensemble of three RCP 4.5 and RCP 8.5 projections for the Moroccan Highlands

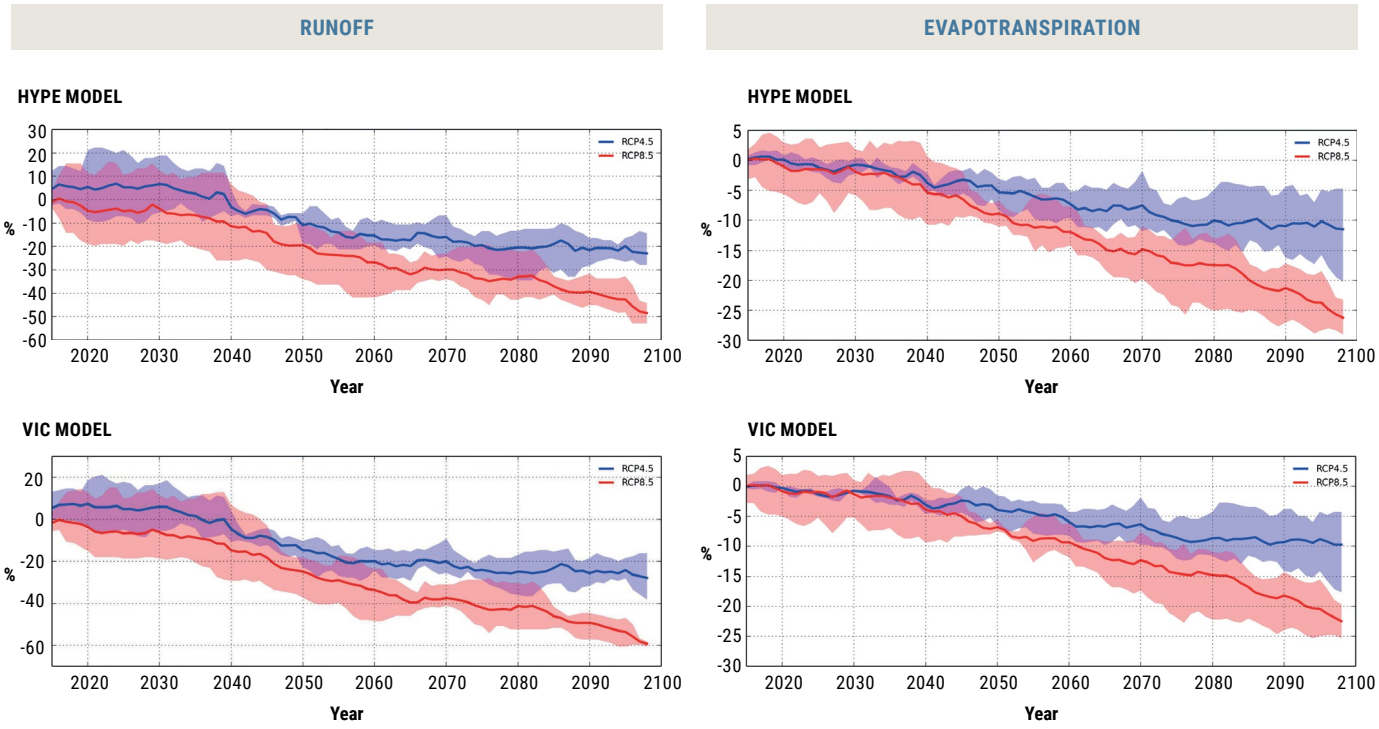

FIGURE 49: Comparison between 25 km (MNA22) and 50 km (MNA44) resolutions for mean change in runoff (using HYPE) over time for two RCP 8.5 projections for the Moroccan Highlands

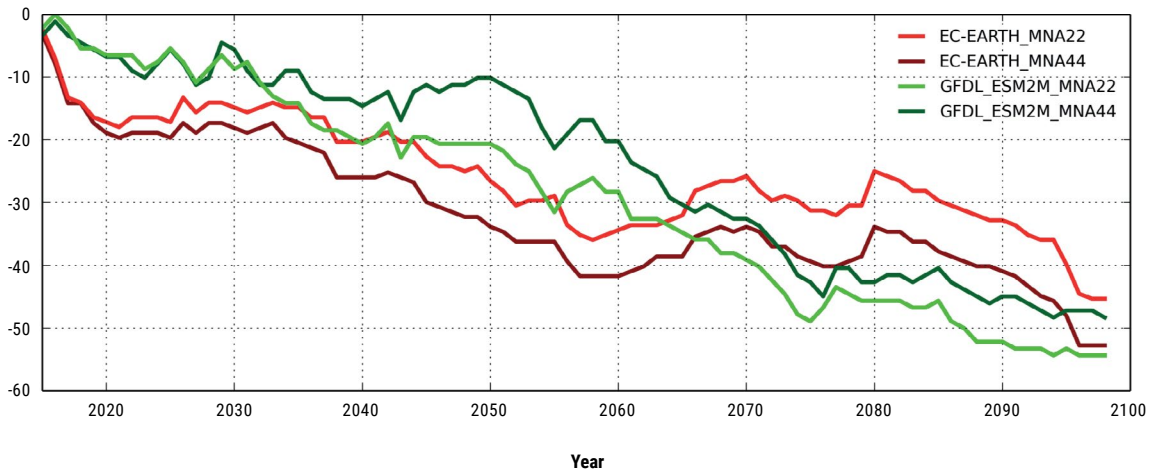

3.3 MEDITERRANEAN COAST

Changes in runoff and evapotranspiration for the Mediterranean Coast subdomain are displayed in Figure 50. Projections of changes in runoff comprise a wide range of values for both models and thus no clear trend in projections can be concluded. Concerning evapotranspiration, the VIC model results show a mean decrease of 14% at end-century for RCP 8.5, which is also apparent in the winter and summer season for this emission scenario and time period. While results for mid-century and from the HYPE model also show an overall reduction in evapotranspiration, the wide range of values does not allow providing a conclusive trend for these conditions. The mixed climate signals for runoff in the near term along the Mediterranean coast may be attributable to climate variability and the intermittent nature of shallow surface waters in the region. The longer-term trends for runoff in the subdomain, however, demonstrate slightly more consensus on the decline in runoff under the pessimistic RCP 8.5 projection towards end of the century.

FIGURE 50: Mean change in runoff and evapotranspiration (using HYPE and VIC) over time for ensemble of three RCP 4.5 and RCP 8.5 projections for the Mediterranean Coast

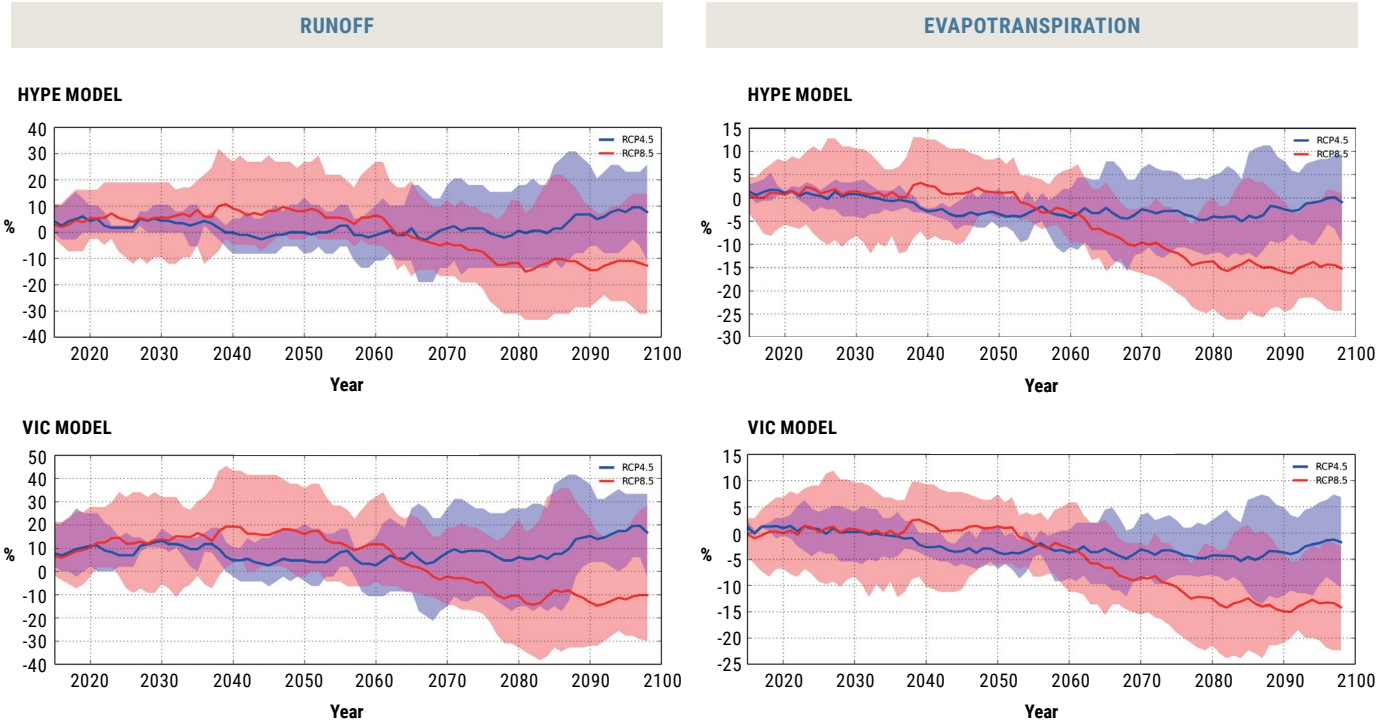

FIGURE 51: Comparison between 25 km (MNA22) and 50 km (MNA44) resolutions for mean change in runoff (using HYPE) over time for two RCP 8.5 projections for the Mediterranean Coast

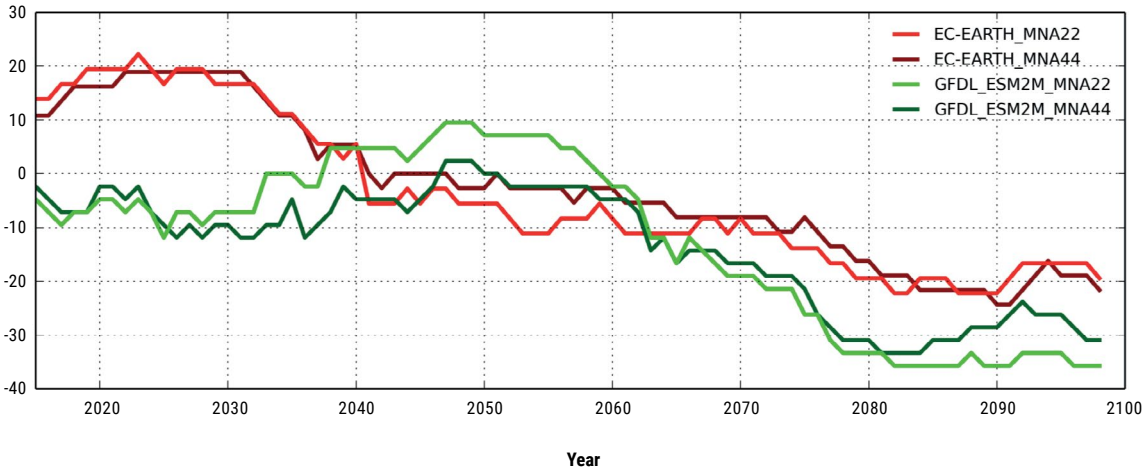

ENDNOTES

1. Groundwater discharge was also considered but, as data were limited, only simple analysis using a hydrological model was conducted, as noted in Chapter 2. Soil moisture was also analysed, but is not included in this report.

REFERENCES

AlSarmi, S. H. and Washington, R. 2014. Changes in Climate Extremes in the Arabian Peninsula: Analysis of Daily Data. *International Journal of Climatology*, 34: p.1329-1345.

CHAPTER 4

FINDINGS FOR SELECTED SHARED WATER BASINS IN THE ARAB REGION

Shared water resources are of considerable importance in the Arab region, with over 66% of freshwater resources in Arab States originating from outside national borders[1] and 14 out of 22 Arab States sharing a surface-water body. All Arab States, with the exception of Comoros, share a transboundary groundwater resource. The high dependency on shared surface- and groundwater resources in the region makes them of strategic importance for achieving sustainable development, especially since some river systems extend across the borders of non-Arab countries.

Policy efforts aiming at national policy integration across water-dependent sectors are thus complicated by the interdependency of the water resources shared by riparian countries each seeking to achieve their own development goals. The impacts of climate change and climate variability projected over the coming years are expected to further complicate shared water resources management efforts. Regional climate and hydrological modelling outputs can thus help to create a common starting point to assist neighbouring States discuss shared water resources management under changing climate conditions.

Given the importance of these shared resources for the region, Arab States laid particular emphasis on the necessity of considering shared basins within RICCAR's scope of work and to include climate change projections and analysis of extreme events on selected shared water basins in the Arab region in the assessment report. This was requested during the RICCAR Fifth Expert Group Meeting in 2013[2] and the tenth session of the Arab Ministerial Water Council Technical Scientific Advisory Committee (Doha, May 2014).[3]

This chapter thus includes selected essential climate variables and extreme climate indices produced from the regional climate modelling projections and regional hydrological modelling outputs for five shared surface water basins in the region: the Nile, the Tigris and Euphrates, the Medjerda, the Jordan River Basin and the Senegal River Basin.

For each of these, a brief overview of general basin characteristics is provided, including a review of selected sectors deemed to be vulnerable to climate change. This is followed by results from regional climate modelling and regional hydrological modelling simulation outputs for a specific subdomain within each basin.

The location of these subdomains (overview map in Chapter 1) was strategically identified, based on the basin's characteristics and the availability of reliable data. For most basins, subdomain delineation mainly included headwaters areas, as further downstream, water flow is often heavily influenced by human interventions such as water regulation structures. In a context of future projections, providing a better future representation of changes in the entire river basin would require an assessment of changes in water management systems (agricultural practices, energy system changes, etc.) as well as population projections in conjunction with climate change projections, which goes beyond the scope of the study. Projections of changes at the river basin headwaters serves as a starting point to assess overall impacts on available water within the basin.

In addition to the considerations reviewed in Chapter 3, it is noted that a broad set of variables were studied (runoff, evapotranspiration, soil moisture, mean discharge, high-flow value and low-flow value) for each subdomain, but only runoff and mean discharge are presented in this chapter.

The projection changes for each variable were generated through the end of the century (and at the seasonal level) for RCP 4.5 and RCP 8.5 emission scenarios at 50-km resolution. Comparisons with results from 25-km resolution are available for changes in runoff and discharge for the RCP 8.5 projections, noting that at this resolution only two projections were available and were thus not combined as an ensemble. Additional outputs are included in the Technical Annex.

4.1 NILE RIVER BASIN

4.1.1 Overview and subdomain selection

The Nile River (Figure 52) is one of the world's major rivers and an important freshwater reservoir. It is 6,695 km long with a basin area of 3,180,000 km^2 shared among the following 11 riparian countries: Burundi, Democratic Republic of the Congo, Egypt, Eritrea, Ethiopia, Kenya, Rwanda, South Sudan, Sudan, United Republic of Tanzania and Uganda. The basin is home to 370 million inhabitants with Egypt having the largest population (80.4 million).[4] The two main tributaries of the Nile River are the White Nile, with sources on the Equatorial Plateau, and the Blue Nile originating in the Ethiopian Highlands. The major lakes in the Nile basin system are Lake Victoria, Lake Kyoga, Lake Albert, Lake Tana, Lake Edward and Lake Nasser.[5]

The Nile River basin is characterized by high climatic diversity and variability. The mean annual rainfall is around 630 mm/yr but is spatially very different. About 28 % of the basin receives less than 100 mm annually and a substantial area (34%) exhibits sub-humid conditions with rainfall ranges of 700–1,300 mm. Rainfall is negligible from northern Sudan across Egypt (less than 50 mm/yr) and precipitation in excess of 1,000 mm is restricted to two areas: the equatorial region from south-western Sudan to most of the Lake Victoria basin (1,200-1,350 mm/yr) and the Ethiopian Highlands (around 1,300 mm/yr at the Roseires Dam station).[6] Evapotranspiration losses account for more than 70% of the water balance in the wettest areas of the Nile Basin, such as the Blue Nile and the equatorial lakes sub-basins and even a higher percentage in drier areas.[7]

Historically, the Nile River has shown significant fluctuations in flow, with most of it coming from the tributaries. The Blue Nile contributes more than 60% of the total flow of the Nile (measured at Aswan Dam) and the other major river systems, namely the Sobat and the Atbara, contribute slightly less than 15% each. The White Nile contributes about 18%.[8] The Blue Nile is characterized by a marked seasonal regime following the rainfall pattern at the headwaters, with most of the flow generated during the rainy season from June to September. The long-term (1912–2010) mean annual discharge of the Blue Nile at the Ethiopia-Sudan border (Roseires Dam/ El Diem station) is 49.3 billion m^3/yr.[9] The long-term mean annual flow of the Nile at Aswan is 85 billion m^3.[10]

4.1.2 Vulnerable sectors

The size and complexity of the Nile River basin display a range of vulnerabilities that vary from one riparian country to another. There are numerous areas in the basin which, through the combination of precarious environmental, economic and social conditions, become vulnerable to additional threats. The key sectors with potential vulnerabilities to climate change impacts in this basin are summarized below.

FIGURE 52: Map of the Nile River basin and extent of subdomain

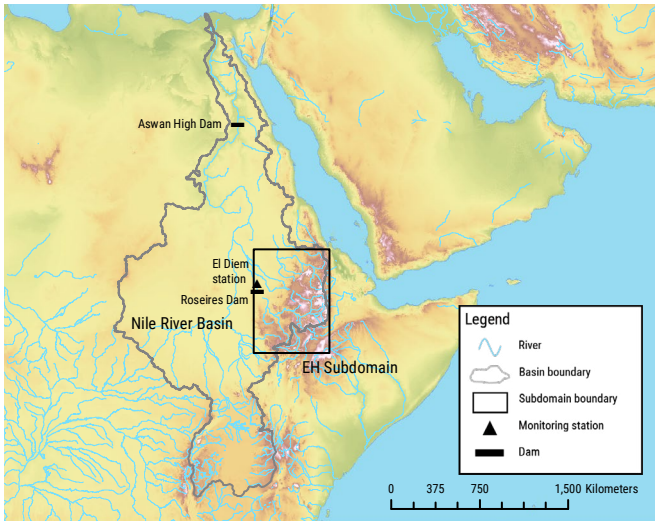

Agriculture, food security and livelihoods

Most of the water use in the Nile basin countries is directed towards agriculture, accounting for more than 80% of all water uses. In the arid and semi-arid downstream regions, the Nile constitutes the sole source of water for agriculture. In Egypt and Sudan for instance (representing some 80% and 17% of total basin wide abstraction for irrigation, respectively), the amount of water used for irrigation is almost as much as the total annual renewable water resources.[11] The irrigation potential of the other countries is also extensive, with agriculture contributing to one third of the overall gross domestic product (GDP) in the basin and providing more than 75% of the total labour force.[12] Already high levels of poverty and underdevelopment in the region put rural communities particularly at risk, as they are also dependent on rainfed agriculture (particularly Ethiopia, Sudan and the upper basin around Lake Victoria). The overdependence on rainfall leaves the countries extremely vulnerable to droughts, floods and extreme weather conditions. In the past, this has led to massive agricultural losses and food insecurity and is now eliciting a move towards urgent investment in water-storage capacity to counteract the uncertainty caused by the climate. Ethiopia, for example, has prioritized investments in large-scale hydrological infrastructure for electricity and storage.

Energy sector and hydropower

The Nile River is an important source of hydropower generation. Several dams have been constructed for this purpose, notably in Egypt and Sudan, and also at the Owen

Falls in Lake Victoria. Hydropower plays an increasing role in water management in the basin's development with, for instance, the 6,000 MW Renaissance Dam on the Blue Nile underway in Ethiopia and the 80 MW Regional Rusumo Falls Hydroelectric Project being developed in Rwanda. Changing climatic conditions have the potential to impact the operation regimes of dams built along the river, with effects on hydropower generation and flow volumes to downstream countries.[13]

Sensitivity to extreme events
The climate of the Nile basin varies considerably over both space and time, resulting in recurrent fluctuations in river flows. Research on the Nile basin has shown that the river's natural flow is particularly sensitive to precipitation that falls on the Ethiopian Highlands. Several events of extreme-flow conditions, including floods and droughts, occurred in the Blue Nile Basin, with the example of a devastating drought in the Ethiopian Highlands in the 1980s due to long dry spells within the rainy season. Another example is the severe flooding experienced in Sudan in 1988 resulting from heavy rainfalls over Khartoum and Atbara. Possibly shifting temperature and precipitation patterns due to climate change will have an impact on the recurrence of extreme conditions, as well as contributing to changes in the river's flow regime.[14]

Groundwater resources
Groundwater resources within the basin are highly variable, both in terms of their recharge and their extent. Groundwater is used increasingly to irrigate during the dry season: in the most arid zones, groundwater may be the only supply source for all types of farm activities. Groundwater resources are under pressure from increased water demand due to rapid population growth and surface pollution, with unsustainable abstractions in many areas, posing a threat in climate change conditions.[15]

Public health-related issues
The population of the Nile basin has long been vulnerable to waterborne diseases associated with interannual fluctuations in rainfall and temperature. Moreover, despite water development projects being vital for increasing agricultural productivity and improving the socio-economic status of rural communities, it has been shown that these projects also have the potential to modify hydrological processes in a way that increases the risk of water-associated diseases.[16] There is also growing evidence that these infrastructure projects can facilitate the transmission of water-associated diseases by providing favourable environments for vectors, hosts and pathogens, such as cholera, schistosomiasis and malaria, all prevalent water-associated diseases within the Nile basin. Published data on cholera case numbers and incidence all suggest that the countries of the Nile basin form a geographic hotspot for cholera in Africa.[17]

Transportation sector
The Nile River is a critical waterway for the transportation of people and goods, as well as for the tourism sector. The river and its tributaries are seasonally navigable and people living along the river have always used it as a vital mode of transporting both goods and people. River steamers represent an important means of transport during the flood season upstream, when transport is not possible by road. Most major cities and towns in Egypt and Sudan are situated on or near the riverbanks. Potentially declining Nile flows due to climate change could increase the vulnerability of the sector.[18]

Highly urbanized areas
Rapidly growing cities in the Nile Basin and the concentration of services in densely populated areas are often located in the zones most sensitive to climate variability. One example is the Nile Delta region which accounts for 30%-40% of Egypt's agricultural production and for most of its tourism and industrial base. As this coastal zone lies in a low elevation area, it would be considerably affected by sea-level rise, saltwater intrusion and other potential social and economic impacts of climate change.[19]

In addition to the key sectors mentioned above, several potential vulnerabilities require consideration and further analysis in the context of climate change. These include population dynamics and projections in the basin, including migration patterns, and their links with future changes in water supply and demand. In this context, poverty, which is widespread in the region as well as gender aspects, ought to be taken into account especially with regard to implications in a shifting climate and availability of water resources. Moreover, attention should be given to transboundary impacts of changing rainfall and temperature patterns in terms of hydrology and socio-economic implications, as they relate to the effects of upstream developments on downstream conditions.

Finally, given the current hydropolitical transboundary configurations in the basin, institutional and cooperative structures play a pivotal role of either alleviating or exacerbating the vulnerabilities due to a changing climate in their consideration and implementations of plans, policies, and projects addressing climate change issues.

4.1.3 Regional climate modelling findings

Changes projected for temperature, precipitation and related extreme events until the end of the century are presented in Figure 53 for the Blue Nile Headwaters. Results show an overall projected increase in temperatures and decrease in precipitation.

FIGURE 53: Mean change in temperature, precipitation and selected extreme events indices over time for ensemble of three RCP 4.5 and RCP 8.5 projections for the Blue Nile Headwaters

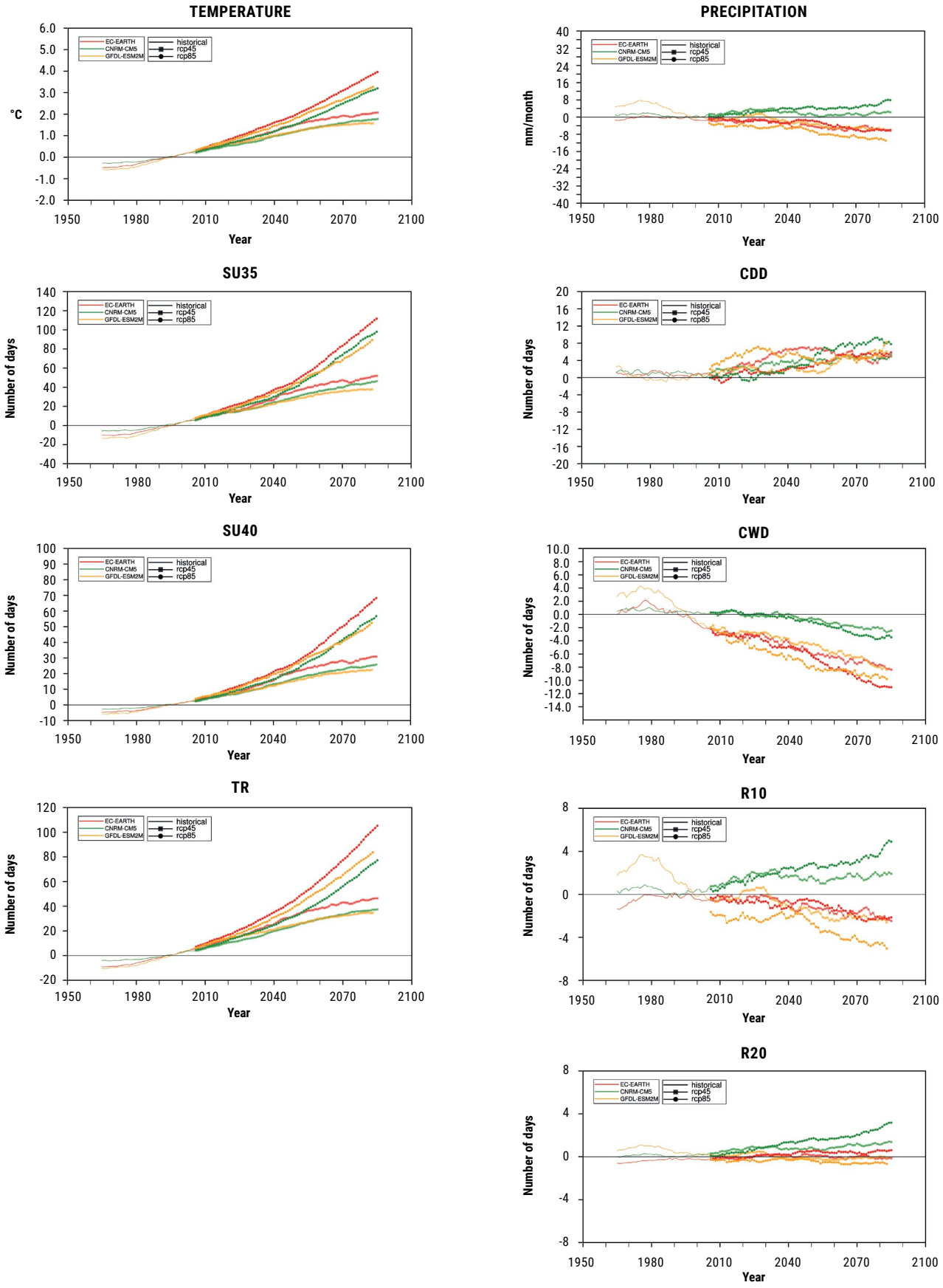

The change in mean temperature for RCP 4.5 shows an increase of 1.5 °C at mid-century and 1.8 °C at end-century. For RCP 8.5, temperatures increase to 2 °C for mid-century and 3.6 °C at end-century. At the seasonal level, the highest increase in temperature is shown to occur in winter with an increase of as much as 3.9 °C by the end of the century for RCP 8.5. As for precipitation, results for RCP 4.5 show a close projected change of –6% and –5% at mid- and end-century respectively. For RCP 8.5, precipitation change is –3% for mid-century and –5% by end-century, reaching the highest reduction in winter with a 7% decrease.

4.1.4 Regional hydrological modelling findings

The headwaters of the Blue Nile in the Ethiopian Highlands show wide variation between the individual ensemble members for runoff for both models (Figure 54) and no conclusive trend can be perceived. The mean values from discharge changes show a decrease over time but, given the high-value ranges in this case too, this trend cannot be considered conclusive. For instance, the change in mean discharge for end-century is –8% for RCP 8.5, but values range from –68% to 86%.

FIGURE 54: Mean change in runoff (using HYPE and VIC) and discharge (using HYPE) over time for ensemble of three RCP 4.5 and RCP 8.5 projections for the Blue Nile Headwaters

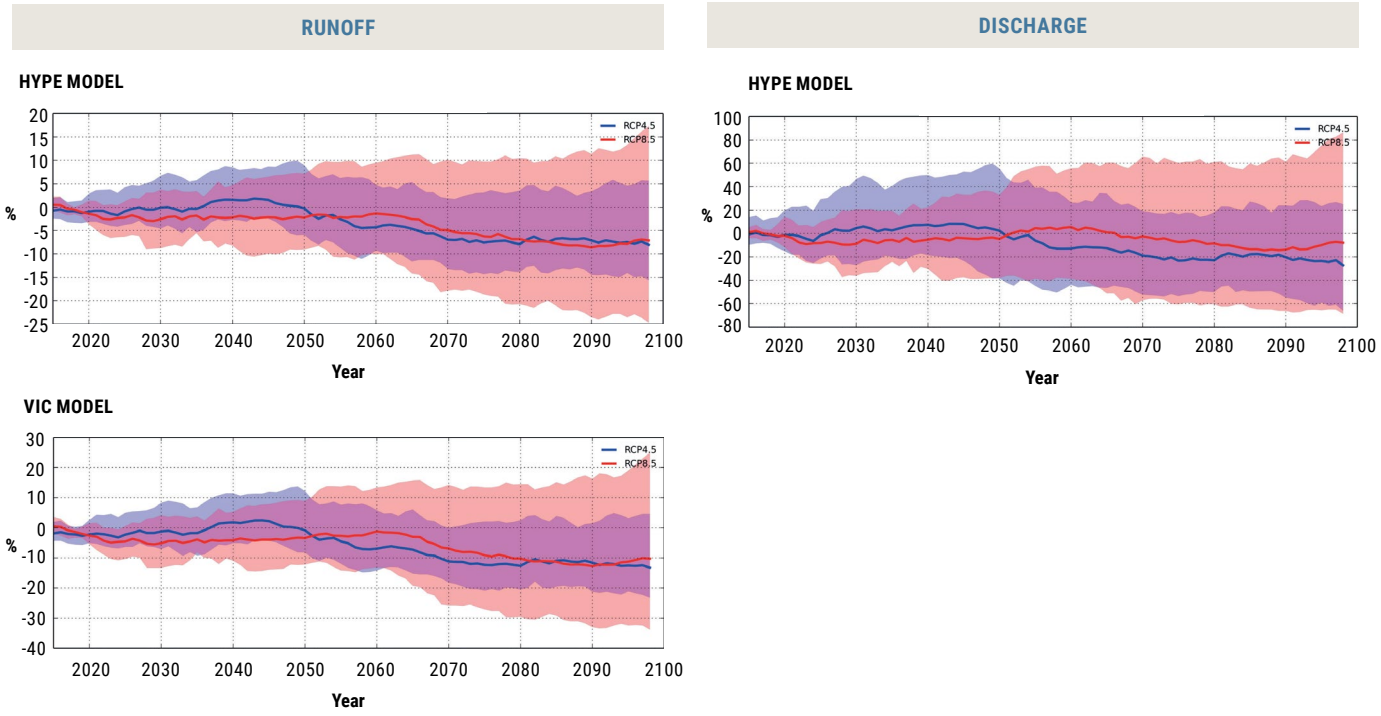

FIGURE 55: Comparison between 25 km (MNA22) and 50 km (MNA44) resolutions for mean change in runoff and discharge (using HYPE) over time for two RCP 8.5 projections for the Blue Nile Headwaters

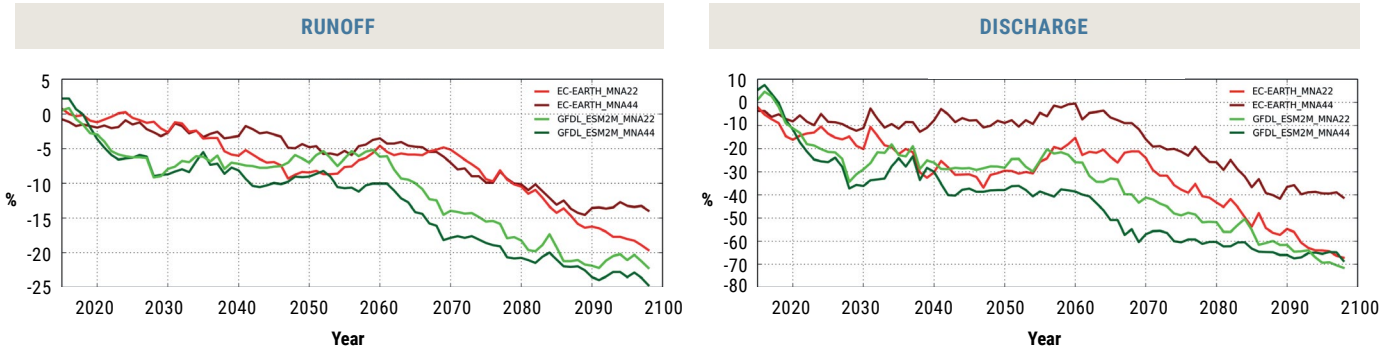

4.2 TIGRIS RIVER AND EUPHRATES RIVER BASINS

4.2.1 Overview and subdomain selection

The Euphrates River (Figure 56) originates in the mountains of eastern Turkey and reaches a length of 2,786 km as it flows through the Syrian Arab Republic and Iraq. It is joined by three tributaries in the Syrian Arab Republic: the Sajur, the Balikh and the Khabour rivers. The 1,800 km long Tigris River has four basin riparian countries: the Islamic Republic of Iran, Iraq, Syrian Arab Republic and Turkey. It originates in the Armenian Highlands in Turkey, flows south and merges with the Euphrates River in southern Iraq. The Tigris has a number of tributaries that make significant contributions to runoff along its course, most of which are shared by Iraq and Turkey or the Islamic Republic of Iran and Iraq. The Tigris and Euphrates merge to feed the Mesopotamian marshlands in southern Iraq. The combined catchment area of the Euphrates and Tigris river basins, including its outlet Shatt al Arab, is around 90,000 km^2, with the overall basin home to more than 50 million people in the Islamic Republic of Iran, Iraq, the Syrian Arab Republic and Turkey.[20] The basin climate is considered similar to a Mediterranean climate, with snowfall in winter in the mountainous Turkish headwater area, and an increasingly hot and dry (arid) climate as the rivers approach the sea. Mean annual precipitation in the basin ranges from approximately 1,000 mm in the Turkish headwaters in the north to 150 mm in the Syrian Arab Republic and just 75 mm in southern Iraq. Mean precipitation in the Tigris basin area is significantly higher than in the Euphrates Basin, owing to the high precipitation rates in the Zagros Mountains in the east of the Tigris basin, which contribute to Tigris streamflow. Most of the precipitation in the Tigris and Euphrates basin falls as snow and remains in the snowpack until the spring snowmelt.[21]

Most of the Euphrates streamflow originates from precipitation in the Armenian Highlands, with Turkey providing about 89% of the total Euphrates flow. While the three Euphrates tributaries used to make up around 8% of the annual Euphrates flow, their contribution has dropped today to 5% or less, due to decreased flow of the Khabour. In Iraq, there are no major surface-water contributions to the Euphrates, except for rare runoff events generated by heavy storms. Before 1973, the mean annual flow of the Euphrates at Jarablus was around 30 billion m^3, but this figure dropped to 25.1 billion m^3 after 1974 and fell to 22.8 billion m^3 after 1990. This is most likely due to climate variability and more frequent periods of drought and the construction of large dams in Turkey as part of the Southeastern Anatolia Project (GAP). Compared to the long-term mean discharge over the period of record from 1937 to 2010, the Euphrates records have shown below-average discharge at Jarablus and Hussaybah since 1999, possibly reflecting a combination of

FIGURE 56: Map of the Tigris and Euphrates river basins and subdomain extent

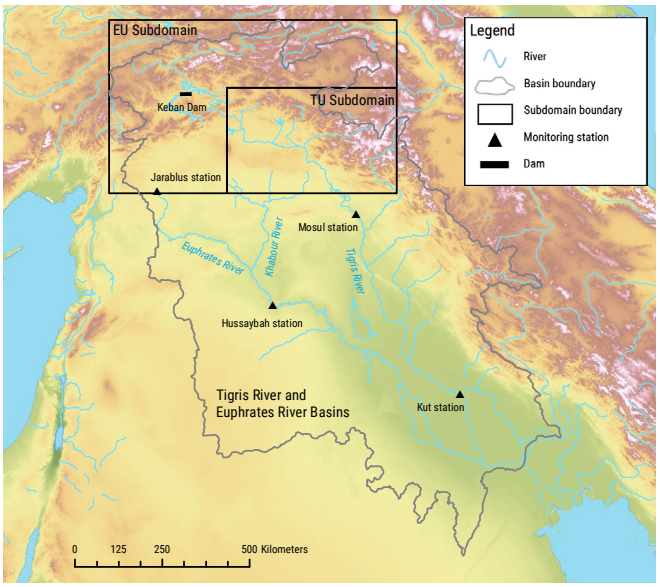

drier weather conditions and the effects of extensive dam-building. With the construction of large water-engineering structures in upstream Turkey and Syrian Arab Republic such as the Keban Dam in 1974 and the Tabqa Dam in 1975, the Euphrates flow regime has shifted towards less pronounced seasonal flow variation starting in the mid-1970s compared to the near-natural flow regime (1937 until the 1970s). The Tigris River exhibits mean annual flows of 20 billion m^3 at Mosul (1931–2011) and 25.7 billion m^3 at Kut station further downstream (1931–2005). Flow contribution to the mean annual flow volume of the Tigris from tributaries located between Mosul and Kut amount to an estimated 25 billion m^3.[22] The construction of several dams in Iraq may have led to a significant reduction in flow volumes in the course of the river, especially after Mosul, reflected in the changes in flow volumes at Kut since 1973 with a mean annual flow volume from 32 billion m^3 before 1973 to 16.7 billion m^3 for the period 1974–2005.[23] Compared to the Euphrates flow regime, the Tigris high-flow season is much longer and more pronounced due to higher winter precipitation over a much greater basin area. Its flow regime can be considered natural before the 1970s, with limited water regulation in the runoff generation area in Turkey, Islamic Republic of Iran and Iraq upstream of Mosul. Because of the extremely high seasonal and annual flow fluctuations in the Euphrates and Tigris rivers, storage facilities are a key concern for water resources management for the riparian countries in both basins.

4.2.2 Vulnerable sectors

The Euphrates and Tigris river basins are faced with increasing challenges in terms of demographic pressures, hydro-infrastructure developments and water-quality

concerns. These factors, in addition to changes in climate patterns and recent conflict situations, are set to deeply affect future water availability and associated socio-economic impacts in the basins yet further. The key vulnerable sectors to climate change in the Tigris–Euphrates basin are presented below.

Agriculture, food security and livelihoods

Agricultural development and food production in the Euphrates and Tigris riparian countries rely heavily on the availability of water in the basin. The droughts that were experienced in the 2000s convey important messages about what could happen in this area in the future if drought intensification occurs. Other extreme events such as dust storms (see next section), which have become more and more common over recent years, are also intrinsically linked to agricultural productivity in the basin. In Iraq, drought and land degradation are major factors jeopardizing food production, with the north depending on rainfall and the central and southern parts relying on irrigation. The extreme droughts of 2007–2009 that affected the country damaged almost 40% of the cropland, with higher intensity in the northern governorates and reaching over 50% in Ninawa and Erbil governorates. The situation caused 20,000 rural inhabitants to move in search of more sustainable access to drinking water and livelihoods. Crops for which Iraq was famous, such as dates, rice and grain, could no longer be grown because the Euphrates River was flowing well below its usual level. Syrian Arab Republic also experienced similar effects due to severe droughts: hundreds of thousands of Syrians lost their livelihoods and had migrated to cities by 2009. It was reported that around 160 villages in northern Syria were abandoned during this period due to reduced water availability. Several studies even connect the Syrian uprising and subsequent outbreak of civil war due to the drought and its consequences. Agriculture has long been a cornerstone of the Syrian economy and this sector is highly vulnerable to changes in climate patterns.[24]

Sensitivity to extreme events

Major impacts of extreme events have been observed in the basin in the last few years. In 2012, Baghdad suffered its worst recorded floods in 30 years; in May 2013, nearly 600 families were displaced by severe flooding and more than 30,350 ha of crops were damaged or destroyed by floodwaters in Missan, Qadissiya and Wassit governorates. Syrian Arab Republic was also affected by a series of floods and extreme weather, such as the snowstorms in Damascus in December 2013, as well as during the winter of 2014/2015 with torrential rain and flooding throughout the country putting a halt to all activities. Other common extreme event phenomena in the basin are dust- and sandstorms. The Euphrates and Tigris basin has been identified as a significant source area for dust storms in Iraq and across the region, with fallow agricultural lands considered the main

Tigris River, Iraq, 2015. Source: Ihab Jnad.

hotspots of dust generation. These storms have had severely negative socio-economic impacts such as budgetary losses, reduced visibility, which significantly disrupted transport, and increases in surface heat. It also further aggravated drought effects, damaged crops and soil and affected the public health sector with acute and chronic respiratory affections. Potential future changes in climate patterns in terms of extreme weather events are aspects of major importance to consider in the basin.[25]

Groundwater resources

It has been reported that, apart from pressures on surface-water availability, heavy exploitation of groundwater poses serious concerns for resource sustainability. A study published in 2013 with the use of NASA images from Gravity Recovery and Climate Experiment (GRACE) satellites revealed a dramatic increase in the dryness of the soil and depletion of below-ground water levels between January 2003 and December 2009. It indicated that the Euphrates and Tigris basins registered the second fastest rate of regional groundwater storage loss in the world after India. As strong interlinkages exist between surface- and groundwater in the Euphrates and Tigris river basins, groundwater depletion is thus also an issue of concern in the context of a changing climate.[26]

Water quality and ecosystems

Pollution from agricultural and domestic sources seriously affects water quality in the basin, with both rivers suffering from severe salinity which increases along the course of the river in Iraq. Moreover, in the Tigris basin region, the Mesopotamian marshes have suffered severe damage as a result of upstream damming projects in the 20th century, reducing the marshes to 14% of their original size. Water quality and ecosystems are thus also important aspects to consider in a context of changing climate and upstream water-regulation developments.[27]

Hydropower sector
The hydropower sector, including micro-hydrological installations, presents opportunities to improve access to electricity in Syrian Arab Republic, Lebanon, Tunisia and other parts of the region. In Iraq, hydropower represents 9.22% of the electricity supply. Temperature and precipitation effects from climate change and upstream developments could alter future hydrological conditions in these countries and, as a result, future hydropower generation.

A study by Pilesjo and Al-Juboori (2016) has shown that a reduction in rainfall by 10% in Iraq has the potential to cause a 25%–50% loss in hydropower generation. As a result of temperature increases of a few degrees, the impact of higher evapotranspiration on hydropower might result in a substantial decrease in generated electricity and thus in lower energy security.[28]

Geopolitical context
In addition to the role that hydrological conditions and water availability play in contributing to economic disruptions, the unrest that erupted in Syrian Arab Republic and Iraq have had severe impacts on urban water-distribution systems, including intentional attacks owing to their strategic value. Armed groups took control of many of the water-storing and regulating structures on the Euphrates in both Syrian Arab Republic and Iraq during the past few years, such as the Tabqah Dam in Syrian Arab Republic in early 2013, which put the water intake for the Aleppo governorate and parts of the Raqqah governorate out of service, depriving more than 5 million Syrians of access to safe water.

Another example is the control of the Mosul Dam in Iraq with major concerns over a cut in water supply, but most importantly a risk of dam collapse which is threatening the life 1.5 million inhabitants in the surroundings areas. This context of political instability is placing additional pressures on the resource and its management in Syrian Arab Republic and Iraq, especially in a context of potential reduced water availability due to climate impacts.[29]

These issues constitute the key current sector with potential severe implications in terms of climatic impacts; several other vulnerabilities also exist such as future changes in water demand and supply due to population and demographic patterns, as well as impacts of upstream developments.[30] Institutional frameworks for transboundary cooperation are also crucial components to take into account in view of future climate variability to ensure effective formulation and implementation of policies and strategies to address future climate variability and its potential impacts on the sectors mentioned above.

4.2.3 Regional climate modelling findings

Projected changes in temperature, precipitation and extreme events indices are presented in Figure 57 and Figure 58 for the Tigris and Euphrates headwaters, respectively.

The change in mean temperature for the Tigris headwaters show an overall increase towards end-century and more marked for RCP 8.5. At mid-century, the projected increase for RCP 4.5 is 1.8 °C and 2.2 °C at end-century. For RCP 8.5, the change is 2.5 °C for mid-century and up to 4.5 °C by end-century. Temperature in the summer season sees larger increases than the winter for this subdomain. Annual projected patterns of precipitation are variable for the Tigris headwaters with increases for RCP 4.5 (4% at mid-century and 1% at end-century). For RCP 8.5, precipitation change is negative with a reduction in 3% for mid-century and 4% for end-century. At the seasonal level, both the Tigris and Euphrates headwaters show a decrease of precipitation during winter and an increase during summer. For RCP 4.5, however, an increase in these basins is projected even for the winter. In general, precipitation changes are milder for RCP 4.5 than for RC 8.5.

Changes in mean temperature of the Euphrates headwaters follow the same trends as the Tigris headwaters in terms of increases towards end-century, with projected increases of 1.9 °C for RCP 4.5 at mid-century and of 2.3 °C at end-century. More marked changes are exhibited for RCP 8.5, with a temperature increase of 2.6 °C for mid-century and 4.8 °C for end-century. As for precipitation, increases are projected for RCP 4.5 (4% at mid-century and 3% at end-century). For RCP 8.5, no significant precipitation change is projected for either time period. Concerning precipitation extremes, in particular for the SDII indicator (not shown), four out of six projections displayed an increasing trend for the Tigris headwaters, while all projections showed increases for the Euphrates headwaters. The Euphrates headwaters subdomain, along with the Senegal River, were the only ones displaying increasing trends for the R20 index in all its projections, compared to the other subdomains where little change was projected.

Euphrates River, Iraq, 2017. Source: Naji Geha.

FIGURE 57: Mean change in temperature, precipitation and selected extreme event indices over time for ensemble of three RCP 4.5 and RCP 8.5 projections for the Tigris River Headwaters

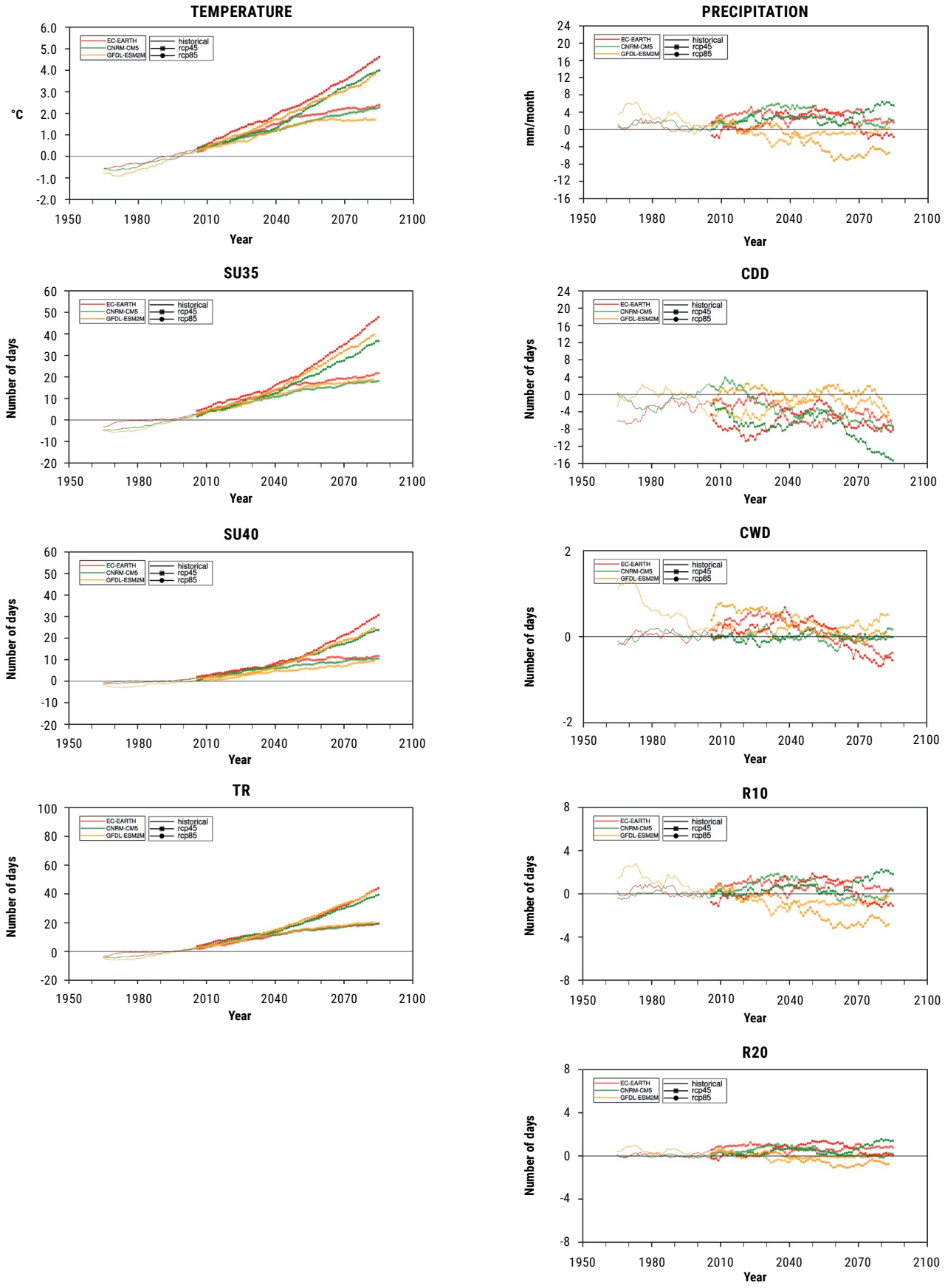

FIGURE 58: Mean change in temperature, precipitation and selected extreme events indices over time for ensemble of three RCP 4.5 and RCP 8.5 projections for the Euphrates River Headwaters

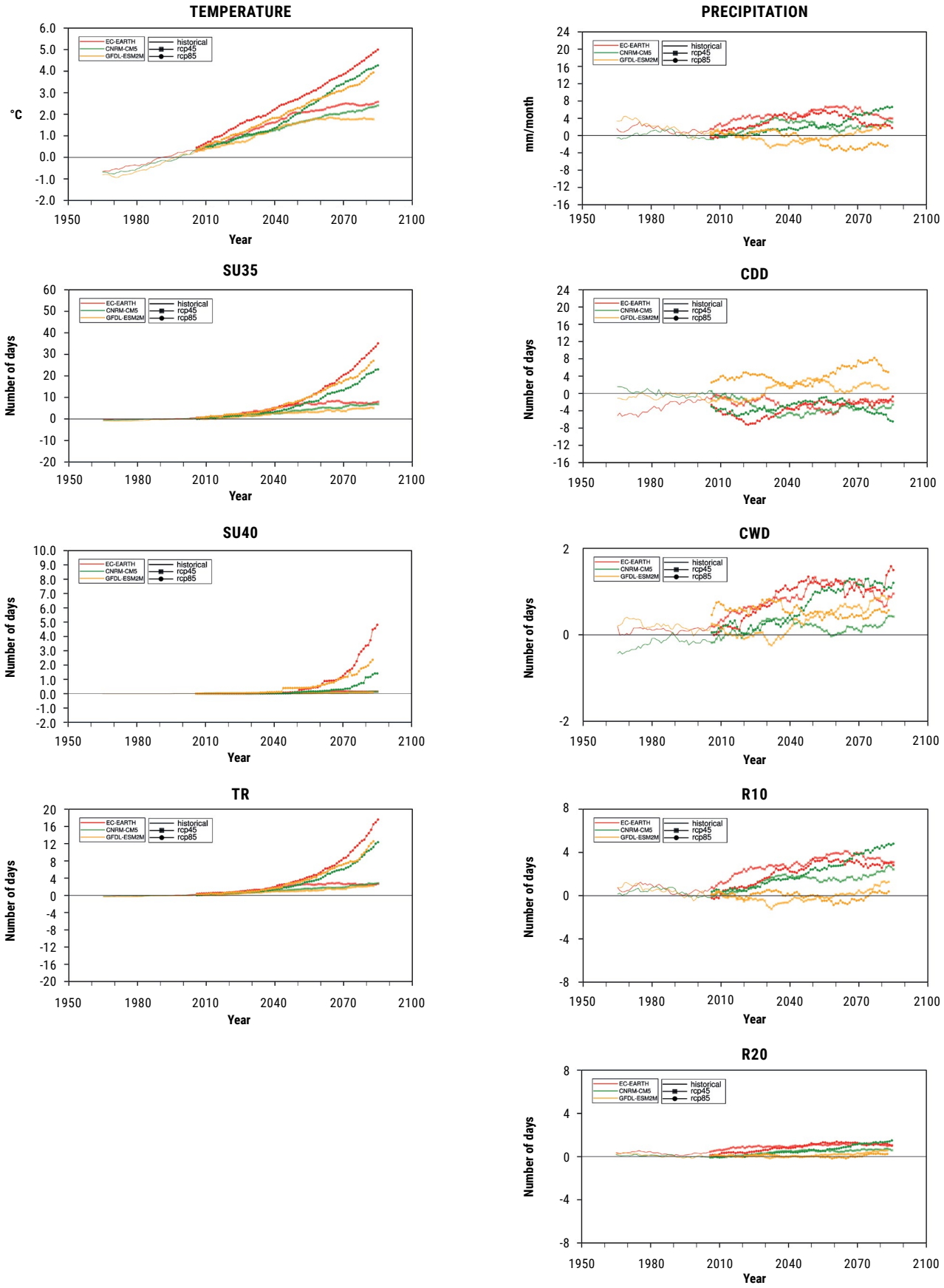

4.2.4 Regional hydrological modelling findings

The Tigris and Euphrates headwaters show small increases in winter runoff (Figure 59 and Figure 61) even when precipitation changes are negative. This is likely due to less snow storage compared to the reference period and thus increased runoff during winter followed by reduced runoff during the summer months, as there is reduced snowmelt, which is seen in the summer pattern of runoff for these basins.

For the Euphrates headwaters, both models project increases at the end of the century for RCP 4.5 (2%–6%, depending on the model), as well as increases in the winter season for these conditions (12%–14%, depending on the model). Moreover, a decrease in mean runoff is projected by the HYPE model in the summer season at the end of the century for RCP 4.5 (–5%) and RCP 8.5 (–22%). This decrease in runoff in the summer season is also projected for the Tigris headwaters, with both models showing a reduction at the end of century for both emission scenarios ranging from 6% to 9% for RCP 4.5 and from 15% to 22% for RCP 8.5, depending on the model.

Concerning change in discharge, no definite trend can be observed for mid-century for the Tigris and Euphrates headwaters due to the wide value ranges. At the end of the century, however, there is a projected decrease of 3% in mean discharge for the Tigris headwaters for RCP 4.5 (values varying from –5% and –2%) and –17% for RCP 8.5, though the latter range is from –28% change to no change. A signal of projected decrease in mean discharge for the summer period is also apparent (–18%) at end-century at RCP 8.5 with the range of values all indicating a decrease (–27% to–6%).

Projections for the Euphrates headwaters for the end of century exhibit a decrease of 17% in mean discharge (varying from –27% and –4%) for RCP 8.5. Mean discharge values are also projected to decrease in the summer season for the mid- and end-century time periods for RCP 8.5. The choice of GCM appears to have more influence on the discharge results for the Tigris and Euphrates than the resolution applied for the analysis, as observed in the figures below presenting the RCP 8.5 results for the 50-km and 25-km resolutions, although both signal a decline compared to the reference period by the end of the century.

It is worthy to note that projections for the change in the high flow value (100-year flow value) in the Euphrates show a decrease of 26% for RCP 8.5. A decrease is also reflected in the summer at both time periods and in the winter at end-century for this emission scenario. On the other hand, the Tigris headwaters exhibit a possible projected increase ranging from 6% to 11% in the high-flow value for RCP 4.5 for the end-century period.

FIGURE 59: Mean change in runoff (using HYPE and VIC) and discharge (using HYPE) over time for ensemble of three RCP 4.5 and RCP 8.5 projections for the Tigris River Headwaters

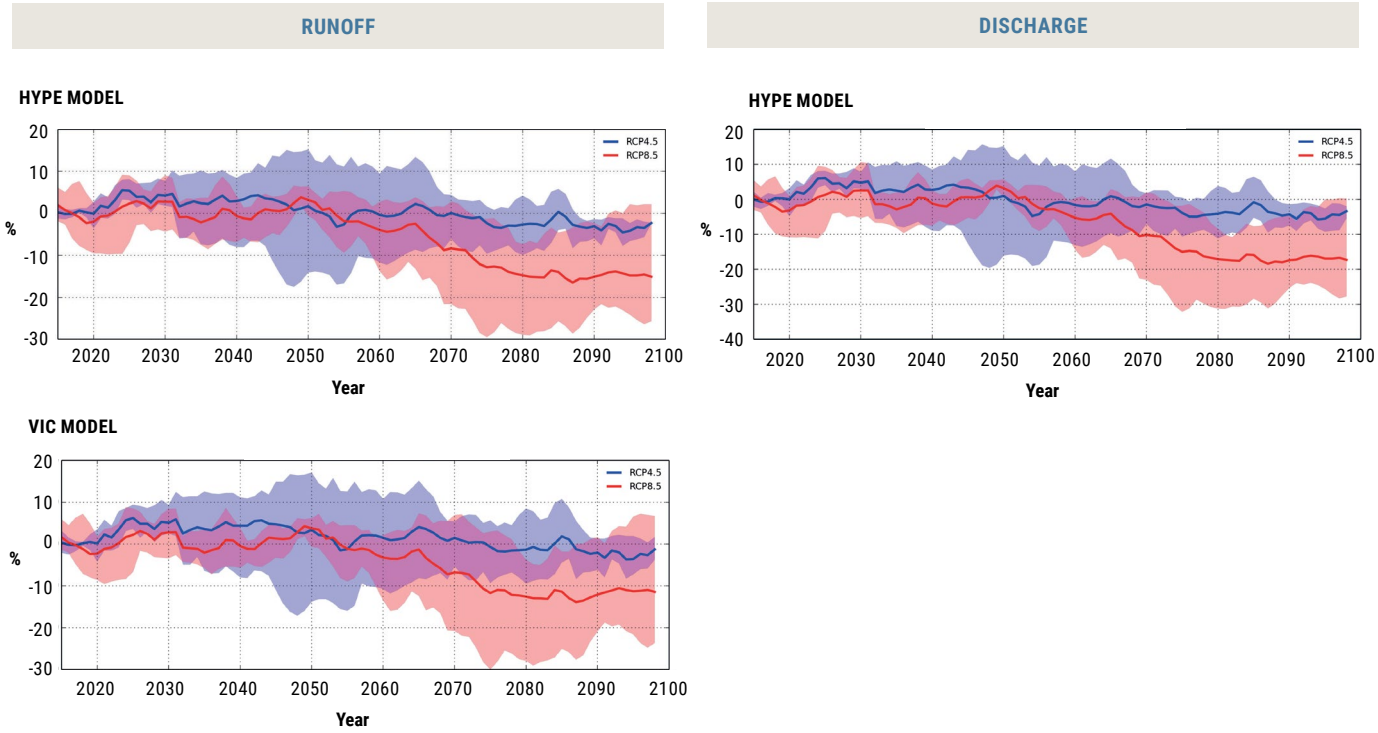

FIGURE 60: Comparison between 25 km (MNA22) and 50 km (MNA44) resolutions for mean change in runoff and discharge (using HYPE) over time for two RCP 8.5 projections for the Tigris River Headwaters

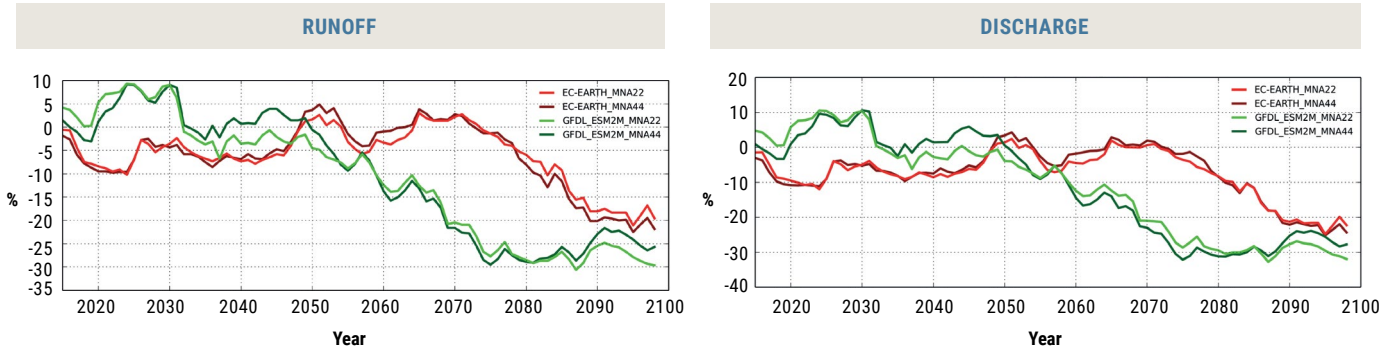

FIGURE 61: Mean change in runoff (using HYPE and VIC) and discharge (using HYPE) over time for ensemble of three RCP 4.5 and RCP 8.5 projections for the Euphrates River Headwaters

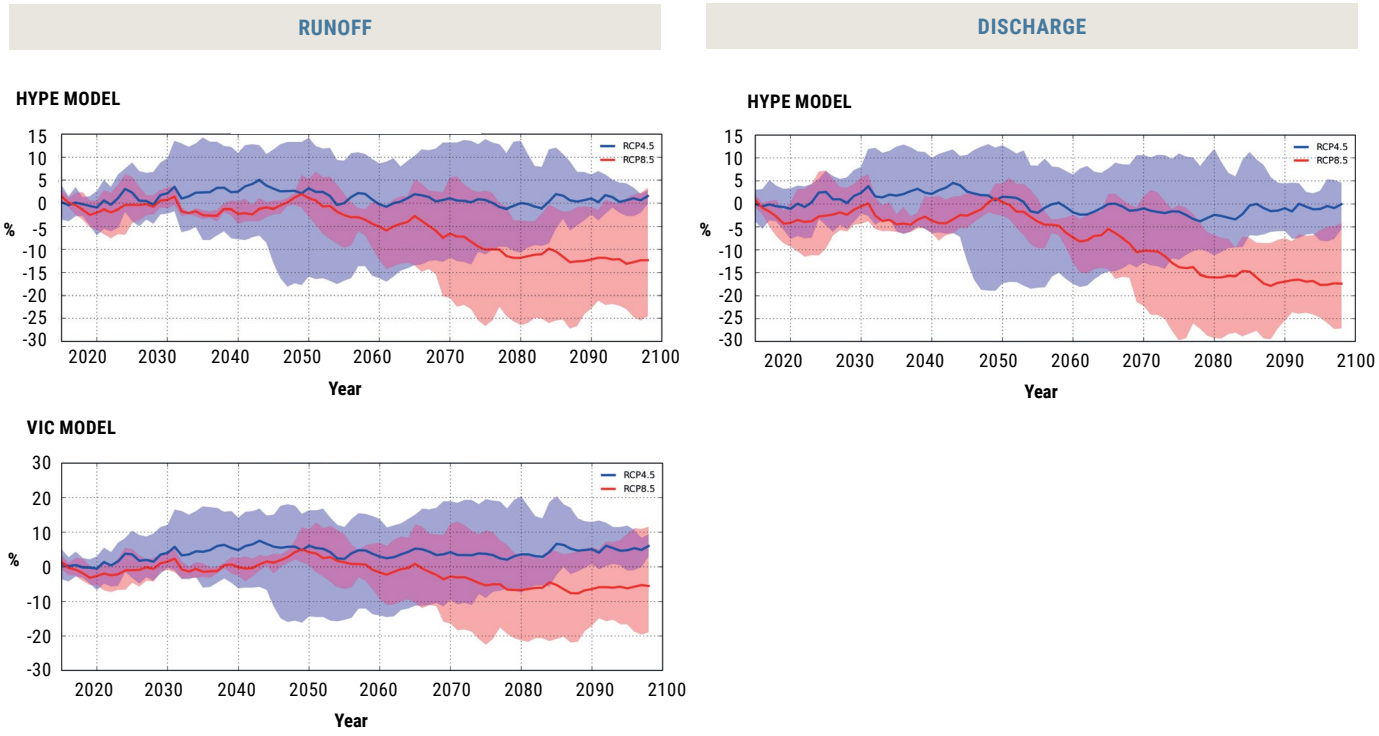

FIGURE 62: Comparison between 25 km (MNA22) and 50 km (MNA44) resolutions for mean change in runoff and discharge (using HYPE) over time for two RCP 8.5 projections for the Euphrates River Headwaters

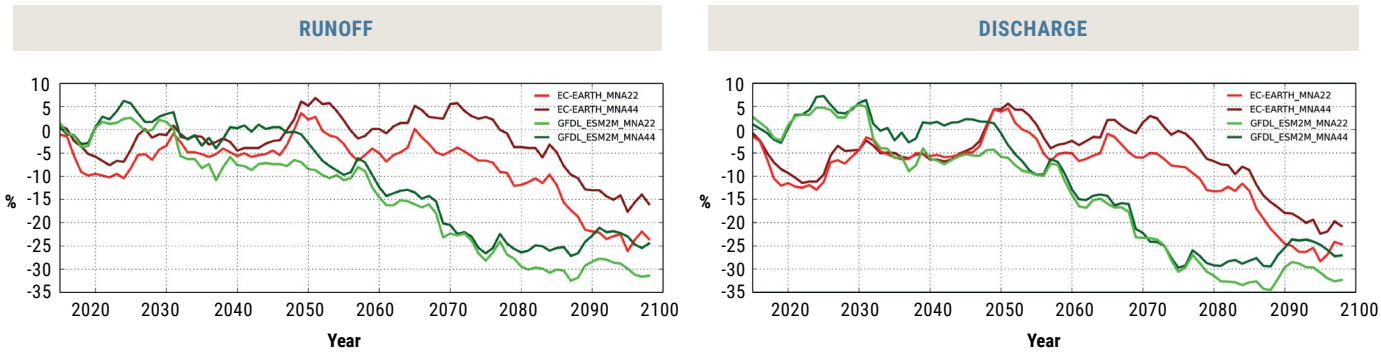

4.3 MEDJERDA RIVER BASIN

4.3.1 Overview and subdomain selection

The 484-km long Medjerda River originates in north-eastern Algeria, flows eastwards to Tunisia, and then discharges to the Gulf of Utica in the Mediterranean Sea (Figure 63). It is the longest river in Tunisia and the most important for this country in terms of water supply, providing around 37% of its surface water and 22% of its renewable water resources. Some 32% and 68% of the basin area (22,070 km²) are located in Algeria and Tunisia, respectively. In 2010, the total population in the basin was estimated to be 2.2 million.[31]

The Medjerda River basin climate can be classified as Mediterranean sub-humid to semi-arid with hot, dry summers and a winter rainy season. The source areas of the northern tributaries are the humid Kroumir Mountains (Souk Ahras area in Algeria), where summits exceed 1,400 m asl and annual precipitation ranges between 600 mm and 800 mm. The catchment area reaches over to the Dorsal Mountain range in the south, where semi-arid conditions prevail with precipitation not exceeding 400 mm/yr. Although situated near the Kroumir Mountains, the presence of a topographically induced rain shadow in the mid-Medjerda valley renders it a relatively dry region. The rainy season extends from September to May, with erratic rainfall and frequent high-magnitude flood events resulting in vast inundations of the floodplains. The annual average precipitation in the basin ranges from 350 mm/yr to 600 mm/yr.[32]

Even though the river is perennial, its hydrological regime is irregular, characterized by low flows with a regular appearance of extreme floods often exceeding 980 m^3/s. In 1973, the discharge reached 3,500 m^3/s at Medjez El Bab station (downstream of Sidi Salem Dam). These overflows threaten towns and rural populations living along the river, as well as important infrastructure such as irrigation systems and bridges in the lower valley and the Medjerda Delta. On average, the river's mean daily discharge is 30 m^3/s and thus constitutes up to 1 billion m^3/yr. A total of 11 dams are in operation in the river basin providing 59% (1,200 million m^3) of the total resources mobilized by dams in northern Tunisia. Another seven dams are planned or are under construction (300 million m^3).

It is widely reported that the dams have modified the river's flow regime since the implementation of these infrastructure development projects and, more precisely, after the construction of the largest Sidi Salem Dam in 1982, with the downstream channel progressively narrowing.[33]

FIGURE 63: Map of the Medjerda River Basin and subdomain extent

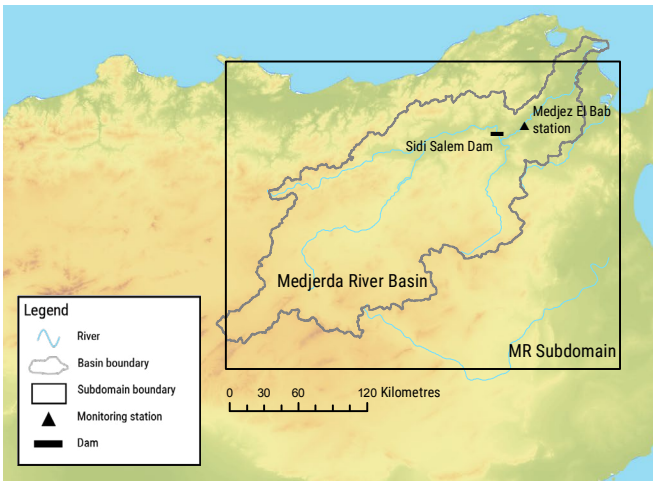

4.3.2 Vulnerable sectors

The Medjerda River is Tunisia's principal watercourse and constitutes, totally or partially, the water supply for more than half the Tunisian population, with some 2 million inhabitants living along the river and its tributaries and approximately 4 million additional inhabitants in the north-east and the centre-east of the country who are also supplied by water transfers from the basin. The vulnerable key sectors to climate change identified during the research are presented below.

Agriculture, food security and livelihoods
Agriculture is the primary economic activity in the basin and constitutes the bulk of production and employment with more than 87,000 people employed by this sector. The river occupies an essential place in the national strategy for food security as agricultural production in the basin contributes about half the total food production in Tunisia. The food security of the entire country is thus dependent on water supply from the river, knowing that it is used to irrigate about 90,000 ha, to which an additional 18,000 ha are partially irrigated with water transfers through the Larousia Dam. Given the river's importance for the rural livelihoods (63% of the basin population being rural), pluri-annual droughts are an issue of concern. Despite the presence of dams and water-transportation infrastructure, the risk of water deficit due to potential climate change impacts still exists, threatening the livelihoods of small-income farmers and their vulnerability to face supplementary investments as a result of droughts.[34]

Sensitivity to extreme events and dam siltation
An important characteristic of the Medjerda's River's hydrological regime is the regular appearance of extreme floods in the past (1969, 1973) as well as in recent years (2000, 2003, 2004, 2005, 2009 and 2012).

These floods have been devastating on both sides of the river, submerging villages and causing considerable loss of life. The flood of January 2003 in northern and central Tunisia was fatal to eight people and resulted in the displacement of 27,000 others.

The floods were exacerbated by the effect of the storage dams that are subject to significant siltation and have modified the river's flow regime. In particular, the construction of the Sidi Salem Dam in 1982 has caused the downstream channel to narrow down progressively. The purpose of the dam was to control and level off the interannual variable inflows to secure adequate domestic and agricultural irrigation water supply for the northern and central parts of the country, especially in Tunis. Water from the dam is also used to cool several power plants. Although it has contributed greatly to the development of the northern regions of Tunisia, it has also had significant adverse implications due to the silting of its reservoir, not only diminishing basin yield, but also impacting hydropower potential.

Some studies indicate that the dams that have been subject to siltation due to erosion and thus to reduced storage capacity, are expected to have even more storage reduction in the order of 30%-40% by the year 2030 as a result of the potential effects of climate change. During the flood of January 2003, the Sidi Salem and Mellegue Dams required releases of flood volumes of up to 1,300 m^3/s, causing an overflow of the riverbed, which was followed by the transport of large volumes of sediment. This contributed to increased flooding, as well as increases in the delta formation of the river mouth (equivalent to 6.2 km^2 during the 20th century time frame) and thus also affecting biodiversity. These overflows threaten towns and rural populations living along the river, as well as important infrastructures such as irrigation schemes and bridges in the lower valley and the Medjerda Delta. Moreover, as a densely populated area, the Medjerda River basin is at considerable risk if flooding events are to be more frequent in the future with potentially severe impacts on infrastructure, human security and economic development.[35]

Water quality and public health issues

The Medjerda River basin is characterized by many sources of pollution that are of considerable concern. During large floods, releases to agricultural plains downstream of dams cause the accumulation of sediments along the wadi beds, turning the coastal areas into "delta-like" structures, which also affects biodiversity. In addition, the basin is subject to deep waterlogging and salinization due to stagnation of saline runoff water resulting in land degradation of up to 60% of the land. Runoff and drainage waters enriched with soluble elements flow towards the lower parts of watersheds where salts migrate to the particular detriment of drinking-water quality and agricultural productivity.

In addition to natural conditions, water quality in the basin is largely affected by pollution from anthropogenic sources. These include industrial pollution due mainly to the food industry, such as the manufacture of dairy products, with industrial discharges estimated at 221 m^3/day. In addition, urban domestic pollution occurs due mainly to discharge of untreated domestic wastewater estimated at 1.27 million m^3/yr, as well as treated sewage discharge from 19 wastewater treatment plants estimated at 12 million m^3/yr that carry high pollutant loads of nitrogen and phosphorus. These loads are responsible for eutrophication observed in the reservoirs of the Sidi Salem and Siliana Dams.

Urban pollution also arises from the dumping of solid waste, estimated at 149,000 t/yr for the four northwest governorates of the Medjerda basin. This figure is tripled when all six governorates within the river basin are taken into account. Water quality and public health issues thus constitute an important sector to consider for further analysis in conditions of climate change due to their strong interlinkages with river hydrology and climate variability.[36]

Energy sector and hydropower

Hydropower capacity in the basin is expected to be further developed by both countries over the coming years. This is to be taken into account in view of potential changes in climate and climate variability, particularly in terms of water supply, to ensure the successful development of this sector.

4.3.3 Regional climate modelling findings

Figure 66 shows projected changes in temperature, precipitation and extreme events indices for the Medjerda River until the end of the century. All projected changes in temperatures indicate an increase over time as compared to the reference period, with the most marked for RCP 8.5, reaching a change of 3.5 °C by the end of the century. The highest change is projected in the summer season for these conditions, with an increase of 4.1 °C. For the emission scenario RCP 4.5, increases are 1.2 °C and 1.6 °C at mid- and end-century, respectively.

Changes in precipitation indicate an overall reduction, with considerable differences between both emission scenarios, in particular at end-century. Projected change for RCP 4.5 is –6% at mid-century and –4% at end-century. On the other hand, for RCP 8.5, precipitation change is –9% for mid-century and –19% for end-century. These differences are especially apparent in the projected change for the winter season, where the change is –8% in mid- and end-century for RC4.5, while the change is –13% at mid-century and –21% at end-century for RCP 8.5.

FIGURE 64: Mean change in temperature, precipitation and selected extreme events indices over time for ensemble of three RCP 4.5 and RCP 8.5 projections for the Medjerda River basin

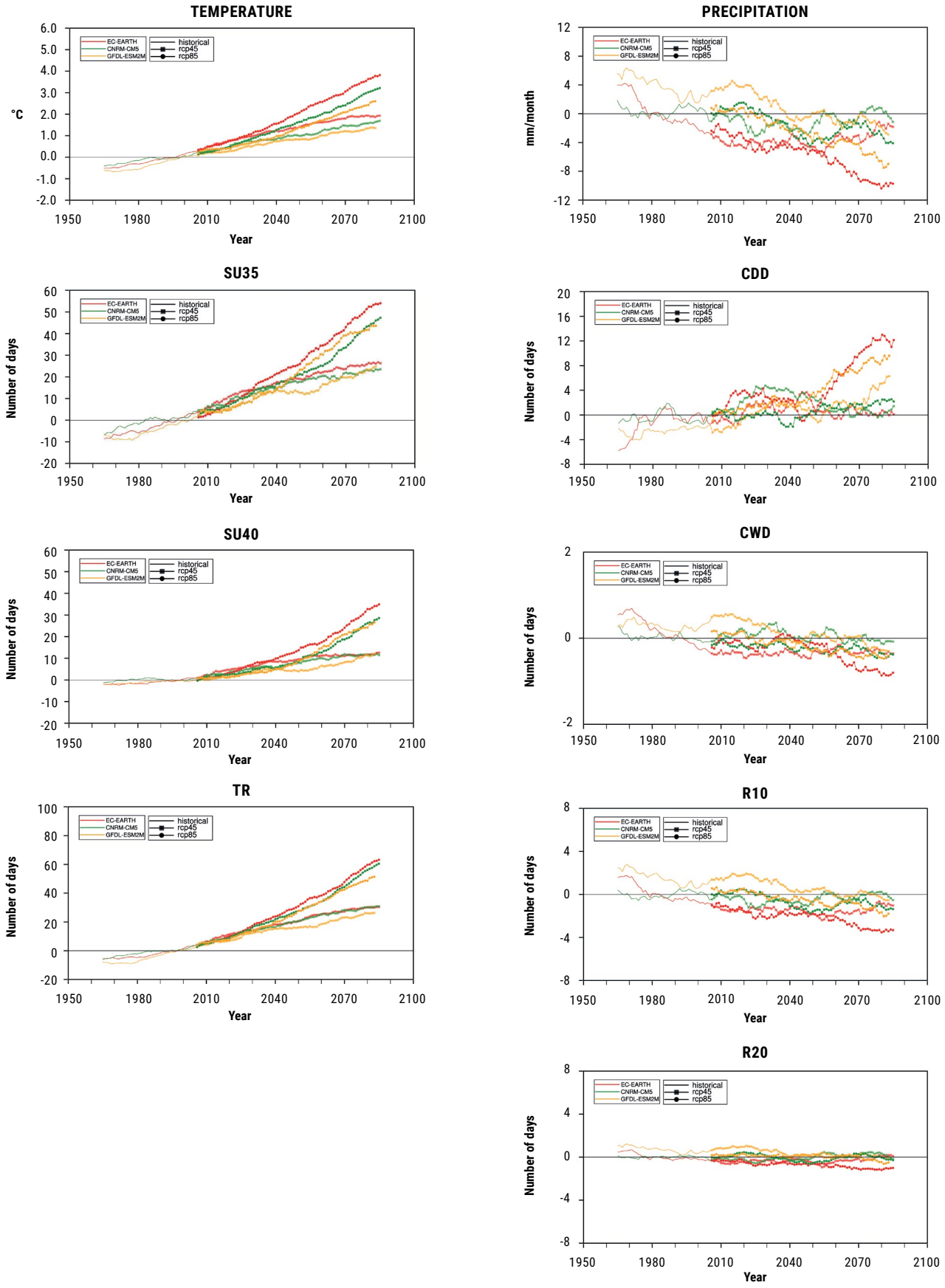

4.3.4 Regional hydrological modelling findings

The Medjerda River basin shows results similar to those of the Moroccan Highlands in terms of mean runoff change with a decrease over time, but not as severe (Figure 65). Both models project a decrease at mid-century for both emission scenarios, with 15%–16% reduction at RCP 4.5 and 31%–32% at RCP 8.5, depending on the model. A 41%–42% reduction in runoff is also projected at end-century for the RCP 8.5 emission scenario.

The same patterns appear at the seasonal level with no difference between the winter and the summer seasons.

Changes in mean discharge projections hold a wide range of values for RCP 4.5 and thus no trend can be concluded. For the RCP 8.5 emission scenario, projections for both time periods show a marked decrease, with –42% change at mid-century (ranging from –47% to –37%) and –53% at end-century (ranging from –60% to –40%).

It is worth noting that decreases are projected in the high-flow value compared to the reference period for RCP 8.5 at mid-century. On the other hand, projections show a mean increase of 60% at end-century for RCP 4.5, however the range of values (–54% to 170%) cannot allow this increase to be confirmed.

FIGURE 65: Mean change in runoff (using HYPE and VIC) and discharge (using HYPE) over time for ensemble of three RCP 4.5 and RCP 8.5 projections for the Medjerda River

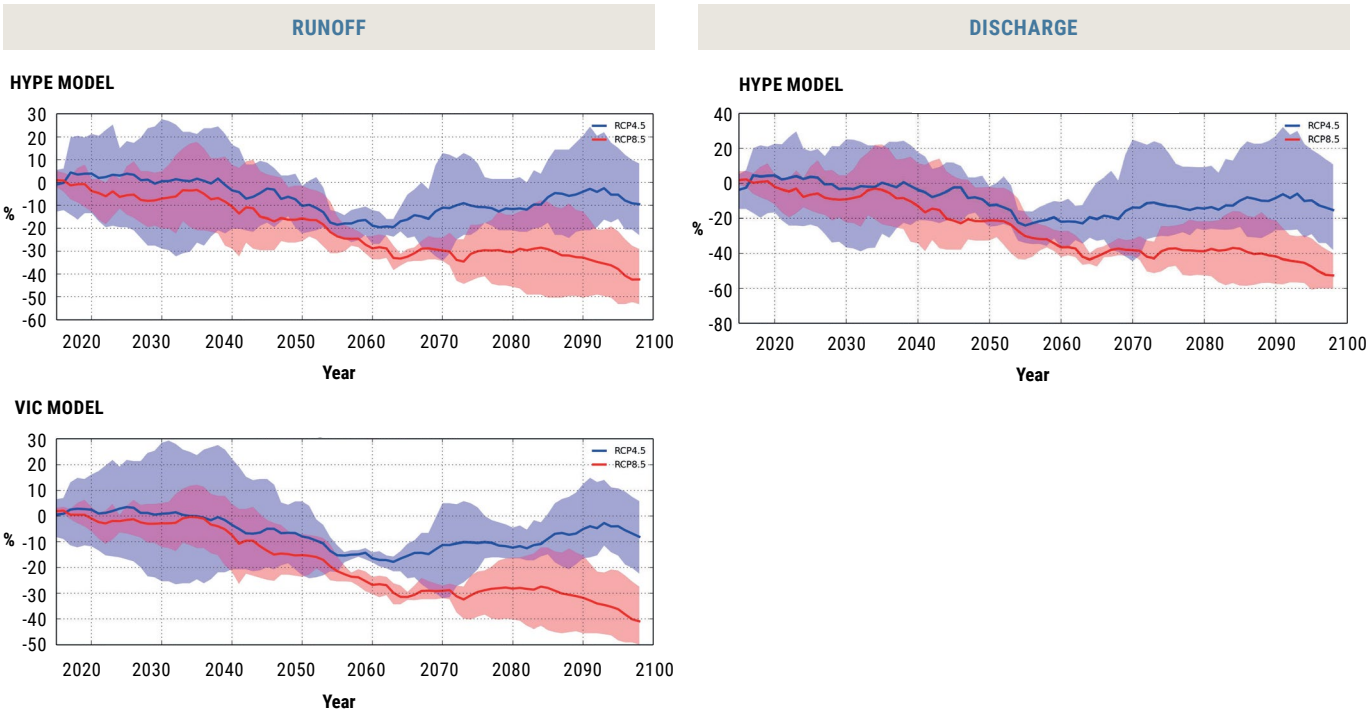

FIGURE 66: Comparison between 25 km (MNA22) and 50 km (MNA44) resolutions for mean change in runoff and discharge (using HYPE) over time for two RCP 8.5 projections for the Medjerda River

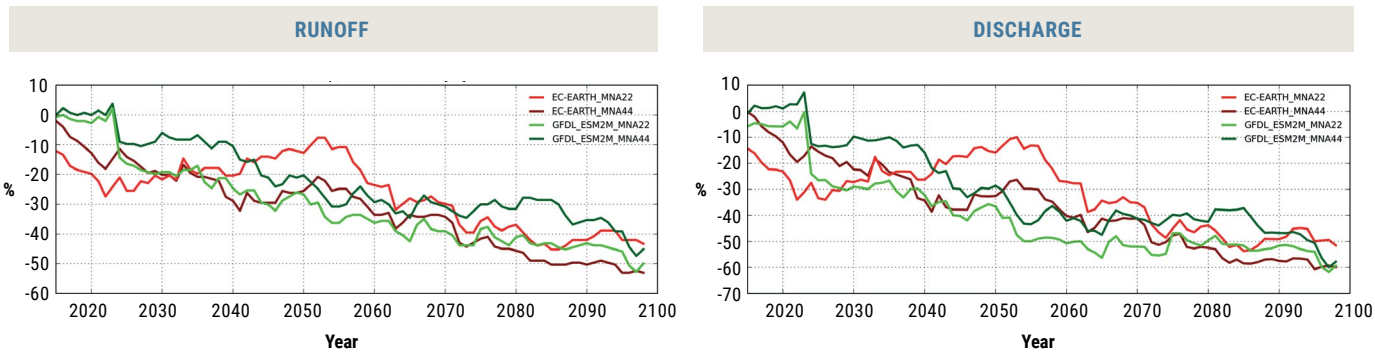

4.4 JORDAN RIVER BASIN

4.4.1 Overview and subdomain selection

The Jordan River (Figure 67) originates in the Anti-Lebanon and Jabal el Sheikh mountain ranges and covers a distance of 223 km from the confluence of the headwaters to the point of discharge into the Dead Sea. Its basin area is estimated at 18,285 km^2 (excluding the Dead Sea), distributed among several riparian countries.[37] Tributaries of the river include the Hasbani, the Liddan, and Banias rivers, which converge and flow into Lake Tiberias. As the flow leaves Lake Tiberias, it receives the waters of the Yarmouk River, which is the longest tributary in the basin and contributes significantly to it. The river is further joined by the Zarqa River in Jordan as well as several eastern and western side wadis in its lower course.

The Jordan River basin displays broad climatic variations within a relatively small area due to the rapidly changing topography which creates different microclimates. A small area in the northern part of the basin consists of mountains in Lebanon and Syrian Arab Republic, while the slopes of the north-eastern mountain ridges and parts of the east bank of the Jordan River are characterized by a dry, temperate Mediterranean climate.

The hillsides of the West Bank and the Jordan Valley have a steppe climate with low precipitation and mean annual temperatures above 18 °C. Parts of the Syrian plateaus and most of the Jordanian Highlands have an arid climate. Precipitation rates in the basin vary from 1,600 mm to 2,400 mm on the eastern slopes of Jabal el Sheikh in the north to less than 200 mm/yr in the lower West Bank and less than 100 mm/yr on the Dead Sea coast. Rainfall declines from north to south and from west to east. The basin has pronounced seasonal climate variability, with strong fluctuations in rainfall from year to year.[38] At its outlet at the Dead Sea, the river had a historic average annual discharge of some 1,300 million m^3 in the 1950s but this value has dropped dramatically to 20–200 million m^3 at present due to high levels of water abstraction through regulation and diversion structures over its course.[39]

4.4.2 Vulnerable sectors

The Jordan River basin is the focus of long-standing water disputes and territorial conflicts; the management of water resources in the basin is thus intimately linked to the regional geopolitical situation. Numerous attempts at cooperation between riparian countries in the basin have been pursued since the early 20th century, but with limited success,

FIGURE 67: Map of the Jordan River Basin and subdomain extent

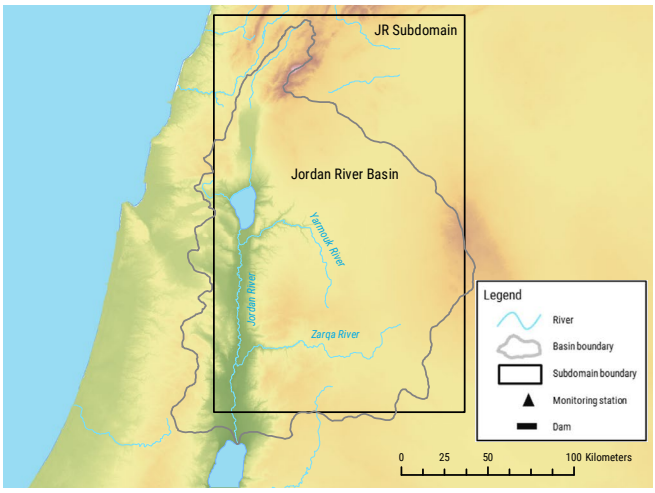

which adds to the difficulty of responding to climate change challenges on scarce water resources and water-dependent sectors. The key vulnerable sectors to consider in this context are presented below.

Agriculture, food security and livelihoods

Given its large consumption of water and importance as the key source of rural livelihoods, agriculture is the sector most sensitive to climate variability and change in the West Bank. The bulk of the cultivated land is located in the Jordan River Valley, which is considered "the food basket" in the State of Palestine. This sensitivity is heightened by a reliance on rainfed agriculture (94 % of the agricultural area in the West Bank). Agricultural livelihoods, particularly within rural rainfed farming communities, are always directly affected by rainfall and drought incidence. Rainfall reduction and variability are the most important climate risk to rural livelihoods and can lead to severe negative effects on agricultural yields: completely altering a growing season if a reduced or delayed rainfall event occurs, for example.

This situation has taken place in several regions of the West Bank, where the northern governorate of Tubas is economically dependent on agriculture and has experienced repeated droughts contributing to reduced spring flow, limiting the time farmers have for irrigation and producing second or third harvests. Dry years also result in freshwater cuts by the Mekorot water utility to residents in the Jordan River Valley (as was the case during the dry year of 2008), thereby limiting the number of harvests. In Jordan, agricultural production is concentrated in two main regions, namely the western highlands where rainfall is relatively high, and the Jordan Valley. While the Jordan Valley is a much smaller area of land compared to highlands, this is where the bulk of the country's agricultural production occurs and thus where most of Jordan's surface water resources are directed.

Water pumped from the Yarmouk River and nearby wells into the King Abdallah Canal has served as the major water supplier for agriculture in the Jordan Valley, thus representing the backbone of irrigated agriculture. Even though other sources of supply are increasingly being used for this sector, such as treated wastewater, changes in climate patterns coupled to the natural water scarcity still have the potential to severely harm agricultural productivity in this region.[40]

Sensitivity to extreme events

Abnormally low rainfall in the basin has recurrently triggered drought events, resulting in economic losses, lowered agriculture productivity and threats to social and economic growth. This was witnessed in the State of Palestine, for instance, in particular between 2003 and 2010, which was characterized by below-average rainfall and several episodes of agricultural drought.

One example of extreme impacts is the case of Al-Auja village, a rural community located in the West Bank Jordan Valley which was once famous for its agricultural trade. The rich water and soil resources in the area enabled the village to be one of the few that could cultivate several crops and its agricultural productivity was completely dependent on the Auja Spring as the sole irrigation source.

Pressured water resources, drought and decreased precipitation rates ultimately resulted in a significant decline in water availability and the drying-out of the spring. This has had a destructive impact on the Palestinian agricultural economy with thousands of square kilometres lying dry or abandoned today due to lack of access to water and declining rates of precipitation (projected decline of up to 3.8 mm/month on average for RCP 8.5, end-century).

As outlined previously, risks of drought also severely impact livelihoods, particularly with the lack of access to water in situations of scarcity. Restrictions on movement and access to land resources and markets jeopardize the watering and seasonal migration of herds, reduce grazing land and, in many cases, prevent access to closer filling points. This has forced herders to purchase water from more distant (but accessible) filling points, incurring higher transportation costs. Impacts of droughts were also severe in Syrian Arab Repuglic and Jordan.[41]

Energy sector and hydropower

The direct energy consequences of climate change impacts are most likely insignificant in relation to bulk power supply priorities in the State of Palestine. There is continuing growth in energy demand across all sectors and a heavy reliance on energy imports.

Expected vulnerabilities from climatic changes relate to increased energy demands to cope with more temperature extremes at the household level, and to mitigate effects on human health and the agriculture sector. Jordan does not have indigenous energy sources, which makes the country fully dependent on imported fossil fuel.

However, some recent developments and water infrastructure plans should be taken into consideration within a context of climate change, since the water and energy sectors are closely interrelated. For instance, the proposed Red Sea–Dead Sea Canal Project involves pumping seawater from sea level at Aqaba, up 230 m in order to cross over the mountains in its path and then down to 420 metres below sea level to the Dead Sea.

The downward flow of water would be used to generate hydropower, which would partially or wholly provide the energy to desalinate the seawater for consumption in Amman and surrounding population centres. The Disi-Amman water-conveyance project also involves pumping requirements reported to be 50 MW or 2% of Jordan's annual energy consumption. The interlinkages between water resources and energy production/consumption should thus be considered and further investigated in climate change conditions with possible impacts on water and energy supply in the Jordanian part of the basin.[42]

Groundwater

Groundwater is by far the main source of water for the West Bank. With groundwater being extracted beyond sustainable limits in this area, potentials of precipitation decline and warming would exacerbate stresses on water quantity and quality. The western and southern governorates of the West Bank constitute recharge zones for groundwater, which is dependent on precipitation and evapotranspiration rates, and thus affects water availability in the east which fall within the Jordan River basin delineation.

A case of potential decline in rainfall in the coming years could also pose a significant problem for Jordan as precipitation is the only source of recharge for aquifers. Moreover, an overall increase in local and regional irrigation demand has serious implications in the country since further stress, including increased salinity, will be put on the groundwater resource which contributes about 50% to the total freshwater supply in the Lower Jordan River Basin.

The overexploitation of groundwater in the highlands also negatively affects spring discharges and base-flow runoff in rivers that constitute the major sources of water for irrigated agriculture in the Jordan Valley.

This hydrological connection between rainfall, surface- and groundwater is of major importance in terms of vulnerabilities under conditions of climate change.[43]

Water quality and public health issues

Water quality is a serious issue in the basin with the river's quality rapidly deteriorating along its course, displaying extremely high saliniy and pollution rates, particularly in its lower portion. These water-quality issues could be exacerbated and should be taken into consideration in a context of climate change. Issues of public health are also of concern. For instance, Palestinians living in the Jordan Valley area are set to face increased public health issues related to the lack of water, such as dehydration, diarrheal diseases and cholera. A major issue is the growing populations and distribution of mosquitos which are expensive to treat. The risk of parasitic disease should be taken into account in a context of climate change as changes in annual and seasonal climate variability, elevated mean temperature and extreme weather events may allow the spread of existing vectors and the establishment of new, invasive ones.[44]

Geopolitical context

Civil unrest has affected, and continues to affect, water resources management in the basin. In Lebanon, governmental plans to develop and make full use of the water resources of the Hasbani River and Wazzani springs has been the subject of recurrent tensions. In the West Bank, the occupation and restrictions on access to agricultural lands is compounded by climate-induced pressures on water resources and places health and livelihoods at risk.

Jordan has been subjected to additional water stress due to the influx of displaced peoples from neighbouring States. Since 2011, Jordan has received approximately 657,000 Syrian refugees,[45] who are situated in urban settlements throughout the country and are placing additional pressures on Jordan's scarce water resources. There have also been indications of risks of pollution of the main aquifer lying beneath the Zaatari camp due to wastewater leakages. Additionally, overpumping of the Amman-Zarqa aquifer is another source risk facing water resources in this region.[46]

In addition to the above-mentioned issues, further vulnerabilities in conditions of climate change are also of importance, such as demographic development and the vast urban expansion which leads to considerable increases in water demand.

Potential decreases in precipitation could worsen the existing water scarcity problems in the lower Jordan River basin, for instance, where more than 80% of Jordan's water resources and population are concentrated. Moreover, institutional frameworks and transboundary cooperation aspects are crucial sectors to consider in order to ensure the development of policies to counteract the potential negative effects of a changing climate, noting that the prolonged conflict in the basin region directly affects the prospects of joint water management.[47]

King Talal Dam, Jordan, 2017. Source: Carol Chouchani Cherfane.

4.4.3 Regional climate modelling findings

Changes in temperature, precipitation and extreme events indices until end-century for the Jordan River are presented in the plotted time series in Figure 68. Increases in mean temperatures are projected over time, with changes of 1.2 °C at mid-century and 1.5 °C at end-century for RCP 4.5. For RCP 8.5, temperatures projections show increases of 1.7 °C at mid-century and 3.2 °C by end-century.

Precipitation is projected to decrease and become more marked at end-century for RCP 8.5. For this emission scenario, projected precipitation change is –7% for mid-century and –13% by the end of the century, as compared to RCP 4.5, which exhibits a change of –7% at end-century. A decrease in precipitation of 22% is projected in the summer for RCP 8.5 at end-century. As for precipitation extremes, four out of six projections showed an increasing trend for the SDII indicator (not shown) indicating higher precipitation intensity.

FIGURE 68: Mean change in temperature, precipitation and selected extreme events indices over time for ensemble of three RCP 4.5 and RCP 8.5 projections for the Jordan River Basin

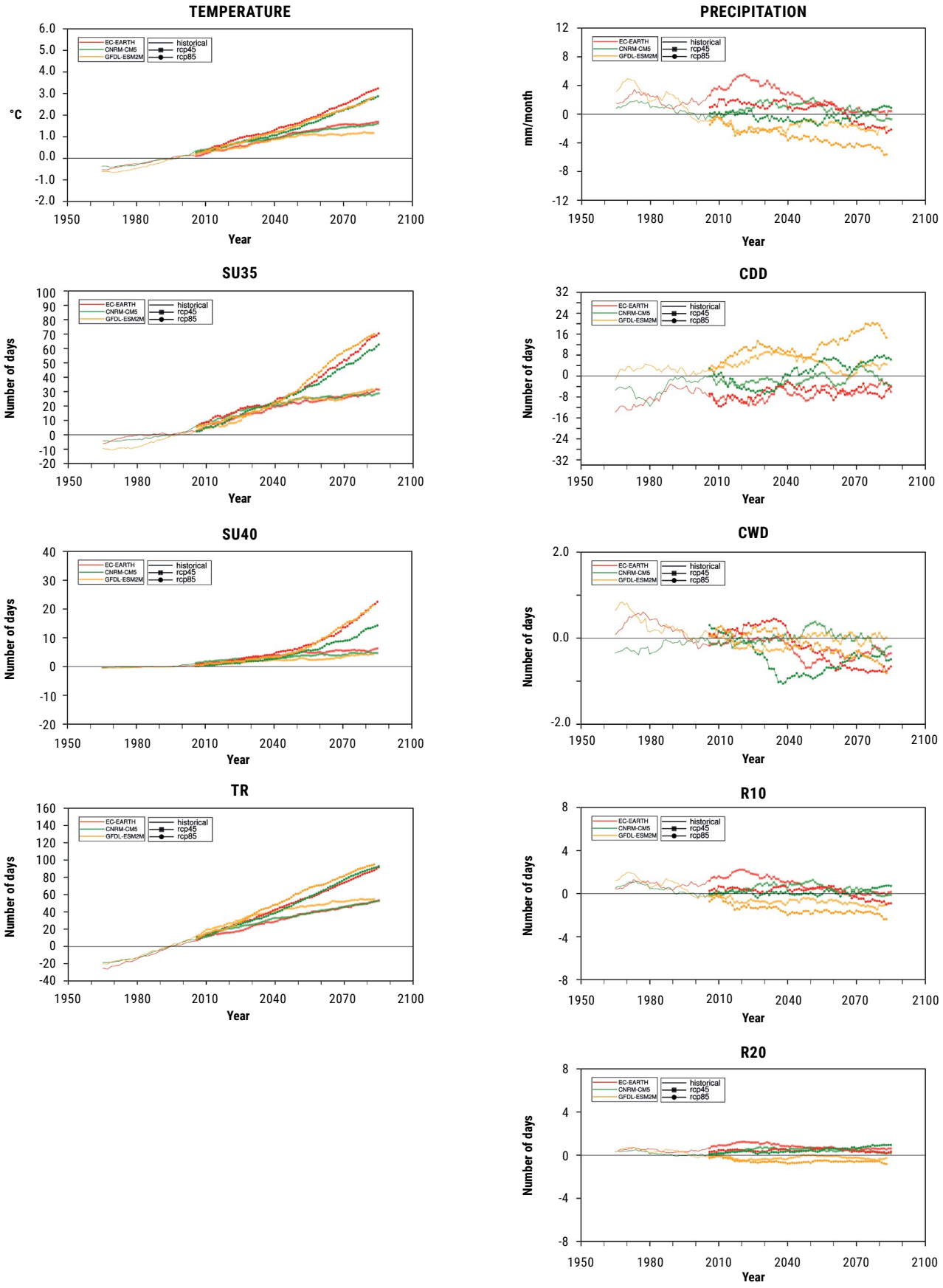

4.4.4 Regional hydrological modelling findings

Overall projections for runoff using both models exhibit a wide range of values and thus no confirmed trend can be concluded, as shown in Figure 69. The only consistent range of values is exhibited by projections from the model HYPE in the summer season for RCP 8.5, with a projected mean decrease in runoff of 21% at mid-century and 23% at end-century. Projections for change in mean discharge show an overall decrease at mid-century for RCP 8.5, as well as for both RCPs at end-century. Given the wide value range, however, no trend can be concluded as to the extent of the reduction in discharge. For instance, the decrease in mean discharge for RCP 8.5 at end-century is 37% but values range between –58% and –4%. As previously mentioned, high uncertainties remain with regard to discharge results for this subdomain, as human influence is not accounted for and can have significant effects on the hydrology, especially considering the size of the river basin.

FIGURE 69: Mean change in runoff (using HYPE and VIC) and discharge (using HYPE) over time for ensemble of three RCP 4.5 and RCP 8.5 projections for the Jordan River

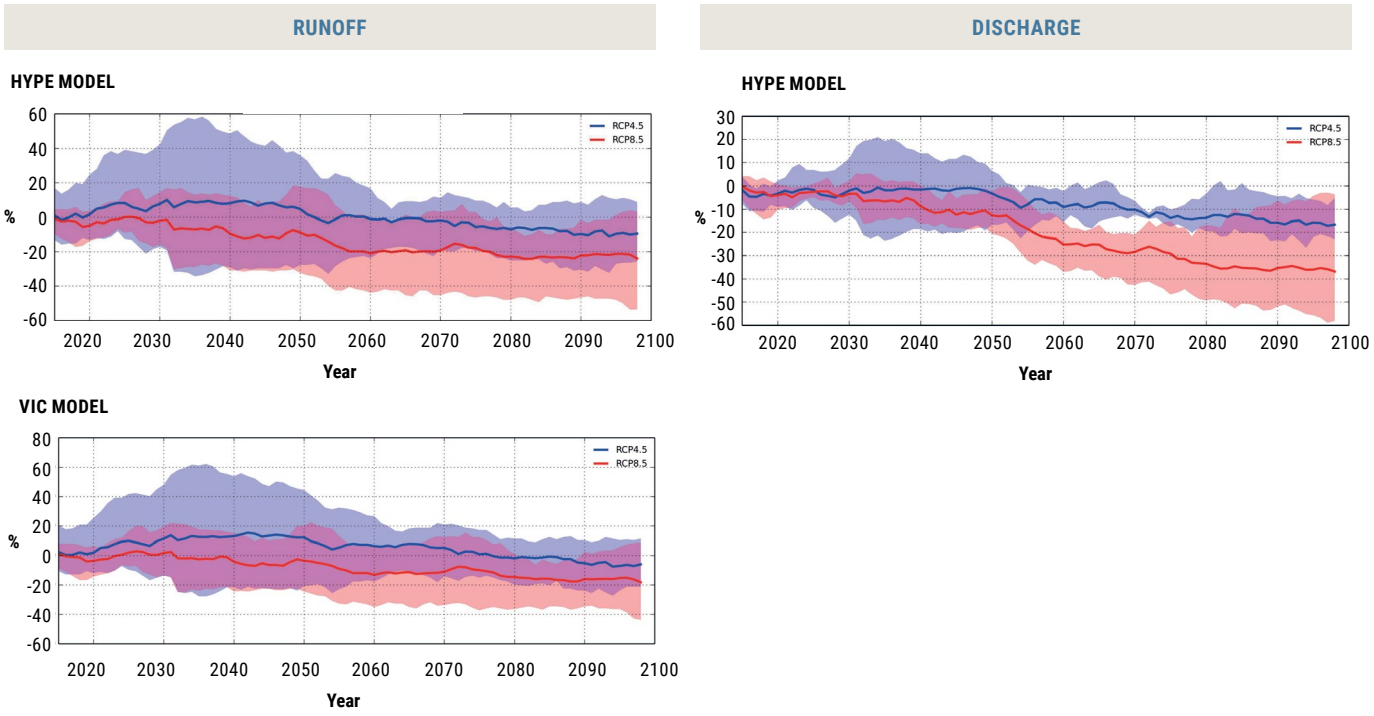

FIGURE 70: Comparison between 25 km (MNA22) and 50 km (MNA44) resolutions for mean change in runoff and discharge (using HYPE) over time for two RCP 8.5 projections for the Jordan River

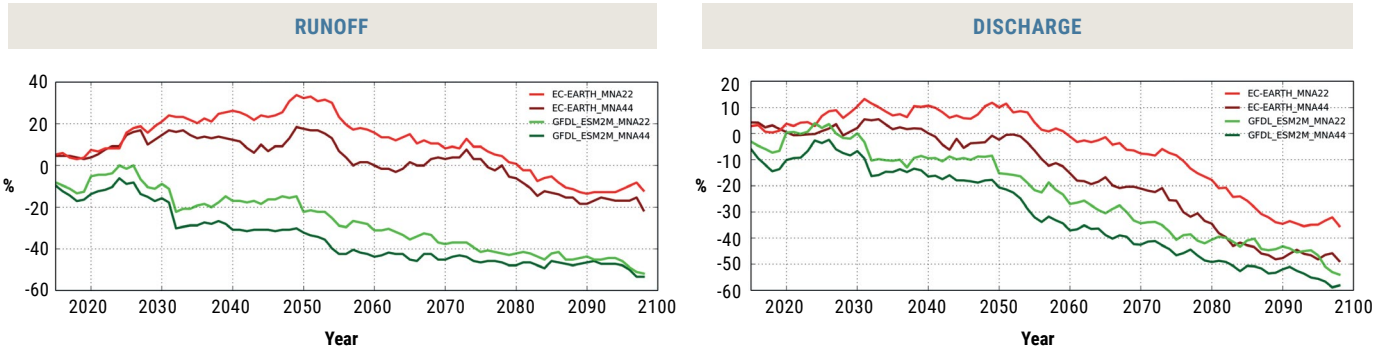

4.5 SENEGAL RIVER BASIN

4.5.1 Overview and subdomain selection

With a length of 1,800 km, the Senegal River is the second-largest river in western Africa. It originates in Guinea, flows through western Mali and then forms the border between Mauritania and Senegal on its way to the Atlantic Ocean (Figure 71). The basin covers a surface area of some 300,000 km^2 mostly in Mali (53%), followed by Mauritania (26%), Guinea (11%) and Senegal (10%).[48] The river's main tributaries are the Bafing, Bakoye and Faleme and all have their source in the Fouta Djallon mountains in Guinea and contribute 80% of the river's flow.[49] The population of the basin is estimated at around 6 million[50], with nearly 85% living along the river and its tributaries.[51]

Most of the Senegal River basin has a sub-Saharan desert climate and is characterized by a contrast in rainfall across different regions. The average annual rainfall is 550 mm/yr, with a varying north-south precipitation gradient from 200–250 mm/yr in the northernmost part to more than 1, 800 mm/yr in the Guinean part of the basin in the south. The predominantly natural vegetation of the region follows this gradient, with a semi-arid savannah in the north to sub-humid forest in the south.[52] The contrasting climate between the upper basin and lower valley is also accompanied by a high interseasonal and interannual variability. The basin underwent a long-lasting period of drought starting in the 1970s that lasted more than 30 years, with sharp drops in rainfall causing the region to suffer a succession of chronic annual deficits.[53]

The river's average flow at Bakel (generally considered a reference station due to its location below the confluence with the last major tributary, Faleme) is estimated at around 690 m^3/s, (about 22 billion m^3/yr). This figure decreased from 1,374 m^3/s during 1903–1950, to 840 m^3/s in 1950–1972 and 419 m^3/s in the period 1973–2002.[54]

Since the late 1980s, the valley region has become progressively more artificially regulated with the creation of embankments, free-flow canals and irrigation ditches. These were developed in direct connection with the construction of two larger hydraulic structures, namely the Manantali Dam, located on the Bafing tributary, and the Diama Dam, located near the mouth of the river in Senegal.

The latter (0.25 billion m^3 storage) has functioned since 1986 with the purpose of blocking seawater intrusion and raising the level of the upstream water body (confined by dykes along both shores) to facilitate irrigation, navigation and the filling of lakes in Senegal and Mauritania.

FIGURE 71: Map of the Senegal River Basin and subdomain extent

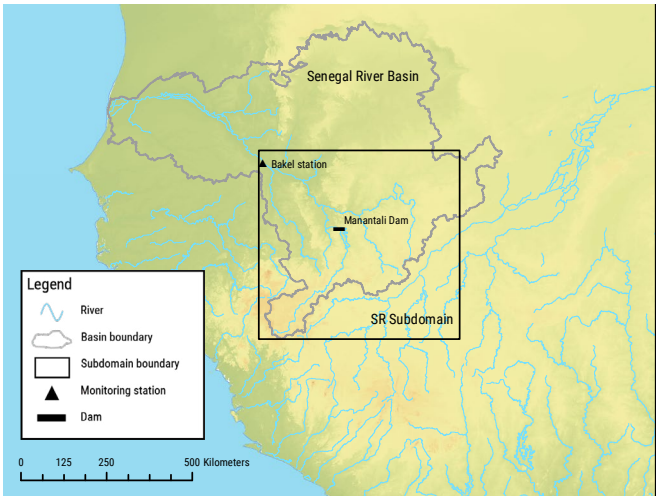

The Manantali Dam (12 billion m^3 storage) has regulated the flow of the Bafing River since 1988 with the purpose of attenuating extreme floods, generating hydropower and storing water in the wet season to augment dry-season flows for irrigation and navigation purposes.

The installation of the dams has allowed year-round availability of freshwater in sufficient quantities and thus the development of irrigated agriculture in the valley, as well as access to drinking-water installations for populations living near the dams.

4.5.2 Vulnerable sectors

It has been widely reported that two major factors have exerted pressure on the basin's water resources in recent years: variability in the climate and rainfall patterns, as well as dam construction. The major vulnerable sectors in conditions of climate change are directly or indirectly related to these factors and are presented below.

Agriculture, food security and livelihoods

A major part of water use in the basin is directed towards agriculture (around 85% of water withdrawals), a sector which employs more than 50% of the labour force in all riparian countries. The upper basin has remained largely an area of subsistence agriculture, based on shifting cultivation. In the downstream valley and delta, traditional production systems (flood-recession cropping, livestock-farming, fishing) and the practice of modern irrigation with water pumped from the river exist side by side.

In its natural regime, the Senegal River's main channel overflowed during high waters in the rainy season and

flooded the wide depression of the middle and lower valley for hundreds of hectares in low-flood years and more than 500,000 ha in wetter years. In these conditions and in the absence of drought, flood-recession farming substantially contributed to achieving self-sufficiency for 50% in the upper valley (the Bakel area) and for 68% in the middle valley (Podor area).

Over the last decades, this farming system was profoundly affected first by drought and chronic water deficits, as well as by the dams, particularly the Manantali Dam, which regulated the river's flow. The other important agricultural activities throughout the basin are livestock-farming and fishing, which were both also affected by the dam construction to varying degrees. For example, there were noted changes in terms of fish stocks with a 50%–70% decline in stocks downstream of Diama; increases in the Diama reservoir and the Lac de Guiers; and substantial decreases in the middle valley (particularly following disturbances in the flood cycle of the alluvial plain, which is a preferred area for fish reproduction).

The agricultural sector and all its related activities is thus a field of particular concern to consider in terms of vulnerability to climate change, as this sector is strongly linked to socioeconomic development and the preservation of livelihoods in the basin.[55]

Land degradation and desertification
Land degradation and desertification are issues of great concern in the basin. Inappropriate land use in various areas of the Fouta Djallon and the Manding plateau have caused soil erosion, land degradation and loss of soil fertility, leading to the creation of vast denuded areas. The spread of deforestation throughout the basin in combination with the overexploitation of natural resources has also modified the basin dynamics in terms of human-settlement patterns.

In addition, phenomena such as decreases in rainfall, increase in the frequency of severe droughts, the occurrence of the harmattan dust-bowl, sand-dune movements and the associated loss of arable land and livestock were precursors to an increase in land degradation and desertification over the years, which progressed toward the south of the basin. The delta has been most affected by land degradation caused by salinization. All these observed phenomena could be intensified in conditions of climate change, leading to decreased land productivity and loss of biodiversity but, most importantly, jeopardizing food security and standards of living for basin communities.[56]

Water quality, ecosystems and public health issues
The dams and associated dykes have brought about major ecological changes in the floodplain on both the Mauritanian and Senegalese sides of the river. The Diama Dam has

Senegal River, Mauritania, 2010. Source: Ihab Jnad.

created a permanent freshwater body whose shores have been subject to the invasion of aquatic plants (*Typha australis, Pistia startioles* and *Salvinia molesta*).

This proliferation has considerably affected agricultural activities by colonizing irrigated areas and blocking irrigation canals, as well as fishing, by obstructing fishermen's mobility and constituting inaccessible refuges for fish.

These conditions have also contributed to the spread of prevalent waterborne diseases such as malaria and schistosomiasis with the invasive aquatic plants and stagnant water offering ideal conditions for the development of mosquito and snail populations. Schistosomiasis has become a major public health problem in the delta, in particular among children. The rapid increase in intestinal schistosomiasis three years after the dams started operating clearly demonstrates the causal link between the development of this disease and modification in the river regime. Similarly, before the opening of the dams, transmission of malaria primarily occurred during the rainy season but is currently being observed in the off-season (December and May).

The basin is still important for migratory birds, notably water birds, which arrive in large numbers during the European winter to wetlands in the Senegal Valley and Delta. Important delta wetlands have been preserved at four Ramsar Convention sites, including the Diawling (Mauritania) and Djoudj (Senegal) national parks.

The considerations listed above, combined with alteration of the river regime and degradation of natural habitats, put the basin's biological diversity in danger. Water quality, ecosystems and public health issues thus constitute an important sector to consider for further analysis in conditions of climate change due to their strong interlinkages with river hydrology and climate variability.[57]

Sensitivity to extreme events
A severe drought occurred in the basin in the 1970s and lasted for over three decades, with sharp drops in rainfall. The impact of the drought on water resources of the basin has been very marked, namely through the downward trend in annual flow volumes causing the region to suffer a succession of chronic annual deficits.

Also, even though the climate variability in the basin makes it prone to floods that cover large parts of the valley for several days or weeks during August to September, a very severe flood event occurred in August 1999 and lasted until mid-October in many areas. This led to the destruction of several villages and irrigation infrastructure, people abandoning their houses and vast rice-crop losses.

Further downstream, the city of Saint-Louis, located near the mouth of the river, experienced great damage due to inundation of areas built up during the drier years in the 1980s. There have also been indications of changes in local sea level in this low-lying area, which should be taken into consideration in a context of changing climate.[58]

In addition to the issues presented above, the extreme poverty which characterizes the area makes the population very vulnerable to changes in climate. The severe drought encountered in the 1960s and 1970s has pushed the riparian countries to search for ways in which they could cooperate to lessen its impacts.

This situation is unique in the region: drivers for cooperation among riparian countries were the severe drought and consequent vulnerability of the population rather than conflict over river resources.

These pressures on water resources, added to those linked to fast demographic growth and various production activities, have recently had repercussions on the basin's natural environment and its ecological diversity, which might be further threatened by the effects of climate change.

4.5.3 Regional climate modelling findings

Changes projected for temperature, precipitation and related extreme events until the end of the century for the Senegal River headwaters are presented in Figure 72.

Both results of projected temperature and precipitation changes follow an increasing trend. The positive change in mean temperature for RCP 4.5 is 1.6 °C at mid-century and 2.1 °C at end-century. For RCP 8.5, temperatures increase of 2.3 °C for mid-century and 4.3 °C by end-century compared to the reference period. A larger increase in temperatures is projected in the winter season.

Precipitation changes also show increases of 1% at mid-century and 2% at end-century for RCP 4.5. For RCP 8.5, precipitation change is more accentuated with 3% at mid-century and 9% by end-century. In terms of precipitation extremes, outputs based on the SDII indicator (not shown) indicate an increasing trend for all projections. Along with the Euphrates headwaters subdomain, projected change in the R20 indicator for the Senegal River represent an exception: all the projections showed increasing trends (compared to little change for the other subdomains).

4.5.4 Regional hydrological modelling findings

The Senegal River basin, which otherwise shows runoff increases in particular at end-century for RCP 8.5 (mean increase of 8%–18%, depending on the model), exhibits a slight decrease of runoff at end- century for RCP 4.5 (of 2%–3%, depending on the model) even though precipitation shows an increase (Figure 73). A likely explanation for this is that the increase in precipitation is offset by increases in evapotranspiration.

Concerning mean discharge change, no definite trend can be observed due to the wide value ranges. At the seasonal level, there are however, signals of an increase of 13% for the winter season at end-century for RCP 8.5 with the range of values all showing an increase (2%–26% range). When examining projected changes in high-flow value, the range of values show that an increase of 15% is projected for mid-century RCP 4.5 and 25% at end-century RCP 8.5. These projected changes are concordant with the changes exhibited in the summer season. For the winter season, increases are projected at end-century.

FIGURE 72: Mean change in temperature, precipitation and selected extreme events indices over time for ensemble of three RCP 4.5 and RCP 8.5 projections for the Senegal River Headwaters

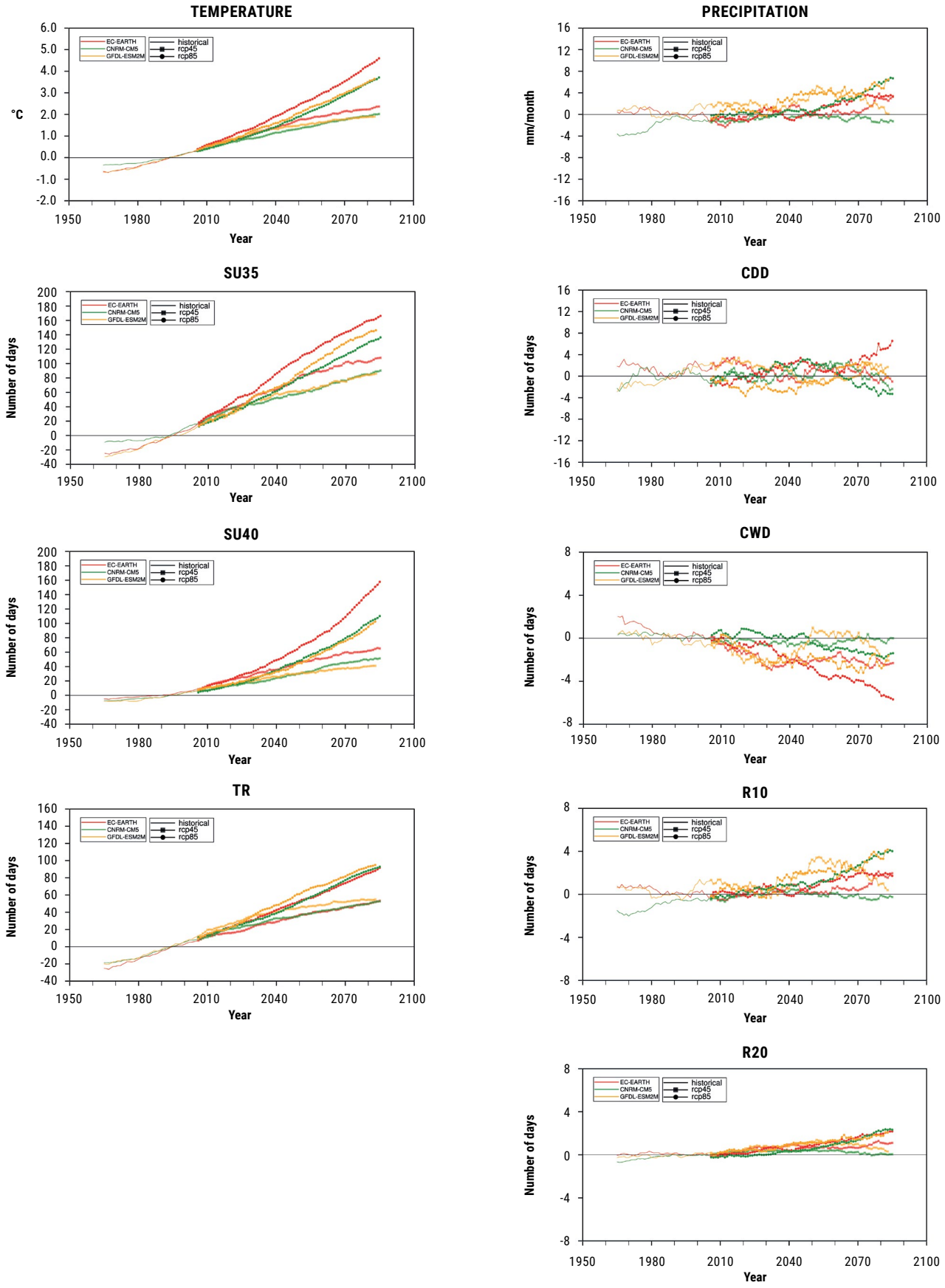

FIGURE 73: Mean change in runoff (using HYPE and VIC) and discharge (using HYPE) over time for ensemble of three RCP 4.5 and RCP 8.5 projections for the Senegal River Headwaters

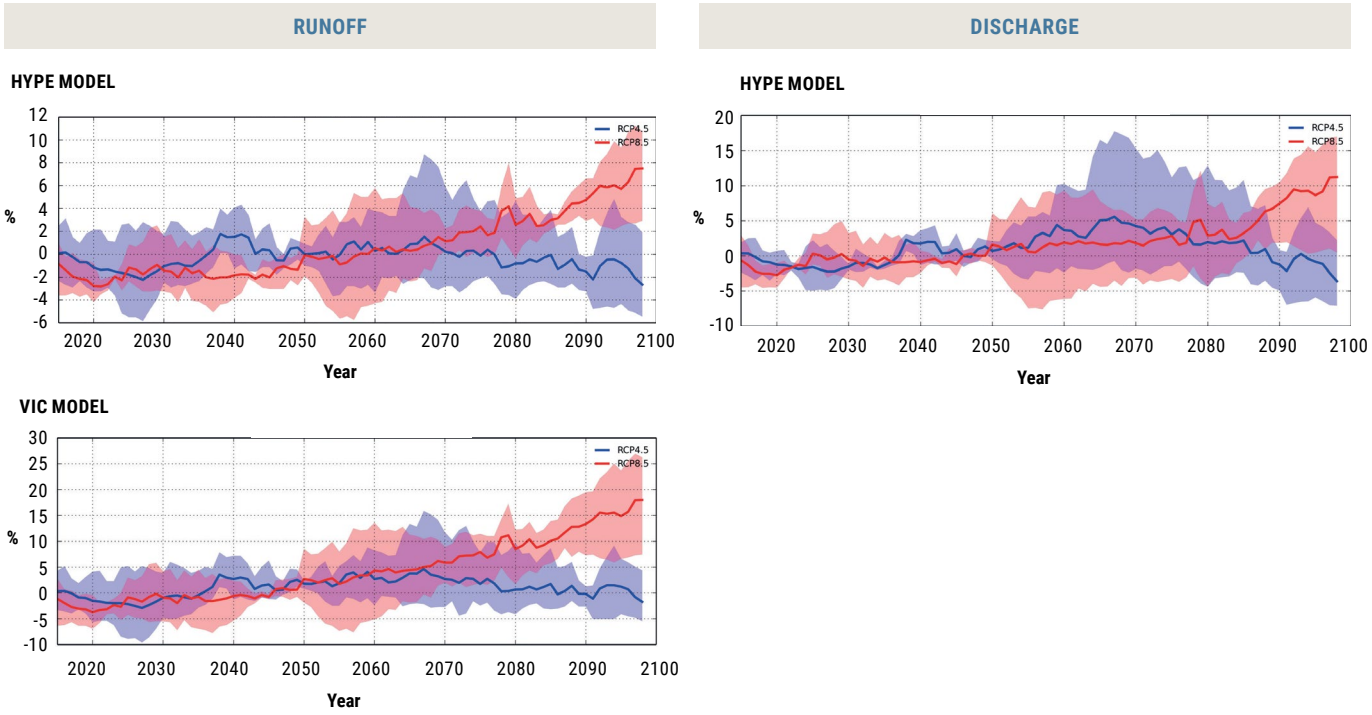

FIGURE 74: Comparison between 25 km (MNA22) and 50 km (MNA44) resolutions for mean change in runoff and discharge (using HYPE) over time for two RCP 8.5 projections for the Senegal River Headwaters

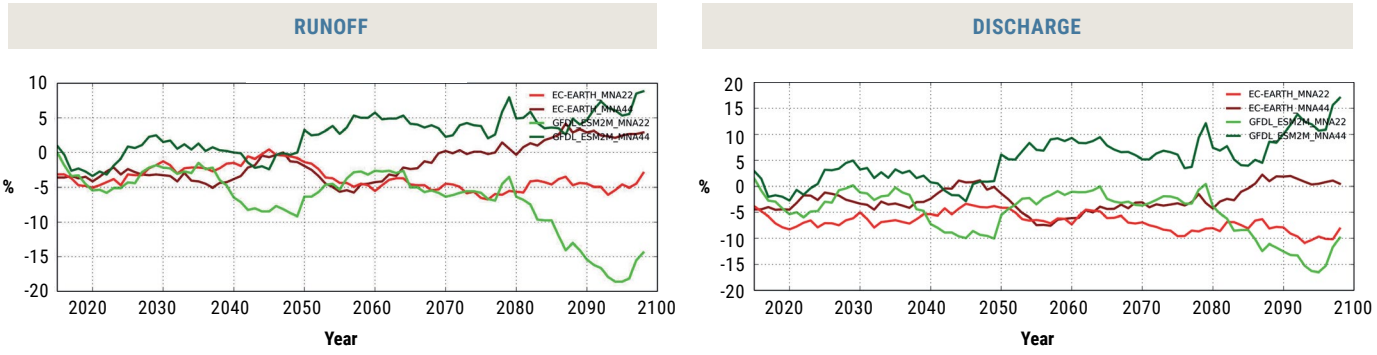

BOX 5: Using RICCAR outputs to inform further basin research

In line with one of its pillars to serve knowledge dissemination and inform further research on climate assessments in the Arab region, RICCAR's generated outputs are being used in ongoing projects related to water resources assessments in the region. One example is the Collaborative Programme on the Euphrates and Tigris (CPET) which aims to improve dialogue and cooperation among the basin countries through increased access to information and knowledge transfer regarding water management in the Euphrates and Tigris region. Building on RICCAR outcomes as it relates to hydrological climate modelling, the HYPE model schematization was used as a basis for an improved hydrological model set-up at the basin level, and the output data projections are expected to be further used within this project for simulation of river behaviour under various management options in a changing future climate.

The CPET project is implemented in collaboration with the International Centre for Biosaline Agriculture (ICBA); the Swedish Meteorological and Hydrological Institute (SMHI), the Stockholm International Water Institute (SIWI) and is funded by the Swedish International Development Cooperation Agency (Sida).

Source: SMHI (2017)

ENDNOTES

1. AMWC, 2012
2. Fifth Expert Group Meeting on the Regional Initiative for the Assessment of the Impact of Climate Change on Water Resources and Socio-Economic Vulnerability in the Arab Region (Amman, 11-12 December 2013)
3. Ninth session of the Arab Ministerial Water Council Technical Scientific Advisory Committee (Cairo, 26-28 January 2014)
4. NBI, 2012; Allam et al., 2016
5. Melesse et al., 2014
6. Camberlin, 2009; Senay et al., 2014
7. NBI, 2014
8. Sutcliffe and Parks, 1999; Allam et al., 2016
9. Ali, 2014
10. Melesse et al., 2014
11. NBI, 2016
12. Karimi et al., 2012
13. Kitaw and Yitayew, 2014; Jeuland 2010; Whittington et al., 2014
14. Taye et al., 2015; Awadallah, 2014
15. Senay et al., 2014; Sherif and Singh, 1999
16. Kibret et al., 2015
17. Melesse et al., 2014; Wimberly and Midekisa, 2014
18. NBI, 2008; UNEP, 2013
19. Frihy and El-Sayed, 2013; Hassaan and Abdrabo, 2013
20. UN-ESCWA and BGR, 2013
21. Isaev and Mikhailova, 2009; Daggupati et al., 2017
22. USGS, 2012
23. ESCWA and BGR, 2013
24. Sumer, 2014; UN-Iraq, 2013b; Janabi, 2013; Kucukmehmetoglu and Geymen, 2014
25. UN-Iraq, 2013a; Middleton and Sternberg, 2013
26. Voss et al., 2013
27. Stevens, 2012; Awadh and Ahmed, 2013; Varol et al., 2011
28. Pilesjo and Al-Juboori, 2016
29. Milillo et al., 2016; Wall Street Journal, 2016
30. Bozkurt and Sen, 2013; Issa et al., 2014; Shamout and Lahn, 2015
31. Djebbi, 2012; SWIM, 2012; ACSAD, 2015
32. Moldenhauer et al., 2007; Zahar et al., 2008; Hermassi et al., 2014
33. Zahar et al., 2008; Jelassi et al., 2015; Hermassi et al., 2014
34. Hermassi et al., 2014; Chabchoub, 2011; Wiebelt et al., 2014
35. Bargaoui et al., 2014; Gharbi et al., 2016; Louati et al., 2015; Khoualdia et al., 2014
36. Arif, 2012; Abidi et al., 2015; Etteieb et al., 2015
37. UN-ESCWA and BGR, 2013
38. Zeitoun et al., 2012
39. UN-ESCWA and BGR, 2013. Courcier et al., 2005 estimates about 275 million m^3 for the year 2000 and FoEME, 2011, reports 20–30 million m^3 in 2009.
40. Wolff et al., 2007; Dobricic, 2013;Mason and Mimi, 2014; Al-Bakri et al., 2013; Lund, 2014
41. Shatanawi et al., 2013; Shadeed, 2013; WFP, 2014; Törnros and Menzel, 2014
42. Jaber, 2012; Ismail et al., 2013
43. Froukh, 2010; Mizyed, 2009;; Hashemite Kingdom of Jordan, 2010; Altz-Stamm, 2012
44. Mason and Mimi, 2009; FoEME, 2010; Mason et al., 2010
45. Reporting as of March 2017, as per UNHCR, 2017
46. Ministry of Environment, 2013; Farishta, 2014; Müller et al., 2016
47. Haering et al., 2010; Earle et al., 2015; Quba'a et al., 2017
48. OMVS, 2014c
49. FAO, 2007; OMVS, 2014a
50. This estimate is based on the assumption that 16% of the total population for the four riparian countries are living in the basin
51. OMVS, 2014b
52. Stisena et al., 2008
53. Oyebande and Odunuga, 2010; OMVS, 2014b
54. Mbaye et al., 2015
55. Varis and Fraboulet-Jussila, 2002; WFP, 2013; Djaman et al., 2016
56. OMVS, 2014c; UNEP, 2009
57. OMVS, 2014c; Mbaye et al., 2016; Manikowski and Strapasson, 2016
58. Dia, 2007; Osorio and Galiano, 2012; Yacoub and Tayfur, 2017
59. Dione, 2004; Mbengue, 2014

REFERENCES

Abidi, S., Bejaouia, M., Jemlia, M. and Boumaizaa, M. 2015. Water Quality of the Oued Medjerda, Tunisia and Algeria, and three of its Northern Tributaries. *Hydrological Sciences Journal*, 60(9).

ACSAD (The Arab Center for the Studies of Arid Zones and Dry Lands). 2015. Case study of the Medjerda River Basin using HEC-HMS. In *RICCAR Regional Workshop on Moving from Climate Change Impact Assessment to Socio-Economic Vulnerability Assessment in the Arab Region, 8-10 June 2015*. ESCWA, Beirut. Available at: https://www.unescwa.org/events/riccar-regional-workshop-moving-climate-change-impact-assessment-socio-economic-vulnerability.

Al-Bakri, J. T., Salahat, M., Suleiman, A., Suifan, M., et al. 2013. Impact of Climate and Land Use Changes on Water and Food Security in Jordan: Implications for Transcending "The Tragedy of the Commons". *Sustainability*, 5: p. 724-748.

Ali, Y. S. A. 2014. The Impact of Soil Erosion in the Upper Blue Nile on Downstream Reservoir Sedimentation. DoctorateThesis. Delft University of Technology, UNESCO-IHE Institute for Water Education. Delft. Available at: http://repository.tudelft.nl/islandora/object/uuid:8ac9e0a5-ec7e-4173-ada4-255a3b2ed908.

Allam, M. M., Figueroa, A. J., McLaughlin, D. B. and Eltahir, E. A. B. 2016. Estimation of Evaporation over the Upper Blue Nile Basin by Combining Observations from Satellites and River Flow Gauges. *Water Resources Research*, 52(2).

Altz-Stamm, A. 2012. Jordan's Water Resource Challenges and the Prospects for Sustainability. Available at: http://www.caee.utexas.edu/prof/maidment/ giswr2012/TermPaper/Altz-Stamm.pdf.

AMWC (Arab Ministerial Water Council). 2012. Arab Strategy for Water Security in the Arab Region to Meet the Challenges and Future Needs for Sustainable Development 2010-2030. Published by League of Arab States. Cairo. Available at: http://www.accwam.org/Files/Arab_Strategy_for_Water_Security_in_the_Arab_Region_to_meet_the_Challenges_and_Future_Needs_for_Sustainable_Development_-_2010-2030.pdf.

Arif, S. 2012. Coût de la Dégradation des Ressources En Eaux - Le Bassin Versant de la Medjerda Atelier de Concertation. Published by SWIM (Sustainable Water Integrated Management).

Awadallah, A. G. 2014. Evolution of the Nile River Drought Risk Based on the Streamflow Record at Aswan Station, Egypt. *Civil Engineering and Environmental Systems*, 31(3): p. 260-269.

Awadh, S. M. and Ahmed, R. M. 2013. Hydrochemistry and Pollution Probability of Selected Sites along the Euphrates River, Western Iraq. *Arabian Journal of Geosciences*, 6(7): p. 2501–2518.

Bargaoui, Z., Tramblay, Y., Lawinc, E. A. and Servatb, E. 2014. Seasonal Precipitation Variability in Regional Climate Simulations over Northern Basins of Tunisia. *International Journal of Climatology*, 34: p. 235-248.

Bozkurt, D. and Sen, O. L. 2013. Climate Change Impacts in the Euphrates–Tigris Basin Based on Different Model and Scenario Simulations. *Journal of Hydrology*, 480: p. 149-161.

Camberlin, P. 2009. Nile Basin Climate. H. Dumont (eds). In *The Nile: Origin, Environments, Limnology and Human Use*. Published by Springer. Available at: http://link.springer.com/chapter/10.1007%2F978-1-4020-9726-3_16

Chabchoub, M. A. 2011. Evaluation des Systèmes de Production Méditerranéens dans un Contexte de Changement Climatique: Cas de la Basse Vallée de la Medjerda en Tunisie. MSc Thesis. Institut Agronomique Mediterranéen de Montpellier, CIHEAM, Available at: http://www.iamm.fr/ressources/opac_css/doc_num.php?explnum_id=7399.

Courcier, R., Venot, J. P. and Molle, F. 2005. Historical Transformations of the Lower Jordan River Basin (in Jordan): Changes in Water Use and Projections (1950-2025). In *Comprehensive Assessment Research Report 9*. Published by Comprehensive Assessment Secretariat. Colombo, Sri Lanka. Available at: http://www.iwmi.cgiar.org/assessment/files_new/publications/CA%20Research%20Reports/ColouredCARR9.pdf. Accessed on May 25, 2012.

Daggupati, P., Srinivasan, R., Ahmadi, M. and Verma, D. 2017. Spatial and Temporal Patterns of Precipitation and Stream Flow Variations in Tigris-Euphrates River Basin. *Environmental Monitoring and Assessment*, 189(50).

Dia, A. M. 2007. Adapting to Climate Variability in the Senegal River Basin in West Africa. Published by African Global Change Research Grants, University of Dakar, Senegal. Available at: http://start.org/download/gec07/dia-final.pdf.

Dione, O. 2004. Thirty Years Of Cooperation In The Senegal River Basin: A Success Story in Cooperative River Basin Management. In *Lecture at Tufts University*. Available at: http://www.tufts.edu/water/pdf/WaterConflict/OusmaneDione.pdf.

Djaman, K., Balde, A. B., Rudnick, D. R., Ndiaye, O., et al. 2016. Long-term Trend Analysis in Climate Variables and Agricultural Adaptation Strategies to Climate Change in the Senegal River Basin. *International Journal of Climatology*.

Djebbi, M. 2012. Delineation of the Flood Prone Zones Along the Medjerda River Downstream of Sidi Salem Dam in Tunisia. *Journal of Sustainable Watershed Science & Management*, 1(2): p. 46-52.

Dobricic, K. 2013. Water Scarcity in the Jordan Valley; Impacts on Agriculture and Rural Livelihoods. Master's Thesis. Uppsala University, Department of Earth Sciences. Uppsala, Sweden. Available at: http://uu.diva-portal.org/smash/get/diva2:651322/FULLTEXT01.pdf.

Earle, A., Cascao, A. E., Hansson, S., Jägerskog, A., et al. 2015. Transboundary Water Management and the Climate Change Debate. Published by Routledge. Available at: https://www.routledge.com/products/9780415835152?utm_source=adestra&utm_medium=email&utm_campaign=sbu3_mbs_4mx_1em_9env_rnl15_x_x

ESCWA and BGR (United Nations Economic and Social Commission for Western Asia; Bundesanstalt für Geowissenschaften und Rohstoffe). 2013. Inventory of Shared Water Resources in Western Asia. Beirut. Available at: www.waterinventory.org.

Etteieb, S., Cherif, S. and Tarhouni, J. 2015. Hydrochemical Assessment of Water Quality for Irrigation: A Case Study of the Medjerda River in Tunisia. *Applied Water Science*.

FAO (Food and Agriculture Organization of the United Nations). 2007. Irrigation potential in Africa a Basin Approach. Available at: http://www.fao.org/docrep/w4347e/w4347e00.htm.

Farishta, A. 2014. The Impact of Syrian Refugees on Jordan's Water Resources and Water Management Planning. Master of Science Thesis. Columbia University, Faculty of Architecture and Planning and Preservation. New York. Available at: http://earth.columbia.edu/sitefiles/file/students/showcase/2014/Aleena-Farishta.pdf.

FoEME (Friends of the Earth Middle East). 2010. Towards a Living Jordan River: An Environmental Flows Report on the Rehabilitation of the Lower Jordan River. Available at: http://foeme.org/uploads/publications_publ117_1.pdf. Accessed on February 17, 2012.

FoEME (Friends of the Earth Middle East). 2011. Roadmap for the Rehabilitation of the Lower Jordan River. Available at: http://foeme.org/uploads/13209208250~%5E$%5E~DHV_Full_Report_11.2011.pdf. Accessed on March 10, 2012.

Frihy, O. E. and El-Sayed, M. K. 2013. Vulnerability Risk Assessment and Adaptation to Climate Change Induced Sea Level Rise along the Mediterranean Coast of Egypt. *Mitigation and Adaptation Strategies for Global Change*, 18: p. 1215-1237.

Froukh, L. 2010. The Impact and Management of Recent Drought on the West Bank Groundwater Aquifer System. A. López-Francos (eds). In *Economics of Drought and Drought Preparedness in a Climate Change Context*. Published by CIHEAM / FAO / ICARDA / GDAR / CEIGRAM / MARM. Zaragoza, Spain. Available at: http://om.ciheam.org/om/pdf/a95/00801357.pdf

Gharbi, M., Soualmia, A., Dartus, D. and Masbernat, L. 2016. Floods Effects on Rivers Morphological Changes Application to the Medjerda River in Tunisia. *Journal of Hydrology and Hydromechanics*, 64.

Haering, M., Al-Karablieh, E. and Salman, A. 2010. Unmet Irrigation Water Demands Due to Climate Change in the Lower Jordan River Basin. In *ICARDA International Conference on Food Security and Climate Change in Dry Areas*. Amman. Available at: http://icardablog.files.wordpress.com/2011/04/foodsecurityandclimatechange1.pdf.

Hashemite Kingdom of Jordan. 2010. National Environmental and Economic Development Study for Climate Change: Jordan National Report Submitted to the UNFCCC. Available at: https://unfccc.int/files/adaptation/application/pdf/jordanneeds.pdf.

Hassaan, M. A. and Abdrabo, M. A. 2013. Vulnerability of the Nile Delta Coastal Areas to Inundation by Sea Level Rise. *Environmental Monitoring and Assessment*, 185: p. 6607–6616.

Hermassi, T., Jebari, S., Nouna, B. B., Safouane, M., et al. 2014. Characterization of Medjerda River Basin. In *First Project Meeting: Participatory Planning for Improving Water Use Efficiency in River Basins, 18-19 March 2014*.

Isaev, V. A. and Mikhailova, M. V. 2009. The Hydrography, Evolution, and Hydrological Regime of the Mouth Area of the Shatt al-Arab River. *Water Resources*, 36(4): p. 380-395.

Ismail, M. S., Moghavvemi, M. and Mahlia, T. M. I. 2013. Energy Trends in Palestinian Territories of West Bank and Gaza Strip: Possibilities for Reducing the Reliance on External Energy Sources. *Renewable and Sustainable Energy Reviews*, 28: p. 117-129.

Issa, I. E., Al-Ansari, N. A., Sherwany, G. and Knutsson, S. 2014. Expected Future of Water Resources within Tigris-Euphrates Rivers Basin, Iraq. *Journal of Water Resource and Protection*, 6: p. 421-432.

Jaber, J. O. 2012. Prospects and Challenges of Small Hydropower Development in Jordan. *Jordan Journal of Mechanical and Industrial Engineering*, 6(2): p. 110-118.

Janabi, H. 2013. Climate Change Impact on Iraqi Water and Agriculture Sectors. Article by Iraqi Economists Network. Available at: http://iraqieconomists.net/en/2013/04/05/climate-change-impact-on-iraqi-water-and-agriculture-sectors/.

Jelassi, A., Gaaloul, N., Laignel, B. and Turki, I. 2015. Caractérisation Hydrologique de l'Oued Medjerda (Tunisie) dans le Cadre de la Future Mission Spatiale SWOT. In *Conference Internationale FRIEND/UNESCO/ Programme Hydrologique International sur L'hydrologie des Grands Bassins Africains, 26-30 Octobre 2015, Hammamet, Tunisie*.

Karimi, P., Molden, D., Notenbaert, A. and Peden, D. 2012. Nile Basin Farming Systems and Productivity. S. B. S. Awulachew, Vladimir; Molden, David; Peden D. (eds). In *The Nile River Basin: Water, Agriculture, Governance and Livelihoods*. Published by Earthscan, Routledge. Abingdon, United Kingdom.

Khoualdia, W., Djebbar, Y. and Hammar, Y. 2014. Caractérisation de la Variabilité Climatique: Cas du Bassin Versant de La Medjerda (Nord-Est algérien). *Revue des Sciences technologiques*, 29: p. 6-23.

Kibret, S., Lautze, J., McCartney, M., Wilson, G. G., et al. 2015. Malaria Impact of Large Dams in sub-Saharan Africa: Maps, Estimates and Predictions. *Malaria Journal*, 14(339).

Kitaw, M. and Yitayew, M. 2014. Water Governance in the Nile Basin for Hydropower Development. A. M. Melesse, W. Abtew and S. G. Setegn (eds). In *Nile River Basin: Ecohydrological Challenges, Climate Change and Hydropolitics*. Published by Springer, Switzerland.

Kucukmehmetoglu, M. and Geymen, A. 2014. The Significance and Impacts of Large Investments over the Determination of Irrigated Agricultural Land Use:The Case of the Euphrates & Tigris River Basin. *Land Use Policy*, 41: p. 514–525.

Louati, M., Saïdi, H. and Zargouni, F. 2015. Shoreline Change Assessment Using Remote Sensing and GIS Techniques: A Case Study of the Medjerda Delta Coast, Tunisia. *Arabian Journal of Geosciences*, 8(6): p. 4239–4255.

Lund, A. 2014. Drought, Corruption, and War: Syria's Agricultural Crisis. Carnegie Endowment for International Peace. Issued on April 18, 2014. Available at: http://carnegieendowment.org/syriaincrisis/?fa=55376.

Manikowski, S. and Strapasson, A. 2016. Sustainability Assessment of Large Irrigation Dams in Senegal: A Cost-Benefit Analysis for the Senegal River Valley. *Frontiers in Environmental Science*, 4(18).

Mason, M. and Mimi, Z. 2009. Climate Change Adaptation Strategy for the Occupied Palestinian Territory (Final report of consultants). Published by United Nations Development Programme. Available at: http://www.preventionweb.net/files/26380_climatechangeadaptationstrategyfort.pdf.

Mason, M. and Mimi, Z. 2014. Transboundary Climate Security: Climate Vulnerability and Rural Livelihoods in the Jordan River Basin. Published by London School of Economics and Birzeit University. Available at: http://eprints.lse.ac.uk/60242/.

Mason, M., Mimi, Z. and Zeitoun, M. 2010. Climate Change Adaptation Strategy and Programme of Action for the Palestinian Authority. Published by United Nations Development Programme (UNDP), Programme of Assistance to the Palestinian People. Jerusalem. Available at: http://www.undp.ps/en/newsroom/publications/pdf/other/climatechange.pdf.

Mbaye, M., Hagemann, S., Haensler, A., Stacke, T., et al. 2015. Assessment of Climate Change Impact on Water Resources in the Upper Senegal Basin (West Africa). *American Journal of Climate Change*, 4: p. 77-93.

Mbaye, M. L., Gaye, A. T., Spitzy, A., Dähnke, K., et al. 2016. Seasonal and Spatial Variation in Suspended Matter, Organic Carbon, Nitrogen, and Nutrient Concentrations of the Senegal River in West Africa. *Limnologica - Ecology and Management of Inland Waters*, 57: p. 1-13.

Mbengue, M. M. 2014. A Model for African Shared Water Resources: The Senegal River Legal System. *Review of European, Comparative & International Environmental Law, Special Issue: International Water Law*, 23(1): p. 59-66.

Melesse, A. M., Abtew, W. and Setegn, S. G. 2014. Nile River Basin: Ecohydrological Challenges, Climate Change and Hydropolitics. Published by Springer.

Middleton, N. J. and Sternberg, T. 2013. Climate Hazards in Drylands: A review. *Earth-Science Reviews*, 126: p. 48-57.

Milillo, P., Bürgmann, R., Lundgren, P., Salzer, J., et al. 2016. Space Geodetic Monitoring of Engineered Structures: The Ongoing Destabilization of the Mosul dam, Iraq. *Nature Scientific Reports*, 6: p. 1-7.

Ministry of Environment, Hashemite Kingdom of Jordan, . 2013. The National Climate Change Policy of the Hashemite Kingdom of Jordan 2013-2020. Available at: http://www.jo.undp.org/content/dam/jordan/docs/Publications/Climate%20change%20policy_JO.pdf.

Mizyed, N. 2009. Impacts of Climate Change on Water Resources Availability and Agricultural Water Demand in the West Bank. *Water Resources Management*, 23: p. 2015-2029.

Moldenhauer, K.-M., Zielhofer, C. and Faust, D. 2007. Heavy Metals as Indicators for Holocene Sediment Provenance in a Semi-arid Mediterranean Catchment in Northern Tunisia. *Quaternary International*.

Müller, M. F., Yoon, J., Gorelick, S. M., Avisse, N., et al. 2016. Impact of the Syrian Refugee Crisis on Land Use and Transboundary Freshwater Resources. *Proceedings of the National Academy of Sciences of the United States of America*, 113(52): p. 4932-14937.

NBI (Nile Basin Initiative). 2008. Physical and Non-Physical Barriers to Cross-Border Trade in the Navigation of the River Nile. In *Socio-economic Development and Benefit Sharing Project*. Available at: file:///C:/Users/924046/Desktop/NBIEgypt2009.pdf.

NBI (Nile Basin Initiative). 2012. State of the River Nile Basin Report. Entebbe, Uganda. Available at: http://nileis.nilebasin.org/content/state-river-nile-basin-report.

NBI (Nile Basin Initiative). 2014. Understanding Nile Basin Hydrology: Mapping Actual Evapotranspiration over the Nile Basin. In *Nile Waters Technical Bulletin Issue 1*. Available at: file:///C:/Users/924046/Downloads/Understanding%20Nile%20Basin%20Hydrology%20Bookle.pdf.

NBI (Nile Basin Initiative). 2016. The Nile Basin Water Resources Atlas. Published by Nile Information System. Available at: http://nileis.nilebasin.org/content/nile-basin-water-resources-atlas.

OMVS (Organisation pour la Mise en Valeur du Fleuve Sénégal). 2014a. Caractéristiques Physiques. Available at: http://www.portail-omvs.org/gestion-ressource-et-environnement/fleuve-senegal/caracteristiques-physiques.

OMVS (Organisation pour la Mise en Valeur du Fleuve Sénégal). 2014b. Strategic Action Plan for the Management of Priority Environmental Problems in the Senegal River Basin. In *GEF Project/Senegal River Basin, Component 3*. Available at: file:///C:/Users/924046/Downloads/senegal_sap_eng.pdf.

OMVS (Organisation pour la Mise en Valeur du Fleuve Sénégal). 2014c. Transboundary Diagnostic Environmental Analysis of the Senegal River Basin. In *GEF Project/Senegal River Basin, Component 3*. Available at: file:///C:/Users/924046/Downloads/senegal_tda_eng.pdf.

Osorio, J. D. G. and Galiano, S. G. G. 2012. Non-stationary Analysis of Dry Spells in Monsoon Season of Senegal River Basin using data from Regional Climate Models (RCMs). *Journal of Hydrology*, 450: p. 82-92.

Oyebande, L. and Odunuga, S. 2010. Climate Change Impact on Water Resources at the Transboundary Level in West Africa: The Cases of the Senegal, Niger and Volta Basins. *The Open Hydrology Journal*, 4: p. 163-172.

Pilesjo, P. and Al-Juboori, S. S. 2016. Modelling the Effects of Climate Change on Hydroelectric Power in Dokan, Iraq *International Journal of Energy and Power Engineering*, 5(2-1): p. 7-12.

Quba'a, R., El-Fadel, M., Najm, M. A. and Alameddine, I. 2017. Comparative Assessment of Joint Water Development Initiatives in the Jordan River Basin. *International Journal of River Basin Management*, 15(1): p. 115-131.

Senay, G. B., Velpuri, N. M., Bohms, S., Demissie, Y., et al. 2014. Understanding the Hydrologic Sources and Sinks in the Nile Basin using Multisource Climate and Remote Sensing Data sets. *Water Resources Research*, 50(11): p. 8625–8650.

Shadeed, S. 2013. Spatio-temporal Drought Analysis in Arid and Semi-arid Regions: A Case Study from Palestine. *Arabian Journal for Science & Engineering* 38: p. 2303-2313.

Shamout, N. and Lahn, G. 2015. The Euphrates in Crisis Channels of Cooperation for a Threatened River. In *Energy, Environment and Resources Research Paper*. Published by Chatham House. Available at: https://www.chathamhouse.org/sites/files/chathamhouse/field/field_document/20150413Euphrates_0.pdf.

Shatanawi, K., Rahbeh, M. and Shatanawi, M. 2013. Characterizing, Monitoring and Forecasting of Drought in Jordan River Basin *Journal of Water Resource and Protection*, 5: p. 1192-1202

Sherif, M. M. and Singh, V. P. 1999. Effect of Climate Change on Sea Water Intrusion in Coastal Aquifers. *Hydrological Processes*, 13(8): p. 1277–1287.

Stevens, M. 2012. Equitable Water Rights: A Holistic Perspective on Eco cultural Restoration to Sustain Biodiversity, Ecosystem Functions and Social Justice in the Tigris Euphrates Watershed. In *9th INTECOL/SWS International Wetlands Conference.* Orlando, Florida. Available at: http://www.conference.ifas.ufl.edu/intecol/presentations/073/1120%20M.Stevens.pdf.

Stisena, S., Jensena, K. H., Sandholta, I. and Grimes, D. I. F. 2008. A Remote Sensing Driven Distributed Hydrological Model of the Senegal River Basin. *Journal of Hydrology*, 354(1-4): p. 131–148.

Sumer, V. 2014. Climate Change and Water Issues in Mesopotamia: A Framework for Fostering Transboundary Cooperation in Euphrates-Tigris Basin. W. L. Filho (eds). In *Handbook of Climate Change Adaptation.* W. L. Filho (eds). Published by Springer.

Sutcliffe, J. V. and Parks, Y. P. 1999. Hydrology of the Nile. In *IAHS Special Publication no.5*. Published by IAHS (International Association of Hydrological Science).

SWIM (Sustainable Water Integrated Management). 2012. Tunisia Cost Assessment of Water Resources Degradation in the Medjerda Basin. Available at: http://www.swim-sm.eu/files/SWIM_medjerda_report_EN_.pdf.

Taye, M. T., Willems, P. and Block, P. 2015. Implications of Climate Change on Hydrological Extremes in the Blue Nile Basin: A review. *Journal of Hydrology: Regional Studies*, 4: p. 280-293.

Törnros, T. and Menzel, L. 2014. Addressing Drought Conditions under Current and Future Climates in the Jordan River Region. *Hydrology and Earth System Sciences*, 18: p. 305-318.

UN-Iraq. 2013a. Sand and Dust Storm Fact Sheet. Published by UN Iraq Joint Analysis and Policy Unit. Available at: http://reliefweb.int/sites/reliefweb.int/files/resources/SDS%20Fact%20Sheet.pdf.

UN-Iraq. 2013b. World Environment Day Factsheet: How Environmental Damage Causes Food Insecurity in Iraq. Published by UN Iraq Joint Analysis and Policy Unit and UNAMI Public Information Office. Available at: http://www.jauiraq.org/documents/1886/Factsheet-WorldEnvironment-English.pdf.

UNEP (United Nations Environment Programme). 2009. Assessment of Transboundary Freshwater Vulnerability in Africa to Climate Change. Available at: http://www.unep.org/dewa/Portals/67/pdf/Assessment_of_Transboundary_Freshwater_Vulnerability_revised.pdf.

UNEP (United Nations Environment Programme). 2013. Adaptation to Climate-change Induced Water Stress in the Nile Basin: A Vulnerability Assessment Report. Available at: www.unep.org/dewa/Portals/67/pdf/Nile_Basin.pdf.

UNHCR (United Nations High Commissioner for Refugees). 2017. Syria Regional Refugee Response. Available at: http://data.unhcr.org/syrianrefugees/regional.php.

USGS (United States Geological Survey). 2012. Stream Gage Descriptions and Streamflow Statistics for Sites in the Tigris River and Euphrates River Basins, Iraq. In *Data Series 540*. Available at: http://pubs.usgs.gov/ds/540/pdf/ds540.pdf.

Varis, O. and Fraboulet-Jussila, S. 2002. Water Resources Development in the Lower Senegal River Basin: Conflicting Interests, Environmental Concerns and Policy Options. *Water Resources Development*, 18(2).

Varol, M., Gotkot, B., Bekleyen, A. and Sen, B. 2011. Water Quality Assessment and Apportionment of Pollution Sources of Tigris River (Turkey) Using Multivariate Statistical Techniques-A Case Study. *River Research and Applications*.

Voss, K. A., Famiglietti, J. S., Lo, M., de Linage, C., et al. 2013. Groundwater Depletion in the Middle East from GRACE with Implications for Transboundary Water Management in the Tigris-Euphrates-Western Iran Region. *Water Resources Research*, 49: p. 904–914.

Wall Street Journal. 2016. Islamic State Uses Huge Syrian Dam As Rampart. Article by Damian Paletta. Issued on January 21, 2016. Available at: https://www.wsj.com/articles/islamic-state-uses-syrias-biggest-dam-as-rampart-and-potential-weapon-1453333531.

WFP (World Food Programme). 2013. Climate Risk and Food Security in Senegal: Analysis of Climate Impacts on Food Security and Livelihoods. Available at: http://www.uncclearn.org/sites/default/files/inventory/wfp10.pdf.

WFP (World Food Programme). 2014. Special Focus Syria: Will Drought Worsen the Impact of Conflict on Food Insecurity? Available at: http://documents.wfp.org/stellent/groups/public/documents/ena/wfp263930.pdf.

Whittington, D., Waterbury, J. and Jeulandc, M. 2014. The Grand Renaissance Dam and Prospects for Cooperation on the Eastern Nile. *Water Policy*: p. 1-14.

Wiebelt, M., Al-Riffai, P., Breisinger, C. and Robertson, R. 2014. Who Bears the Costs of Climate Change? Evidence from Tunisia. Published by International Food Policy Research Institute (IFPRI). Available at: https://www.ifw-members.ifw-kiel.de/publications/who-bears-the-costs-of-climate-change-evidence-from-tunisia.

Wimberly, M. and Midekisa, A. A. 2014. Hydro-Epidemiology of the Nile Basin: Understanding the Complex Linkages Between Water and Infectious Diseases. A. M. Melesse, W. Abtew and S. G. Setegn (eds). In *Nile River Basin: Ecohydrological Challenges, Climate Change and Hydropolitics*. Published by Springer. Available at: http://www.springer.com/us/book/9783319027197

Wolff, H. P., Shechter, M., Fleischer, A., Salman, A., et al. 2007. Forecasting Social and Economic Impacts from Climate Change on Farming Systems in Riparian Countries of the Jordan River –a Combined Model-based Approach. Published by Network for Socio-Economic Research on Water Resource Management in the Middle East. Available at: https://www.uni-hohenheim.de/~hpwolff/pdfs/WS6cWolff.pdf.

Yacoub, E. and Tayfur, G. 2017. Evaluation and Assessment of Meteorological Drought by Different Methods in Trarza Region, Mauritania. *Water Resources Management*, 31: p. 825-845.

Zahar, Y., Ghorbel, A. and Albergel, J. 2008. Impacts of Large Dams on Downstream Flow Conditions of Rivers: Aggradation and Reduction of the Medjerda Channel Capacity Downstream of the Sidi Salem Dam (Tunisia). *Journal of Hydrology*, 351: p. 318-330.

Zeitoun, M., Eid-Sabbagh, K., Dajani, M. and Talhami, M. 2012. Hydro-political Baseline of the Upper Jordan River. Published by Association of the Friends of Ibrahim Abd el Al. Beirut. Available at: https://www.uea.ac.uk/documents/439774/1029261/UJR+Hydropol+Baseline+-+Main+lo-res+%282012%29.pdf/28ae7dc7-e16f-45a4-95a1-d285edbfc528.

IMPACT ASSESSMENT
CASE STUDIES

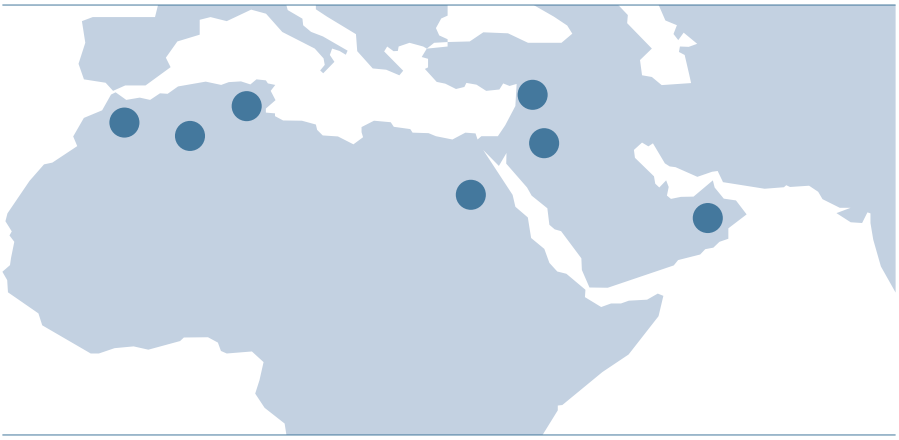

CHAPTER 5

EXTREME EVENTS IMPACT ASSESSMENT FOR SELECTED BASINS

This chapter presents the impacts of climate change in terms of extreme events in three river basins in the Arab region, namely the Nahr el Kabir River basin shared between Lebanon and Syrian Arab Republic[1]; the Wadi Diqah River basin in Oman; and the Medjerda River basin shared between Algeria and Tunisia (Figure 75). For each basin, changes in the following indicators were analysed: extreme temperature and precipitation indices, extreme drought events and extreme flood events. Full details on the methodology, as well as additional results and analysis are available in the RICCAR technical report *Impact of Climate Change on Extreme Events in Selected Basins in the Arab Region* (2017) prepared by ACSAD.[2]

The Nahr el Kabir River is 56 km long and flows along the northern Lebanese border with Syrian Arab Republic and has a total watershed area of some 990 km^2. The river collects its water from tributaries on both sides, flows from east to west and discharges into the Mediterranean Sea at its outlet in Arida, Lebanon. The river basin has been characterized by recurrent floods.

The Wadi Diqah is located 60 km southeast of Muscat and is one of the few wadis continuously flowing throughout the year in Oman. The watercourse is 70 km long and the watershed covers a surface area of some 1,870 km^2. Rainfall varies seasonally and geographically over the study area with an annual average precipitation of about 148 mm/yr (about 276 million m^3).

A detailed description of the Medjerda River is available in Chapter 4, along with a basin map (see Figure 63). The river flows eastwards from north-eastern Algeria to Tunisia and then discharges to the Gulf of Utica in the Mediterranean Sea. Its total watershed area is about 22,700 km^2 and is characterized by a sub-humid to semi-arid climate with a mean annual rainfall of 480 mm/yr with irregular patterns in time and in space.

FIGURE 75: Extreme events case studies: study area

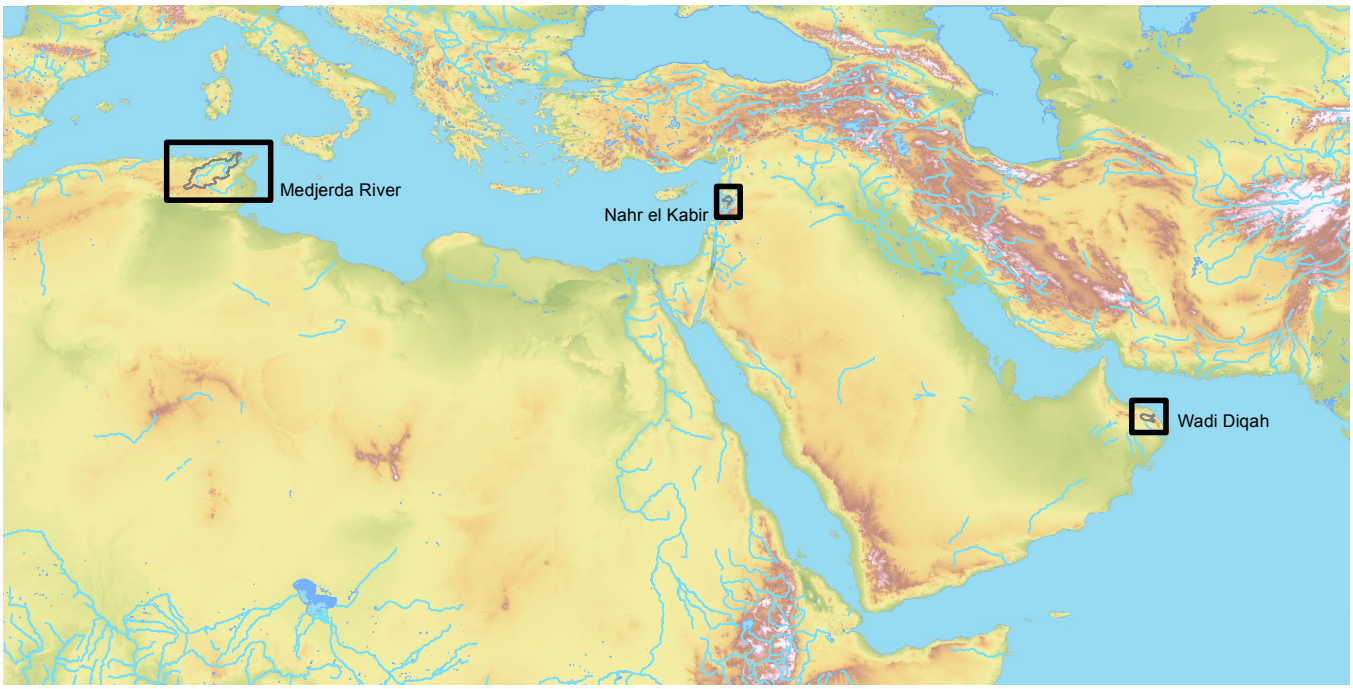

5.1 INDICATORS AND EVENTS SELECTED FOR ANALYSIS

5.1.1 Extreme temperature and precipitation

Projected trends in extreme temperature and precipitation indices were studied for each of the three basins. These were based on RCM daily temperature (Tmax; Tmin) and precipitation projections generated under RICCAR until the end of the century and for both emission scenarios RCP 4.5 and RCP 8.5.

Datasets were quality-controlled and processed into indices of climate extremes using the RClimDex package.[3] The variables analysed were based on the set of extreme climate indices developed by ETCCDI, and those presented in this chapter are listed in Table 13. Additional indices are presented in the related RICCAR technical report.[4]

5.1.2 Drought events

Projected changes in drought events in the three basins were analysed using precipitation projection datasets generated under RICCAR for both emission scenarios until the end of the century. The drought assessment was based on the Standardized Precipitation Index (SPI) according to the method developed by McKee et al.,1993, which measures drought based on the degree to which precipitation in a given time period diverges from the historical median.[5]

SPI indices are timescale-specific and compare precipitation totals for a specific period over all previous years of available data for the same period. Two timescales were selected for this study. The first is the six-month SPI (November to end of April for Nahr el Kabir and Medjerda rivers; May to end of October for Wadi Diqah), which is also referred to as agricultural drought and gives an important indication of rainfall patterns during the agricultural season in the basins.

The other timescale considered is the 12-month SPI (starting November) or hydrological drought, which reflects long-term precipitation. The SPI values were calculated according to a gamma distribution using Microsoft Excel.

It is important to note that the α and β parameters of the γ probability density function were computed for the reference period (1986–2005) then were fixed when SPI was calculated for projected climate data (2006–2100) As defined by McKee et al.,1993, SPI values are classified into different drought categories with SPI < –1.0 indicating a moderate drought, SPI < –1.5 a severe drought, and SPI < –2.0 reflecting an extreme drought.

TABLE 13: Indicators presented

Indicator	unit
Extreme temperatures	
TR (tropical nights)	No. of days/yr
SU35 (hot days)	No. of days/yr
SU40 (very hot days)	No. of days/yr
Extreme Precipitation	
CDD (maximum length of dry spell)	No. of days/yr
CWD (maximum length of wet spell)	No. of days/yr
R10 (10 mm precipitation days)	No. of days/yr
R20 (20 mm precipitation days)	No. of days/yr
SDII (Simple Precipitation Intensity Index)	mm/day
Drought events	
SPI (Standardized Precipitation Index)	-
Flood events	
90th percentile high flow	No. of days
100-yr flood	m^3/s

5.1.3 Extreme flood events

The assessment of the impact of climate change on extreme flow was carried out using the HEC HMS model and the Arc GIS extension HEC-GeoHMS.[6] The Soil Moisture Accounting (SMA) method was selected within HEC-HMS for this analysis. Data sources used to perform the hydrological simulations for each selected basin included observed climate and river discharge data for at least two stations in each basin, as well as topographic, land use and soil data pertaining to each basin. River discharge data were used for model calibration and validation for the three basins. In addition, downscaled RCM daily temperature and precipitation projections generated under RICCAR over the Arab Domain were used as inputs to the hydrological model as the climate data for different time periods and emission scenarios. Potential evapotranspiration was also used as an input and computed within the HEC-HMS model using the Priestley-Taylor method. Hydrological model runs were then performed separately on individual RCM ensemble member simulations (RCA4_EC EARTH, RCA4_CNRM-CM5, and RCA4_GFDL-ESM) covering the period 1970–2100 for RCP 4.5 and RCP 8.5. A total of six runs were thus applied for each basin. For each RCP, the ensemble mean streamflow value from the three model runs was then calculated and used as a result for the analysis. Based on the outputs, two sets of analyses

were used to detect projected changes in the frequency and magnitude of extreme streamflow events until the end of the century in the selected basins. The first aimed at identifying changes in the frequency of extreme peak flow discharges: the number of days exceeding the 90th percentile values of the maximum daily streamflow value. The second analysis investigated changes in the 100-year flood value, which refers to extreme flow events with return periods equal to, or larger than, 100 years. The Gumbel frequency distribution was used for flood-frequency analyses, with the variables estimated using the maximum likelihood method.

5.2 NAHR EL KABIR RIVER BASIN – LEBANON/SYRIAN ARAB REPUBLIC

5.2.1 Extreme temperature and precipitation

All temperature indicators indicate trends towards drier conditions in the basin, apparent from projected increases in warm temperature indicators and decrease in cold spells (Figure 76). For instance, SU35 is projected to increase from 60 days to 88 and 98 days at mid- and end-century, respectively, for RCP 4.5 and up to 93 and 124 days for RCP 8.5 (Table 14).

The trend of increased temperature indicators is more pronounced under RCP 8.5. As for precipitation indicators, results are variable.

For instance, there is a significant amount of variability for the CDD indicator with no obvious temporal pattern: for RCP 4.5, an increase by three days is apparent at mid-century, followed by a decrease of three days at end-century.

On the other hand, less heavy rain (R10) is projected over time, even though very heavy rain is projected to increase (R20). Increases in rain intensity are projected for both scenarios over time as exhibited by the changes in the SDII indicator.

Nahr el Kabir River, Syrian Arab Republic, 2007. Source: Ihab Jnad.

FIGURE 76: Mean change in selected extreme events indices over time for ensemble of three RCP 4.5 and RCP 8.5 projections for the Nahr el Kabir River basin

TEMPERATURE INDICES

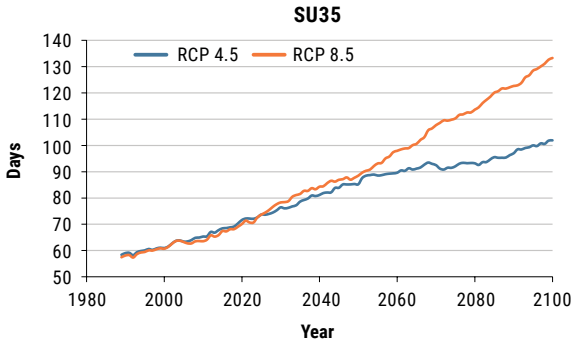

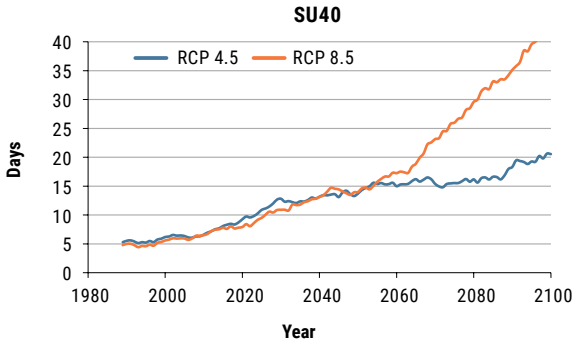

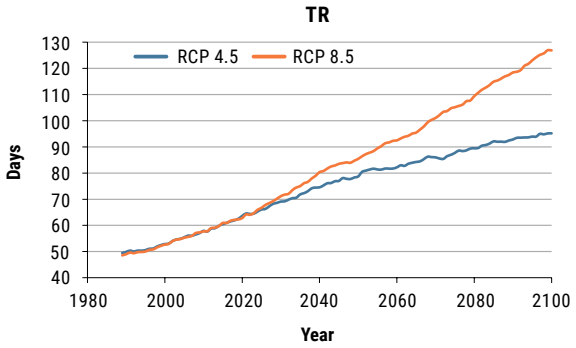

PRECIPITATION INDICES

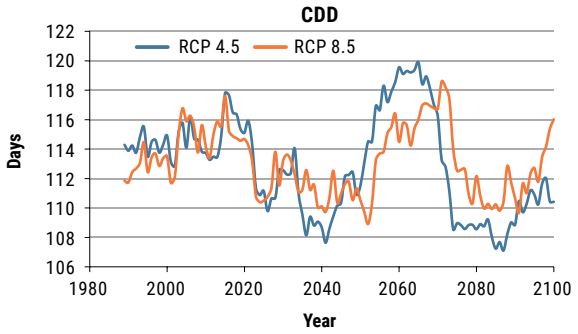

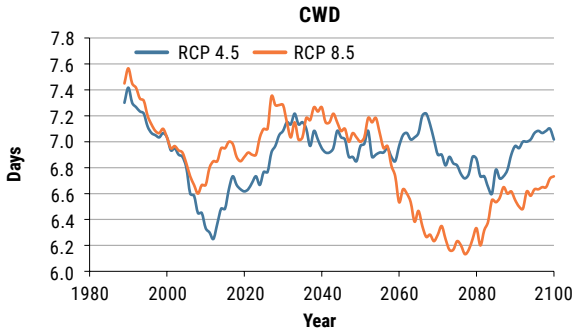

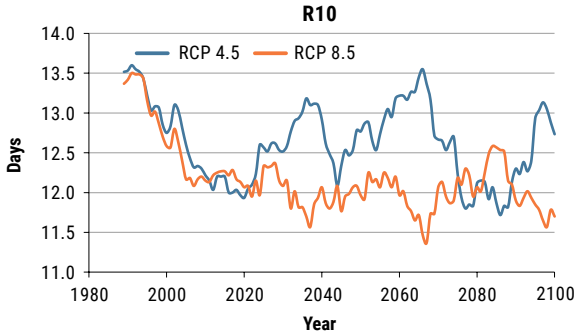

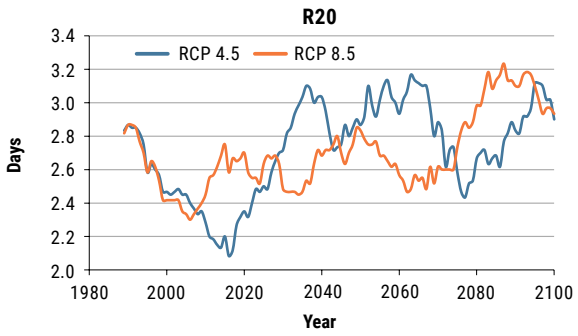

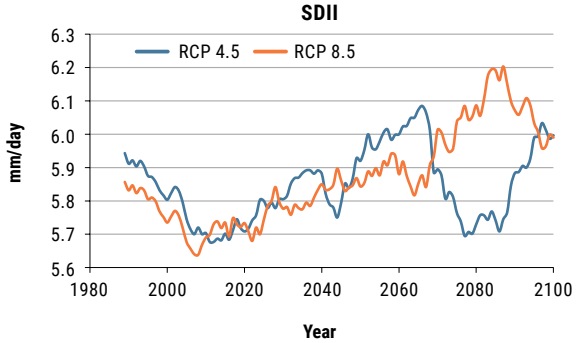

TABLE 14: Extreme event indices values for different emission scenarios and time periods for Nahr el Kabir River basin

Index	Emission scenario	1986-2005	2046-2065	2081-2100
Extreme temperature indices				
TR (days/yr)	RCP 4.5	52	81	93
	RCP 8.5		89	119
SU35 (days/yr)	RCP 4.5	60	88	98
	RCP 8.5		93	124
SU40 (days/yr)	RCP 4.5	5	15	18
	RCP 8.5		16	36
Extreme precipitation indices				
CDD (days/yr)	RCP 4.5	113	116	110
	RCP 8.5		113	112
CWD (days/yr)	RCP 4.5	7.1	7.0	6.9
	RCP 8.5		6.9	6.6
R10 (days/yr)	RCP 4.5	13.0	12.9	12.3
	RCP 8.5		12.0	12.1
R20 (days/yr)	RCP 4.5	2.6	3.0	2.9
	RCP 8.5		2.7	3.1
SDII (mm/day)	RCP 4.5	5.8	6.0	5.9
	RCP 8.5		5.9	6.1

5.2.2 Drought events

When evaluating the six-month SPI (Figure 77), results show that moderate drought occurs 55% of the time (percentage in terms of months) for the reference time period. For RCP 4.5, it changes to 45% and 65% of the time at mid- and end-century, respectively, and becomes more intense for RCP 8.5 with moderate drought occurring 75% and 90% of the time at mid- and end-century, respectively.

When evaluating the 12-month SPI (Figure 78), results show that moderate drought occurs 60% of the time for the reference period and is projected at 55% for mid-century and 65% at end-century for RCP 4.5. A strong increase is projected at RCP 8.5, with occurrences of 75% and 80% at mid- and end-century, respectively. In summary, when comparing future projections, results show that a strong increase in the percentage of time with moderate drought conditions is expected towards end-century. There are no projected severe or extreme droughts in the six- or 12-month SPI in the basin.

FIGURE 77: Projected six-month SPI trends over time for ensemble of three RCP 4.5 and RCP 8.5 projections for the Nahr el Kabir River basin

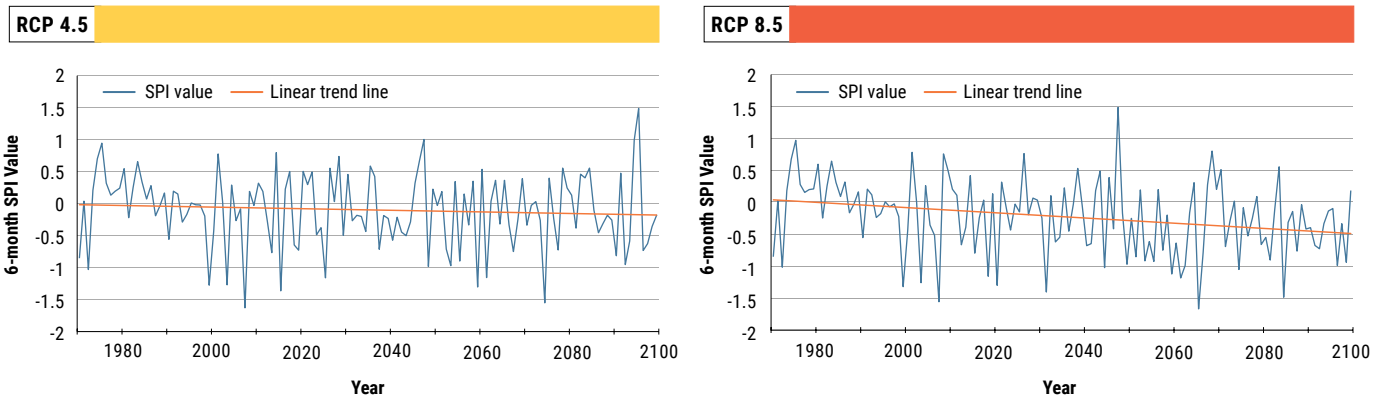

FIGURE 78: Projected 12-month SPI trends over time for ensemble of three RCP 4.5 and RCP 8.5 projections for the Nahr el Kabir River basin

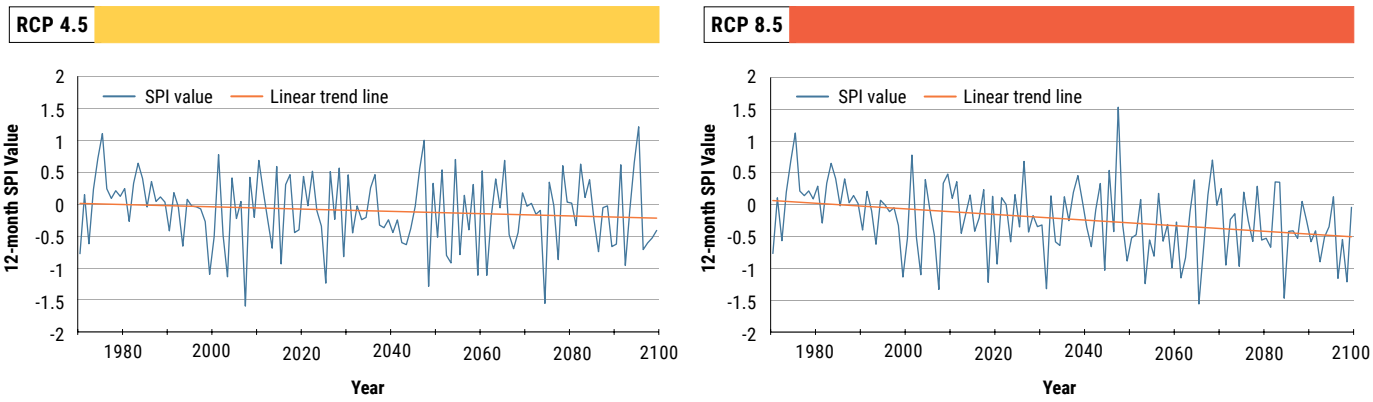

5.2.3 Extreme flood events

Results show that the 90th per centile high flow days are projected to increase for both emissions scenarios in this basin (Figure 79). Moreover, trends for the 100-year flood values (Figure 80) are projected to rise strongly in particular for RCP 8.5. Results for RCP 8.5 show changes in value from 126 m^3/s at the reference period to 131 m^3/s and 149 m^3/s at mid- and end-century, respectively (Table 15).

FIGURE 79: Mean number of 90th percentile high-flow days for different emission scenarios and time periods for the Nahr el Kabir River basin

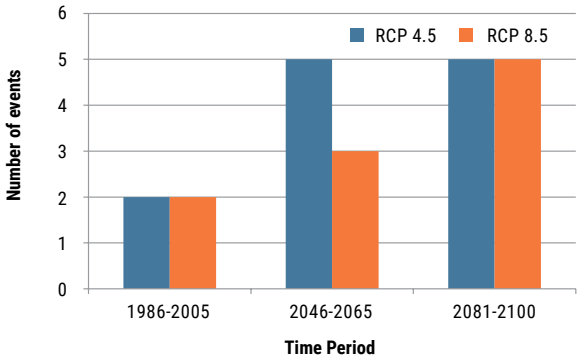

FIGURE 80: Mean change in the 100-year flood value (m^3/s) over time for ensemble of three RCP 4.5 and RCP 8.5 projections for the Nahr el Kabir River basin

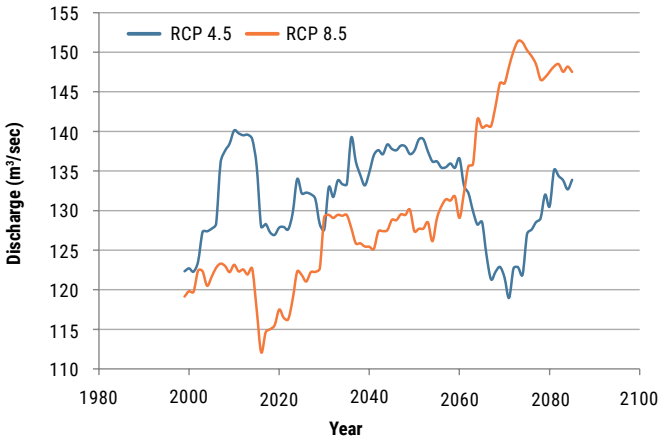

TABLE 15: Mean ensemble 100-year flood values (m^3/s) for different emission scenarios and time periods for the Nahr el Kabir River basin

Emission scenario	1986–2005	2046–2065	2081–2100
RCP 4.5	126	136	128
RCP 8.5	126	131	149

5.3 WADI DIQAH RIVER BASIN

5.3.1 Extreme temperature and precipitation

Results for extreme temperature and precipitation for the Wadi Diqah River basin are presented in Figure 81 and Table 16. All temperature indicators show a trend towards drier conditions in the Wadi Diqah basin. SU35 is projected to increase from 40 days in the reference period to 77 days and 89 days at mid- and end-century, respectively for scenario RCP 4.5. The trends for RCP 8.5 are more pronounced with increases to 88 days and 130 days, respectively, at mid- and end-century. Projections for precipitation indicators indicated a clear increasing trend for CDD in concordance with decreasing trends in CWD. On the other hand, both R10 and R20 show increases towards the end of the century and projected changes in SDII indicate that more intense precipitation events are projected for both emission scenarios.

Wadi Diqah Dam reservoir, Oman, 2011. Source: Ihab Jnad.

FIGURE 81: Mean change in selected extreme events indices over time for ensemble of three RCP 4.5 and RCP 8.5 projections for the Wadi Diqah River basin

TEMPERATURE INDICES

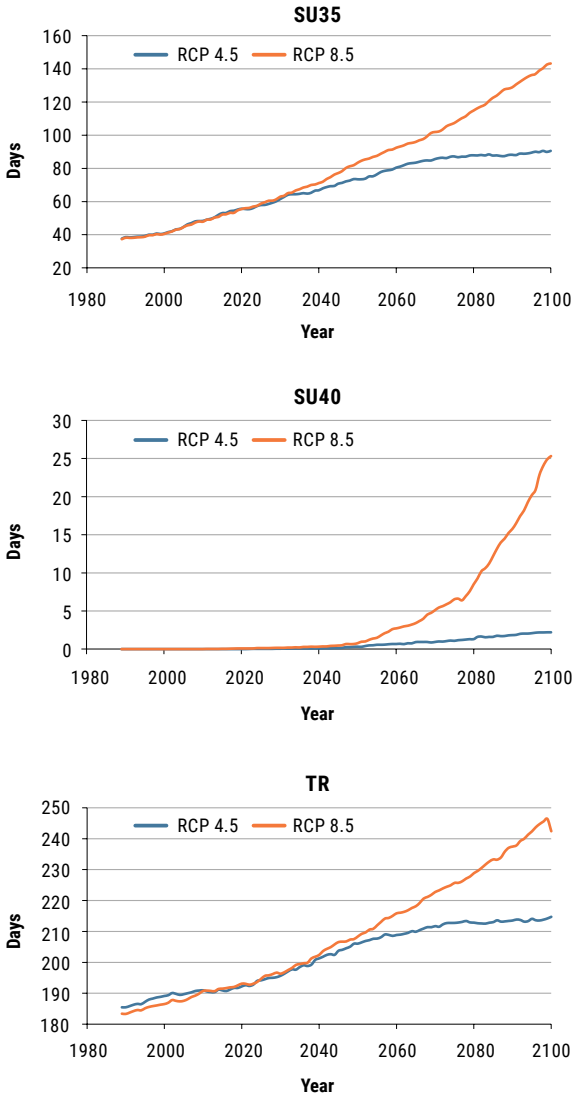

PRECIPITATION INDICES

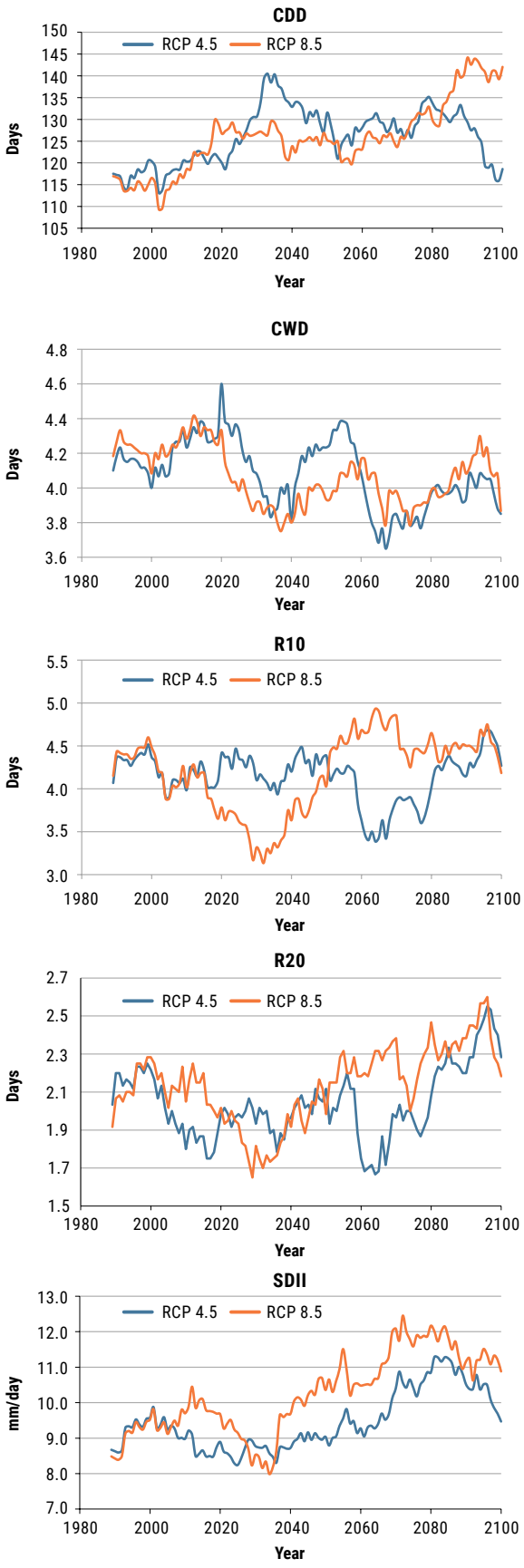

TABLE 16: Extreme event indices values for different emission scenarios and time periods for the Wadi Diqah River basin

Index	Emission scenario	1986-2005	2046-2065	2081-2100
Extreme temperature indices				
TR (days/yr)	RCP 4.5	187	207	213
	RCP 8.5		212	238
SU35 (days/yr)	RCP 4.5	40	77	89
	RCP 8.5		88	130
SU40 (days/yr)	RCP 4.5	0	0.5	1.9
	RCP 8.5		1.8	16.8
Extreme precipitation indices				
CDD (days/yr)	RCP 4.5	115	128	126
	RCP 8.5		124	139
CWD (days/yr)	RCP 4.5	4.1	4.2	4.0
	RCP 8.5		4.0	4.1
R10 (days/yr)	RCP 4.5	4.3	4.0	4.4
	RCP 8.5		4.5	4.5
R20 (days/yr)	RCP 4.5	2.1	2.0	2.3
	RCP 8.5		2.2	2.4
SDII (mm/day)	RCP 4.5	9.1	9.2	10.6
	RCP 8.5		10.6	11.4

5.3.2 Drought events

As shown in Figure 82 and Figure 83, a positive SPI trend is projected for both emission scenarios over the years, though this change in trend is not significant according to the Mann-Kendall test (α=0.05). Evaluation of results in terms of percentage of occurrence shows an overall decrease in the occurrence of moderate drought for the six-month SPI as opposed to an increase for the 12-month SPI. Values for the six-month SPI vary from 60% of the time in the reference period to 50% both at mid- and end-century for RCP 4.5. No change from the reference period is apparent for RCP 8.5 at mid-century (50%) but a decrease to 40% is projected at end-century. As for the 12-month SPI, an increase in moderate drought occurrence is projected for RCP 4.5 compared to the reference period which exhibits an occurrence of 50% (values of 65% and 60% for mid- and end-century, respectively), as well as an increase for RCP 8.5 at mid-century, with the occurrence changing from 50% (reference period) to 55% (mid-century). No severe or extreme droughts are detected in this basin.

FIGURE 82: Projected six-month SPI trends over time for ensemble of three RCP 4.5 and RCP 8.5 projections for the Wadi Diqah River basin

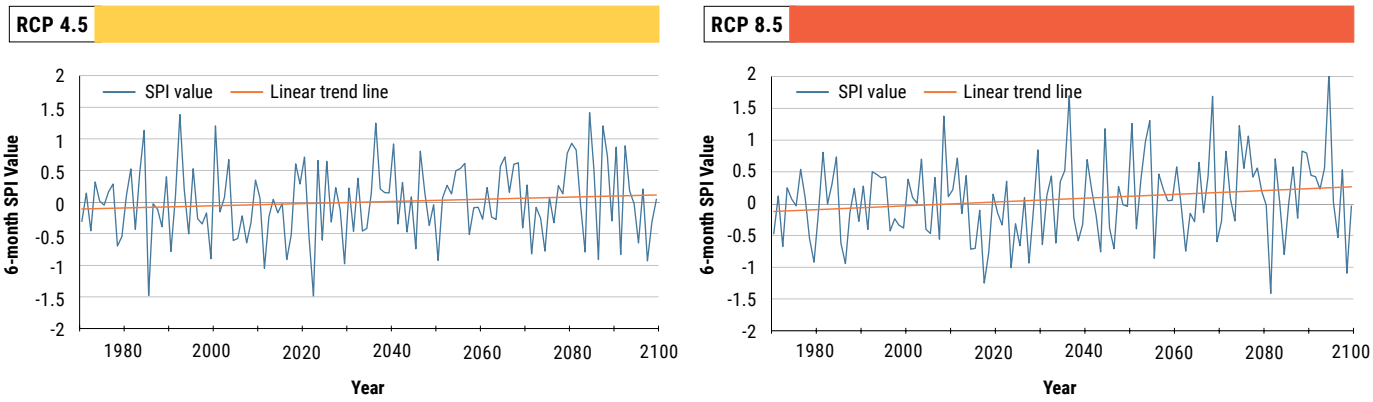

FIGURE 83: Projected 12-month SPI trends over time for ensemble of three RCP 4.5 and RCP 8.5 projections for the Wadi Diqah River basin

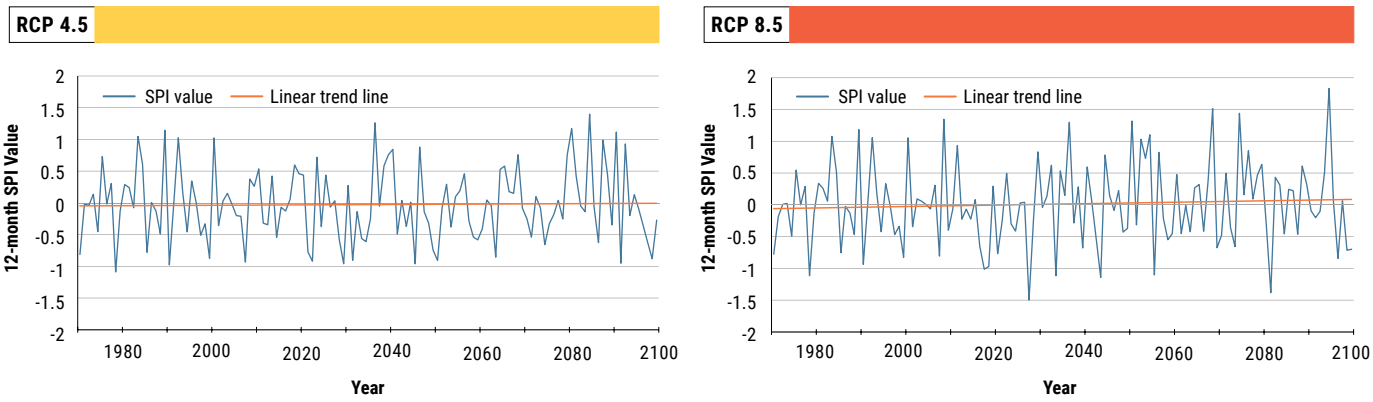

5.3.3 Extreme flood events

As shown in Figure 84, results for the 90th percentile high-flow days for Wadi Diqah reveal a decrease at mid-century compared to the reference period followed by an increase at end-century for both emissions scenarios. The 100-year flood value is projected to rise for both RCPs at the end of the century after a decrease at mid-century (Figure 85 and Table 17).

FIGURE 84: Mean number of 90th percentile high-flow days for different emission scenarios and time periods for the Wadi Diqah River basin

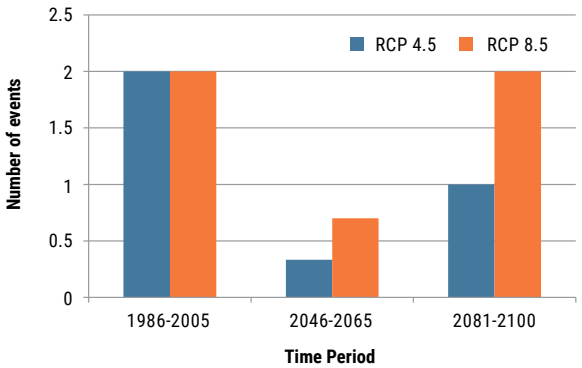

FIGURE 85: Mean change in the 100-year flood value (m^3/s) over time for ensemble of three RCP 4.5 and RCP 8.5 projections for the Wadi Diqah River basin

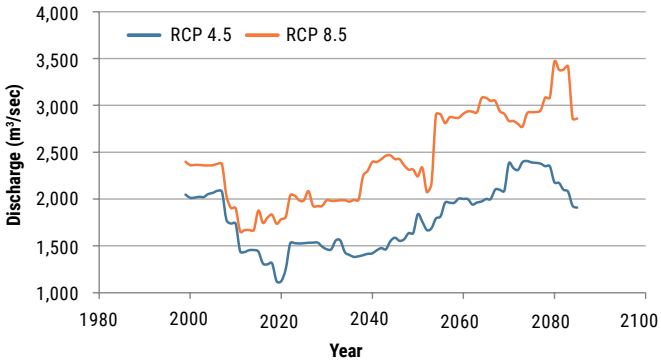

TABLE 17: Mean ensemble 100-year flood values (m^3/s) for different emission scenarios and time periods for the Wadi Diqah River basin

Emission scenario	1986–2005	2046–2065	2081–2100
RCP 4.5	2,200	1,836	2,275
RCP 8.5	2,100	2,667	3,043

5.4 MEDJERDA RIVER BASIN

5.4.1 Extreme temperature and precipitation

As shown in Figure 86 and Table 18, changes in extreme temperature indices in the basin indicate consistent trends towards drier conditions, in particular for RCP 8.5. For example, for the emission scenario RCP 4.5, the indicator SU35 is projected to increase from 45 days in the reference period to 65 days and 74 days at mid and end-century, respectively. These change to 71 and 97 days for RCP 8.5. Results for precipitation extremes are more variable. For instance, CDD show decreases at mid-century and increase at end-century. Both R10 and R20 have consistent decreasing trends at the end of the century, while precipitation intensity is projected to increase at the end of the century (SDII).

Sidi Salem dam, Medjerda River, Tunisia, 2015. Source: Elarbi Alaeddin.

FIGURE 86: Mean change in selected extreme event indices over time for ensemble of three RCP 4.5 and RCP 8.5 projections for the Medjerda River basin

TEMPERATURE INDICES

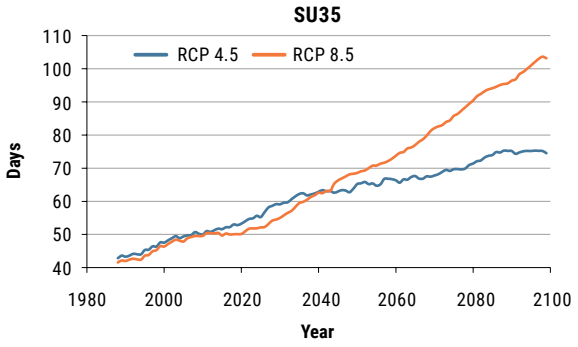

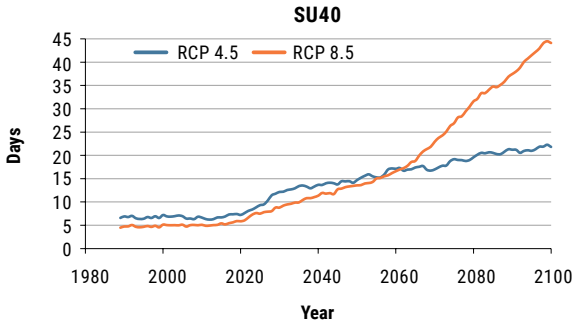

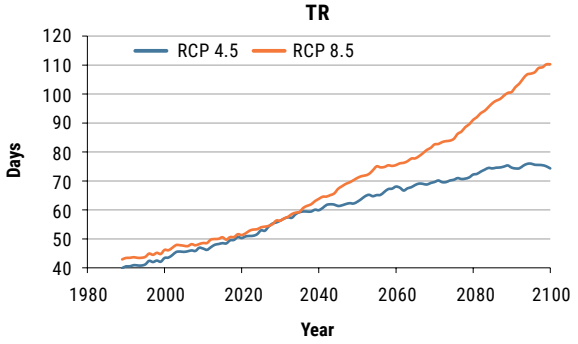

PRECIPITATION INDICES

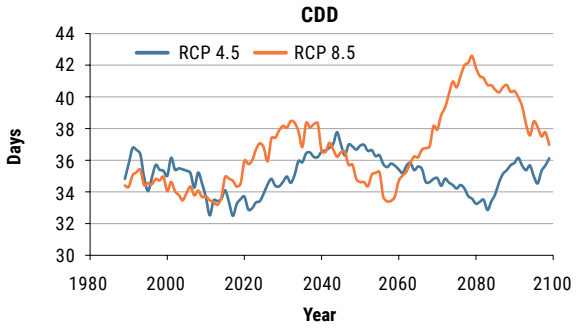

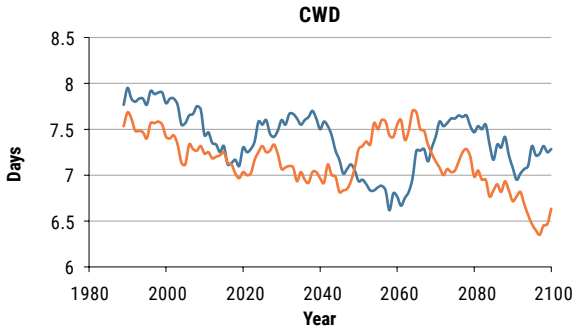

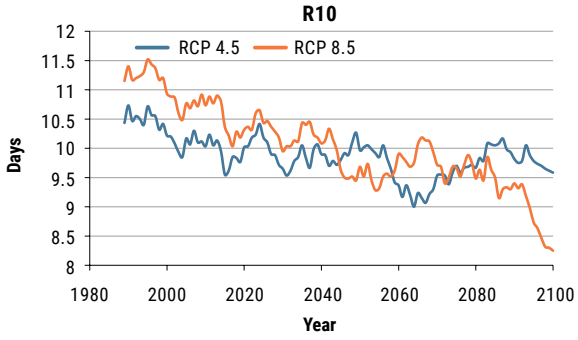

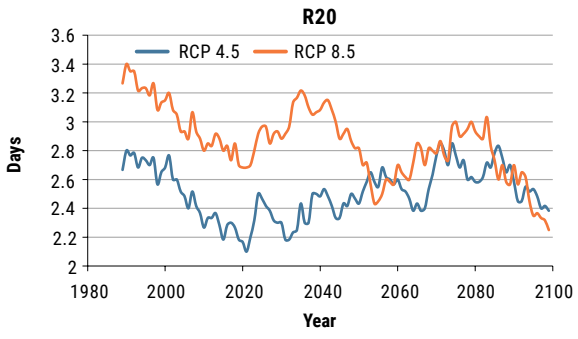

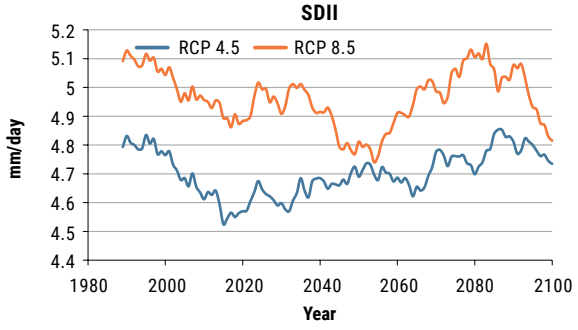

TABLE 18: Extreme event indices values for different emission scenarios and time periods for the Medjerda River basin

Index	Emission scenario	1986-2005	2046-2065	2081-2100
Extreme temperature indices				
TR (days/yr)	RCP 4.5	43	65	75
	RCP 8.5		73	102
SU35 (days/yr)	RCP 4.5	45	65	74
	RCP 8.5		71	97
SU40 (days/yr)	RCP 4.5	6	16	21
	RCP 8.5		15	38
Extreme precipitation indices				
CDD (days/yr)	RCP 4.5	35	36	35
	RCP 8.5		35	40
CWD (days/yr)	RCP 4.5	7.7	6.9	7.3
	RCP 8.5		7.3	6.7
R10 (days/yr)	RCP 4.5	10.9	9.7	9.9
	RCP 8.5		9.6	9.1
R20 (days/yr)	RCP 4.5	3.0	2.5	2.6
	RCP 8.5		2.7	2.6
SDII (mm/day)	RCP 4.5	4.9	4.7	4.8
	RCP 8.5		4.8	5.0

5.4.2 Drought events

Figure 87 and Figure 88 show that SPI values exhibit projected significant negative trends over the years (according to Mann-Kendall test with α=0.05). Unlike the other basins, the Medjerda River exhibits projected episodes of severe and extreme drought in addition to moderate drought for both RCPs over time (Table 19).

Results show a slight increase in the percentage of time with moderate drought for both SPI values and emission scenarios. Furthermore, it can be seen that severe drought conditions are expected to occur much more often by the end of the century. Lastly, extreme drought is projected to occur at the end of the century for the emission scenario RCP 8.5 only.

FIGURE 87: Projected six-month SPI trends over time for ensemble of three RCP 4.5 and RCP 8.5 projections for the Medjerda River basin

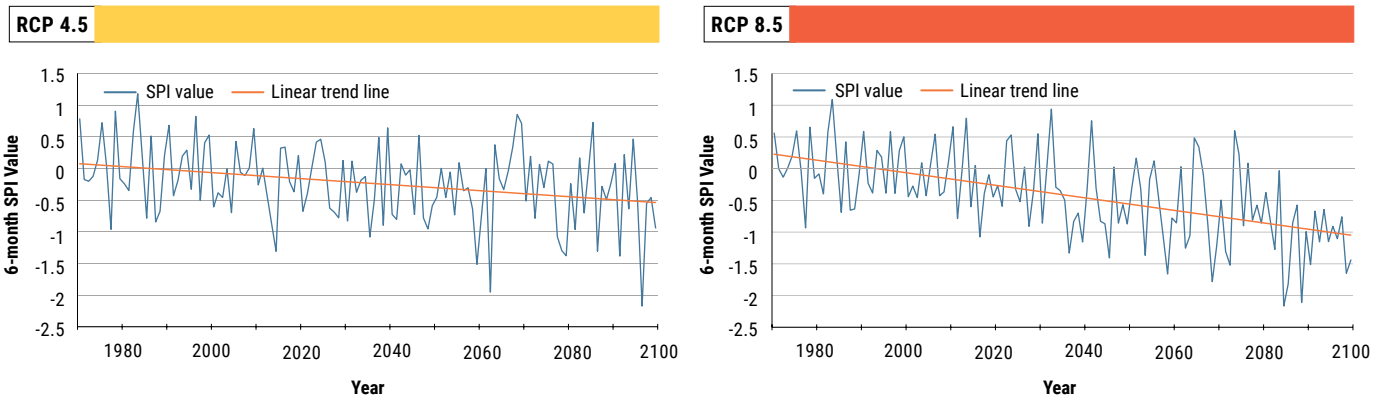

FIGURE 88: Projected 12-month SPI trends over time for ensemble of three RCP 4.5 projections for the Medjerda River basin

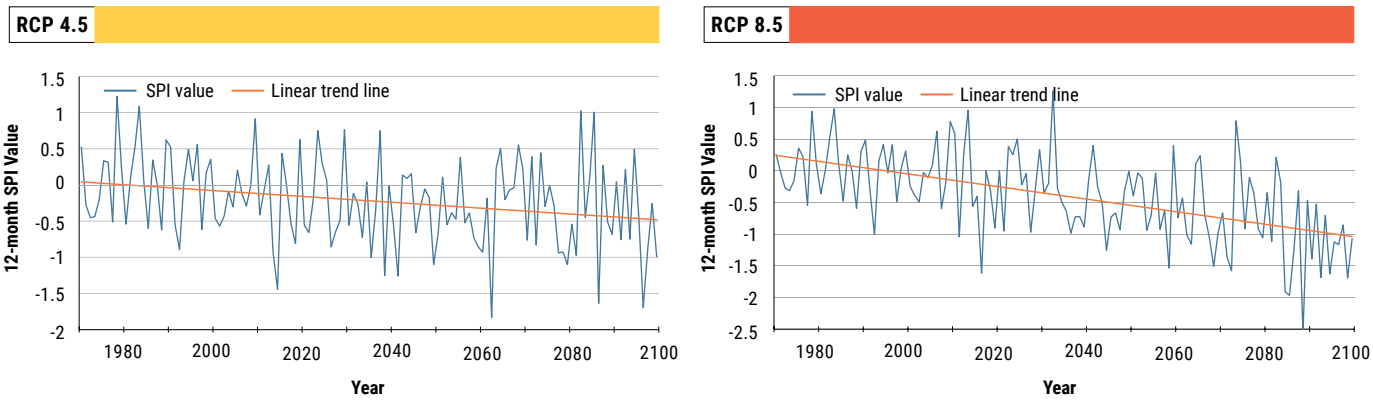

TABLE 19: Projected percentage of time with moderate, severe and extreme drought conditions until the end of the century for the six-month SPI value and the 12-month SPI value in the Medjerda River basin

Drought conditions	Drought occurence (%)				
	Reference period (1986-2005)	Mid-century (2046-2065)		End-century (2081-2100)	
		RCP 4.5	RCP 8.5	RCP 4.5	RCP 8.5
Six-month SPI value					
Moderate	60	70	70	70	75
Severe	0	10	5	0	15
Extreme	0	0	0	5	10
TOTAL	**60**	**80**	**75**	**75**	**100**
12-month SPI value					
Moderate	50	75	85	50	65
Severe	0	5	5	10	25
Extreme	0	0	0	0	5
TOTAL	**50**	**80**	**90**	**60**	**95**

5.4.3 Extreme flood events

Projected changes in the 90th percentile high-flow days are highly variable for the Medjerda basin. As seen in Figure 89, decreases are projected towards end-century for RCP 4.5. On the other hand, results for RCP 8.5 exhibit increases at mid-century and decreases at end-century. Even though the latter indicator exhibits decreases for RCP 4.5, results for the 100-year flood value project increases from 790 m^3/s (reference period) to 8,436 m^3/s at mid-century and a further increase to 9,031 m^3/s at end-century for this emission scenario. For RCP 8.5, values remain in the same range with 7,533 m^3/s and 7,627 m^3/s at mid century and end-century, respectively (Figure 90 and Table 20).

FIGURE 89: Mean number of 90th percentile high-flow days for different emission scenarios and time periods for the Medjerda River basin

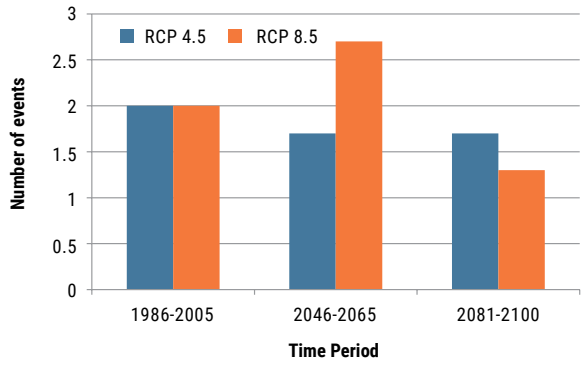

FIGURE 90: Mean change in the 100-year flood value (m^3/s) over time for ensemble of three RCP 4.5 and RCP 8.5 projections for the Medjerda River basin

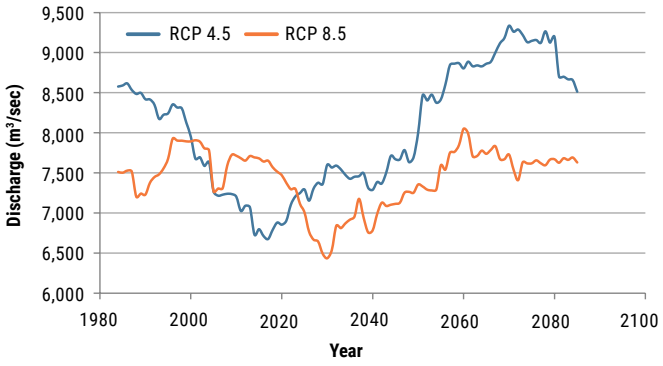

TABLE 20: Mean ensemble 100-year flood values (m^3/s) for different emission scenarios and time periods for the Medjerda River basin

Emission scenario	1986–2005	2046–2065	2081–2100
RCP 4.5	7,890	8,436	9,031
RCP 8.5	7,890	7,535	7,627

5.5 SUMMARY OF KEY FINDINGS

For the Nahr el Kabir basin, by the end of the century and for both emission scenarios:

- There is a notable projected increase in heat extremes such as warm-spell duration, number of hot days, number of very hot days, and tropical nights over time;
- Results indicate an increase in precipitation intensity and very heavy precipitation days, together with an increasing number of consecutive dry days;
- There is a projected tendency towards drier conditions with an increase in the occurrence of moderate drought, but with no severe or extreme droughts events projected to occur;
- The basin is likely to experience an increase in the magnitude of peak flow and flood frequencies over the 21st century.

For the Wadi Diqah basin:

- There is a projected increase in heat extremes such as warm-spell duration, number of hot days, number of very hot days and tropical nights over time and for both emission scenarios;
- Results indicate an increase of precipitation intensity and heavy precipitation days, together with increasing consecutive dry days for future periods under both RCPs;
- In accordance with the reference period, there is no indication of projected severe or extreme droughts over the 21st century, while moderate drought conditions are still projected to occur with few changes compared to the reference period;
- The basin is likely to experience a progressive general increase in the magnitude of peak flow over time for both emission scenarios, together with a decreasing number of extreme flood days at mid-century followed by an increase at end-century.

For the Medjerda basin:

- An increase in all heat extremes is projected, such as warm-spell duration, number of hot days, number of very hot days, and tropical nights by the end of the century for both RCPs;
- There is a projected overall decrease in heavy precipitation days, together with an increase in consecutive dry days over time and for both emission scenarios;
- There is a tendency towards drier conditions with projected episodes of severe and extreme droughts in addition to moderate drought over time and for both emission scenarios;
- The Medjerda basin is likely to experience an increase in the magnitude of peak flows for the moderate emission scenario, together with a decreasing number of extreme flood events. For the high-emission scenario, however, the magnitude of peak flow is projected to decrease.

ENDNOTES

1. Also referred to as Nahr el Kabir Al-Janoubi (the great southern river), not to be confused with the Nahr el Kabir Al Shamali (the great northern river), a river in the Syrian Arab Republic that is not shared.
2. ACSAD and ESCWA, 2017
3. RClimDex was developed by, and is maintained at, the Climate Research Branch of the Meteorological Service of Canada. It provides a graphical user interface to compute the 27 core indices and perform quality control on the input daily data (ETCCDI, 2017).
4. See ACSAD and ESCWA, 2017
5. McKee et al., 1993
6. The Hydrologic Engineering Center Hydrological Modelling System (US Army Corps of Engineers, 2000). Refer to Chapter 1 for more details on this model.

REFERENCES

ACSAD and ESCWA (Arab Center for the Studies of Arid Zones and Dry Lands; United Nations Economic and Social Commission for Western Asia). 2017. Impact of Climate Change on Extreme Events in Selected Basins in the Arab Region. *RICCAR Technical Report*. Published by United Nations Economic and Social Commission for Western Asia (ESCWA). Beirut. E/ESCWA/SDPD/2017/RICCAR/TechnicalReport.5.

ETCCDI (Expert Team on Climate Change Detection and Indices). 2017. Climate Change Indices: Software. Available at: http://etccdi.pacificclimate.org/software.shtml.

McKee, T. B., Doesken, N. J. and Kleist, J. 1993. The Relationship of Drought Frequency and Duration to Time Scales. *Proceedings of the 8th Conference on Applied Climatology*, 17(22): p. 179-183.

US Army Corps of Engineers. 2000. Hydrologic Modeling System (HEC-HMS). Available at: http://www.hec.usace.army.mil/software/hec-hms/.

CHAPTER 6

IMPACT OF CLIMATE CHANGE ON THE AGRICULTURAL SECTOR

The Arab region has the lowest per capita availability of water and arable land in the world. Renewable water resources are currently estimated at about 600 m^3 per person per year, corresponding to 10% of the world average, while arable land is about 0.15 ha per person, corresponding to 20% of the world average. Home to about 5% of the global population, the region has the highest percentage of total renewable water resources withdrawal in the world, with irrigated agriculture representing the lion's share (beyond 80%). In the Mashreq countries, the proportion of irrigated land represents 43% of the total cropland, while the Maghreb countries are much less dependent on irrigation (7%–18%), whereas Egypt is nearly 100% irrigated. Furthermore, the Arabian Peninsula and parts of northern Africa are significantly overexploiting their water resources with a significant over-reliance on fossil non-renewable groundwater. Essentially, the water situation is not sustainable and further challenged by being about 60% transboundary.

Notwithstanding efforts to increase agricultural yield, the region is not self-sufficient in food production and relies mainly on imports: about 50% of its wheat and barley, 40% of its rice and 70% of its maize. Some Gulf countries indeed import all their cereal calories. Moreover, the reliance on food imports is expected to increase by 64% between 2010 and 2030.[1] Such reliance on imports exposes Arab States to supply and price risks, as seen during the 2007/2008 and 2010/2011 global food crises. An additional strain on food and water demand is exerted by a strong population growth (almost 2% per year – about twice the world average), which is expected to double by 2050. In addition to rising population, higher living standards, urbanization and further development in general will all exercise an increasing pressure on the already scarce water resources, in turn deeply interwoven with food-security challenges.

Food security and water scarcity remain critical challenges in the Arab region with strong implications for national security, with additional strains caused by climate change impacts. Within RICCAR and through ACCWaM, this section reports on the climate change impact assessment for given time horizons, carried out on major green sectors, specifically, crop systems, livestock, fishery and aquaculture and forestry. Full details of the methodology, as well as additional results and analysis are available in the RICCAR technical report *Climate Change and Adaptation Solutions for the Green Sectors in the Arab Region* (2017).[2]

Irrigated cotton field, Deir el Zor, Syrian Arab Republic, 2007. Source: Ihab Jnad.

6.1 IMPACT ON CROPPING SYSTEMS

A point of departure for analysing the impact of climate change on crop systems was the identification of the existing farming systems in the region (Figure 91). This map was then superimposed on the vulnerability assessment (VA) maps.

The RICCAR VA maps show that most of the cropped area in the Arab region lies within the highest three vulnerability classes (Figure 92 and Figure 93). The areas with highest vulnerability are the Nile Valley (especially the northern parts: this is in addition to the impact of seawater-level rise on the Delta which is expected to impact negatively about 30% of the Delta land surface within this century), the Tigris–Euphrates basin, the south-western Arabian Peninsula and the western parts of North Africa on the Atlas Mountains. The analysis of the green sectors study area shows that evapotranspiration will increase and runoff will decline, resulting in increased intensity of water scarcity, as confirmed by the crop hotspots characterized by global water scarcity classes. The biophysical characterization of the crop hotspots by global farming systems revealed that the most productive systems of the region, namely irrigated and dry savanna agriculture, are those more prone to climate change: 85%–90% of their combined areas are located under the highest two vulnerability classes.

Consistent results are obtained by overlapping the hotspots with global agro-ecological zones (AEZ), where the most productive (irrigated, good soils and moderate soils) are more vulnerable to climate change under the two scenarios (RCP 4.5 and RCP 8.5) with vulnerability increasing when moving to the worst-case scenario and towards the end of the century. Consequently, the most important crops in the region, particularly wheat and sorghum, are all highly vulnerable to climate change as the majority of their areas are located within the two classes of highest vulnerability.

Sorghum crop, UAE, 2010. Source: Wikimedia commons/Priyag.

FIGURE 91: Major farming systems in the Arab region

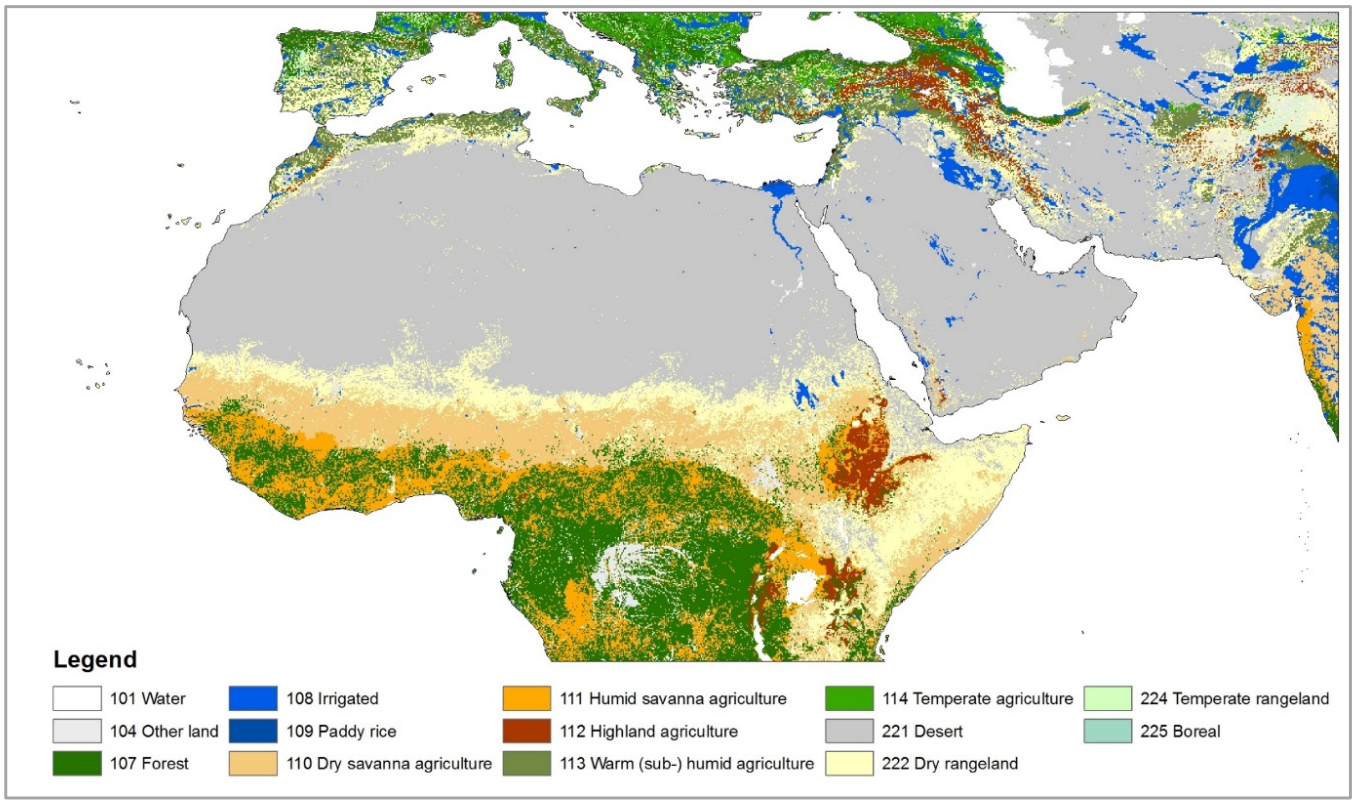

Source: FAO, 2011

Figure 94 and Figure 95 illustrate the distribution of the harvested areas of six crops analysed by vulnerability class under the four climate change scenarios. The most affected crops are wheat and sorghum.

The latter is grown mostly in areas with the highest vulnerability (range 5.9–7.5) while the former is mostly located in the areas with second highest vulnerability (range 5.1–5.8).

It is also evident that the vulnerability of all crops increases when moving from RCP 4.5 to RCP 8.5 and when moving from mid- to end-century scenarios. This is clear in Figure 96 where, for example, the percentage of wheat area falling under the highest two classes of vulnerability increases from 57% under RCP 4.5 mid-century to exceed 65% under RCP 8.5 end-century. Similar trends apply to all the other crops even for olive – the least affected crop with the lowest percentage in the highest vulnerable areas.

FIGURE 92: Distribution (%) of major farming systems in the vulnerability classes (mid-century)

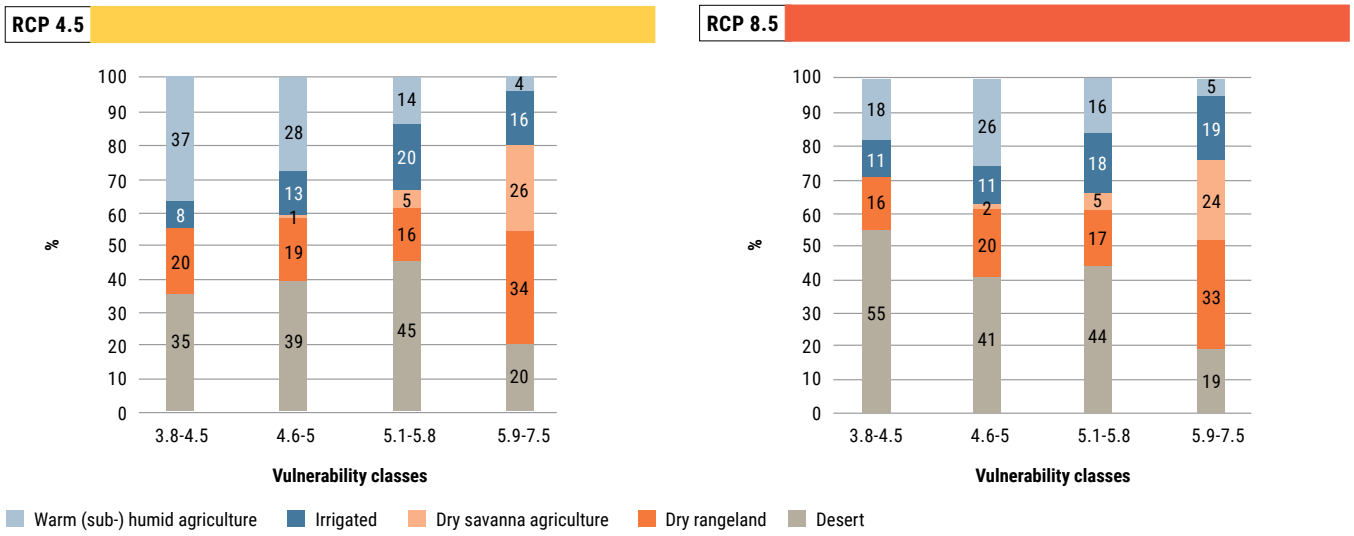

FIGURE 93: Distribution (%) of major farming systems in the vulnerability classes (end-century)

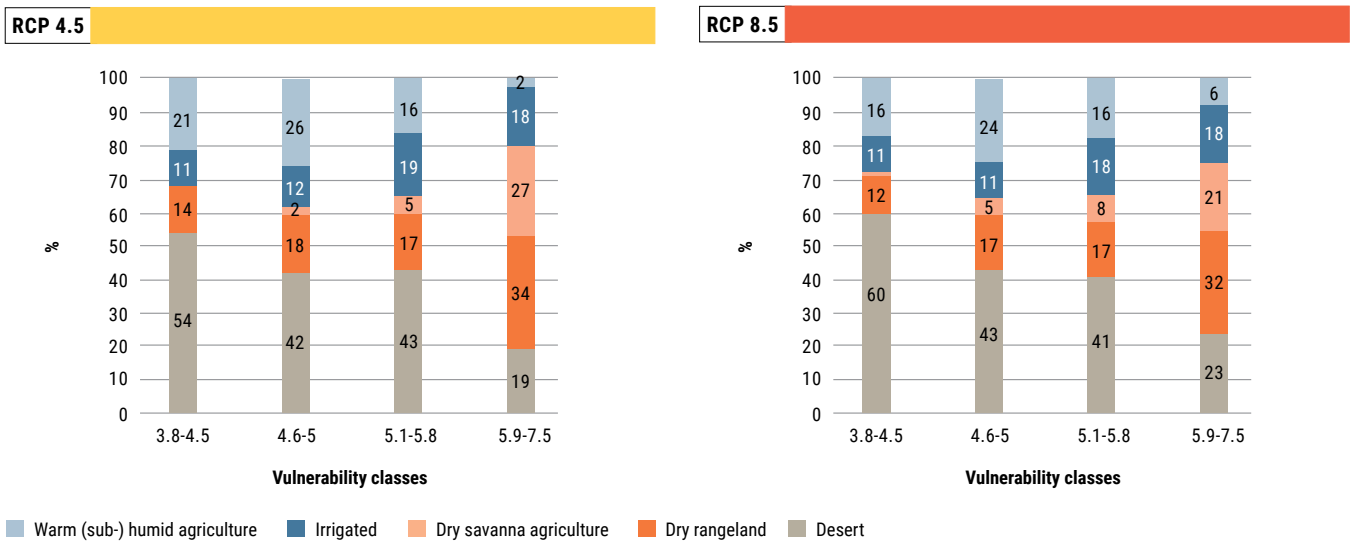

FIGURE 94: Crop area distribution in the vulnerability classes (mid-century)

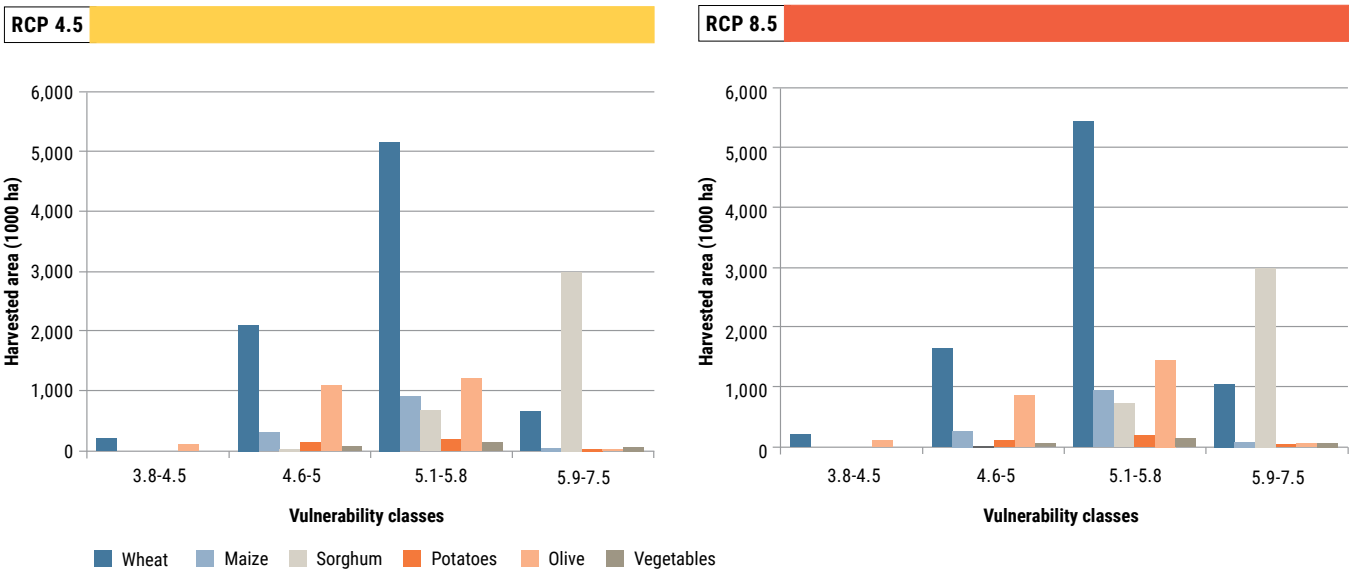

FIGURE 95: Crop area distribution in the vulnerability classes (end-century)

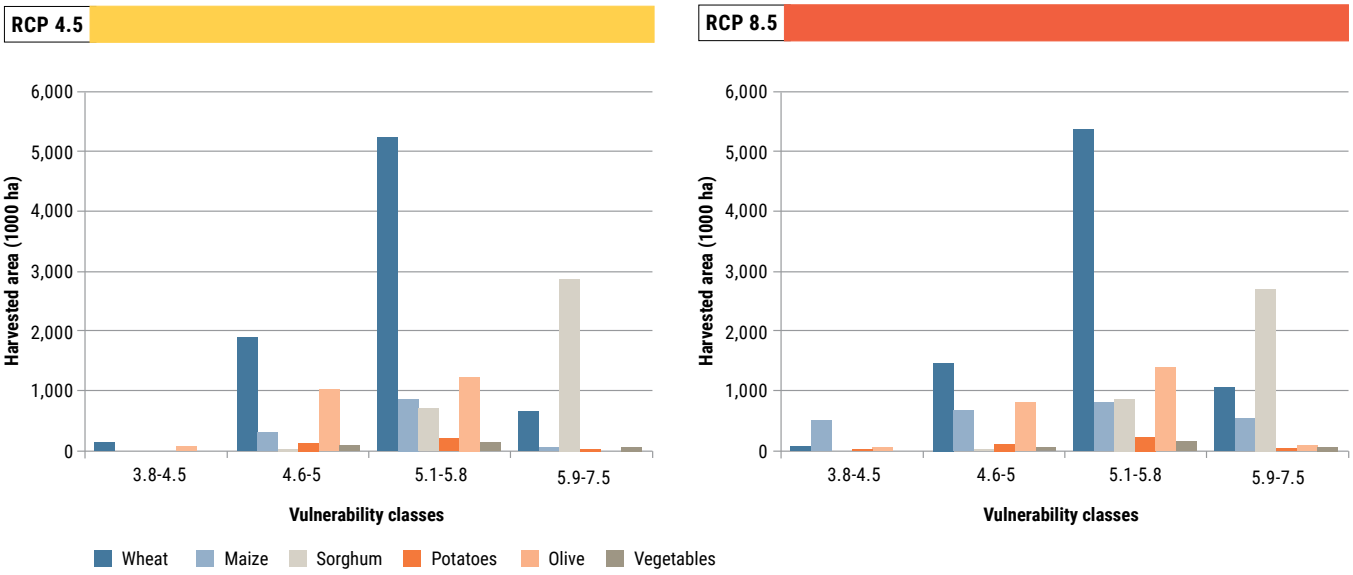

FIGURE 96: Proportion of irrigated crops areas exposed to the highest two classes of vulnerability

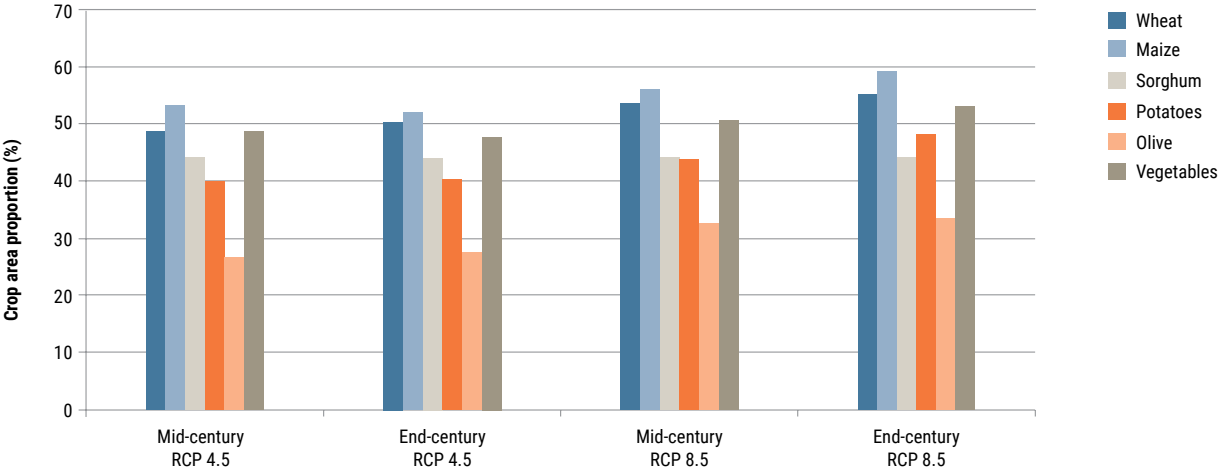

Although some GCMs predict yield increases for some climate scenarios, these increases will occur mostly in areas less important for the relevant crops, while the areas where the crops are concentrated will be negatively affected under all climate scenarios (both moderate and worst-case scenario). For example, irrigated maize is predicted to realize some yield increases within the second and third vulnerability classes. Sorghum, however, which is grown mostly in the highest vulnerable areas, will experience yield declines under all climate change scenarios. Wheat yield is projected to decline under all scenarios, with the largest decline expected in areas with high wheat concentrations. Maize is the least vulnerable cereal and it is expected that reduction in yield will be slight, despite it being located mostly within highly vulnerable areas. Trends for potatoes are similar to those for maize and for olive, which is the only tree crop examined: it was found to be the most vulnerable to climate change, with substantial yield reduction under all scenarios and all GCMs.

6.2 IMPACT ON LIVESTOCK SYSTEMS

The livestock sector in the region contributes to food security, poverty alleviation, employment and economic development and shares 30%–50% of the agricultural output. The vulnerability hotspot map for livestock (see Chapter 11) was produced solely on the basis of water availability without considering the impact on feed production. Adding to that the predicted change in temperature, the results of the hotspots show that the potential impacts of climate change on livestock is related to a dwindling water- and feed-resource base due to recurrent droughts, degradation of rangelands and desertification. Most vulnerable areas are located along the Nile Valley, the Horn of Africa and the south-western Arabian Peninsula, followed by areas of the Fertile Crescent and North Africa, though to a lesser extent. The vulnerability maps showed that the potential impacts of climate change on livestock are slight, compared to their impacts on crops. However, these impacts become significantly negative by the end of century with worst climate scenario. Focusing on sheep, goats, cattle and camels, the majority of these livestock are found in areas with very high vulnerability classes. Excluding camels, which have the lowest density, cattle are the most affected by climate change, followed by goats and sheep, respectively. No noticeable difference in vulnerability is observed between production systems for goats and camels but cattle and sheep – the most important animals in terms of value and number, respectively – raised on grassland production systems will be more prone to climate vulnerability than those raised under mixed systems. The latter is especially true for sheep, whose vulnerability increases dramatically with a grassland system compared to a mixed system under worst-case climate scenario.

Aquaculture near the Orontes river, Lebanon, 2011. Source: Joelle Comair.

6.3 IMPACT ON FISHERIES AND AQUACULTURE

Marine fisheries in the region – and to some extent aquaculture – contribute to food security, poverty alleviation, employment and economic development and share about 25% of agricultural output. In 2011, for example, while the self-sufficiency of cereal in the region reached 45%, the self-sufficiency of fish reached about 75%. Moreover, aquaculture fish production is expected to increase in the coming years, further reducing the gap between domestic supply and demand. However, freshwater aquaculture of many countries in the region is likely to be affected by climate change and may be affected by flooding, drought or high temperatures. It should be noted that the pressure exerted on biodiversity by the pressure of fishing activities has a greater impact on stocks and ecosystems than climate change. Because many fishery resources are heavily overexploited, a change in climate is likely to cause the final collapse of some stocks if fishery management does not reduce exploitation.

6.4 IMPACT ON FORESTRY

In the Arab region, rising atmospheric CO_2 concentrations, higher temperatures, changes in annual and seasonal precipitation patterns and the frequency of extreme events, such as droughts and forest fires, are severely impairing the production, quality and stability of forests and other natural ecosystems. The aridity of the region and low forest cover, coupled with high deforestation rates in some countries, make forests more vulnerable to the negative consequences of climate changes. More specifically, the impact on four major forestry systems were investigated (Figure 97).

FIGURE 97: Location of the pilot sites for investigating the impacts of climate change

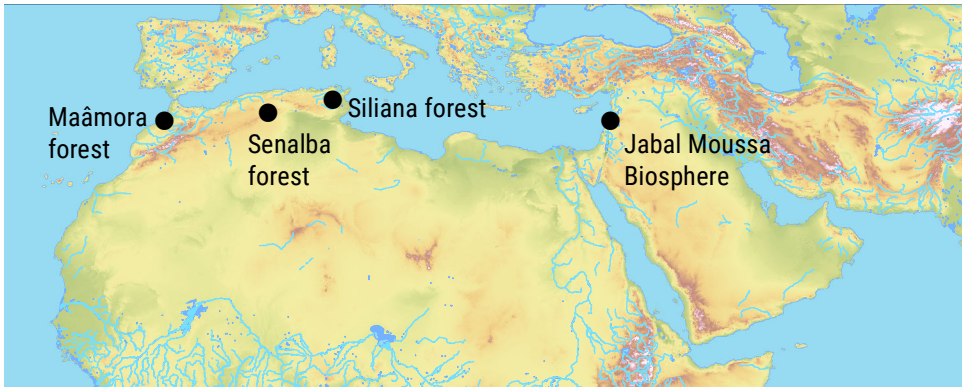

The Maâmora Forest in Morocco is currently undergoing strong anthropic pressure corresponding to wood collection for all uses, overgrazing and systematic collection of cork-oak (*Quercus suber*) acorns for food and trade. Because it prevents natural regeneration, overgrazing is one of the causes of forest ageing. The main impact of climate change on the Maâmora Forest is expected to be water stress. This will be further amplified by anthropic pressure (overgrazing, fuelwood collection, non-wood forest product collection, urbanization, and tourism) and, to a lesser extent, by pest attacks. Eastern zones of the Maâmora Forest are more vulnerable than its western zones.

The mid-century impact of a moderate-case scenario shows an increased vulnerability in all forest areas. Eastern zones will be mostly impacted by water deficit, while western zones will be mostly impacted by forest ageing and health. End-century sees a significant increment in vulnerability.

The Senalba Forest in Algeria has been quite well preserved, thanks to its altitudinal position (900 m–1,600 m asl). There is, however, a strong lack of regeneration of the forest stands, whose average age is 105 years. Moreover, more than 50% of the lands of the Djelfa Wilaya, where the Senalba Forest is located, are sensitive – even highly sensitive – to desertification. The expected impact of climate change will result in an absence of regeneration and an overall ageing of the Aleppo pine populations, defoliation due to water stress and pest attacks and a diminution of the diversity of plants. The vulnerability to climate change of the Senalba Forest for mid- and end-century (and for both scenarios) is mostly influenced by water stress, amplified by overgrazing.

The Siliana Forest in Tunisia decreased in size by 13% from 1990 to 2000 on the basis of various forest inventories. Forest land has mostly been converted into cropland, wooded bushland, non-wooded bushland and young plantations. In the same time frame, 93% of the wooded bushland has been replaced with forest, non-wooded bushland, young plantations and cropland. The vulnerability to climate change of the Siliana Forest is mostly influenced by water deficit, amplified by anthropic activities (overgrazing, fuelwood collection, forest fires, land tenure and land encroachment). As regards climatic factors, forest cover is mostly influenced by extended droughts that bring dieback due to water stress, impede Aleppo pine regeneration and increase tree sensitivity to pest attacks.

In the Jabal Moussa Biosphere Reserve in Lebanon, major tree species like *Quercus cerris* or *Juniperus drupacea* are declining because of climate change, principally because of extreme dry and hot years. Other tree species are also declining because of unregulated activities such as charcoal production and overgrazing.

Moreover, soil erosion is accentuated in degraded areas, resulting in the contamination of watercourses. This process is aggravated by extreme meteorological events that tend to become more frequent according to climate change scenarios. The Jabal Moussa Biosphere Reserve is currently under a humid regime and projections under the moderate-case scenario (RCP 4.5) predict that the northern part of the Reserve will become sub-humid by 2070, while projections under the worst-case scenario (RCP 8.5) predict that the whole Reserve will become sub-humid by 2070.

The most vulnerable forest feature according to the vulnerability assessment is the potentiality for *Quercus cerris* populations for reproduction.

The lessons learned from these case studies in Arab countries is that the vulnerability of Mediterranean forests to climate change is exacerbated by human activities, mostly overgrazing and fuelwood collection and, to a lesser extent, tourism (particularly when coming closer to cities). Even if climate change alone is unlikely to jeopardize the presence of forests, it is likely to impact forest productivity and bring shifts in species composition.

6.5 IMPACT ON SELECTED CROPS IN EGYPT, LEBANON AND JORDAN

When conducting an assessment of projected impacts of climate change on different crops, the so-called fertilizing effect due to CO_2 increase should also be considered.

Moreover, the impact of CO_2 on different crops varies according to their photosynthetic pathway. C3 crops such as wheat, rice or barley are generally expected to benefit from elevated CO_2 concentration in the atmosphere. This is not the case with C4 crops like maize or sorghum.[3]

A specific assessment of the comprehensive impact of climate change on selected crops in pilot areas of selected countries was therefore conducted, using the FAO AquaCrop model, given its ability to consider water-stress conditions and elevated CO_2 concentrations in the atmosphere.

The selected crops were wheat, maize and cotton for the North Delta in Egypt, representing irrigated agriculture; rainfed wheat and barley for Karak Governorate in Jordan, representing very dry (arid) zones; and irrigated eggplant, maize and potato were selected for the Orontes watershed in Lebanon, representing mixed agriculture zones.

After calibration of the model, the simulations were conducted for the selected crops and zones for both moderate-case and worst-case scenarios and for both time horizons (mid-century and end-century). A summary of the impact of climate change on the yield and duration of the growth period are reported in Figure 98, Figure 99 and Figure 100 for Egypt, Lebanon and Jordan, respectively.

The results of the simulation confirm the overall positive response of the C3 crops investigated (wheat, barley, eggplant, potato and cotton) and the non-response of the C4 crop investigated (maize), to elevated atmospheric CO_2 concentration. With C3 crops, we need to distinguish between irrigated and rainfed systems. In fact, irrigated wheat (in Egypt) shows a yield increase of about 14% with both scenarios (RCP 4.5 and RCP 8.5) at mid-century and a yield increase of about 11% and 16% with scenarios RCP 4.5 and RCP 8.5, respectively, at end-century.

This indicates that the projected changes in temperature are not influencing wheat productivity, as long as water is available and that irrigated wheat may take advantage of the climate change due to the increase in CO_2 concentrations. The same can be said for the other C3 plants investigated: cotton (in Egypt), eggplant and potato (in Lebanon) under irrigated conditions. The current, overall water scarcity situation in the Arab region will deteriorate decade by decade, however, and agriculture's share of available water resources will drop continually. This will impact irrigated crop production and crop yield, requiring integrated and highly efficient water resources management.

When we observe the results of the AquaCrop simulation for cereals under rainfed conditions, the yield is affected negatively in all cases, as well as scenarios, with the exception of wheat and barley for mid-century.

The increasingly uneven distribution of rainfall, long periods of dry spells and stronger rainstorms, causing erosion and water losses, will affect rainfed crops significantly. Supplemental irrigation, soil- and water-conservation and water-harvesting measures might ease the negative impacts of climate change on rainfed cropping in the Arab region to a certain extent.

The AquaCrop simulation results also show that climate change will shorten the growing seasons by between 3% and 14% for irrigated wheat in the North Delta in Egypt and between 4% and 27% for the Orontes watershed, Lebanon. This decrease in the length of growing season, mainly due to projected higher temperatures, might result in a slight reduction in crop evapotranspiration.

Wheat harvesting, Egypt, 2017. Source: Amr Hamed.

FIGURE 98: Simulated yield and growing-period duration of maize, wheat and cotton for the reference period, mid-century and end-century for RCP 4.5 and RCP 8.5 in Egypt

Source: FAO, 2017

FIGURE 99: Simulated yield and growing-period duration of eggplant, maize and potato for the reference period, mid-century and end-century for RCP 4.5 and RCP 8.5 in Lebanon

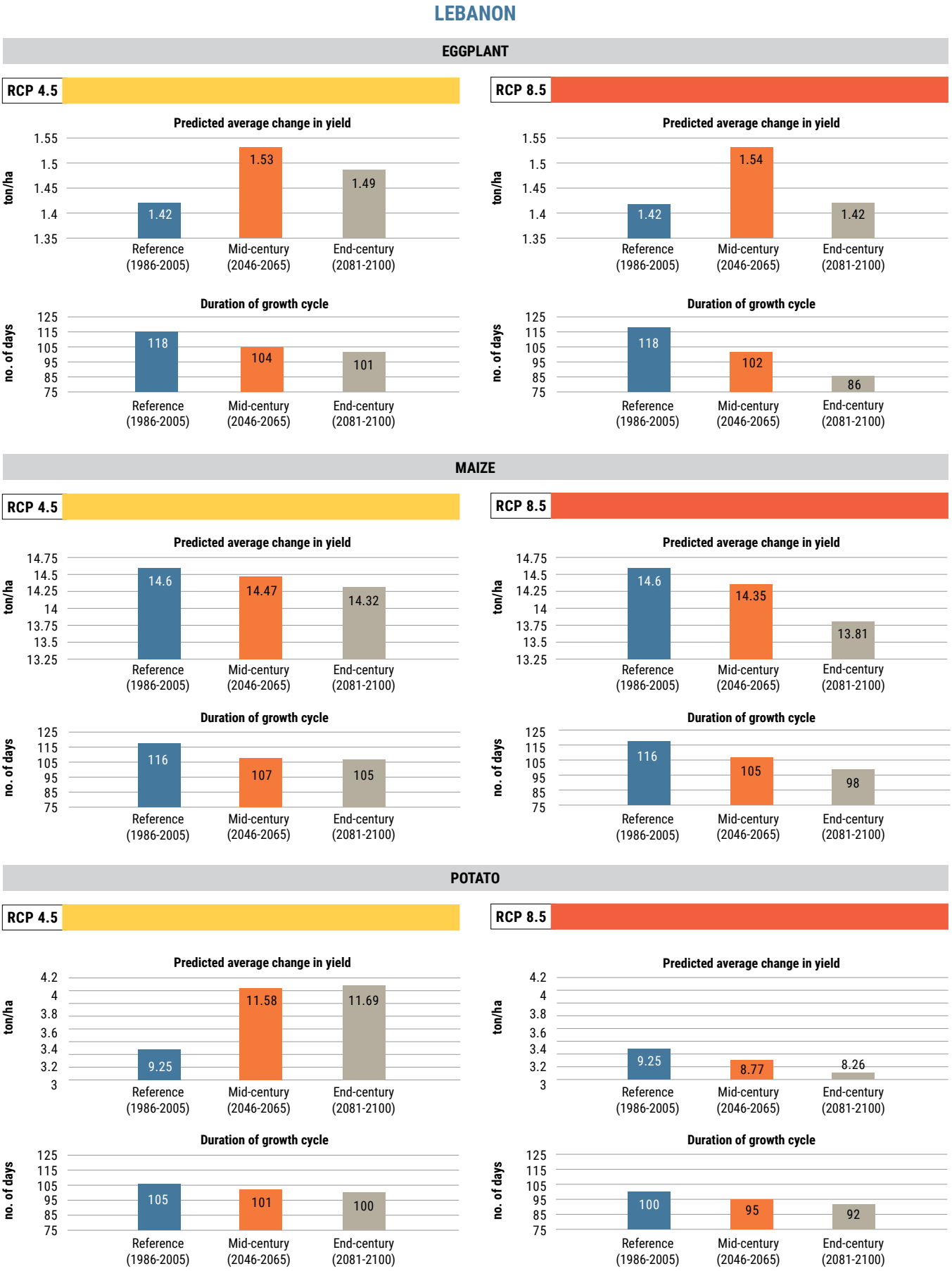

Source: FAO, 2017

FIGURE 100: Simulated yield and growing-period duration of wheat and barley for the reference period, mid-century and end-century for RCP 4.5 and RCP 8.5 in Jordan

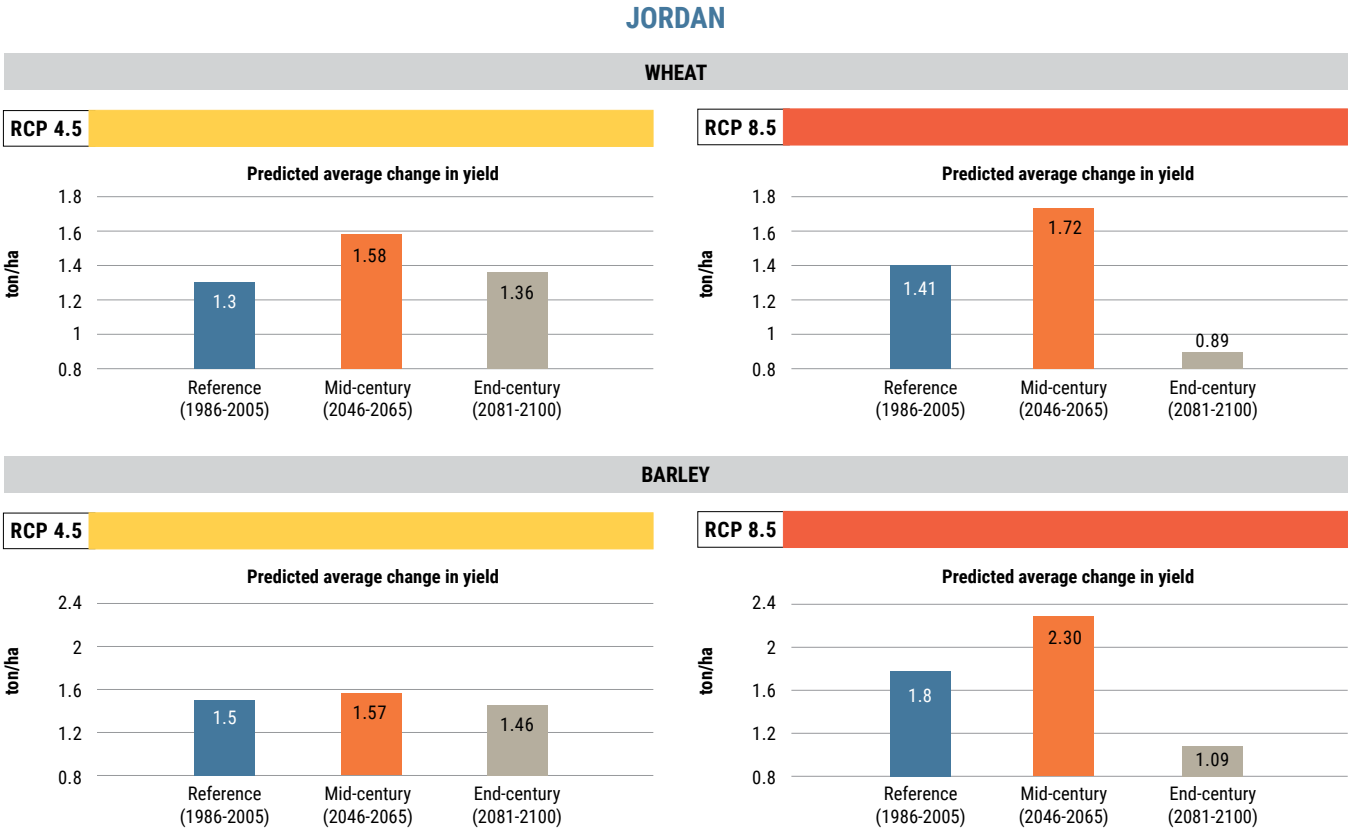

Source: FAO, 2017

6.6 CONCLUSION

The following conclusions can thus be made with respect to the climate change impacts on the productivity of the green sectors of the Arab region:

- Over 50% of the surface area of the Arab region's major cropland systems (including wheat, maize, sorghum, potatoes, vegetables and olives) are exposed to the highest two classes of vulnerability. The highest vulnerability is assessed for the Nile Valley, the Tigris–Euphrates basin, the south-western Arab Peninsula and the western parts of North Africa. As expected, vulnerability increases from the moderate-case to the worst-case scenario and from mid-century to end-century.

- The impact of climate change on livestock is related to the decline of the water and food resource base due to recurrent droughts, degradation of rangelands and desertification. Most vulnerable areas are located along the Nile Valley, the Horn of Africa and south-western Arabian Peninsula, followed by areas of the Fertile Crescent and North Africa. Cattle are the most affected by climate change, followed by goats and sheep. Livestock raised under grassland production systems will be more prone to climate vulnerability than those raised under mixed systems.

- Drought, floods and high temperatures are the major factors of climate change impacts on the fishery and aquaculture sector. Coupled with over-exploitation by humans, climate change may induce the collapse of certain stocks.

- The aridity of the region and low forest cover, coupled with high deforestation rates in some countries make forests more vulnerable to the negative consequences of climate changes. A major impact is expected from water stress (dry and hot years), inducing defoliation, accelerated ageing, reduction in regeneration capacity and increased sensitivity to pest attacks. Overall, a reduction in forest productivity and possible shifts in the composition of species are expected. Vulnerability increases significantly at end-century and with the worst-case scenario. Vulnerability is exacerbated by human activities, mostly overgrazing and the collection of fuelwood.

- C3 crops, such as wheat and cotton under irrigation (non-limited water conditions) appear to benefit from elevated atmospheric CO_2 concentrations. Excellent water management then becomes an adaptation measure for saving water and exploiting the potential in C3 crops to convert the higher CO_2 concentration into higher yields. These findings highlight clearly how the resulting increase in water scarcity is one of the major impacts of climate change on the green sector of the Arab region.

This is particularly the case for crops and forests. If water was not limited, some crops would even benefit from the elevated CO_2 concentrations. Even the impact on livestock is mostly through the grassland production system for feeding the animals. For fishery and aquaculture, the increase in temperature is the more relevant factor. Extreme events such as drought and floods, as further impacts of climate change, can have devastating impacts on all sectors.

ENDNOTES

1. Swain and Jägerskog, 2016
2. See FAO et al., 2017
3. C3 and C4 are the names derived from the first stable compound synthesized by the crop (3 carbon or 4 carbon compound) during CO_2 fixation in photosynthesis. The photosynthetic efficiency of C3 plants is relatively less due to the high rate of photorespiration compared to C4 crops which don't' undergo photorespiration (Furbank and Taylor, 1995).

REFERENCES

FAO (Food and Agriculture Organization of the United Nations). 2011. The State of the World's Land and Water Resources for Food and Agriculture (SOLAW) Managing Systems at Risk. Published by FAO, Rome and Earthscan, London. Available at: http://www.fao.org/docrep/017/i1688e/i1688e.pdf.

FAO (Food and Agriculture Organization of the United Nations). 2017. AquaCrop. Available at: http://www.fao.org/aquacrop/en/.

Furbank, R. T. and Taylor, W. C. 1995. Regulation of Photosynthesis in C3 and C4 Plants: A Molecular Approach *The Plant Cell*, 7: p. 797-807.

FAO, GIZ and ACSAD (Food and Agriculture Organization of the United Nations; Deutsche Gesellschaft für Internationale Zusammenarbeit; Arab Center for the Studies of Arid Zones and Dry Lands). 2017. Climate Change and Adaptation Solutions for the Green Sectors in the Arab Region. *RICCAR Technical Report*. Published by United Nations Economic and Social Commission for Western Asia (ESCWA). Beirut. E/ESCWA/SDPD/2017/RICCAR/TechnicalReport.2.

Swain, A. and Jägerskog, A. 2016. Emerging Security Threats in the Middle East: The Impact of Climate Change and Globalization. Published by Rowman & Littlefield. Lanham, USA.

CHAPTER 7

IMPACT OF CLIMATE CHANGE ON HUMAN HEALTH IN SELECTED AREAS

Climate change in the Arab region has the potential to threaten health and well-being by influencing patterns of communicable and non-communicable diseases through a range of direct and indirect pathways characterized by complex interactions. Direct effects include increases in heat-related illnesses and extreme events, while indirect effects include deterioration of air quality, changes to the distribution of disease vectors, undernutrition and mental health impacts associated with displacement and loss of livelihoods.[1]

For instance, in many parts of the Arab region, the impacts of climate change on agricultural production can threaten food security with significant implications for children's health, as well as contributing disproportionately to undernutrition in low-income households because of the higher costs of food. Many of these climate change impacts on health are amplified in areas where other environmental changes or social and political crises occur, such as desertification or conflict.

The health impacts resulting from climate change will be experienced differently across diverse geographical areas and populations in the region. Varying exposure to health hazards, as well as the susceptibility of different populations and their ability to cope or adapt, will determine the overall impacts on human health and well-being.

The IPCC AR5 states that there has "very likely" been an overall increase in the number of warm days and nights in the region.[2] These increasing temperatures lead to greater risks of heat-related morbidity and mortality in both high- and low-income countries in the Arab region, predominantly in urban areas.[3] Extreme heat causes higher rates of hospitalization and mortality in certain groups, including the elderly, people with existing conditions such as cardiovascular or respiratory disease, people living in lower-quality housing and outdoor workers. While humans can adapt to changes in temperature, there are physiological limits that may be passed in some climate change scenarios.[4]

Additionally, warmer temperatures may magnify the effects of poor air quality, such as ground-level ozone, and increase the production of airborne allergens which can further exacerbate respiratory diseases.

Diseases transmitted by water- or food-borne agents are sensitive to changes in temperature and are common in the Arab region. Higher rates of diarrhoeal disease caused by bacteria such as *Salmonella* and *Campylobacter* occur during warmer temperatures and are projected to rise due to climate change.[5] Transmission of pathogens associated with contaminated drinking water and certain food crops such as enteric viruses and *Cryptosporidium* has additionally been associated with precipitation patterns, including conditions of flooding and drought.

Due to existing gender roles in many countries, this may particularly impact women and girls who spend a great deal of time performing water-, sanitation- and hygiene-related tasks, as well as caring for sick family members. Vector-borne diseases, such as leishmaniasis, malaria, dengue and schistosomiasis, are also very sensitive to a range of climate variables and constitute a major, increasing public health concern in the region. Favourable climate conditions influence the growth, survival and transmission of vectors and rising minimum and maximum temperatures may result in vector range changes or expansions. In addition, climate change can perturb ecosystems and habitats of zoonotic reservoir species, indirectly influencing disease transmission.[6]

Some of these diseases are referred to as neglected tropical diseases (NTDs) a group of infectious diseases which disproportionally impact the poorest people in tropical and subtropical regions. Many NTDs are chronic parasitic infections which reinforce poverty owing to their significant impacts on child development, worker productivity and pregnancy outcomes, costing developing economies billions of dollars every year.[7]

In the Arab region, Egypt and Yemen experience the highest rates of many NTDs followed by Algeria, Libya and Morocco.[8] Understanding how climate change will impact efforts to control and eliminate NTDs is of critical importance to reducing the infectious disease burden in the region.

7.1 HEAT INDEX CONSIDERATIONS AND FINDINGS

Heat stress can induce adverse impacts on human health and is a leading cause of mortality due to meteorological phenomena. Heat-related illnesses are not due solely to extremely high air temperatures, however. High humidity coupled with temperature reduces the body's ability to self-regulate its temperature.[9] The heat index is one of the most common methods to measure apparent temperature and is valid for air temperature exceeding 26.67 °C and over 40% relative humidity.[10] The heat index was calculated for eight selected cities located in coastal areas in the Arab region, which are more likely to be affected by heat-index impacts due to proximity to the sea elevating relative humidity.[11] The heat index was screened for two thresholds: exercise caution (> 26.7 °C), suggesting possible fatigue with prolonged exposure and physical activity; and danger (> 40.6 °C), when heat cramps and heat exhaustion are likely and heatstroke is possible.[12]

The area most vulnerable to heat stress is the African Atlantic coastline (including Nouakchott). For the reference period, there are 194 days/year of caution days and 11 days/year classified as danger days. Caution days increase from 56 (RCP 4.5) to 76 (RCP 8.5) days/year for mid-century, whereby danger days increase from 45 (RCP 4.5) to 68 (RCP 8.5) days/year. For end-century, increases in caution days range from 69 (RCP 4.5) to 144 (RCP 8.5) days/year. Danger days increase from 66 (RCP 4.5) to 143 (RCP 8.5) days/year when compared to the reference period.

The central Arabian Gulf (Doha, Dubai, Manama) is also highly susceptible to heat stress. For the reference period, 181 days/year are recommended to exercise caution due to heat stress. Dangerous heat-stress levels are found 74 days/year. For mid-century, an increase of 13 (RCP 4.5) to 24 (RCP 8.5) days/year is expected in caution days. The increase in the number of danger days is higher, from 33 (RCP 4.5) to 46 (RCP 8.5) days/year. The increase continues for end-century. The number of caution days increases from 21 (RCP 4.5) to 41 (RCP 8.5) days/year when compared to the reference period. Similarly, the number of danger days increase from 45 (RCP 4.5) to 80 (RCP 8.5) days/year.

The heat index is a lesser factor in the northern and southern Arabian Gulf (Kuwait City and Muscat). For the northern Gulf, 30 days/year are recommended to exercise caution, with only 1 day/year with dangerous heat stress levels, for the reference period. More cautionary days are apparent in the southern Gulf (42 days/year) with no danger days. The number of cautionary days increase from 14 (RCP 4.5) to 15 days/year (RCP 8.5) for mid-century in the northern Gulf and from 15 (RCP 4.5) to 20 days/year (RCP 8.5) in the southern Gulf. Likewise, danger days increase from 4 (RCP 4.5) to 10 days/year (RCP 8.5) in the northern Gulf, whereas no increase in danger days is expected in the southern Gulf for mid-century. For end-century, increases in caution days range from 16 (RCP 4.5) to 26 (RCP 8.5) days/year and from 23 (RCP 4.5) to 31 (RCP 8.5) days/year, in the northern and southern Gulf, respectively. The number of danger days increase from 7 (RCP 4.5) to 38 (RCP 8.5) days/year in the northern Gulf with no expected increases in the southern Gulf.

Along the North African coastline near the Mediterranean (Tripoli), 50 days/year are recommended to exercise caution during the reference period, with no danger days. No danger days are expected for future periods. However, caution days increase from 16 (RCP 4.5) to 34 (RCP 8.5) days/year for mid-century and from 31 (RCP 4.5) to 56 (RCP 8.5) days/year for end-century.

The least vulnerable area evaluated is the eastern Mediterranean (Beirut). No heat-stress days were determined for the reference period. Caution days increase from 3 (RCP 4.5) to 6 (RCP 8.5) days/year for mid-century and from 5 (RCP 4.5) to 23 (RCP 8.5) for end-century. No danger days are projected for any future period.

It should be noted that this evaluation was based upon daily average temperature and relative humidity and can be affected by daily maxima, as well as uncertainties stemming from the coarseness of the climate data. Moreover, the heat index is oversimplified and thus underestimated in conditions with full sun and conversely underestimated in very cloudy conditions.[13] Lastly, although the evaluation was conducted in major cities, the urban heat island effect, which can also elevate temperatures, was not considered. Heat stress is expected to increase in coastal regions throughout the Arab region. Outdoor manual labourers are most exposed to impacts, resulting in diminished work capacity (approximately 60% decline) and increased water consumption.[14] The elderly are also at risk because mortality rates are higher on heat-stress days.[15] Nevertheless, heat-related illnesses are preventable. Decision-makers can employ hot-weather warning systems, develop emergency response plans and educate the public. In addition, sufficient breaks should be allowed for outdoor labourers on heat-stress days.

7.2 CASE STUDIES OF NEGLECTED TROPICAL DISEASES

7.2.1 Conceptual framework

This assessment focuses on leishmaniasis and schistosomiasis, two NTDs endemic to the Arab region that are sensitive to changing climate conditions. Cases in western North Africa and Egypt were selected for further investigation due to high prevalence of leishmaniasis and schistosomiasis respectively, and because of the availability of social and environmental datasets that are integrated with climate information. This study focuses in particular on exposure dimensions to understand how climate change will impact conditions required for the transmission of leishmaniasis and schistosomiasis.

This case study adapts the Water-Associated Disease Index (WADI) approach,[16] which aims to improve understanding of vulnerability to health hazards associated with global changes, to the case of leishmaniasis and schistosomiasis in the Arab region. It brings together different types of information in the form of an index, comprising dimensions of exposure, susceptibility and adaptive capacity in order to identify regions most vulnerable to specific health hazards of interest.

In this approach, vulnerability is defined as the propensity to be adversely impacted and exposure is defined as the conditions that support the presence and transmission of a disease agent. Susceptibility refers to sensitivity when exposed to a hazard, which may include social, economic and political conditions.[17] Adaptive capacity is defined as an ability to respond or adapt to a hazard.

To identify components comprising exposure, susceptibility and adaptive capacity, conceptual frameworks were developed for leishmaniasis and schistosomiasis and were used to identify components describing relationships between the disease agent, human health and the environment in the research literature and their potential indicators. Based on these indicators and corresponding thresholds, datasets to populate indicators were identified and included in the assessment.[18]

Data were selected based on the quality and availability of datasets identified from publicly accessible data repositories online. RCM climate projections developed for the MENA Domain were used among other datasets to compare historical exposure conditions for both diseases to those for mid- and end-century using RCP 4.5 and RCP 8.5. Datasets for the exposure components and associated indicators were imported into a geographical information system (ArcGIS) and converted into raster format for manipulation with pixels representing a value from 0 to 1. Monthly temperature and humidity rasters were developed to understand seasonal trends. As susceptibility and adaptive capacity components can be difficult to differentiate in empirical assessments (e.g. education level), they were combined in this analysis to create one map output representing susceptibility and lack of adaptive capacity.[19] These raster layer components contained pixels representing a value from 0 to 1, and were created by normalization.

To create map outputs, components were assumed to have equal importance and were aggregated to form composites for exposure, susceptibility and lack of adaptive capacity using an arithmetic average.[20] While equal weighting was used, other weighting approaches could be adopted with understanding of the local importance of these components, such as expert weighting.

Rather than creating an overall vulnerability index, these separate maps were created for each disease to highlight areas of particular concern for decision-makers. Full details of the methodology, such as dataset selection and sources, are provided in the RICCAR technical report dedicated to this case study prepared by UNU-INWEH.[21]

Casablanca coast, Morocco, 2005. Source: carloszgz-flickr.com

7.2.2 Leishmaniasis

Leishmaniasis is an endemic disease in the region caused by infection with a *Leishmania* parasite transmitted by a sandfly vector and persists as a serious public health concern. There is frequently little information on incidence because surveillance and reporting is limited in many countries affected by the disease.

The zoonotic cutaneous form (ZCL) carried by animals, especially rodents, and the anthroponotic cutaneous form (ACL) carried by humans are both transmitted in the region in rural arid areas and urban areas respectively. ZCL is widely distributed in areas with types of vegetation that support the rodent carrier *(P. obesus)* and occurs in Algeria, Egypt, Iraq, Jordan, Libya, Morocco, State of Palestine, Saudia Arabia, Somalia, Syrian Arab Republic, Sudan, Tunisia and Yemen. ACL is transmitted in areas with densely populated towns and villages and is found in Iraq, Morocco, Saudi Arabia, Syrian Arab Republic and Yemen.[22]

Western North Africa was chosen for this case study because cutaneous leishmaniasis (CL) is a growing public health problem in the region and Morocco was chosen for more detailed analysis of susceptibility and adaptive capacity because relevant datasets were available. Based on the conceptual framework developed for leishmaniasis, current and future exposure were assessed, based on components for suitable temperature and humidity conditions for the sandfly vector that carries the disease, combined with an indicator on land-cover types that support transmission of ZCL. Regionally downscaled future climate projections for the MENA Domain developed as part of RICCAR were used for temperature datasets. Susceptibility to leishmaniasis was determined using available datasets for sanitary conditions which can increase sandfly breeding and resting sites and provide easier access to human hosts[23] as well as migration, which has the potential to bring non-immune people into areas with transmission cycles, which is particularly relevant in the MENA region. Adaptive capacity included prevention and control interventions to stop the transmission of leishmaniasis. For this assessment, this component included the indicator related to education, which ensures that people recognize an infection and seek treatment quickly.

Results of this assessment suggest that changes in climate may have an important impact on the range of leishmaniasis transmission in the Arab region. Like many vector-borne diseases, leishmaniasis incidence displays a strong seasonality due to the influence of climate variables. Minimum temperatures in the study area historically drop below the sandfly vector's survival thresholds (10 °C) during colder months, limiting the transmission of leishmaniasis. Based on exposure projections, results indicate that warmer temperatures during colder months could extend the period of suitability for disease transmission due to minimum temperatures occurring less frequently below the sandfly survival threshold. As shown in Figure 101 for November, areas indicating no exposure (in white) become progressively limited by end- century, in particular for RCP 8.5. In some areas, however, exposure may be reduced where maximum temperatures exceed 40 °C for longer periods, such as in summer months, due to the upper end of the sandfly survival range. Although the extent of areas characterized by temperatures > 40 °C will potentially expand, many of these areas are in sparsely inhabited regions and will therefore have less impact on human populations. In addition to temperature conditions, vegetation for the animal host may decrease in some areas with decreasing moisture availability associated with changes in humidity.

It is, however, important to note that climate conditions are only one aspect of exposure and overall vulnerability and ZCL is characterized within exposed areas by focal outbreaks. Foci occur in areas with suitable vegetation for the rodent reservoir host in proximity to human populations. Foci may also occur where susceptibility is higher due to factors such as poor housing quality and sanitary conditions that provide breeding sites for the vector or high rates of in-migration that increase the non-immune population. Figure 102 indicates that many areas that are exposed to ZCL in Morocco are more susceptible and have lower adaptive capacity than other parts of the country. This means that public health authorities can apportion resources to vector-control activities which decrease exposure during longer seasons of transmission, as well as improving capacity of the population to cope with outbreaks.

The *P. papatasi* sandfly, vector of *Leishmania* parasites. Source: Center for Disease Control and Prevention (USA).

FIGURE 101: Historical and projected exposure to Leishmaniasis in North Africa in November

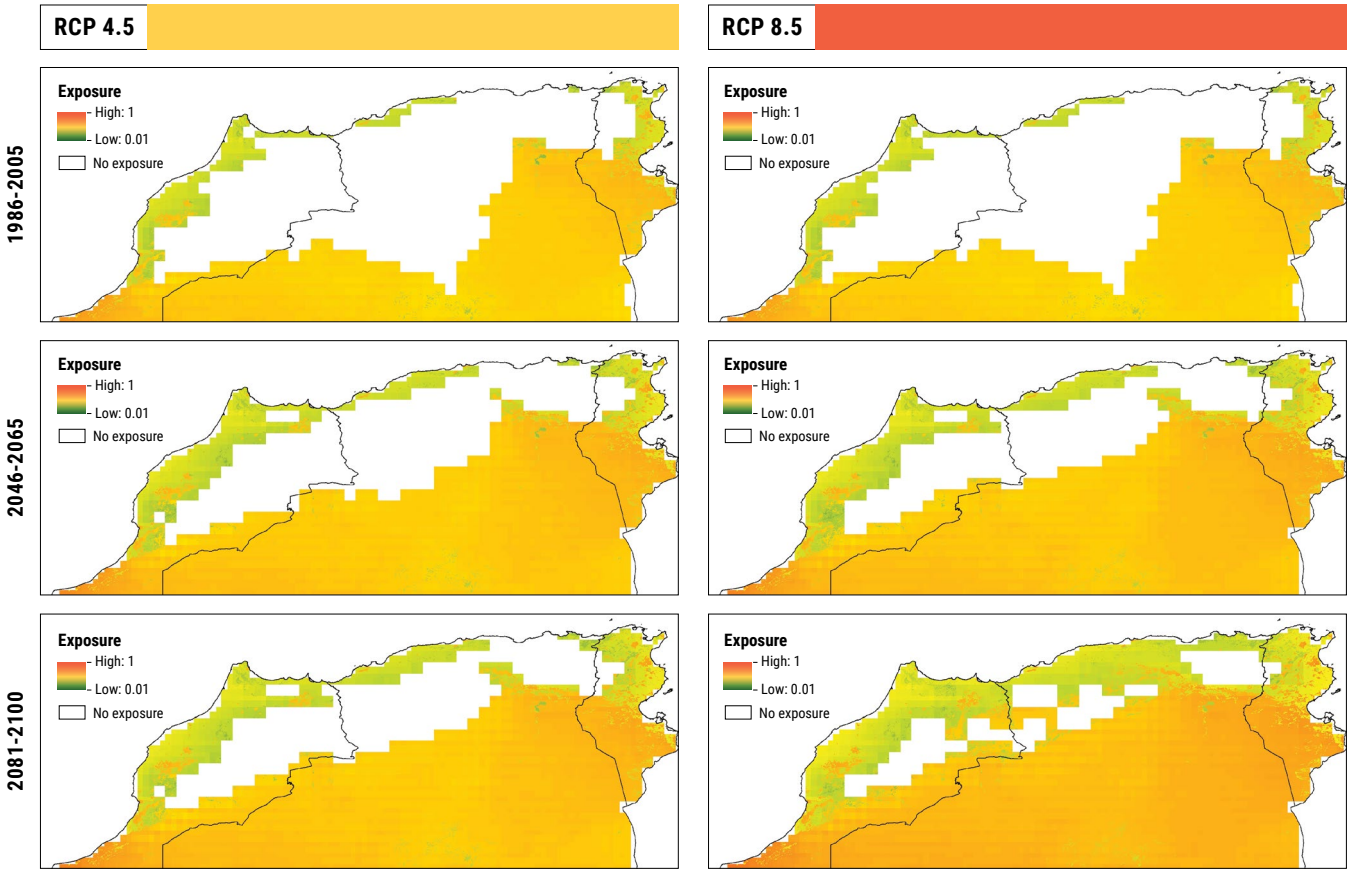

FIGURE 102: Susceptibility and lack of adaptive capacity to leishmaniasis in Morocco

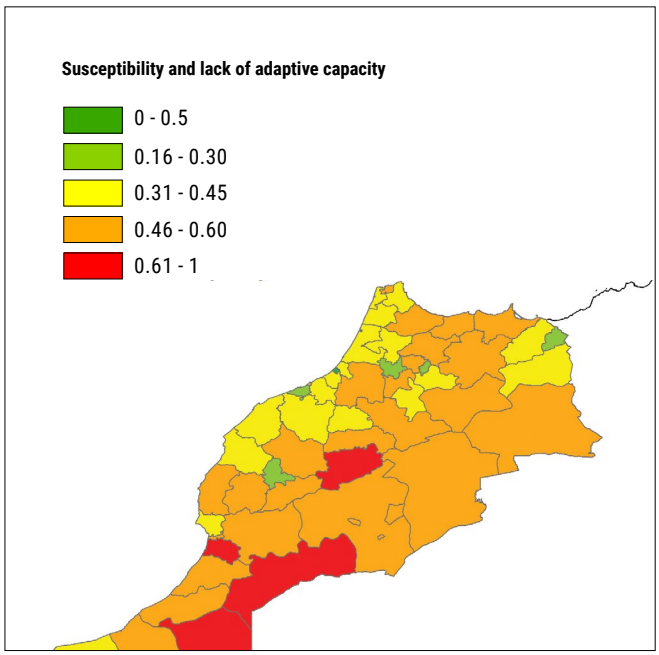

7.2.3 Schistosomiasis

Schistosomiasis is a parasitic disease resulting from contact with contaminated freshwater sources and transmitted by blood flukes known as schistosomes which live in freshwater snail hosts. The disease disproportionately affects the poorest people in endemic areas, including those without access to safe water and sanitation, and those with water-based livelihoods such as fishing and rice cultivation.[24] In the MENA region, schistosomiasis is the second most prevalent NTD with an estimated 12.7 million cases affecting Egypt, Somalia, Sudan and Yemen. The highest prevalence is reported in Egypt where *S. mansoni*, which is the parasite causing intestinal schistosomiasis, is endemic in northern regions and was thus chosen for this case study.[25] While efforts to control schistosomiasis in Egypt have been successful, certain communities in the Nile Delta with high prevalence rates sustain transmission of the disease.[26]

Based on the conceptual framework for schistosomiasis, this case study assessed current and future exposure to the disease in Egypt, based on suitable conditions for *B. alexandrina* snail populations that transmit *S. mansoni*.

FIGURE 103: Historical and projected exposure to schistosomiasis in Egypt in December

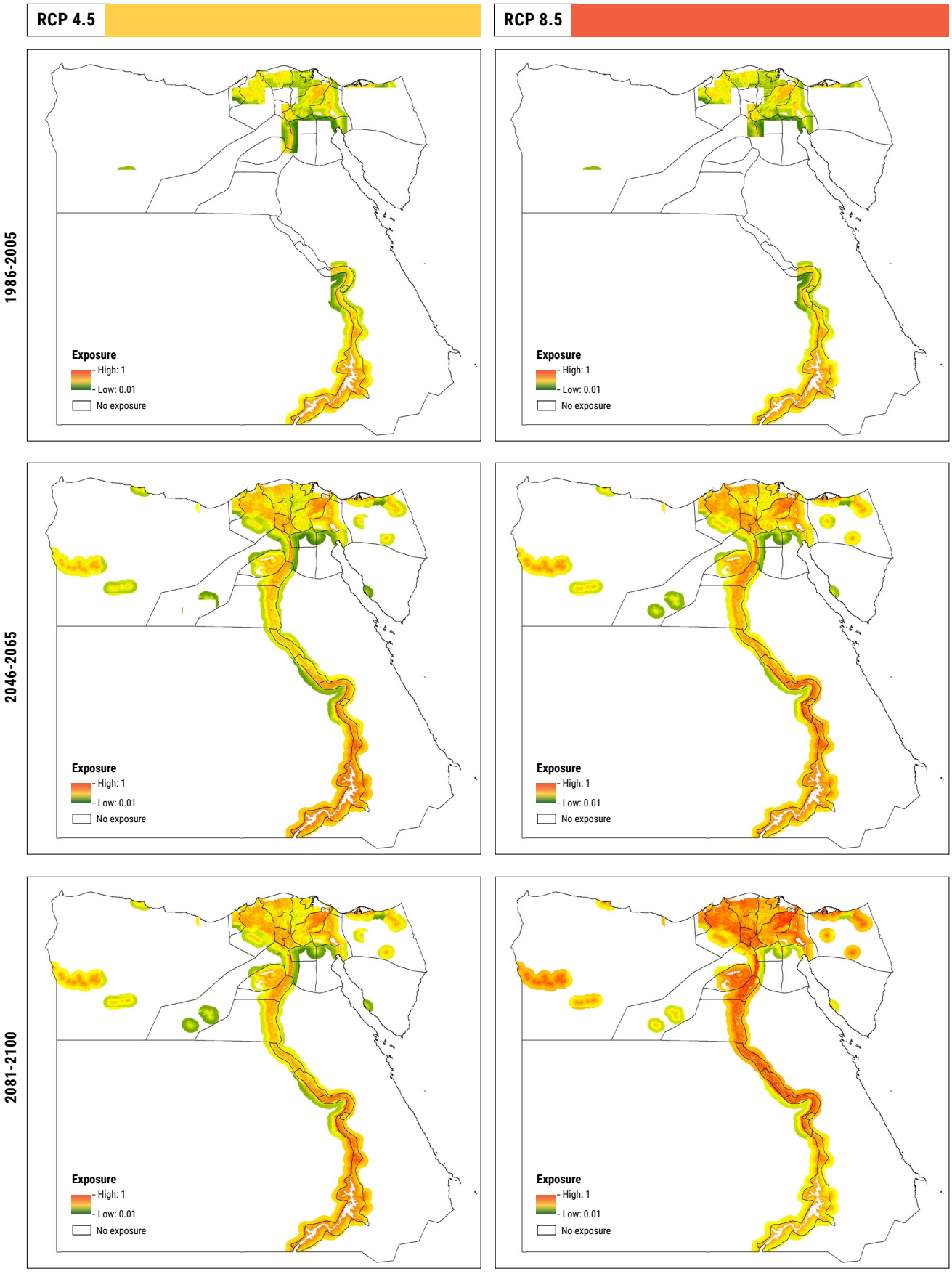

Air temperature was used as a proxy for water temperature, which is not available in climate models, and temperature suitability was integrated with information on proximity to water sources and extent of sewerage networks that impact the transmission cycle. As schistosomiasis is strongly influenced by social determinants, susceptibility was based on indicators related to the access to water resources in rural areas, populations engaged in water-related livelihoods, as well as age and health status indicators. The indicators used to identify areas of adaptive capacity were related to health care access and education.

Results of the assessment indicate that changes in climate may influence the seasonal pattern of schistosomiasis transmission in Egypt. The disease transmission in the region occurs on a seasonal basis, with most cases occurring during the warmer summer months and in the Nile Delta, where there are intensive contacts with water due to water-based livelihoods. While transmission is limited in colder months, the results of this case study suggest that increasing temperatures projected in RCP 4.5 and RCP 8.5 at mid- and end-century in winter will create conditions that increase infection risk during winter months. Figure 103 highlights historical exposure in December during the winter, when fewer cases currently occur, compared to exposure at mid- and end-century. Because these changes in temperature occur near thresholds for schistosome infection risk, small increases can make a large difference. In addition, other species of snail, such as *B. pfeifferi*, the most widespread intermediate host of *S. mansoni* in Africa, survive at slightly warmer temperatures than *B. alexandrina*, so could become established in greater numbers in the area in warmer conditions.[27]

These findings have implications for public health authorities who currently undertake vector-control activities during the warmer months, when most infections occur. Changing climate conditions could also impact the success of treatment measures, such as de-worming programmes, if they are timed for warmer periods. Importantly, changes in exposure are projected to occur in areas in the Nile Delta where the population currently experiences higher susceptibility due to water-based livelihoods and limited sewerage connections (Figure 104).

In these areas, climate change could have a greater impact on the burden of disease by increasing the length of the transmission season. In addition to climate change, other positive or negative social and ecological changes in the Arab region, such as increasing access to sanitation, land degradation or conflicts which disrupt control and elimination efforts, could have important impacts on the disease cycle.

FIGURE 104 : Susceptibility and lack of adaptive capacity to schistosomiasis in Egypt

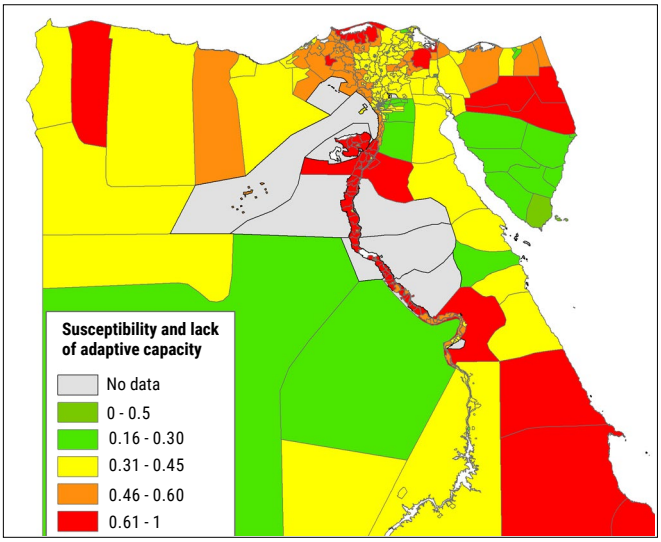

7.2.4 Implications and conclusions

The results of this assessment, which focuses particularly on exposure dimensions, indicate that climate change may impact the seasonal duration of disease transmission. These findings have implications for vector control, surveillance and awareness-building activities carried out by public authorities. Beyond the serious health burden associated with NTDs, these chronic infections can entrap people in a cycle of poverty and are often associated with social stigma.

The impact of climate change is not simply limited to changes in climate variables but also comprises extreme events that may also considerably affect the distribution of NTDs and efforts to develop sustainable control strategies. Moreover, these climate change impacts must be considered within the context of concurrent social and other environmental changes, such as extensive human and animal migrations, conflict and associated breakdowns in public health systems and socio-economic development.[28] In addition, desertification and water resource development projects to address increasing water scarcity have played a role in supporting the transmission of NTDs such as leishmaniasis, as they can increase exposure to the disease.[29] Migrations of people within their countries or to other parts of the region can also lead to large outbreaks in new areas and therefore exacerbate exposure and susceptibility conditions.

It is important to highlight the fact that the burden of NTDs is higher in poor and marginalized communities[30], indicating a disproportionate threat due to changing climate conditions.

In the case of leishmaniasis, the disease has been found to present a greater threat to the health and socio-economic status of women.[31] In Tunisia, women involved in agriculture have higher vulnerability as they receive increased exposure to irrigation activities and are more sensitive to the negative social implications of the disease.[32] In Yemen, the incidence of leishmaniasis was found to be higher among rural children and female populations, which may be due to their work in agriculture and animal care, as well as water collection, when they may be exposed to sandfly bites.[33] In addition, women's limited access to financial resources may reduce access to healthcare for treatment for the disease. Cutaneous leishmaniasis, which can cause disfiguring scars, can have a severe impact on women's psychological well-being, as well as quality of life due to social stigmatization. For schistosomiasis, changes in exposure are projected to occur in areas of the Nile Delta, where the population currently experiences higher susceptibility. As this is a water-associated disease, there are particular implications for women and girls who often spend large amounts of time performing water-, sanitation- and hygiene-related tasks, as well as caring for sick family members.

While significant progress is being made to control and eliminate many NTDs in the Arab region, there is a pressing need to consider how these efforts may be threatened by climate change. This is made challenging by poor surveillance and reporting capacities, as well as a lack of information on incidence rates in many affected countries. Further research to deepen understanding of the complex processes through which climate change will impact NTD dynamics is thus required in order to identify and adapt appropriate and equitable health-promotion strategies.

7.2.5 Limitations

Several limitations should be considered regarding this case study. While this assessment applied regional climate projections, disease incidence is characterized by extremely focal outbreaks within exposed areas. The results should not be taken as being predictive of future prevalence of schistosomiasis or leishmaniasis, but as indicative of areas where projected changes in climate may influence the suitable conditions for transmission. Not all possible indicators are considered in the case studies, as there is limited evidence on some linkages in the Arab region or because datasets are unavailable. For example, given the case of schistosomiasis and the available indicators considered in the exposure assessment, results show that disease exposure covers the course of the Nile River, while the actual disease prevalence is more restricted to the lower Nile River. On the other hand, while not the focus of this study, limited data were freely available on indicators of susceptibility and adaptive capacity in this assessment, which highlights data gaps that could improve vulnerability assessments.

Northern Nile Delta, Egypt, 2015. Source: Ihab Jnad.

BOX 6: Recent disease outbreaks due to climate conditions: yellow fever and other diseases

Over the past decade, the region has witnessed recurrent outbreaks from emerging or re-emerging infectious diseases, leading to numerous cases of morbidity and mortality. The major ones recently detected in the region include yellow fever, dengue and rift valley fever, all transmitted by the Aedes mosquito and presented below. Other infectious diseases also reported include the Middle East respiratory syndrome (Bahrain, Oman, Oatar, Saudi Arabia, UAE and Yemen, 2013–2015) and some cases of cholera in Iraq (2015).

YELLOW FEVER

Yellow fever is commonly transmitted by infected *Aedes aegypti* mosquitoes and known to be endemic in tropical areas of Africa and Latin America. As a highly seasonal disease, rainfall is an important determinant in its prevalence. The warmer the ambient temperature, the shorter the incubation period from the time the mosquito imbibes the infective blood till it is able to transmit by bite. Warmer temperatures also provide shorter time for larvae to mature as water temperatures rise, leading to a greater capacity to produce more offspring during the transmission period. Another important contributing factor to the disease spread is urbanization, with the rapid growth of densely populated towns and cities providing an increasingly favourable environment for transmission. Water-storage containers in urban areas or other similar materials (buckets, flowerpots, discarded tyres, etc.) can also serve as breeding sites if they accumulate rainwater. A recent disease outbreak in the region occurred in Sudan in 2012; 849 suspected cases, including 171 deaths, were reported in Darfur. Prior to this, outbreaks in 2003 and 2005 were the first reports of yellow fever in Sudan in approximately 50 years. Another outbreak occurred in 2013 leading to 15 deaths in the state of West Kordofan. A risk assessment conducted in 2012 in Sudan identified potential areas of risk for yellow fever virus transmission and found it in circulation in all ecological areas of the country, with an estimated 30.7 million people living in areas of high risk or at potential risk of contracting yellow fever. As a result, Sudan launched its first ever mass preventive vaccination campaigns in 2014 with some 7.5 million people vaccinated in seven high-risk states. Apart from Sudan, evidence of circulation of the virus was reported in Djibouti and Somalia based on serological studies.[34]

DENGUE FEVER

In 2012, dengue fever was classified by WHO as the "most important mosquito-borne viral disease in the world" due to its significant geographical spread into previously unaffected areas and the subsequent costly burden of disease. Dengue has recently resurged in the region, causing sporadic yet increasingly common outbreaks, particularly in Saudi Arabia and Egypt (2015), Sudan and Yemen (2012–2015). Smaller outbreaks involving multiple serotypes of the virus are also being reported more frequently from countries such as Djibouti and Somalia, indicating the presence of vectors with the risk of local transmission. Several studies have investigated the role climate change plays in the resurgence of the disease in recent decades and is an ongoing area of research. It has been shown that reasons for the currently observed and predicted expansion are multifactorial, including viral introduction through migration and travel, as well as changes in climatic conditions. While the scarcity of rainfall in the Arab region results in climatic conditions that are not ideal for dengue vectors, expected increasing temperatures and water stress will contribute to stimulate dengue incidence with the increase of water storage containers (ideal for vector breeding) in anticipation of drier conditions.[35]

RIFT VALLEY FEVER

The first outbreak of rift valley fever (RVF) outside the African continent was witnessed along the south-western coast of Saudi Arabia and neighbouring coastal areas of Yemen in September 2000. The outbreak resulted in more than 120 human deaths and major losses in livestock populations from disease and slaughter. It followed increased rainfall in nearby highlands that flooded the coastal areas and created ideal environments for mosquito populations similar to those found in RVF-endemic regions of East Africa. Most RVF activity was associated with flooded wadi agricultural systems, and no cases were reported in the mountains or in the dry sandy regions, where surface water does not accumulate long enough to sustain mosquito breeding. Another spread was reported in Sudan in 2008 and then in six different regions of Mauritania in 2012.[36]

ENDNOTES

1. Watts et al., 2015
2. Hewitson et al., 2014
3. Habib et al., 2010
4. Pal and Eltahir, 2016
5. El-Fadel et al., 2012
6. Haines et al., 2014
7. Hotez, 2009
8. Hotez et al., 2012
9. Willett and Sherwood, 2012
10. Rothfusz, 1990
11. Diffenbaugh et al., 2007
12. NWS, 2016
13. Willett and Sherwood, 2012
14. Tawatsupa et al., 2010
15. Smoyer et al., 2000
16. Dickin et al., 2013
17. Birkmann et al., 2013
18. Alimi et al., 2016
19. De Sherbinin, 2014
20. Dickin et al., 2013
21. See UNU-INWEH, 2017
22. Postigo, 2010
23. WHO, 2017
24. Hotez and Fenwick, 2009
25. Hotez et al., 2012
26. Elmorshedy et al., 2015
27. McCreesh and Booth, 2014
28. Hotez et al., 2012
29. Boubaker and Chahed, 2011
30. Du et al., 2016
31. Al-Kamel, 2016a; Boubaker et al., 2011
32. Boubaker, 2016
33. Al-Kamel, 2016b
34. Reiter, 2001; WHO, 2014; WHO, 2016; Yuill et al., 2013; Karunamoorthi, 2013; Jentes et al., 2010
35. Amarasinghe and Letson, 2012; Murray et al., 2013; IRIN News, 2010; Pinkerton and Rom, 2014; Humphrey et al., 2016
36. Martin et al., 2008; El-Mamy et al., 2011; WHO, 2012; Himeidan et al., 2014; Sayed-Ahmed et al., 2015

REFERENCES

Al-Kamel, M. A. 2016a. Impact of Leishmaniasis in Women: A Practical Review with an Update on my ISD-Supported Initiative to Combat Leishmaniasis in Yemen (ELYP). *International Journal of Women's Dermatology*, 2(3): p. 93-101.

Al-Kamel, M. A. 2016b. Leishmaniasis in Yemen: A Clinicoepidemiological Study of Leishmaniasis in Central Yemen. *International Journal of Dermatology*, 55(8): p. 849–855.

Alimi, T. O., Fuller, D. O., Herrera, S. V., Arevalo-Herrera, M., et al. 2016. A Multi-Criteria Decision Analysis Approach to Assessing Malaria Risk in Northern South America. *BMC Public Health*, 16(221): p. 1-10.

Amarasinghe, A. and Letson, W. G. 2012. Dengue in the Middle East: a Neglected, Emerging Disease of Importance. *Transactions of the Royal Society of Tropical Medicine and Hygiene*, 106.

Birkmann, J., Cardona, O. D., Carreño, M. L., Barbat, A. H., et al. 2013. Framing Vulnerability, Risk and Societal Responses: the MOVE Framework. *Natural Hazards*, 67(2): p. 193–211.

Boubaker, H. B. 2016. Health Impacts of Climate Change in Arab world: Case of Tunisia. In *ESCWA Workshop on Developing the Capacities of the Health Sector for Climate Change Adaptation to Protect Health from the Climate Change Effects on Freshwater Resources, 19-21 April 2016, Amman, Jordan*. Available at: https://www.unescwa.org/sites/www.unescwa.org/files/events/files/health_impacts_of_climate_change_in_arab_countries_-_case_of_tunisia.pdf.

Boubaker, H. B. and Chahed, M. 2011. Des Echos du Terrain: Gestion de la Leishmaniose en Tunisie dans le Contexte des Changements Climatiques. In *Adaptation aux Changements Climatiques en Afrique Rapport Annuel 2010-2011*. Published by International Development Research Centre (IDRC). Available at: https://www.idrc.ca/sites/default/files/sp/Documents%20EN/tunisia_f.pdf.

Boubaker, H. B., Kouni-Chahed, M. and Alaya-Bouafîf, N. B. 2011. Relationship Between Climate Change and Zoonotic Cutaneous Leishmaniasis in Tunisia. *Tropical Medicine & International Health*, 16.

De Sherbinin, A. 2014. Climate Change Hotspots Mapping: What Have We Learned. *Climatic Change*, 123(1): p. 23–37.

Dickin, S. K., Schuster-Wallace, C. J. and Elliott, S. J. 2013. Developing a Vulnerability Mapping Methodology: Applying the Water-Associated Disease Index to Dengue in Malaysia. *PLOS One*, 8(5).

Diffenbaugh, N. S., Pal, J. S., Giorgi, F. and Gao, X. 2007. Heat Stress Intensification in the Mediterranean Climate Change Hotspot. *Geophysical Research Letters*, 34(11).

Du, R., Hotez, P. J., Al-Salem, W. S. and Acosta-Serrano, A. 2016. Old World Cutaneous Leishmaniasis and Refugee Crises in the Middle East and North Africa. *PLOS Neglected Tropical Diseases*, 10(5).

El-Fadel, M., Ghanimeh, S., Maroun, R. and Alameddine, I. 2012. Climate Change and Temperature Rise: Implications on Food-and Water-borne Diseases. *Science of the Total Environment*, 437: p. 15-21.

El-Mamy, A. B. O., Baba, M. O., Barry, Y., Isselmou, K., et al. 2011. Unexpected Rift Valley Fever Outbreak, Northern Mauritania. *Emerging Infectious Diseases*, 17(10): p. 1894-1896.

Elmorshedy, H., Bergquist, R., Abou El-Ela, N., Eassa, S., et al. 2015. Can Human Schistosomiasis Mansoni Control be Sustained in High-risk Transmission Foci in Egypt? *Parasites and Vectors*, 8(1): p. 1-8.

Habib, R. R., Zein, K. E. and Ghanawi, J. 2010. Climate Change and Health Research in the Eastern Mediterranean Region. *Ecohealth*, 7(2): p. 156-175.

Haines, A., Haines, A., Ebi, K. L., Smith, K. R., et al. 2014. Health Risks of Climate Change: Act Now or Pay Later. *The Lancet*, 384(9948): p. 1073-1075.

Hewitson, B., Janetos, A. C., Carter, T. R., Giorgi, F., et al. 2014. Regional Context (Chapter 21). In Climate Change 2014: *Impacts, Adaptation, and Vulnerability. Part B: Regional Aspects. Contribution of Working Group II to the Fifth Assessment Report of the Intergovernmental Panel on Climate Change*. V. R. Barros, C.B. Field, D.J. Dokken, M.D. Mastrandrea, K.J. Mach, T.E. Bilir, M. Chatterjee, K.L. Ebi, Y.O. Estrada, R.C. Genova, B. Girma, E.S. Kissel, A.N. Levy, S. MacCracken, P.R. Mastrandrea, and L.L. White (eds). Published by Cambridge University Press. Cambridge, United Kingdom and New York, USA. Available at: https://www.ipcc.ch/pdf/assessment-report/ar5/wg2/WGIIAR5-Chap21_FINAL.pdf.

Himeidan, Y. E., Kweka, E. J., Mahgoub, M. M., Rayah, E. A. E., et al. 2014. Recent Outbreaks of Rift Valley Fever in East Africa and the Middle East. *Frontiers in Public Health*, 2.

Hotez, P. J. 2009. The Neglected Tropical Diseases and Their Devastating Health and Economic Impact on the Member Nations of the Organisation of the Islamic Conference. *PLOS Neglected Tropical Diseases*, 3(10).

Hotez, P. J. and Fenwick, A. 2009. Schistosomiasis in Africa: An Emerging Tragedy in Our New Global Health Decade. *PLOS Neglected Tropical Diseases*, 3(9).

Hotez, P. J., Savioli, L. and Fenwick, A. 2012. Neglected Tropical Diseases of the Middle East and North Africa: Review of their Prevalence, Distribution, and Opportunities for Control. *PLOS Neglected Tropical Diseases*, 6(2).

Humphrey, J. M., Cleton, N. B., Reusken, C. B. E. M., Glesby, M. J., et al. 2016. Dengue in the Middle East and North Africa: A Systematic Review. *PLOS Neglected Tropical Diseases*, 10(12).

IRIN News. 2010. Yemen: Dengue Fever Spreading in South. Issued on July 14, 2010. Available at: http://www.irinnews.org/report/89826/yemen-dengue-fever-spreading-in-south.

Jentes, E. S., Poumerol, G., Gershman, M. D., Hill, D. R., et al. 2010. The Revised Global Yellow Fever Risk Map and Recommendations for Vaccination, 2010: Consensus of the Informal WHO Working Group on Geographic Risk for Yellow Fever. *Lancet Infectious Diseases*, 11(8): p. 579-650.

Karunamoorthi, K. 2013. Yellow Fever Encephalitis: An Emerging and Resurging Global Public Health Threat in a Changing Environment. S. Tkachev (eds). In *Encephalitis*. S. Tkachev (eds). Published by InTech.

Martin, V., Chevalier, V., Ceccato, P., Anyamba, A., et al. 2008. The Impact of Climate Change on the Epidemiology and Control of Rift Valley Fever. *Revue Scientifique et Technique*, 27(2): p. 413-426.

McCreesh, N. and Booth, M. 2014. The Effect of Simulating Different Intermediate Host Snail Species on the Link Between Water Temperature and Schistosomiasis Risk. *PLOS One*, 9(7).

Murray, N. E. A., Quam, M. B. and Wilder-Smith, A. 2013. Epidemiology of Dengue: Past, Present and Future Prospects. *Clinical Epidemiology*, 5: p. 299-309.

NWS (National Weather Service USA). 2016. Heat Index. Published by National Oceanic and Atmospheric Administration. Available at: http://www.nws.noaa.gov/om/heat/heat_index.shtml.

Pal, J. S. and Eltahir, E. A. B. 2016. Future Temperature in Southwest Asia Projected to Exceed a Threshold for Human Adaptability. *Nature Climate Change*, 6: p. 197–200.

Pinkerton, K. E. and Rom, W. N. 2014. Global Climate Change and Public Health. In *Respiratory Medicine Series*. Published by Humana Press.

Postigo, J. A. 2010. Leishmaniasis in the World Health Organization Eastern Mediterranean Region. *International Journal of Antimicrobial Agents*, 36(Suppl 1): p. 62-65.

Reiter, P. 2001. Climate Change and Mosquito-Borne Disease. *Environmental Health Perspectives*, 109: p. 141-161.

Rothfusz, L. P. 1990. The Heat Index "Equation" (or, more than you ever wanted to know about heat index). NWS Tech. Attachment SR 90-23. Published by National Weather Service, USA.

Sayed-Ahmed, M., Nomier, Y. and Shoeib, S. M. 2015. Epidemic Situation of Rift Valley Fever in Egypt and Saudi Arabia. *Journal of Dairy, Veterinary & Animal Research*, 2(3).

Smoyer, K. E., Rainham, D. G. and Hewko, J. N. 2000. Heat-stress-related Mortality in Five Cities in Southern Ontario: 1980–1996. *International Journal of Biometeorology*, 44(4): p. 190-197.

Tawatsupa, B., Lim, L. Y., Kjellstrom, T., Seubsman, S. A., et al. 2010. The Association between Overall Health, Psychological Distress, and Occupational Heat Stress among a Large National Cohort of 40,913 Thai Workers. *Global Health Action*, 3(1).

UNU-INWEH (United Nations University Institute for Water, Environment and Health). 2017. Climate Change Impacts on Health in the Arab Region: A Case Study on Neglected Tropical Diseases. RICCAR Technical Report. Published by United Nations Economic and Social Commission for Western Asia (ESCWA). Beirut. E/ESCWA/SDPD/2017/RICCAR/TechnicalReport.1

Watts, N., Adger, N., Agnolucci, P., Blackstock, J., et al. 2015. Health and Climate Change: Policy Responses to Protect Public Health. *The Lancet Commissions*, 386(10006): p. 1861–1914.

WHO (World Health Organization). 2012. Rift Valley Fever in Mauritania. In *Disease Outbreak News: Emergencies Preparedness, Response*. Available at: http://www.who.int/csr/don/2012_11_01/en/.

WHO (World Health Organization). 2014. Yellow Fever Fact Sheet. Available at: http://applications.emro.who.int/docs/Fact_Sheet_WHD_2014_EN_1635.pdf.

WHO (World Health Organization). 2016. Progress Report on Emerging and Re-emerging Diseases Including Dengue and Dengue Haemorrhagic Fever. In *Sixty-third Session of thr Regional Committee for the Eastern Mediterranean* Available at: http://applications.emro.who.int/docs/RC_technical_papers_2016_inf_doc_2_19010_EN.pdf?ua=1.

WHO (World Health Organization). 2017. Leishmaniasis Fact Sheet. Available at: http://www.who.int/mediacentre/factsheets/fs375/en/.

Willett, K. M. and Sherwood, S. 2012. Exceedance of Heat Index Thresholds for 15 Regions under a Warming Climate using the Wet-bulb Globe Temperature. *International Journal of Climatology*, 32(2): p. 161-177.

Yuill, T. M., Woodal, J. P. and Baekeland, S. 2013. Yellow Fever Outbreak—Darfur Sudan and Chad. *International Journal of Infectious Diseases*, 17(7): p. 476-478.